Synthesis of High Molecular Weight Polymers as Low-Viscosity Latex Particles by RAFT Aqueous Dispersion Polymerisation

Rory Jacob McBride

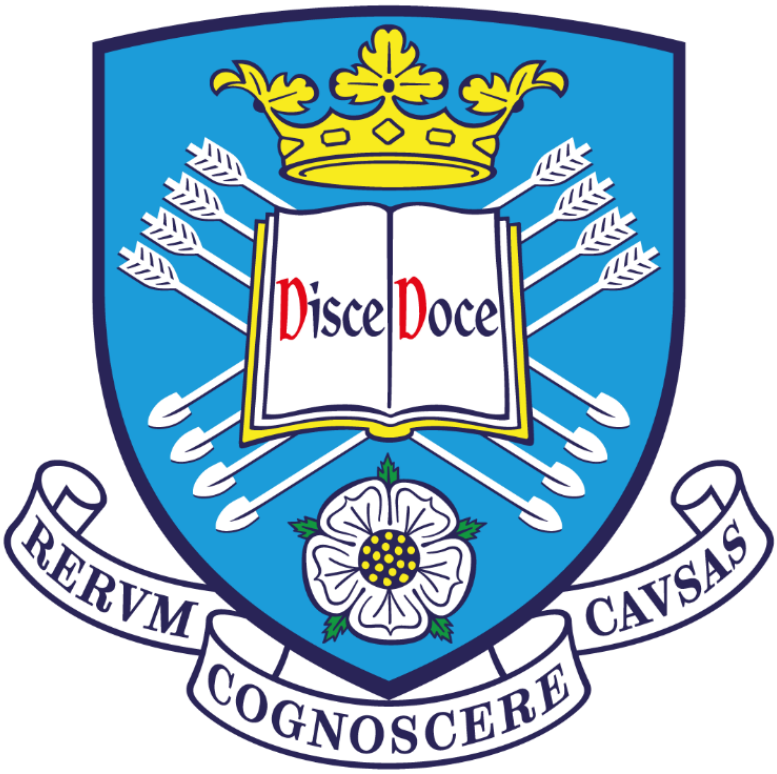

Department of Chemistry

University of Sheffield

PhD Thesis 2019-2023

Supervisor: Prof. Steven P. Armes FRS

Declaration

The work described in this thesis was undertaken at the University of Sheffield under the supervision of Professor Steven P. Armes between October 2019 and December 2023 and has not been submitted, either wholly or in part, for this or any other degree. All the work is the original work of the author, except where acknowledged.

Signed Date

……. ……

RORY MCBRIDE

Acknowledgements

I praise God whose grace sustains me and gives me joy, health and motivation in my work! *He is my strength and refuge, my present help in times of trouble. Ps 46.*

Many thanks to my wonderful wife Amy over the past few years for her patience and understanding, as I eventually got myself to sit down and write this document. Also, sincere appreciation to my parents for their support throughout my time at university – perhaps a copy of this Thesis will be the best way for you to understand what I've been doing for the past 4 years!

I would like to thank Steve Armes for the assistance and direction he has provided me with as my supervisor during this project. Also to Hans-Joachim Hähnle, Christine Rösch and Adam Blanazs from BASF, as well as my secondary supervisor Steve Ebbens. In the Armes group, I'd like to make special mention to Erik Cornel for his direction during my MChem project and who entertained my questions on whether I should even do a PhD! Additionally, to those who went out of their way to help me develop my project; I particularly thank Olly (and his irreplicatable thixotropy), Reb, Debs, Patrick and Andi. Also to those who've helped me with analysis, including Adam and Tom with SAXS, Hubert and Matt with TEM. À Elisa, merci pour le travail que tu as accompli pendant ton stage d'été à Sheffield.

In principle, I have enjoyed the research I have done as part of this project, and it is unfortunate that I missed out on doing a lot of work *owing to* closures caused by COVID-19. *Conversely*, I certainly made up for it with the work and opportunities I had in the following years. *Judicious* use of my time has still enabled me to write this Thesis *(REF)*. During my placement at BASF, I am grateful to Christina Niedberg for practical support in the laboratory and the time she spent helping me enjoy my time in beautiful Ludwigshafen. Also, to the many interns I got to know, particularly the D104 lunch group including Marc (and car), Felix (and family), Mery & Nicole (and quality Italian cooking), Clemens & Olivia (and bicycles!).

I shall remember well… i) 'safely' scooting around late at night at BPC Bordeaux with the extended Sheffield contingent after a memorable midnight meal at the palace, ii) the awe-inspiring view from the Sears Tower during ACS Chicago with Amy, Chill and Derek, iii) the lavish food and accommodation when attending ECIS Chania with Csilla, Oleta, Saul, Ed, Derek and Spyros, iv) coincidently sitting next to Oliver on the plane to ACS San Francisco whose talk preceded mine and v) watching the state ballet and opera in Prague during the ISP with Hubert, as well as catching up with native Pragovians: Niccolo and Vyshakh.

I hadn't intended to stay in Sheffield so long, but this meant I was blessed with getting to know (and marry) Amy and I wouldn't want it any other way! It's been great that the summer of '23 has seen five F-floor weddings and getting to share in these celebrations. It's been a pleasure doing my PhD and a privilege to work for Steve and I look forward to what comes next!

Publications and Conference Presentations

Publications

1. **Rory J. McBride**, John F. Miller, Adam Blanazs, Hans-Joachim Hähnle, and Steven P. Armes, “Synthesis of High Molecular Weight Water-Soluble Polymers as Low-Viscosity Latex Particles by RAFT Aqueous Dispersion Polymerization in Highly Salty Media”, *Macromolecules*, 2022, **55**, 7380−7391
2. **Rory J. McBride**, Elisa Geneste, Andi Xie, Anthony J. Ryan, John F. Miller, Adam Blanazs, Christine Rösch and Steven P. Armes, "A Low-Viscosity Route to High Molecular Weight Water-Soluble Polymers: Exploiting the Salt Sensitivity of Poly(*N*-acryloylmorpholine)", *Macromolecules*, 2024, **57**, 2432−2445
3. Hubert Buksa, Edwin C. Johnson, Derek H. H. Chan, **Rory J. McBride**, George Sanderson, Rebecca M. Corrigan and Steven P. Armes, “Arginine-functional Methacrylic Block Copolymer Nanoparticles: Synthesis, Characterization and Adsorption onto a Model Planar Substrate”, *accepted by Biomacromolecules*.

Conference Talks

1. American Chemical Society Conference, Chicago, August 2022
2. 36th European Colloid & Interface Society Conference, Chania, September 2022
3. American Chemical Society Conference, San Francisco, August 2023
4. International Symposium on Polyelectrolytes, Prague, September 2023

Conference Posters

1. Bordeaux Polymer Conference, Bordeaux, June 2022
2. Young Researchers Meeting, Nottingham, July 2022
3. Young Researchers Meeting, Warwick, June 2023

Abstract

This Thesis uses reversible addition-fragmentation chain transfer (RAFT) polymerisation to develop new aqueous dispersion polymerisation formulations in either salty or acidic aqueous media. A suitable steric stabiliser is chain-extended with a second block, which becomes insoluble at a critical degree of polymerisation (DP). Hence the resulting amphiphilic diblock copolymer chains self-assemble to form spherical nanoparticles via polymerisation-induced self-assembly (PISA), which ensures a low-viscosity colloidal dispersion. To identify suitable steric stabilisers and core-forming blocks for the high (or low) salt formulations studied in Chapters 2 to 5, various hydrophilic homopolymers were subjected to aqueous solubility tests. This involved attempted dissolution of each homopolymer in a series of known concentrations of ammonium sulfate, thus identifying the minimum salt concentration required for their insolubility. Various cationic, anionic, zwitterionic and non-ionic stabilisers proved to be suitable water-soluble precursors for chain extension with acrylamide-based core-forming blocks. Formulations include poly(2-(acryloyloxy)ethyl trimethylammonium chloride)–poly(*N*,*N*-dimethylacrylamide) (PATAC−PDMAC), poly(2-(methacryloyloxy)ethyl phosphorylcholine−poly(*N*,*N*-dimethylacrylamide) (PMPC−PDMAC), poly(sodium acrylate)–polyacrylamide (PNaAc−PAM), poly(2-hydroxyethyl acrylamide)−poly(*N*-acryloylmorpholine) (PHEAC−PNAM) in the presence of added salt and poly(2-acrylamido-2-methylpropanesulfonic acid, sodium salt)−poly(2-carboxyethyl acrylate) (PAMPS−PCEA) at pH 2.0. In this latter case, the PCEA core block is insoluble at this pH owing to protonation of its pendent carboxylic acid groups.

Dilution of the first four colloidal dispersions with deionised water or increasing the pH of the latter formulation leads to molecular dissolution to produce a viscous solution. If the core-forming block is sufficiently long, transparent free-standing gels can be obtained. Such dilution- or pH-triggered viscosity modification has potential applications for home and personal care products or as a dewatering flocculant in oilfield applications. In this Thesis, various synthesis parameters are optimised with the aim of maximising this thickening effect, including the upper limits solids content, final monomer conversion, chain extension efficiency and core-forming block DP. Furthermore, experimental reproducibility was optimised by judicious selection of the initiator type, reaction temperature and solution pH. For example, $PMPC_{139}$-$PDMAC_{6000}$ particles were prepared at 20% w/w solids using a potassium persulfate/ascorbic acid redox initiator at 30°C in the presence of 2.0 M ammonium sulfate.

These diblock copolymer particles were characterised using dynamic light scattering (DLS), laser diffraction, electrophoretic mobility and optical microscopy. Their mean diameter is significantly larger than those typically reported in the PISA literature. This is partly because of the relatively high DP targeted for the core-forming block but also because the particle cores are not fully dehydrated. ^{1}H NMR spectroscopy was used to calculate monomer conversions and to assess the relative degree of hydration of the core-forming block at various salt concentrations. The diblock copolymer chains were also analysed by gel permeation chromatography (GPC) using a pH 7.0 TRIZMA buffer eluent combined with a refractive index detector. This technique indicated high chain extension efficiencies but broad molecular weight distributions (M_w/M_n ~ 1.5-2.5). The latter is consistent with the relatively low [RAFT agent]/[initiator] molar ratios required for such formulations. In addition, static light scattering in aqueous eluent was used to determine absolute M_w values of up to 2.5 MDa for the 'low salt' PHEAC−PNAM formulation. Finally, rotational rheometry was used to determine the solution viscosity of the initial low-viscosity dispersions and highly viscous solutions obtained after either lowering the salt concentration or raising the solution pH. In this context, it is worth emphasising that relatively high dispersities are beneficial for maximising the solution viscosity, because this parameter is much more sensitive to M_w than M_n.

Ultimately, the scope for potential commercial applications will depend on the relative cost and reproducibility of these aqueous PISA syntheses. Thus, cost-effective monomers such as acrylic acid, acrylamide and acrylonitrile were investigated in this work.

List of Abbreviations

ACVA	4,4'-Azobis(4-cyanopentanoic acid)
ADH	Adipic acid dihydrazide
AIBA	2,2'-Azobisisobutyramidinium chloride
ALAM	Allyl acrylamide
Alcomer-115	Industrial UHMW anionic polyacrylamide powder
APS	Ammonium persulfate
AsAc	Ascorbic acid
ATRP	Atom transfer radical polymerisation
BASF	Badische Anilin- und Sodafabrik
BDMAT	S-butyl-S′-(α,α′-dimethyl-α″-acetic acid)trithio-carbonate
B-FF7	Disodium 2-hydroxy-2-sulfinatoacetate
BM1433	4-(((2-(carboxyethyl)thio)carbonothioyl)thio)-4-cyanopentanoic acid
CCC	Critical coagulation concentration
CMC	Critical micelle concentration
CTA	Chain transfer agent
Đ	Dispersity
DLVO	Theory to account for the coagulation of lyophobic colloids proposed by B. Derjaguin, L. Landau, E. Verwey and T. Overbeek.
DMF	Dimethylformamide
DP	Degree of polymerisation
D_v	Volume-average diameter
D_z	Z-average hydrodynamic diameter
EDA	Ethylenediamine
EDL	Electrical double layer
EGDA	Ethylene glycol diacrylate
EGDMA	Ethylene glycol dimethacrylate
ESR	Electron spin resonanc
E_{ster}	Steric repulsion
E_{VdW}	van der Waals attraction
FRP	Free radical polymerisation
GPC	Gel permeation chromatography (see also SEC)
IEP	Isoelectric point
IR	Infrared
IUPAC	International Union of Pure and Applied Chemistry
k	Rate constant
KPS	Potassium persulfate
k_BT	Thermal energy
LAM	Less-activated monomer
LAP	Living anionic polymerisation
LCST	Lower critical solution temperature
MALLS	Multi-angle laser light scattering
MAM	More-activated monomer
MBS	Sodium metabisulfite
M_n	Number-average molecular weight
M_v	Viscosity-average molecular weight
M_w	Weight-average molecular weight

MW	Molecular weight
MWD	Molecular weight distribution
NG-ELS	Next generation electrophoretic light scattering
NMP	Nitroxide-mediated polymerisation
NMR	Nuclear magnetic resonance
OM	Optical microscopy
P	Packing parameter
P(2-HBA)	Poly(2-hydroxybutyl acrylate)
P(3-HPMA)	Poly(3-hydroxypropyl methacrylate)
PAA	Poly(acrylic acid)
PAM	Polyacrylamide
PAMPS	Poly(2-acrylamido-2-methylpropanesulfonic acid, sodium salt)
PATAC	Poly(2-(acryloyloxyethyl)trimethylammonium chloride)
PB	Polybutadiene
PBS	Phosphate buffered saline
PBzDA	Poly(2-(acryloxyethyl)benzyldimethylammonium chloride)
PBzDMA	Poly(2-(methacryloxyethyl)benzyldimethylammonium chloride)
PBzMA	Poly(benzyl methacrylate)
PCEA	Poly(2-carboxyethyl acrylate)
PCMAM	Poly(*N*-cyanomethyl acrylamide)
PDAAM	Poly(diacetone acrylamide)
PDEA	Poly(2-(diethylamino)ethyl methacrylate)
PDEAM	Poly(*N,N*-diethylacrylamide)
PDEGMA	Poly(di(ethylene glycol)methyl ether methacrylate)
PDIPEMA	Poly(2-(diisopropylamino)ethyl methacrylate)
PDMAC	Poly(*N,N*-dimethylacrylamide)
PDMS	Polydimethylsiloxane
PE	Polyethylene
PEG	Poly(ethylene glycol) (see also PEO)
PEO	Poly(ethylene oxide) (see also PEG)
PETTC	4-cyano-4-(2-phenylethanesulfanylthiocarbonyl)sulfanylpentanoic acid
PGMA	Poly(glycerol monomethacrylate)
PHBA	Poly(4-hydroxybutyl acrylate)
PHBMA	Poly(2-hydroxybutyl methacrylate)
PHEA	Poly(2-hydroxyethyl acrylate)
PHEAC	Poly(2-hydroxyethyl acrylamide)
PHEMA	Poly(2-hydroxyethyl methacrylate)
PHEMAC	Poly(2-hydroxyethyl methacrylamide)
PHMMAC	Poly(hydroxymethyl methacrylamide)
PHPMA	Poly(2-hydroxypropyl methacrylate)
PHPMAC	Poly(*N*-(2-hydroxypropyl) methacrylamide)
PIB	Polyisobutylene
PiBuOMAM	Poly(isobutoxymethyl acrylamide)
PISA	Polymerisation-induced self-assembly
PMAA	Poly(methacrylic acid)
PMEA	Poly(2-methoxyethyl acrylate)
PMEMA	Poly(2-*N*-morpholinoethyl methacrylate)
PMETAC	Poly(2-(methacryloyloxyethyl)trimethylammonium chloride)

PMMA	Poly(methyl methacrylate)
PMPC	Poly(2-(methacryloyloxy)ethyl phosphorylcholine)
PNaAc	Poly(sodium acrylate)
PNAEP	Poly(2-(*N*-acryloyloxy)ethyl pyrrolidone)
PNAM	Poly(*N*-acryloylmorpholine)
PNIPAM	Poly(*N*-isopropylacrylamide)
PNMEP	Poly(*N*-2-(methacryloyloxy)ethyl pyrrolidone)
PS	Polystyrene
PSEMA	Poly(2-hydroxyethyl methacrylate, monosuccinic acid ester)
PTHFA	Poly(tetrahydrofurfuryl acrylate)
PVAC	Poly(vinyl acetate)
R	Rate of reaction
RAFT	Reversible addition-fragmentation chain transfer
RDRP	Reversible-deactivation radical polymerisation
R_g	Radius of gyration
SAXS	Small angle X-ray scattering
SEC	Size exclusion chromatography (see also GPC)
SEM	Scanning electron microscope
SFS	Sodium formaldehyde sulfoxylate
SLS	Static light scattering
$t_{1/2}$	Ten hour half life temperature
T-21S	2-Ethylhexanoyl tert-butyl peroxide
TBHP	t-Butyl hydroperoxide
TEM	Transmission electron microscopy
THF	Tetrahydrofuran
TMEDA	*N,N,N′,N′*-Tetramethylethylenediamine
TRIZMA	Tris(hydroxymethyl)aminomethane
UCST	Upper critical solution temperature
UHMW	Ultra-high molecular weight
UV	Ultraviolet
VA-044	2,2'-Azobis(2-(2-imidazolin-2-yl)propane)dihydrochloride
VA-50	2,2'-Azobis(2-methylpropionamidine)dihydrochloride
ΔG_{mix}	Gibbs free energy of mixing
ΔH_{mix}	Enthalpy of mixing
ΔS_{mix}	Entropy of mixing
ε	Molar extinction coefficient
ε_{max}	Kinetic energy barrier
ε_{min}	Potential energy minimum
η	Viscosity
χ_{AB}	Flory-Huggins AB interaction parameter

Table of Contents

Chapter 1: Introduction

1.1 Polymer Chemistry

1.1.1 General Concepts

Over a century ago, Staudinger hypothesised the existence of high molecular weight (MW) 'macromolecules' comprising long chains with many covalently-linked repeat units.[1] This new concept did not become widely accepted until Carothers provided experimental evidence for the synthesis and characterisation of various polymers in the 1930s.[2] Since these pioneering studies, many more synthetic polymers have been developed for a range of applications, including car tyres, household appliances, packaging, contact lenses, textiles and as bank notes. It has been estimated that more than nine billion tonnes of such plastics have been manufactured over the past 70 years.[3] Recently, the environmental impact and end-of-life persistence of polymers has come under increasing scrutiny and is now subject to new legislation.[4]

Carothers distinguished between addition and condensation polymers on the basis of their differing chemical structures. Thus, polymers formed from vinyl monomers were denoted addition polymers, whereas polyesters formed from diacids and diols were termed condensation polymers since a small molecule is eliminated when forming each repeat unit. However, modern nomenclature classifies polymers as either chain or step polymers based on their differing polymerisation mechanisms. Generally addition polymers are equivalent to chain polymers and condensation polymers are essentially the same as step polymers, but with some notable exceptions. For example, polyurethanes are structurally similar to condensation polymers such as polyesters and polyamides, but no small molecules are eliminated during their synthesis. Nonetheless, mechanistic insight means that polyurethanes are considered to be step polymers.[5] Chain-growth polymerisations usually involve the reaction between a vinyl (or cyclic) monomer and an initiator or catalyst, with regeneration of the active site on the polymer chain-ends at the end of each growth step.[6]

The average number of monomer repeat units per polymer chain is defined as the degree of polymerisation (DP).[7] The number-average molecular weight (M_n) is biased towards lower molecular weight species and is defined according to **Equation 1.1**, where M_i is a given molecular weight and n_i is the number of chains possessing that weight. The weight-average molecular weight (M_w) is biased towards higher molecular weight species and is defined according to **Equation 1.2**. Gel permeation chromatography (GPC) can be used to assess the whole molecular weight distribution (MWD) as well as M_n and M_w values. Although the use of a refractive index detector requires calibration standards to be used, which assumes variation in elution time depends only on mass, ignoring any chemical differences. Alternatively, colligative properties or end-group analysis via nuclear magnetic resonance (NMR) spectroscopy or osmometry can be used to determine M_n, whereas static light scattering (SLS) or small-angle X-ray scattering (SAXS) can be used to determine M_w.[5]

$$M_n = \frac{\Sigma n_i M_i}{\Sigma n_i} \quad \textbf{(1.1)} \qquad\qquad M_w = \frac{\Sigma n_i {M_i}^2}{\Sigma n_i M_i} \quad \textbf{(1.2)}$$

The polydispersity index, now known as the dispersity (Đ), is obtained by dividing the weight-average molecular weight by the number-average molecular weight, as shown in **Equation 1.3**. This parameter provides an indication of the breadth of the MWD. Đ is always greater than unity because $M_w > M_n$. A dispersity value which is close to unity indicates a relatively narrow MWD whereas larger Đ values indicate much broader distributions.[8]

$$Đ = \frac{M_w}{M_n} \quad \textbf{(1.3)}$$

1.1.2 Polymer Architectures

The monomer repeat units (A, B) on a linear polymer chain can be varied according to the schematic structures shown in **Figure 1.1**. The structure of a homopolymer is shown in (a) and four types of copolymers, which comprise two different monomers, are shown in (b-e). Random copolymers comprise chains with a random sequence of the A and B repeat units. An alternating copolymer has a strictly alternating sequence of these two monomers, which are present in an equimolar ratio. Gradient copolymers exhibit a gradual change in composition from one monomer to the other along the chain. Block copolymers can be formed by sequential addition of one monomer followed by another. It is also possible to incorporate other monomers into a linear polymer, which will form alternative sequences of the repeat units along the chain.[9,10]

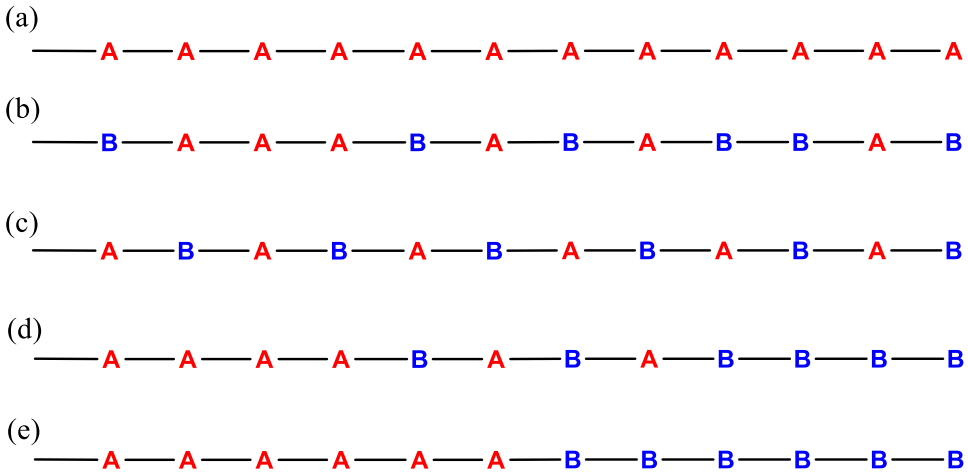

Figure 1.1 Schematic representations of various linear copolymers where A and B represent different monomers: (a) homopolymer, (b) random copolymer; (c) alternating copolymer; (d) gradient copolymer; (e) block copolymer.[7]

It is also possible to form non-linear polymers by using either bifunctional or multifunctional monomers, via chain transfer to polymer, or via reaction with a di(meth)acrylate impurity.[11–13] In this case, either branched copolymers or gel networks are formed.[10,14] This Thesis will consider the formation of homopolymers, linear diblock copolymers and lightly branched polymers.

1.2 Polymerisation Techniques

1.2.1 Free Radical Polymerisation (FRP)

Free radical polymerisation is an example of a chain-growth polymerisation where high molecular weight polymers can be obtained even at low monomer conversions. Many vinyl monomers are suitable for this technique, for example the chemical structure of (meth)acrylates and (meth)acrylamides; shown in **Figure 1.2**. FRP is best performed in the absence of air, because oxygen forms a resonance-stabilised peroxy radical product that either retards or inhibits the polymerisation.[15] However, FRP is not adversely affected when using protic solvents such as water and minimal purification of solvents and monomers is required. It is tolerant of a wide range of vinyl monomers, but potential side reactions should be considered.[16]

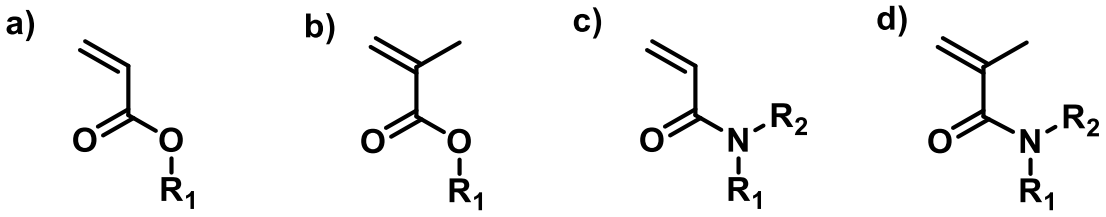

Figure 1.2 Common vinyl monomers where R_1 and R_2 represent substituent groups: (a) acrylate, (b) methacrylate, (c) acrylamide, (d) methacrylamide.

The FRP mechanism is shown in **Figure 1.3** and includes four steps: initiation, propagation, chain transfer and termination. The decomposition of the initiator, where radical formation usually occurs via homolytic cleavage, is often facilitated by heating or irradiation. This step is usually slow compared to the subsequent steps where the chain end is now a highly reactive radical.[17]. It is well-known that most FRP syntheses usually suffer from chain transfer side reactions. Chain transfer from a polymer radical to either solvent or monomer leads to a reduction in M_n, whereas chain transfer to polymer usually leads to branched polymers and hence a higher M_w.[18]

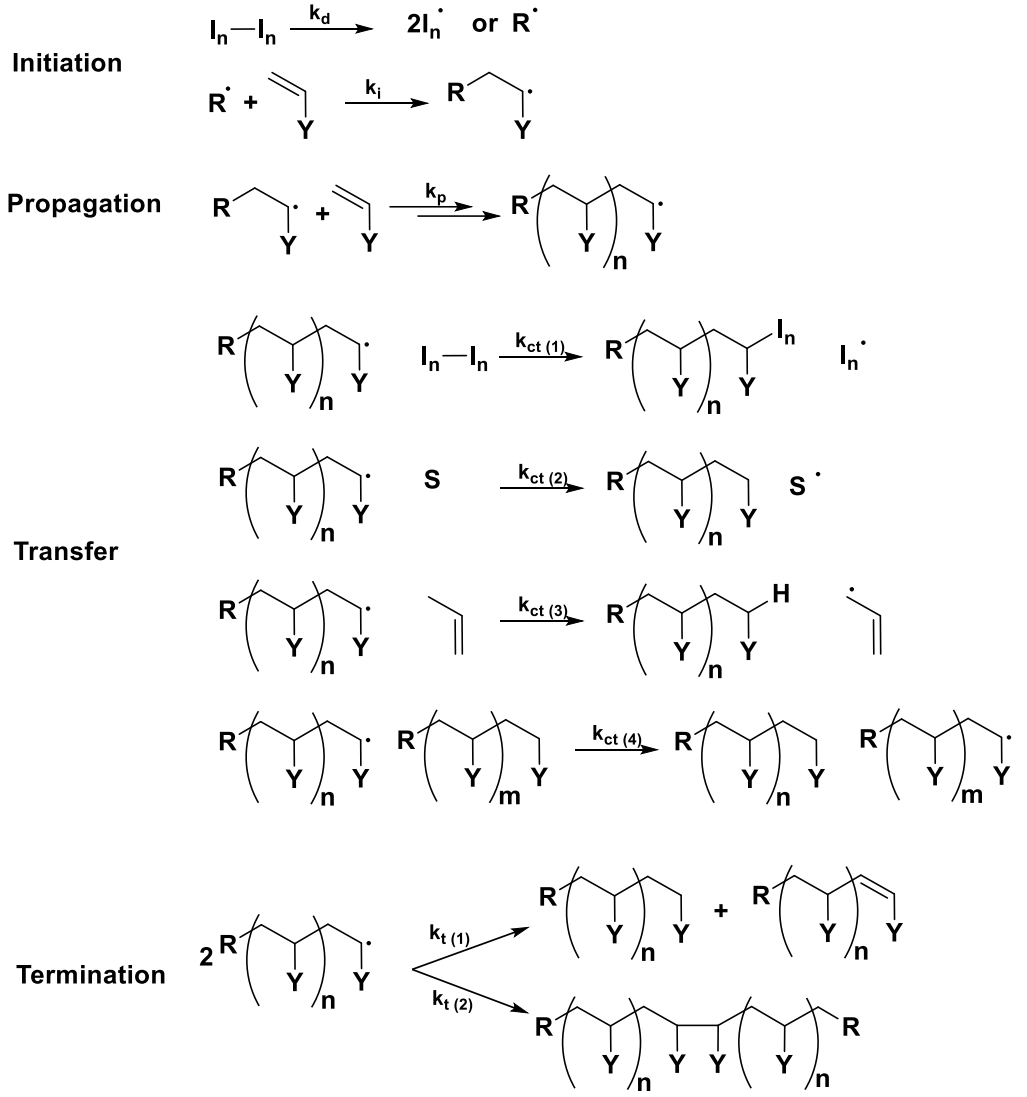

Figure 1.3 Mechanism for free radical polymerisation (FRP) showing decomposition of I_n-I_n into two radicals, initial reaction with monomer, then propagation. There are four possible transfer reactions; 1) to initiator, 2) to solvent, 3) to monomer, 4) to polymer. There are two modes of termination; 1) disproportionation, 2) combination. Rate constants are also included for each reaction.[16,19]

The structural arrangement of repeat units in the above mechanism shows substituents located isoregically, on alternating backbone carbon atoms.[5] Propagation could theoretically occur via either head-to-head (H-H) or head-to-tail (H-T) monomer addition, but the latter is overwhelmingly predominant for both steric and resonance reasons. More specifically, the α-carbon atom of a vinyl group is more sterically hindered than the β-carbon atom. Moreover,

the propagating radical formed on the α-carbon atom after radical addition to the β-carbon atom is stabilised by the Y substituent group, see **Figure 1.4**.

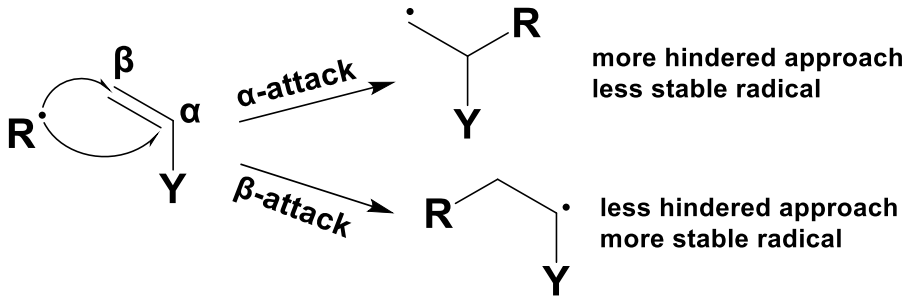

Figure 1.4 Schematic representation of radical addition to either the α-carbon or β-carbon, which results in head-to-head (H-H) or head-to-tail (H-T) addition, respectively. In practice, the latter is strongly preferred.

The rate constant for the decomposition of the initiator (k_d) is several orders of magnitude lower than the rate constants for initiation and propagation, so the initial formation of radicals is the rate-limiting step for FRP.[16] High MW chains are formed at low monomer conversions and a high initiator concentration will result in more shorter polymer chains.

Commonly used thermal initiators include peroxides and azo compounds. When the central bond is cleaved, this typically leads to the formation of two identical radicals via homolytic fission.[20] Thermal initiators can be classified by their ten-hour half-life temperature ($t_{1/2}$) which is the temperature at which half of the initiator decomposes to form radicals within ten hours. To ensure a constant supply of free radicals during the polymerisation, the reaction temperature is usually set to be equal to $t_{1/2}$, this is calculated from k_d, as shown in **Equation 1.4**.[5,10]

$$t_{1/2} = \frac{ln(2)}{k_d} \qquad \textbf{(1.4)}$$

Water-soluble thermal initiators include: *2,2'*-azobis(2-(2-imidazolin-2-yl)propane dihydro-chloride (VA-044: $t_{1/2}$ = 44°C), *2,2'*-azobisisobutyramidinium chloride (AIBA: $t_{1/2}$ = 56°C) and *4,4*-azobis(*4*-cyanovaleric acid) (ACVA: $t_{1/2}$ = 70°C), as shown in **Figure 1.5**.

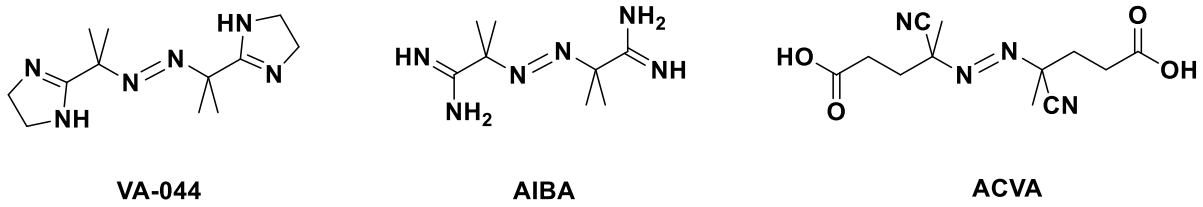

Figure 1.5 Structures of three water-soluble azo-initiators: 2,2'-azobis(2-(2-imidazolin-2-yl) propane dihydrochloride (VA-044), 2,2'-azobisisobutyramidinium chloride (AIBA) and 4,4-azobis(4-cyanovaleric acid) (ACVA).

In principle, polymer radicals may also react with initiator, solvent, monomer, or dormant (terminated) polymer chains via chain transfer reactions, which can cause a reduction in polymer chain length and an increase in their dispersity. In some monomers, a diacrylate or dimethacrylate impurity may exist from when the monomer was prepared, which will cause branching in the polymer structure.[21] For example, relatively low levels of ethylene glycol dimethacrylate (EGDMA) impurity in 2-hydroxyethyl methacrylate (HEMA) monomer can have a significant impact on the molecular weight and solubility of the resulting poly(2-hydroxyethyl methacrylate (PHEMA).[13,22]

However, because radicals are preserved in such side reactions, the overall polymerisation kinetics remain the same. The respective rates of initiation, propagation and termination are denoted as R_i, R_p and R_t. The rate of thermal decomposition of the initiator, R_d, is given in **Equation 1.5,** where f is the initiator efficiency and $[I]$ is the initiator concentration. This step is relatively slow and is hence the rate-limiting step for the overall rate of polymerisation (R_{poly}). Moreover, the rate of decomposition (R_d) is approximately equal to R_i.

$$R_d = 2fk_d[I] \approx R_i \qquad \textbf{(1.5)}$$

When the initiator efficiency is less than unity, not all the generated radicals react with monomer to form a polymer chain. Instead, a minor proportion of the radicals become trapped for a short period within a solvent cage, which increases the probability of their recombination. This is known as the 'cage effect' and results in a reduction in the initiator efficiency, f, which usually varies between 0.30 and 0.80.[9]

Electron spin resonance (ESR) spectroscopy has been used to determine the polymer radical concentration, but in practice this technique is not widely available. The rate of polymerisation (R_{poly}) is equivalent to R_p, because each propagation has the same rate constant and it is the sum of them. Furthermore, if the steady-state approximation is valid, the rate of initiation (R_i) is equal to the rate of termination (R_t), so the polymer radical concentration can be eliminated from the rate equation.[9] The rate equations for propagation and termination are given by **Equations 1.6** and **1.7** below.

$$R_p = k_p[M][M\bullet] \approx R_{poly} \qquad \textbf{(1.6)}$$

$$R_t = 2k_t[M\bullet]^2 \approx R_i \qquad \textbf{(1.7)}$$

Here [M] is the monomer concentration, [M•] denotes the concentration of all radicals, k_p is the rate constant for propagation and k_t is the rate constant for termination. Termination via disproportionation results in two polymer chains; one chain-end is saturated and the other has an unsaturated group that is capable of further reaction. In contrast, termination by combination results in just one polymer chain, whose MW is the sum of the two reacting polymer radicals. While there are two pathways for termination, most polymer radicals tend to undergo termination predominantly by combination.[5] It can be challenging to determine the ratio between the rate constants for disproportionation ($k_{t\,(1)}$) and combination ($k_{t\,(2)}$) owing to the influence of chain transfer reactions.[5] Methods such as mass spectrometry and end-group analysis are used to evaluate $k_{t\,(1)}$ / $k_{t\,(2)}$.[23] The proportion of polymer radicals that undergo

disproportionation increases when the propagating radical is sterically hindered or has a β-hydrogen available for transfer. For example, methyl acrylate appears to undergo termination exclusively by combination at 25°C while polystyrene has been reported to have a $k_{t\,(1)} / k_{t\,(2)}$ ratio of ≈ 0.15.[24,25] In contrast, a $k_{t\,(1)} / k_{t(2)}$ ratio of approximately unity has been observed for methyl methacrylate at 90°C.[5,23]

Combining the rate equations for propagation and termination enables derivation of an expression for R_{poly}, which eliminates the polymer radical concentration term, see **Equation 1.8.**

$$R_{poly} = k_p[M]\sqrt{\frac{R_i}{2k_t}} \qquad \textbf{(1.8)}$$

Combining **Equation 1.8** with the rate equation for initiation (**Equation 1.5**) leads to **Equation 1.9**.

$$R_{poly} = k_p[M]\sqrt{\frac{fk_d[I]}{k_t}} \qquad \textbf{(1.9)}$$

Derivation of **Equation 1.9** requires two assumptions: (i) the steady-state approximation (i.e. $R_i = R_t$) and (ii) that the number of monomer units consumed during initiation is negligible compared to that consumed during propagation. Inspecting **Equation 1.9**, faster rates of polymerisation can be achieved by increasing [*M*] and [*I*]. The relatively slow rate of initiation (owing to the low k_d value) plus chain termination leads to a relatively broad MWD (typically Đ = 1.5 – 3.0), which is characteristic of polymers prepared by FRP. Moreover, significantly shorter chains are formed under monomer-starved conditions, which also contributes to a broader MWD.[5,9]

The kinetic chain length (ν) is defined as the average number of monomers polymerised for each radical that initiates a polymer chain.[26] This quantity is equal to the ratio of propagating

to initiating (or terminating) rates – that is R_p/R_i.[5] The rate laws can be combined to give ν, see **Equation 1.10**.

$$\nu = \frac{R_p}{R_t} = \frac{R_p}{R_i} = \frac{k_p[M]}{2\sqrt{fk_d k_t[I]}} \qquad \textbf{(1.10)}$$

$$\nu \propto \frac{[M]}{\sqrt{[I]}} \qquad \textbf{(1.11)}$$

Equation 1.11 shows ν is proportional to the monomer concentration [*M*] and has an inverse square root dependence on the initiator concentration [*I*]. The degree of polymerisation (DP) is equivalent to 2ν for disproportionation and ν for combination.

In principle, low-temperature polymerisations can be conducted using either redox initiators or photoinitiators. The early history of redox polymerisation has been described by Bacon.[27] Baxendale and co-workers described initiation of vinyl polymerisations using a hydrogen peroxide-ferrous salt system.[28] More recently, Lamb and co-workers reported the use of *t*-butyl hydroperoxide (TBHP) combined with reducing agents such as sodium formaldehyde sulfoxylate (SFS), sodium metabisulfite (MBS) or ascorbic acid (AsAc).[29]

It is not possible to make well-defined diblock copolymers by FRP. If two (or more) vinyl monomers are present in the reaction mixture, a statistical copolymer will be obtained whose structure is governed by the respective relative comonomer reactivity ratios. Moreover, the mean lifetime of an individual growing polymer radical is far too short ($< 10^{-4}$ s) to allow sequential monomer addition.[15] Instead, the synthesis of diblock copolymers requires a polymerisation mechanism that confers much greater control. Well-defined block copolymers can be prepared using (pseudo-)living polymerisation methods, as outlined in the following sections.

1.2.2 Living Anionic Polymerisation (LAP)

In order to synthesise polymers with narrow MWDs, the conventional chain-growth polymerisation mechanism must be modified to prevent intrinsic termination and substantially extend the lifetime of each propagating chain. Such a polymerisation is said to be 'living' because polymerisation continues indefinitely if further monomer is added to the reaction mixture. [30,31] The IUPAC definition for a living polymerisation is 'a chain-growth polymerisation from which chain transfer and chain termination are absent'.[32] Szwarc was the first to report the concept of 'living polymers' in 1956.[33] This seminal study involved the living anionic polymerisation (LAP) of styrene using sodium naphthalenide initiator in anhydrous tetrahydrofuran (**Figure 1.6**) with this system exhibiting a negligible tendency to undergo termination. An anionic adduct (active centre) forms when the initiator adds to styrene monomer, which is then able to react with further monomer to produce polystyrene chains with carbanion end-groups.[33]

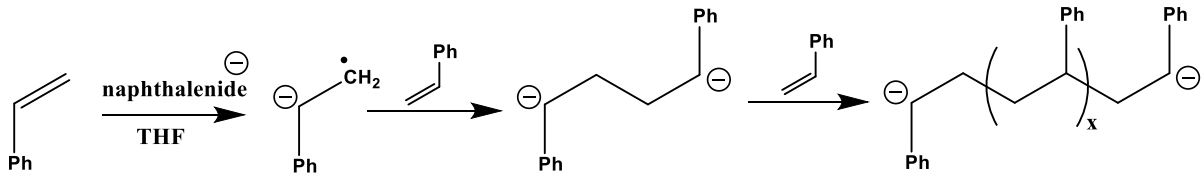

Figure 1.6 LAP of styrene to form polystyrene, using anionic naphthalenide anions as the electron transfer agent.[33]

Initiation is effectively instantaneous for LAP, resulting in immediate growth of all polymer chains at approximately the same rate. The anionic chain-ends cause chains to repel each other; which suppresses any intrinsic termination mechanism. These conditions lead to a relatively narrow MWD polymers compared to those obtained by FRP, as shown in **Figure 1.7**.

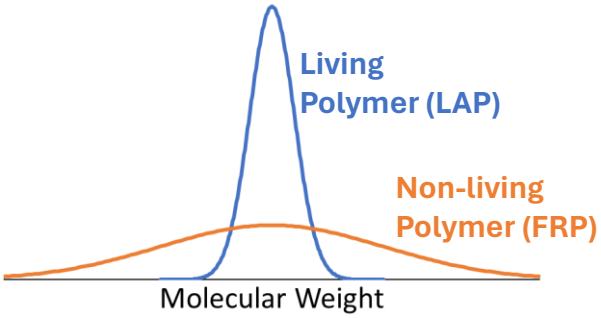

Figure 1.7 Schematic representation of MWDs exhibited by a living polymer (LAP) and a non-living polymer (FRP).

Due to the uniform simultaneous growth of polymer chains, living polymers exhibit a linear evolution of molecular weight with monomer conversion (**Figure 1.8)**. Furthermore, even after polymerisation is complete, the living character of the chains is retained, enabling the synthesis of well-defined block copolymers via sequential monomer addition while maintaining a narrow MWD (e.g. Đ = 1.10).[34,35]

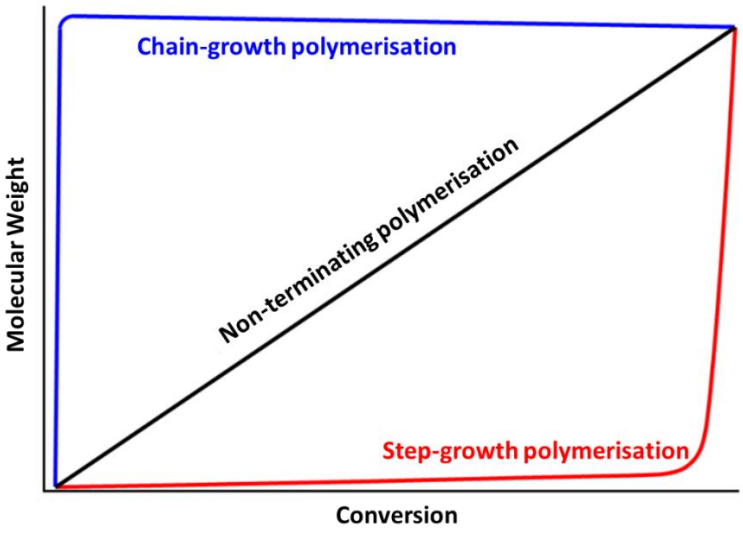

Figure 1.8 Molecular weight evolution against monomer conversion for a typical chain-growth polymerisation, step-growth polymerisation and a non-terminating polymerisation.

During LAP, the rate of initiation is much faster than the rate of propagation. Thus, the rate of polymerisation is simply equal to the rate of propagation because the latter is the rate-limiting step (**Equation 1.12**). The kinetic chain length can be determined at any given

conversion using **Equation 1.13**, which is derived from the integrated form of the rate equation. The complete absence of transfer reactions and termination is assumed when deriving such formulae.

$$R_p = k_p[P_n^-][M] \qquad \textbf{(1.12)}$$

$$\nu = \frac{[M]_0 - [M]}{[I]_0} \qquad \textbf{(1.13)}$$

Here, R_p is the rate of polymerisation, k_p is the propagation rate constant, $[P_n^-]$ is the concentration of propagating anionic chains, $[M]$ is the monomer concentration at any given time, ν is the kinetic chain length, $[M]_0$ is the initial monomer concentration and $[I]_0$ is the initiator concentration. LAP enables the facile production of near-monodisperse homopolymers with pre-determined DPs by simply adjusting the $[M]_0$ / $[I]_0$ molar ratio, as summarised in **Equation 1.14**.

$$DP \approx \frac{Moles\ of\ Monomer}{Moles\ of\ Initiator} \qquad \textbf{(1.14)}$$

LAP suffers from some practical limitations compared to conventional FRP. It is restricted to a few non-functional vinyl monomers that are compatible with a highly nucleophilic initiator (e.g. styrene, isoprene, butadiene etc.). It is also necessary to rigorously exclude protic impurities (e.g. water) from the reaction solution, so this also restricts the choice of solvent (e.g. THF, toluene or benzene). However, one benefit of this technique is that the living polymer chains can be capped by addition of a suitable reagent such as methanol.

1.2.3 Reversible-Deactivation Radical Polymerisation (RDRP)

In the 1990s several strategies were developed for suppressing the termination of polymer radicals. These techniques were initially termed *living radical polymerisations*, but because termination and chain-transfer reactions are still possible, they were subsequently renamed

controlled radical polymerisations. In 2009, the term *reversible-deactivation radical polymerisation (RDRP)* was recommended by IUPAC which more accurately captures the modus operandi of the polymerisation mechanisms.[10,36]

The basic principle of RDRP is to reversibly trap or otherwise temporarily deactivate chain radicals in order to suppress termination, thus establishing pseudo-living character. Techniques generally involve either reversible end-capping of the polymer radicals or rapid reversible chain transfer between an end-capped polymer radical and a polymer radical. Each chain grows with approximately equal probability in short bursts of activity, which results in a relatively narrow Poisson MWD (Đ = 1.10-1.20).[10] Like other radical polymerisation methods, RDRP requires an inert atmosphere to avoid oxygen inhibition. However, the conditions are much less demanding than those required for LAP because protic impurities are not detrimental to RDRP.[32,37] Alike LAP, the rate limiting step for RDRP is propagation because initiation should be very quick to allow all polymer radical chains to grow for the same length of time.

RDRP is characterised by a linear evolution in molecular weight with conversion, which is similar to that for a non-terminating polymerisation, see **Figure 1.8**. The three main RDRP techniques are nitroxide-mediated polymerisation (NMP), atom transfer radical polymerisation (ATRP) and reversible addition-fragmentation chain transfer (RAFT) polymerisation. NMP works very effectively for styrene and acrylates, but is incompatible with methacrylic monomers and often requires prolonged heating to achieve high conversions. On the other hand, RAFT and ATRP are more versatile and easier to conduct at lower temperatures with faster reaction kinetics.[38] Conventional ATRP in aqueous solution is complicated by several factors that can lead to premature termination, so certain modifications are often made to such formulations. The range of functional vinyl monomers that are amenable to RAFT polymerisation is relatively broad and includes both (meth)acrylates and (meth)acrylamides. This polymerisation method is the subject of this Thesis and is discussed in more detail below.[39]

1.2.4 Reversible Addition-Fragmentation Chain Transfer (RAFT) Polymerisation

RAFT polymerisation was first reported by Chiefari et al. in 1998.[32,40] RAFT polymerisations are based on the principle of rapid reversible transfer between active and dormant polymer chains.[32] Unlike NMP or ATRP, it does not rely on the persistent radical effect, but instead uses degenerative transfer whereby the radical is transferred from the active centre to another species, which alters its reactivity.[41] The RAFT mechanism (**Figure 1.9**) is similar to that of FRP, but the addition of a highly reactive organosulfur-based chain transfer agent (CTA) that fragments during chain transfer leads to pseudo-living character.[10,42–45] This chain transfer agent restricts the number of active polymer radicals that are present at any given time by creating an equilibrium between active and dormant species. All polymer chains have an equal probability to grow as they become successively activated and deactivated while premature termination can be effectively suppressed by judicious choice of the RAFT CTA.[42]

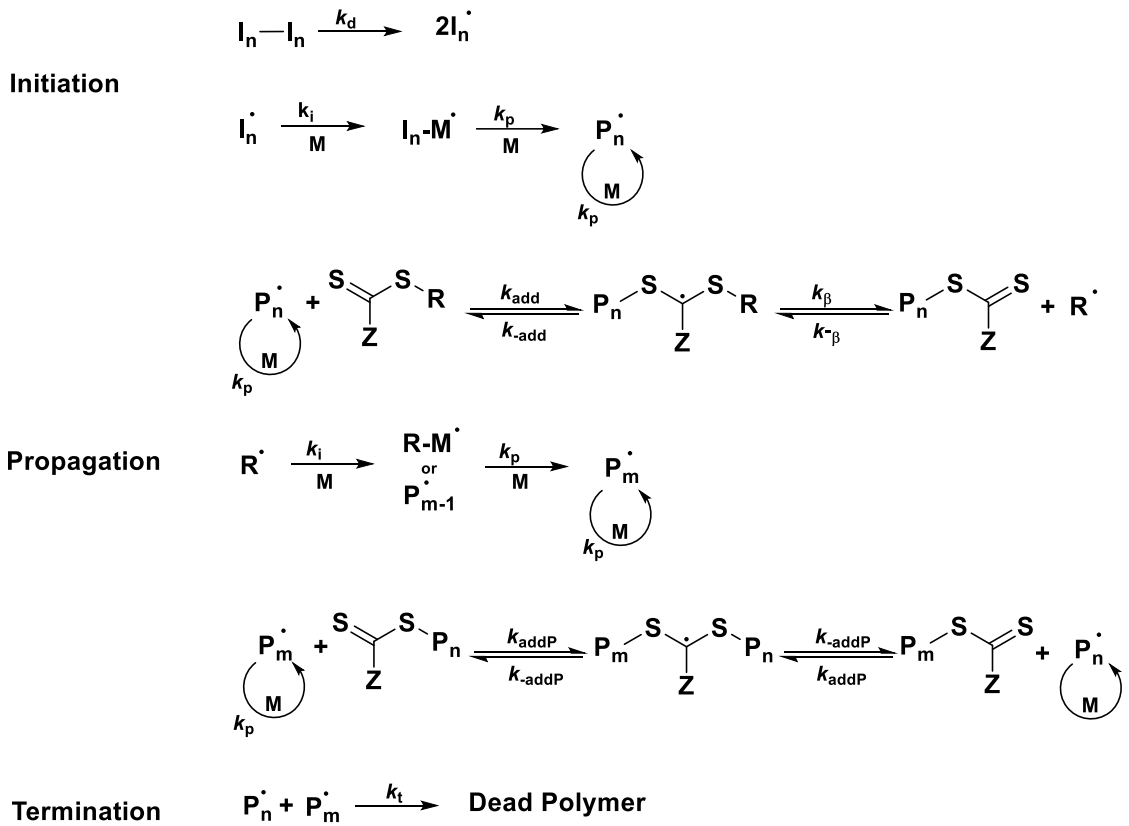

Figure 1.9 Mechanism for reversible addition-fragmentation chain transfer (RAFT) polymerisation as proposed by Rizzardo and co-workers.[42,43]

Most vinyl monomers can be classed as either "more-activated" monomers (MAMs) or "less-activated" monomers (LAMs). MAMs have conjugation between the vinyl double bond and a carbonyl group (e.g. acrylamide), whereas LAMs have no such conjugation (e.g. vinyl acetate). In general, a well-controlled polymerisation of a MAM can be achieved using either dithioesters or trithiocarbonates, whereas poorly controlled polymerisations are usually observed when using either dithiocarbamates or xanthates. For LAMs, the opposite behaviour is observed. In principle, the kinetics of a RAFT polymerisation should be similar to that of FRP, because the overall rate should not be affected by chain transfer side-reactions. However, inhibition prior to polymerisation and retardation during polymerisation are often observed.[45,46] In some cases, this has been attributed to inappropriate selection of the organosulfur RAFT agent, see **Figure 1.10**.[47–49]

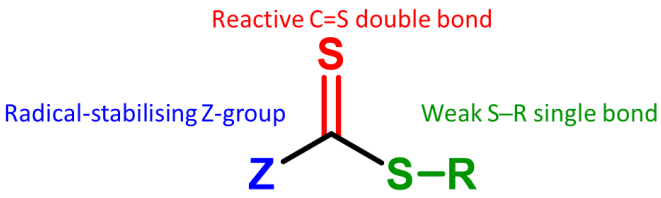

Figure 1.10 General chemical structure of a RAFT chain transfer agent (CTA)

The RAFT CTA enables rapid reversible capping of the active propagating polymer radical (P_n•) to form a dormant radical species. The C=S bond should be highly reactive to enable rapid reaction of the CTA with any P_n•; thus it gives rise to a high rate constant of addition (k_{add}). The Z group on the RAFT CTA must be capable of stabilising this intermediate radical species to reduce the instantaneous concentration of P_n• and hence gain control over the polymerisation. The R group on the RAFT CTA must be a good radical leaving group and the resulting radical (R•) must be capable of re-initiating polymerisation to form new propagating species (P_m•).

Judicious selection of a suitable CTA is required to achieve controlled polymerisations for a specific type of vinyl monomer, some possible Z and R group substituents are shown in **Figure 1.11**.[42,45,46]. Polymerisation of acrylates works best when using RAFT agents that contain no cyano groups, whereas polymerisation of methacrylates is well-controlled when using RAFT agents bearing cyano groups.[42] A more active RAFT agent is required for polymerisation of MAMs, to make the propagating radical more reactive towards polymerisation and a less reactive RAFT agent is required for polymerisation of LAMs in order to destabilise the intermediate radical and favour fragmentation.[46]

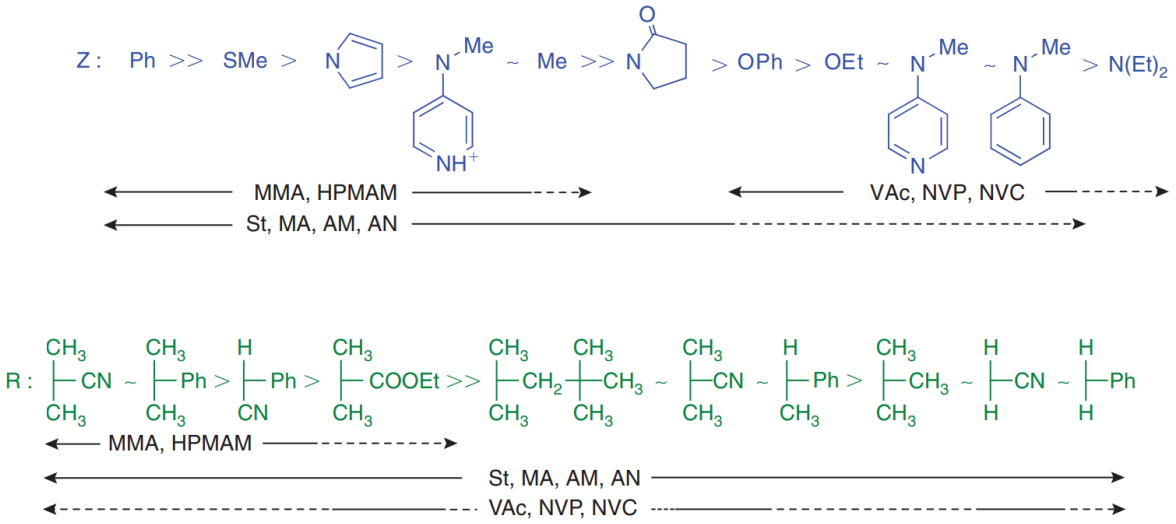

Figure 1.11 Guidelines for RAFT agent selection for the polymerisation of various MAM and LAM monomers: solid lines represent good control, whereas dashed lines indicate partial control. Figure reproduced from Moad and co-workers.[45]

Poorly controlled polymerisation of LAMs is observed when using dithioesters or trithiocarbonates. This is often accompanied by both inhibition and retardation owing to the relatively high stability of the intermediate radical relative to the leaving ability of the propagating radical.[50] Polymerisation of MAMs using dithiocarbamates or xanthates is also ineffective owing to the relatively poor reactivity of such CTAs towards the monomer. However, more controlled polymerisations can be achieved if the heteroatom is part of an aromatic ring or if electron-withdrawing groups are present.[45,46,51] Retardation becomes more

pronounced at higher CTA concentrations when dithiobenzoates are employed, although low-dispersity polymers can still be prepared.[45,51,52] Two plausible explanations have been proposed: side reactions with intermediates[53] or slow fragmentation of the intermediate radical species.[54] Inhibition has been attributed to slow fragmentation of the initial intermediate to afford R•, followed by slow re-initiation of new polymer chains.[55,56]

There are four main classes of RAFT agents: trithiocarbonates, dithiobenzoates, dithiocarbamates and xanthates.[51] The RAFT agents primarily used in this Thesis are trithiocarbonates, which are appropriate for the vinyl monomers of interest. To form an AB diblock copolymer via RAFT polymerisation, the first step is to react the RAFT CTA with the monomer chosen for the first block. When this polymerisation has reached a sufficiently high conversion, the monomer chosen for the second block can be added. Two examples of precursor homopolymers amenable to this protocol are shown in **Figure 1.12**.

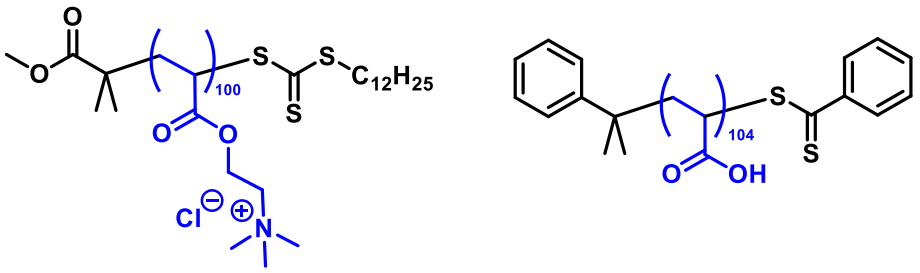

Figure 1.12 Chemical structures of poly(2-(acryloyloxyethyl)trimethylammonium chloride)-*trithiocarbonate* CTA (PATAC$_{100}$-*TTC*) and poly(acrylic acid)-*dithiobenzoate* CTA (PAA$_{104}$-*DB*).[57,58]

RAFT polymerisation enables the synthesis of polymers with narrow MWDs and tunable DPs. It is compatible with a wide range of monomer functionality such as -COOH, -OH, -NR$_2$, without requiring protection group chemistry.[40] However, thiocarbonylthio species can be susceptible to hydrolysis in alkaline solution, while aminolysis can occur in the presence of primary or secondary amines to afford thioamines and thiols.[46] The main disadvantages of

RAFT formulations are the cost, colour, toxicity and malodour conferred by the organosulfur-based CTA.[45,59]

The quantity of initiator used in RAFT polymerisation is employed at a suitable molar ratio relative to the CTA (typically at a CTA/initiator molar ratio of five to ten). Therefore, when targeting high MW polymers the initiator concentration is relatively low. When targeting very high MW polymers, this will ultimately cause the polymerisation to fail (or proceed very slowly) owing to too few radicals being generated within a given timescale. In this case, it may be necessary to increase the initiator concentration to achieve high conversions. However, this will be inevitably accompanied by a reduction in RAFT control over the MWD. A brief inhibition period may occur at the beginning of a polymerisation, as reported by Feldermann and co-workers when using cumyl dithiobenzoate.[60] This phenomenon may be associated with pre-equilibrium of the RAFT agent or perhaps the presence of low levels of impurities (e.g. inhibitor).[5]

Redox initiators for RAFT polymerisations include: (i) *t*-butyl hydroperoxide/ascorbic acid (TBHP/AsAc)[61], (ii) *t*-butyl hydroperoxide/disodium 2-hydroxy-2-sulfinatoacetate (TBHP/B-FF7)[61,62], and (iii) ammonium persulfate/sodium formaldehyde sulfoxylate (APS/SFS); see **Figure 1.13**.[63] Perrier's group compared each of these systems for the aqueous RAFT polymerisation of *N*-acryloylmorpholine (NAM) at 30°C.[64] Employing an oxidising agent / reducing agent molar ratio of unity (or higher) was optimal and the fastest rate of polymerisation was achieved using the TBHP/B-FF7 redox pair. High monomer conversions and relatively low dispersities (Đ > 1.1) were observed at 50°C, even in the presence of oxygen.[64]

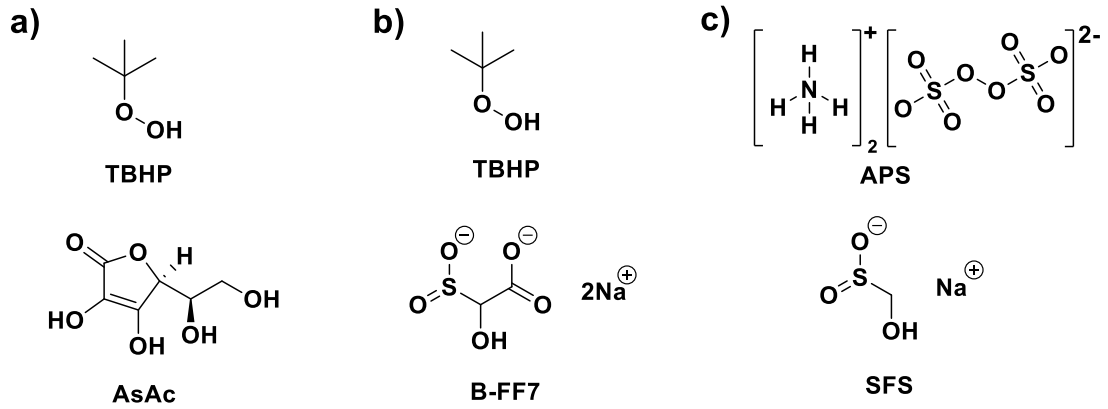

Figure 1.13 Chemical structures of the three redox initiator pairs compared by Perrier et al. for the RAFT polymerisation of NAM at 50°C.[64]

The Armes group has recently reported using a redox initiator comprising AsAc and potassium persulfate (KPS) at 30°C.[65] In this case, the RAFT polymerisation of 2-(*N*-(acryloyloxy)ethyl pyrrolidone) (NAEP) produced low-dispersity homopolymers and high conversions were achieved up to a target DP of 400.[66]

1.3 Self-Assembly

1.3.1 Surfactant Self-Assembly

In this thesis, 'self-assembly' is used to describe the autonomous organisation of components into patterns or structures without external intervention, as defined by Whitesides and Grzybowski.[67] In principle, self-assembly by non-covalent interactions enables the design of materials smaller than the limits of conventional manufacturing. Self-assembly is driven by an unfavourable enthalpy mixing term (ΔH_{mix}) and a relatively small entropy term (ΔS_{mix}).

A surfactant is an amphiphilic molecule that has a hydrophilic head-group and a hydrophobic tail. In aqueous media, the covalent bond that links these two components prevents macroscopic phase separation, so demixing is confined to the nanoscale. The resulting microphase separation leads to the formation of spherical micelles, where the head-groups remain in contact with the water while the tails are shielded from the aqueous solution within

the hydrophobic cores. The formation of micelles only occurs above the critical micelle concentration (CMC), when a large ΔH_{mix} term outweighs the loss in ΔS_{mix}.[68] Increasing the surfactant concentration above its CMC results in the formation of further micelles, while the unimer concentration remains constant (see **Figure 1.14**). For small molecule surfactants, there is a rapid dynamic equilibrium between the unimers and micelles. According to Israelachvili,[69] the CMC is given by **Equation 1.15**:

$$CMC = exp\left[-\frac{(\mu_1^0 - \mu_N^0)}{k_B T}\right] \qquad \textbf{(1.15)}$$

Here μ_1^0 is the chemical potential of the free amphiphile, μ_N^0 is the chemical potential of a micelle composed of N surfactant molecules, k_B is Boltzmann's constant and T is the absolute temperature.

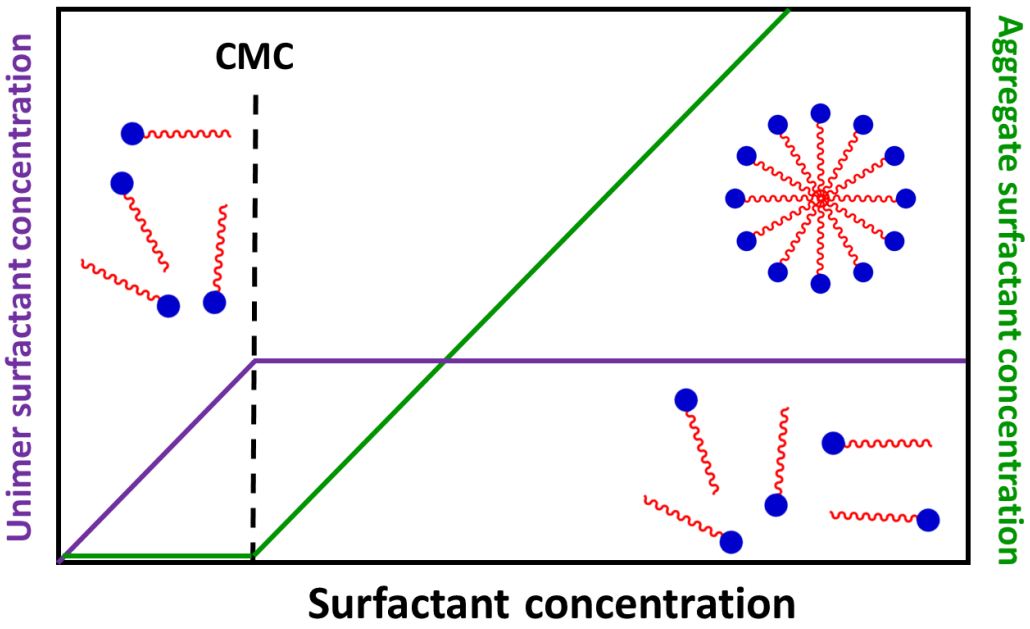

Figure 1.14 Increasing the surfactant concentration leads to the formation of surfactant micelles in aqueous solution. The vertical dashed line represents the critical micelle concentration (CMC), above which surfactant molecules undergo self-assembly to form micelles, which undergo rapid dynamic exchange with unimers.[69]

Studies of surfactants suggest that the primary factor driving the formation of various morphologies is the inherent molecular curvature, depicted in **Figure 1.15**. The resulting

geometric packing of the surfactant can be described using a dimensionless packing parameter *P*, as shown in **Equation 1.16**.[68,70]

$$P = \frac{v}{l_c \times a_0} \qquad \textbf{(1.16)}$$

Here, v is the volume of the hydrocarbon chain, a_0 is the surface area occupied by the head group, and l_c is the maximum effective length that the hydrocarbon chain can extend.[68,70] Formation of self-assembled nanostructures in water involves a delicate balance between van der Waals attractive forces between adjacent hydrophobic chains and a steric/ionic repulsive force arising from interactions between neighbouring hydrophilic head groups as shown in **Figure 1.15**. The surface area of the head-group (a_0) can be estimated from the minimum in a plot of the total interaction free energy (calculated from the sum of the attractive and repulsive potential energy curves) versus the surface area per molecule.

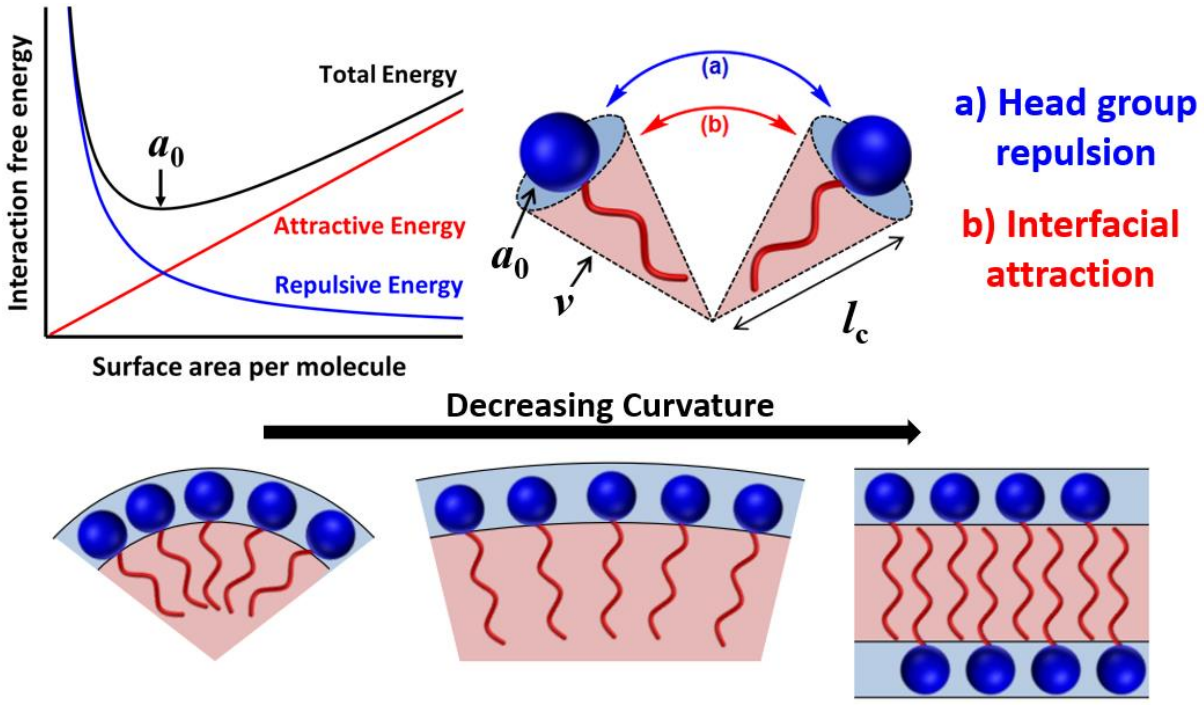

Figure 1.15 Schematic illustration of the relationship between a) hydrophilic repulsion and b) hydrophobic attraction, which results in a minimum energy for the surface area per molecule that corresponds to the optimum head-group area, a_0. The cartoon underneath depicts the geometrical constraints and inherent molecular curvature which enables surfactant self-assembly into different nano-structures.[69]

1.3.2 Block Copolymer Self-Assembly

The geometrical packing parameter can be used to describe stabilised diblock copolymers where spherical micelles are favoured when $0 < P < 1/3$, cylindrical micelles when $1/3 < P < 1/2$, and membrane structures (e.g. vesicles and lamellae) when $1/2 < P < 1$ (**Figure 1.16**).[71]

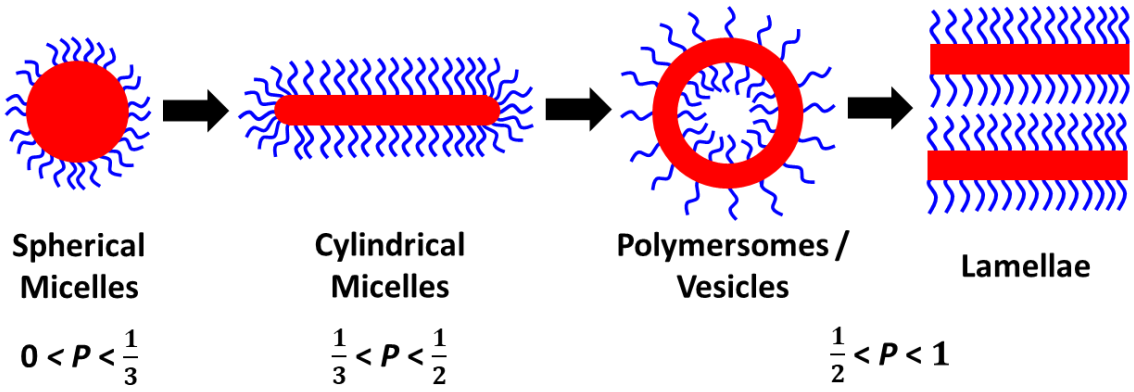

Figure 1.16 2D cross-section schematic of self-assembled diblock copolymer morphologies and their theoretical packing parameter ranges.[71]

Flory[72] and Huggins[73] developed a lattice model to calculate the Gibbs free energy of mixing (ΔG_{mix}) for a two component liquid mixture. This enables the modelling via self-consistent mean-field theory of two similarly sized molecules with a random distribution on a theoretical lattice, as shown in **Figure 1.17a**.[74] When modelling a polymer chain in solution, the chains are divided up into segments of comparable size to that of the solvent molecules, and the two components are randomly distributed on a lattice, with the polymer chains forming sequences of adjacent cells **Figure 1.17b**.

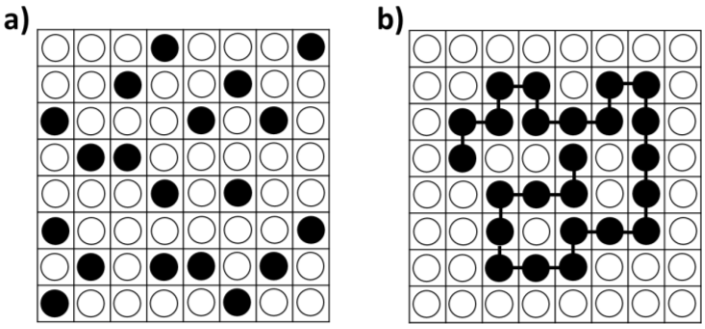

Figure 1.17 Schematic representation of a 2D lattice model: a) a mixture of molecules of equal size and b) a mixture of solvent molecules with a polymer chain illustrating the connectivity of polymer segments. Reproduced from Young and Lovell.[10]

The dimensionless Flory-Huggins interaction parameter (χ_{AB}) contains both enthalpic and entropic terms based on interactions with self and nearest neighbours and is included in the Flory-Huggins equation for $\Delta G_{mix,}$ as given by **Equation 1.17**.

$$\Delta G_{mix} = RT[n_A ln\phi_A + n_B ln\phi_B + n_A \phi_B \chi_{AB}] \qquad \textbf{(1.17)}$$

Here R is the universal gas constant, T is the absolute temperature, n_A and n_B are the number of moles of the two components (denoted A and B), and ϕ_A and ϕ_B are the volume fractions of these two components.[10] In the case of diblock copolymers in the bulk, the χ_{AB}-parameter identifies the degree of incompatibility between the polymer blocks (denoted A and B), which drives their microphase separation as shown in **Equation 1.18**.

$$\chi_{AB} = \left(\frac{z}{k_B T}\right)[\varepsilon_{AB} - \frac{1}{2}(\varepsilon_{AA} - \varepsilon_{BB})] \qquad \textbf{(1.18)}$$

Here z is the number of nearest neighbours per polymer repeat unit, k_B is the Boltzmann constant, and ε_{AB}, ε_{AA} and ε_{BB} are the interaction energies per repeat unit for A-B, A-A and B-B interactions, respectively. A positive χ_{AB} indicates net repulsion between species A and B, which is required for microphase separation and self-assembly, whereas a negative value indicates a preference towards mixing with a dependence on temperature.[75]

Block copolymers exhibit distinctive microphase behaviour and have been well studied over the past six decades.[76–78] In block-selective solvents (which solubilise one block but not the other), a range of copolymer morphologies can be obtained via self-assembly in an analogous way to surfactants.[68,74] Block copolymers may show amphiphilic behaviour in aqueous solution if one block is hydrophilic and the other is hydrophobic: this drives self-assembly to form various nano-objects. This is because one block is water-soluble and acts as a steric stabiliser, while the other block is water-insoluble and forms the core.[75] Traditionally, block copolymer self-assembly has required post-polymerisation processing. Typically, the diblock copolymer

is first prepared via solution polymerisation in a good solvent for both blocks. Then a second solvent that is selective for one of the two blocks is added to drive self-assembly. Eisenberg and co-workers reported the synthesis of various block copolymers that undergo micellisation according to this protocol.[75,79–81] For example, poly(styrene)-*block*-poly(ethylene oxide) (PS-*b*-PEO) and poly(styrene)-*block*-poly(acrylic acid) (PS-*b*-PAA) were prepared via anionic polymerisation in THF at −78°C.[82] Subsequently, a 75/25 w/w DMF/water mixture was added to induce self-assembly, thus forming nanoparticles. Such self-assembly occurs spontaneously and is a thermodynamically-driven process.[76] In the case of aqueous block copolymer formulations, self-assembly can sometimes be induced by simply changing the pH or temperature, rather than by introducing a second solvent.[82]

1.3.3 Colloidal Stabilisation of Polymer Nanoparticles

For many potential applications of nanoparticles, such as in enhanced oil recovery[83], paint formulations[84], pharmaceuticals[85] and pesticides[86] it is important that they remain colloidally stable to prevent aggregation or precipitation. In principle, addition of a surfactant or a good solvent for both blocks, or adjusting the solution temperature or pH may result in loss of the original copolymer morphology or particle aggregation.[87] Generally, particles are either sterically-stabilised or charge-stabilised, as discussed in the following sections.

1.3.4 Steric Stabilisation of Polymer Nanoparticles

Steric stabilisation is conferred by energetically and entropically unfavourable interpenetration and compression of adsorbed polymer chains located at the particle surface.[88,89] When two such ‘hairy’ particles approach each other, a sharp increase in repulsion is observed when the interparticle separation distance (*h*) becomes less than twice the adsorbed layer thickness (δ). The resulting potential energy diagram assumes additivity between the steric repulsion (E_{ster}) and van der Waals (E_{VdW}) attraction curves. A shallow potential energy

minimum (ε_{min}) exists at a distance ~2δ and the condition for elastic (non-sticky) collisions between particles (i.e. colloidal stability) is that $\varepsilon_{min} << k_BT$, where k_BT is the thermal energy of the particles.[90] This is shown in **Figure 1.18**.

In a good solvent for the adsorbed polymer chains, their local segment density increases when the interparticle separation distance is less than 2δ. This causes an increase in osmotic pressure within the overlap region and a reduction in configurational entropy, which causes strong steric repulsion.

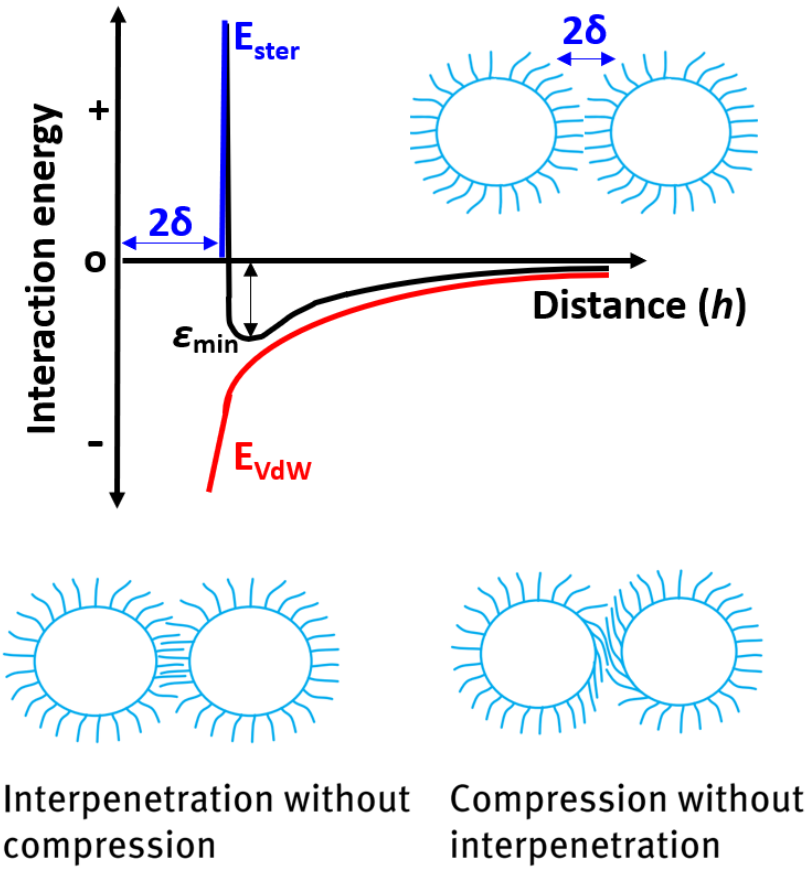

Figure 1.18 Potential energy diagram comprising steric repulsion (E_{ster}) and van der Waals attraction (E_{VdW}) curves and the combined interaction potential (black line) between two sterically-stabilised colloidal particles. The potential energy minimum is relatively shallow and the condition for colloidal stability is that $\varepsilon_{min} << k_BT$, where k_BT is the mean thermal energy of the particles. Below is shown a schematic representation of the interaction between two particles coated with adsorbed polymer layers. Modified from Tadros.[90]

In a poor solvent, segment−segment interactions are preferred over segment−solvent interactions, thus the particles can approach to within a distance δ. In this case, ε_{min} is significantly deeper so the particles no longer have the required thermal energy to overcome the van der Waals attractions. Hence such collisions are 'sticky', which leads to flocculation. Depending on the thickness of the adsorbed polymer layer, the surface coverage and the solvency, sterically-stabilised particles may undergo either strong (irreversible) or weak (reversible) flocculation.[90]

1.3.5 Charge Stabilisation of Polymer Nanoparticles

Charge stabilisation involves repulsive forces generated by the unfavourable overlap of electrical double layers (EDLs).[90,91] The EDL model was originally developed by Gouy[92] and Chapman for charged flat plates:[93] the surface potential leads to an ion gradient in the surrounding aqueous solution. Short-range electrostatic ordering of the counterions occurs near the surface, whereas thermal randomisation is observed over longer length scales. Subsequent modifications were made by Stern[94] and Graham[95] to address certain unsatisfactory assumptions, i.e. the solvent was originally treated as a structureless dielectric of constant permittivity and the electrolyte ions were simply regarded as point charges. These two workers introduced the concept of specifically adsorbed ions contributing to a non-diffuse component to an otherwise diffuse double layer.

This EDL model is applicable to charged colloidal particles.[90] Deryaguin & Landau[96] and Verwey & Overbeek[97] independently developed a quantitative 'DLVO' theory to account for the coagulation of lyophobic colloids that occurs on addition of salt. This theory assumes additivity between the EDL repulsion (E_{elec}) and van der Waals (E_{VdW}) attraction forces operating between two colloidal particles. This results in an energy–distance curve comprising a secondary minimum at longer interparticle separation distances, a primary minimum at shorter distances and an energy barrier (ε_{max}) at intermediate distances. The kinetic energy

barrier to coagulation (ε_{max}) prevents particles from getting too close to each other and the condition for colloidal stability is that the ε_{max} is significantly greater than the particle thermal energy (k_BT).[90] The potential energy graph and corresponding cartoon is shown in **Figure 1.19**.

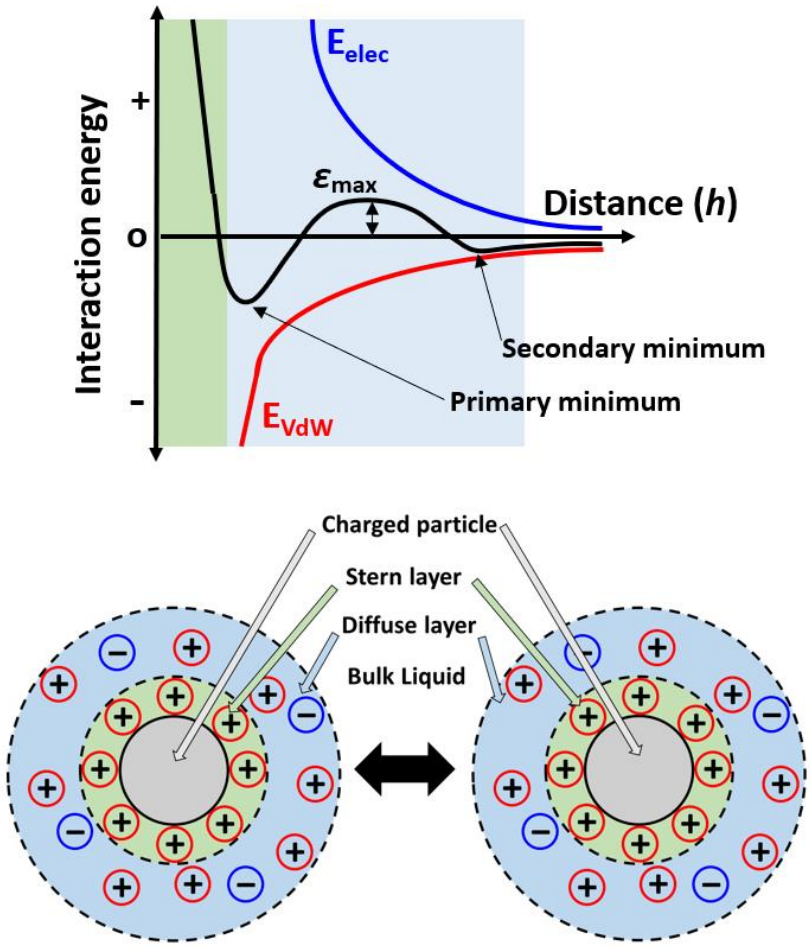

Figure 1.19 Potential energy diagram comprising the EDL repulsion (E_{elec}) and van der Waals attraction (E_{VdW}) curves and the combined DLVO interaction potential (black line) between two colloidal particles. A kinetic energy barrier ε_{max} ensures colloidal stability provided that $\varepsilon_{max} >> k_BT$, where k_BT is the thermal energy of the particles.[98–100] Also shown is a schematic illustration of charge stabilisation arising from unfavourable EDL overlap between approaching colloidal particles.

Charge stabilisation of polymer particles in water can be compromised by addition of an electrolyte.[87] The EDL shrinks as the salt concentration increases, which causes ε_{max} to shrink. This lower kinetic energy barrier leads to loss of colloidal stability and hence coagulation of polymer nanoparticles. This is summarised by the Schultze-Hardy rule,[101,102] which is based on the following two experimental observations: (i) lyophobic sols are coagulated on addition of

electrolyte and (ii) the minimum critical electrolyte concentration required to induce coagulation depends strongly on the valency of the counter-ion.[101–103] These empirical findings were made over a century ago and were subsequently rationalised by the development of DLVO theory.

The critical coagulation concentration (CCC) is the minimum amount of added salt required to induce coagulation. This parameter depends on the lyotropic nature of the counterion, as calculated for the Hofmeister series.[104] Poiseuille realised that some ions make water more viscous, while others reduce the solution viscosity relative to that of pure water at a given temperature .[105] Jones and Dole[106] showed that the salt concentration, electrostatic interactions and the solution viscosity could be related by the following **Equation 1.19**:

$$\frac{\eta}{\eta_0} = 1 + A\sqrt{C} + BC \quad \textbf{(1.19)}$$

Where η is the solution viscosity, η_0 is the solvent viscosity, A is a coefficient that depends on the electrostatic interactions as calculated from Debye–Hückel theory, B is a coefficient that depends on the solute–solvent interactions and C is the solute concentration. The Hofmeister series distinguishes between kosmotropic (high charge density) ions from chaotropic (low charge density) ions. Kosmotropes such as ammonium sulfate cause an increase in solution viscosity owing to a strengthening of the hydrogen bond network, whereas chaotropes such as ammonium chloride produce less viscous solutions owing to the weakening of the network. For higher concentrations of both types of salt (usually above 1.0 M), the aqueous solution viscosity increases significantly.[107,108] Kosmotropic salts are more effective at salting out water-soluble polymers (or proteins) from solution.[107]

1.3.6 Minimal Charge Stabilisation of Polymer Nanoparticles

Armes and co-workers[109–112] performed initial work on minimal charge stabilisation using terminal carboxylic acid or tertiary amine groups. RAFT chain ends are retained on poly(glycerol monomethacrylate)$_x$-poly(2-hydroxypropyl methacrylate)$_y$ (PGMA$_x$–PHPMA$_y$) diblock copolymers synthesised by aqueous dispersion polymerisation (**Figure 1.20**). These chain ends contain carboxylic or morpholino groups that are pH-responsive, where their degree of ionisation enables the formation of a range of different morphologies.[109–112]

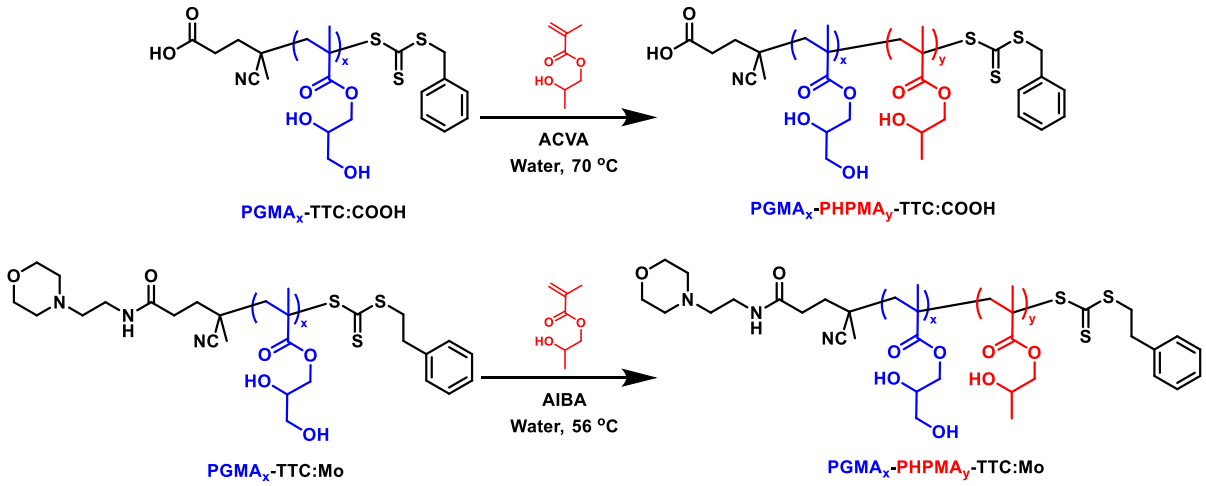

Figure 1.20 Reaction scheme for the synthesis of PGMA$_x$-PHPMA$_y$ diblock copolymers with pH-responsive carboxylic acid and morpholino end-groups.[109–112]

The TEM images of PGMA$_{56}$–PHPMA$_{155}$ nanoparticles shown in **Figure 1.21**, demonstrates that using a carboxylic acid functionalised CTA enables the pH-dependent preparation of either worms or spheres. On the other hand, the methyl ester functionalised CTA, which has no pH response, only permits the preparation of the worm morphology.[109]

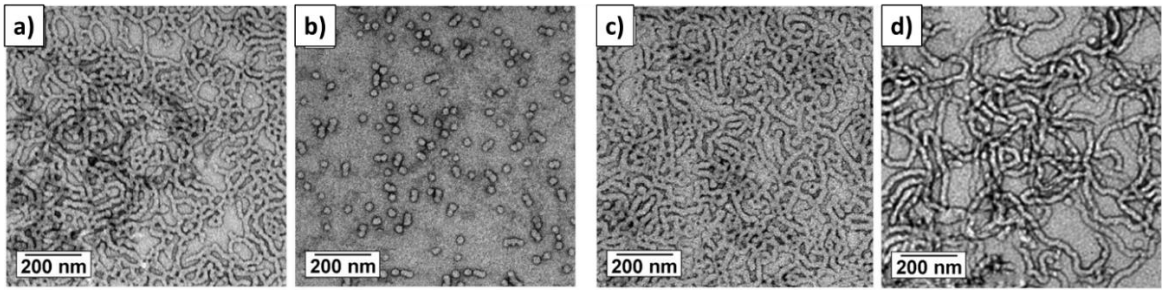

Figure 1.21 TEM images of PGMA$_{56}$–PHPMA$_{155}$ nanoparticles: a) HOOC–TTC worms at pH 3.5, b) HOOC–TTC spheres at pH 6.0, c) MeOOC–TTC worms at pH 3.5 and d) MeOOC–TTC worms at pH 6.0.[109]

Rieger and co-workers synthesised a BAB triblock copolymer using a benzoic acid-based bifunctional RAFT agent to polymerise *N*,*N*-dimethylacrylamide (DMAC) and then chain-extend this precursor with diacetoneacrylamide (DAAM) in aqueous solution, as shown in **Figure 1.22**.[113] The '*flower-like*' PDMAC loop-stabilised structure was unable to stabilise nanoparticles at pH 3.0. In contrast, spheres, colloidally stable worms and vesicles were formed at pH 4.2, but only spheres were produced at pH 5.0. This is because the central benzoic acid group derived from the RAFT agent plays a key role in conferring colloidal stability. A certain minimum degree of ionisation is required to produce a range of stable nanoparticle morphologies, whereby further ionisation leads to kinetically-trapped spheres.[113]

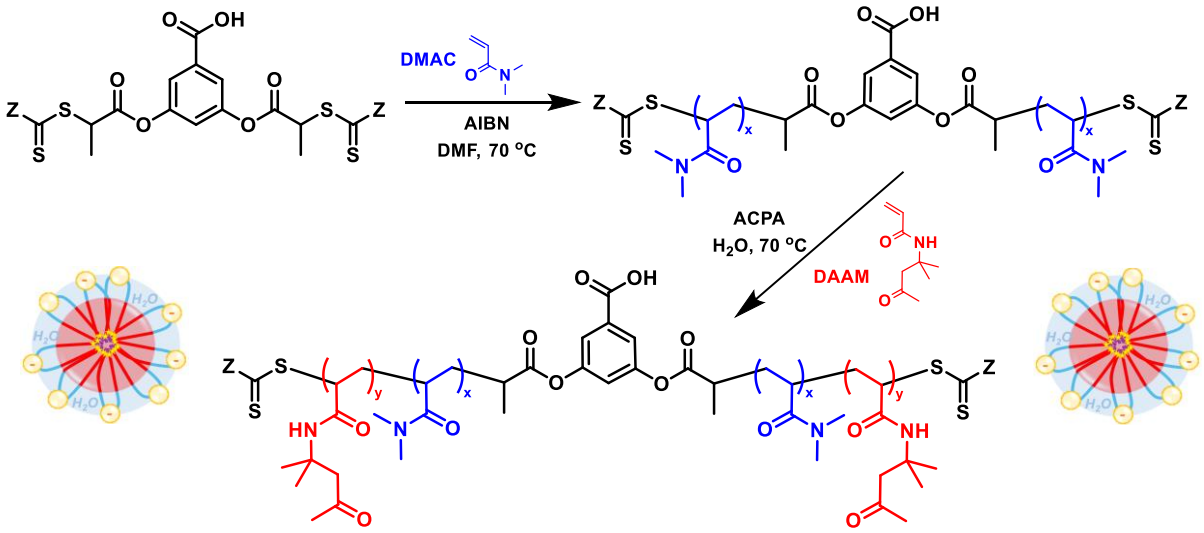

Figure 1.22 Reaction scheme for the synthesis of the bifunctional PDMAC precursor and its subsequent chain extension with DAAM to produce $PDAAM_y$-*b*-$PDMAC_{2x}$-*b*-$PDAAM_y$ triblock copolymers via RAFT aqueous dispersion polymerisation. The degree of ionisation of the central benzoic acid group dictates whether colloidally stable block copolymer nano-objects are obtained or not.[113]

The Armes group showed that for certain formulations, the solution pH can also be critical for colloidal stability.[114,115] Gibson et al. reported that either too low a solution pH or the addition of 60 mM KCl caused the reversible flocculation of poly(*N*-2-(methacryloyloxy)ethyl pyrrolidone)$_{42}$-poly(2-hydroxypropyl methacrylate)$_x$ ($PNMEP_{42}$-$PHPMA_x$) nanoparticles.[114] Such colloidal instability is the result of (i) protonation of the anionic carboxylate end-groups

or (ii) charge screening, respectively. Similarly, Beattie and co-workers found that poly(2-hydroxyethyl acrylate)$_{73}$-poly(4-hydroxybutyl acrylate)$_x$ (PHEA$_{73}$–PHBA$_x$) nanoparticles undergo flocculation below pH 5.1.[115] Incorporation of a morpholine group on the steric stabiliser chain-ends (via esterification of a carboxylic acid-based RAFT agent) produced nanoparticles exhibiting complementary pH-dependent colloidal stability. Polymer structures are shown in **Figure 1.23**. Thus, colloidally stable nanoparticles were obtained below pH 5 whereas flocculation was observed above pH 5.[115]

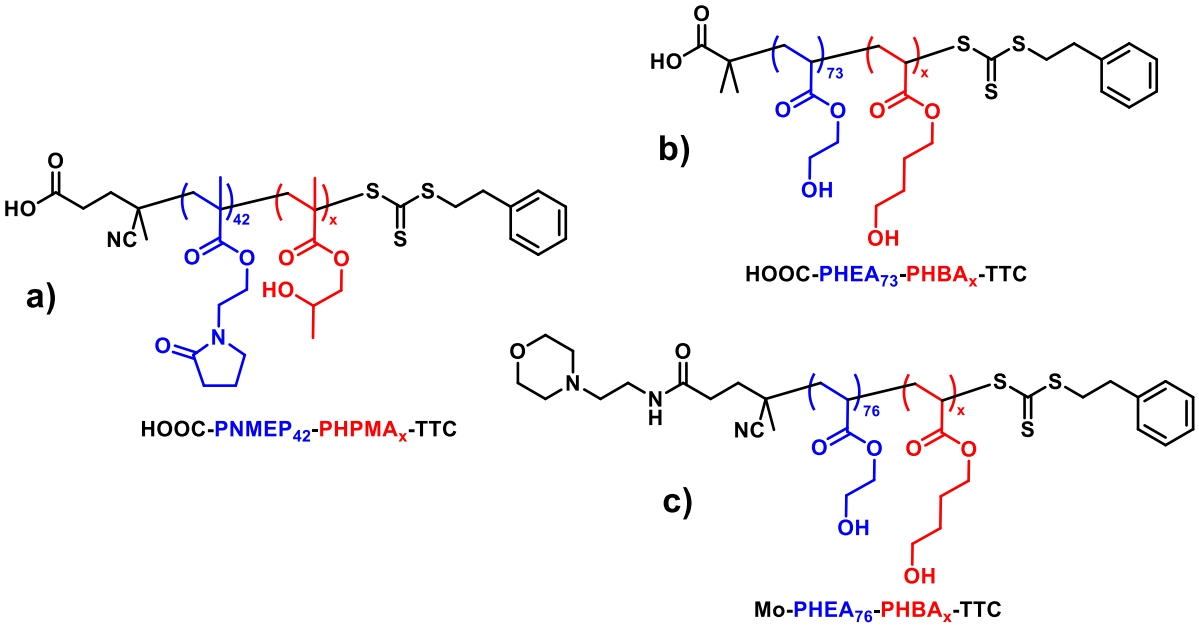

Figure 1.23 Chemical structures of (a) poly(*N*-2-(methacryloyloxy)ethyl pyrrolidone)$_{42}$-poly(2-hydroxypropyl methacrylate)$_x$ (PNMEP$_{42}$-PHPMA$_x$) bearing a carboxylic acid end-group, (b) poly(2-hydroxyethyl acrylate)$_{73}$-poly(4-hydroxybutyl acrylate)$_x$ (PHEA$_{73}$–PHBA$_x$) bearing a carboxylic acid end-group, (c) PHEA$_{76}$–PHBA$_x$ bearing a morpholine end-group.[114,115]

Furthermore, they have demonstrated that if the RAFT agent carboxylic chain end is deprotonated, this affects the copolymer morphology.[65,116] For example, Byard et al. showed that PDMAC$_{56}$–P(HBA-*stat*-DAAM)$_{264}$ formed worms at pH 3 but spheres at pH 7.[65] Similarly, Deane et al. showed that PNAEP$_{85}$-PHBA$_x$ nano-objects formed four distinct copolymer morphologies at pH 3, whereas only spheres were obtained at pH 7.[116]

1.3.7 Electrosteric Stabilisation of Polymer Nanoparticles

A third type of colloidal stabilisation mechanism is electrosteric stabilisation.[88,117] This is when the steric stabiliser chains exhibit polyelectrolyte character. Unlike purely electrostatic interactions, electrosterically stabilised particles remain stable even at high salt concentrations.[118,119] If a weak polyelectrolyte is used in this context, the particle surface charge will vary with solution pH. In this case, electrosteric stability is only conferred within a specific pH range.

1.3.8 Polymerisation-Induced Self-Assembly (PISA)

Polymerisation-induced self-assembly (PISA) involves the synthesis of diblock copolymers via either dispersion or emulsion polymerisation whereby a soluble precursor block is chain-extended with a second monomer whose corresponding homopolymer is insoluble in the chosen solvent.[120] The polymer chains in the growing second block become insoluble at some critical DP which drives *in situ* self-assembly to form nano-objects from the dispersed chains. Spherical micelles are the first morphology to be formed in a PISA formulation. However, as the polymerisation progresses, the higher order morphologies can also be obtained if certain conditions are fulfilled. PISA can be performed at high solids (up to 50% w/w solids) and typically only relatively short reaction times are required to achieve high monomer conversions.[121,122] This is because once micellar nucleation occurs, the unreacted monomer diffuses into the growing nanoparticles and this high local monomer concentration leads to a rate acceleration.[70,123] Under suitable conditions, these monomer-swollen copolymer micelles can undergo fusion to form anisotropic worms which can evolve to form branched worms and then wrap up to produce vesicles.[124] The final morphology is determined by various parameters depending on the nature of the diblock copolymer.[120,125] Since the first report in 2002 by Ferguson et al.,[126] many successful PISA formulations have been devised.[122,127] For example,

Charleux and co-workers have reported many successful RAFT aqueous emulsion polymerisation formulations.[123,128–130]

In 2007, Hawker and co-workers reported the synthesis of well-defined diblock copolymer micelles via so-called RAFT 'precipitation' polymerisation of *N*-isopropylacrylamide (NIPAM) at 70°C using a PDMAC precursor.[131] PNIPAM has a lower critical solution temperature (LCST) of around 32°C.[132] At a certain critical DP, the growing PNIPAM blocks become sufficiently hydrophobic to induce micellar nucleation. In the absence of any cross-linker, the nanoparticles simply undergo molecular dissolution because the PNIPAM chains are below their LCST and hence are no longer hydrophobic.[133] However, if the same aqueous PISA synthesis is conducted in the presence of a *N*,*N*-methylenebisacrylamide (BIS) comonomer, the growing PNIPAM chains become crosslinked. Thus, the nanoparticles become water-swollen microgels on cooling to 20°C as shown in **Figure 1.24**.[131]

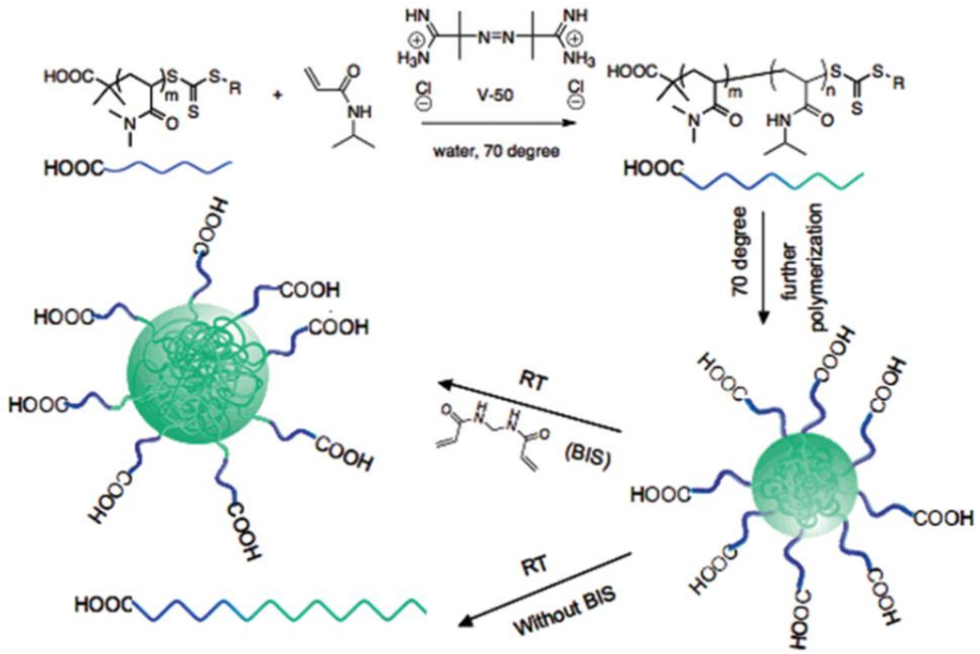

Figure 1.24 Schematic representation of the RAFT 'precipitation' polymerisation of NIPAM at 70°C to form spherical micelles. Introducing BIS crosslinker into such polymerisations led to the microgel formation on cooling, rather than molecular dissolution. Reproduced from Hawker et al.[131]

Over the last decade PISA has garnered considerable attention. This can be explained by its relative ease of use and its applicability towards a wide range of monomers and solvents. The technique provides a convenient method for efficient nanoparticle self-assembly and avoids the requirement for post-polymerisation processing. RDRP techniques have been primarily used to conduct PISA syntheses, with particular attention being given to RAFT polymerisation.[134]

PISA is generic: it can be performed in polar solvents such as water and ethanol or using non-polar solvents such as *n*-alkanes.[122,135] This Thesis will focus on RAFT-mediated PISA in aqueous media which has a range of potential commercial applications.

1.4 RAFT Aqueous Dispersion Polymerisation

1.4.1 Phase Diagrams

The synthesis of poly(glycerol monomethacrylate)$_x$-poly(2-hydroxypropyl methacrylate)$_y$ (PGMA$_x$−PHPMA$_y$) nano-objects via RAFT aqueous dispersion polymerisation has been well-studied by the Armes group, see **Figure 1.25**.[110,136–139] This dithiobenzoate-based RAFT formulation enables a range of copolymer morphologies to be obtained by simply adjusting the DP of each block and the target solids contents. For example, Li and Armes reported the efficient synthesis of either well-defined spherical nanoparticles or polydisperse vesicles within a few hours at 70°C.[136]

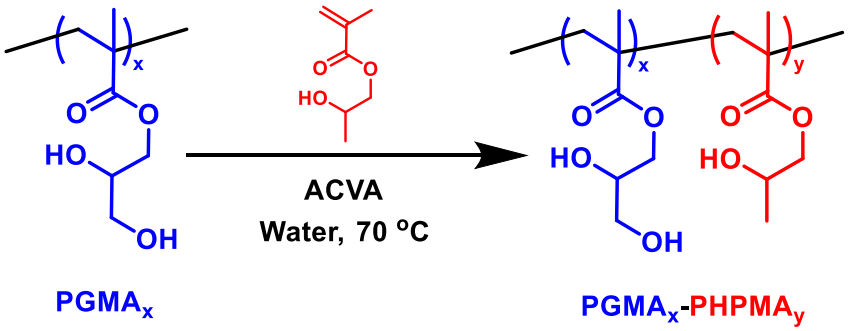

Figure 1.25 Reaction scheme for the synthesis of sterically-stabilised PGMA$_x$-PHPMA$_y$ nanoparticles via RAFT aqueous dispersion polymerisation of HPMA at 70°C.

A pseudo-phase diagram can be constructed to identify the conditions required to form a specific morphology for a given diblock copolymer.[70,140,141] **Figure 1.26** summarises experimental data obtained for the synthesis of a series of $PGMA_x$–$PHPMA_y$ nano-objects, as reported by Blanazs et al.[137] The shortest stabiliser block ($PGMA_{47}$) enables the formation of a range of copolymer morphologies with no concentration dependence (**Figure 1.26a**). In this case, systematic variation of the core block DP provides convenient control over the final copolymer morphology. The use of a $PGMA_{78}$ stabiliser requires a correspondingly longer core-forming block to obtain each pure copolymer morphology (i.e. spheres, worms or vesicles), see **Figure 1.26b**. Moreover, this evolution in morphology is only observed at a sufficiently high copolymer concentration; only kinetically trapped spheres are obtained at a copolymer concentration of 10% w/w. This is because the $PGMA_{78}$ stabiliser confers greater steric stabilisation than $PGMA_{47}$, which means that sphere-sphere fusion is less likely to occur (but can still occur at higher copolymer concentration). The pseudo-phase diagram constructed for the longest stabiliser block ($PGMA_{112}$) shows a relative lack of morphological complexity, with kinetically-trapped spheres being the predominant morphology (**Figure 1.26c**). Similar pseudo-phase diagrams have been constructed for many other diblock copolymers.[142–146]

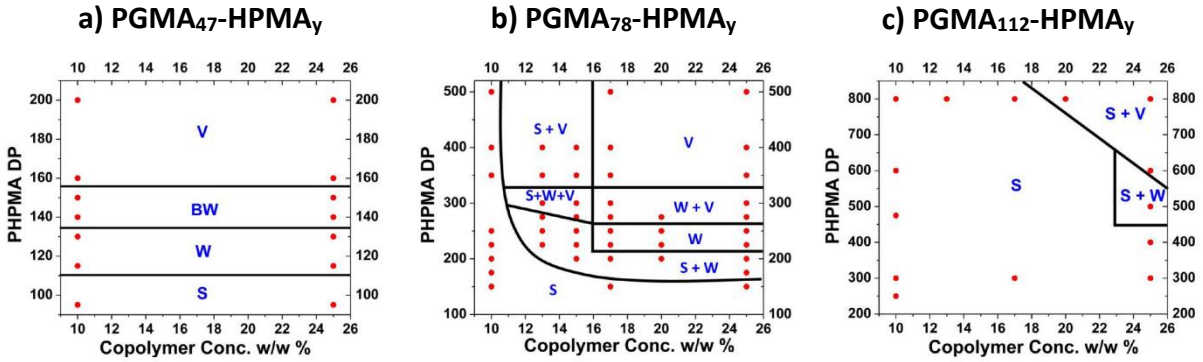

Figure 1.26 Three pseudo-phase diagrams constructed for $PGMA_{47}$-$PHPMA_y$, $PGMA_{78}$-$PHPMA_y$ and $PGMA_{112}$-$PHPMA_y$ nano-objects prepared by RAFT aqueous dispersion polymerisation of HPMA at 70°C [S = spheres, W = worms, BW = branched worms and V = vesicles]. Reproduced from Blanazs and co-workers.[137]

Williams et al. constructed a phase diagram for a similar polymer, but which contained some cationic character in the stabiliser block, by using poly(2-(methacryloyloxy)ethyl]-trimethylammonium chloride) (PMETAC). The ([1 - *n*]PGMA$_x$-[*n*]PMETAC$_y$)-PHPMA$_z$ formulation enables facile synthesis of spheres, worms and vesicles (**Figure 1.27**).[142]

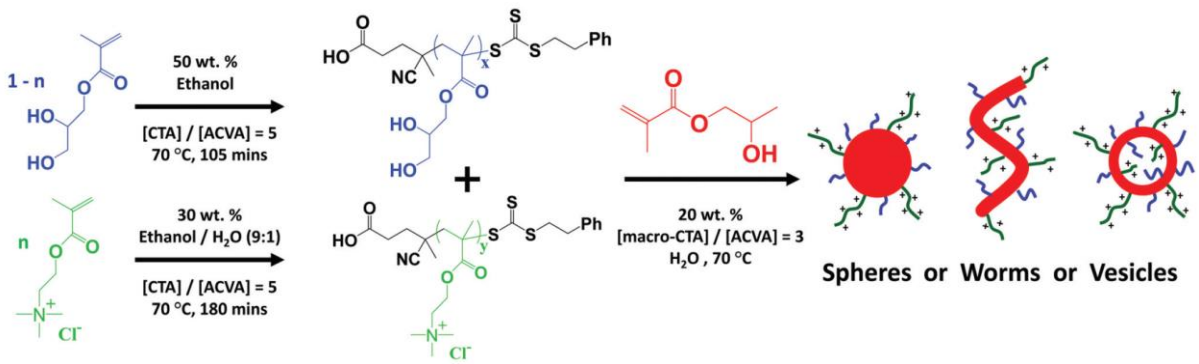

Figure 1.27 Synthesis of cationic diblock copolymer nanoparticles of general formula ([1 - *n*]PGMA$_x$-[*n*]PMETAC$_y$)-PHPMA$_z$ by RAFT aqueous dispersion polymerisation of HPMA using a binary mixture of non-ionic and cationic water-soluble precursors. Optimisation of n, x, y, and z enables the formation of cationic spheres, worms or vesicles.[142]

As the cationic character of the PMETAC stabiliser block was increased relative to that of the non-ionic PGMA, it became more difficult to access higher-order morphologies, with spheres being formed over a wide range of PHPMA DPs, as shown in **Figure 1.28**. The worm-gel formulation was found to be bacteriocidal and bacteriostatic towards *S. aureus*.[142]

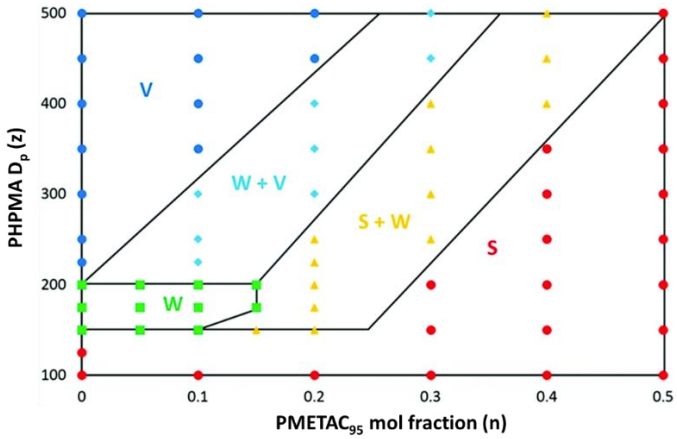

Figure 1.28 Pseudo-phase diagram constructed for a series of diblock copolymer nanoparticles of general formula ([1 − *n*]PGMA$_{62}$ + [*n*]PMETAC$_{95}$)−PHPMA$_z$ prepared by RAFT aqueous dispersion polymerisation of HPMA at 20% w/w solids. S = spheres, W = worms, V = vesicles, S + W = mixed phase of spheres and worms, W + V = mixed phase of worms and vesicles. Figure reproduced from Williams and co-workers.[142]

1.4.2 Suitable Monomers

There are relatively few vinyl monomers which meet the solubility requirements for an aqueous dispersion polymerisation formulation.[120,147] Such monomers should be water-miscible but their corresponding homopolymers must be water-insoluble to be suitable core-forming blocks. The seven vinyl monomers shown in **Figure 1.29** meet these two criteria and have made up the majority of aqueous PISA formulations over the past decade or so.[148]

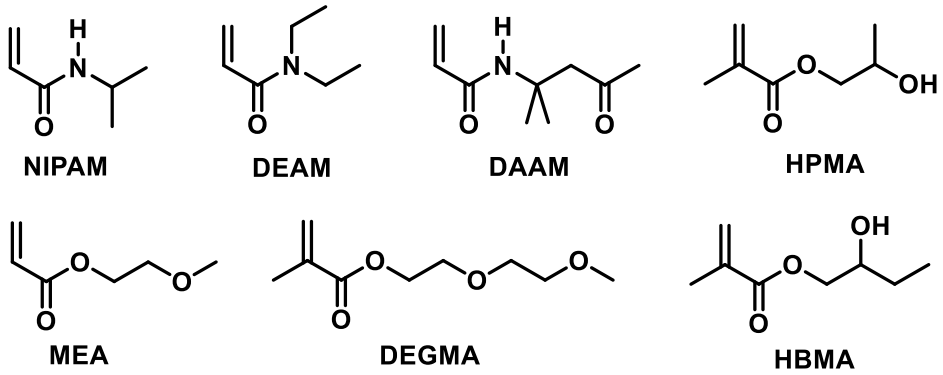

Figure 1.29 Chemical structures of vinyl monomers reported for aqueous dispersion polymerisation. *N*-isopropylacrylamide (NIPAM), *N*,*N*-diethylacrylamide (DEAM), diacetoneacrylamide (DAAM), 2-hydroxypropyl methacrylate (HPMA), 2-methoxyethylacrylate (MEA), di(ethylene glycol)methyl ether methacrylate (DEGMA) and 2-hydroxybutyl methacrylate (HBMA).[148]

Diacetone acrylamide (DAAM) was identified as a suitable core-forming block by Zhou et al.[149] in 2015. Its pendent ketone group is useful because it can be readily derivatised by post-polymerisation modification.

In 2018, Foster et al. reported a computational method to predict suitable core-forming monomers for aqueous dispersion polymerisation. Mathematical modelling based on the partition coefficient for the monomer between *n*-octanol and water (which provides a measurement of its hydrophilicity) and the head group surface area, was used to identify suitable monomers. Five vinyl monomers are shown in **Figure 1.30.**[148]

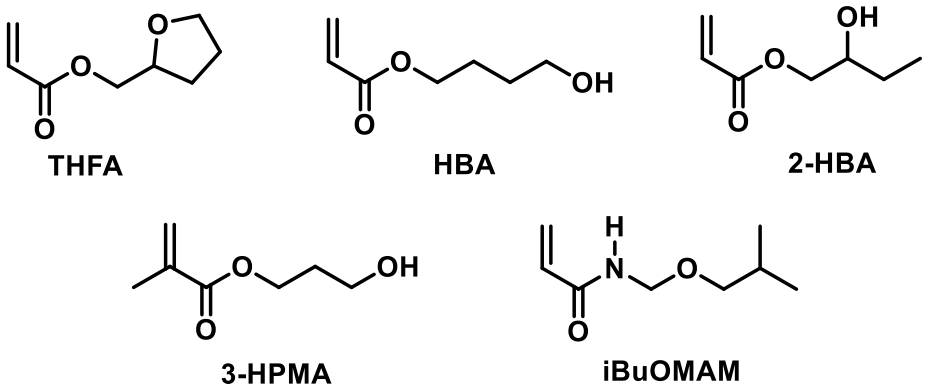

Figure 1.30 Chemical structures of five vinyl monomers predicted to be suitable for aqueous dispersion polymerisation: tetrahydrofurfuryl acrylate (THFA), 4-hydroxybutyl acrylate (HBA), 2-hydroxybutyl acrylate (2-HBA), 3-hydroxypropyl methacrylate (3-HPMA) and isobutoxymethyl acrylamide (iBuOMAM).[148]

According to the PISA literature, there are three main causes of kinetically-trapped spheres: (i) low copolymer concentration[150,151], (ii) a high steric stabiliser DP,[150] and (iii) polyelectrolyte character in the stabiliser.[57,142] Each of these factors can prevent the efficient fusion of pairs of spheres, which is the critical first step in copolymer morphology evolution during PISA.[142,150]

Byard et al. statistically polymerised a binary mixture of 4-hydroxybutyl acrylate (HBA) and DAAM using a poly(*N*,*N*-dimethacrylamide) (PDMAC) homopolymer precursor to form a thermoresponsive diblock copolymer, as shown in **Figure 1.31**.[65] When the solution temperature was raised from 1 – 70°C, the copolymer morphology reversibly switched from spheres to worms to vesicles to lamellae (**Figure 1.32**). Such rich self-assembly behaviour had not been previously reported for any amphiphilic diblock copolymer or surfactant.

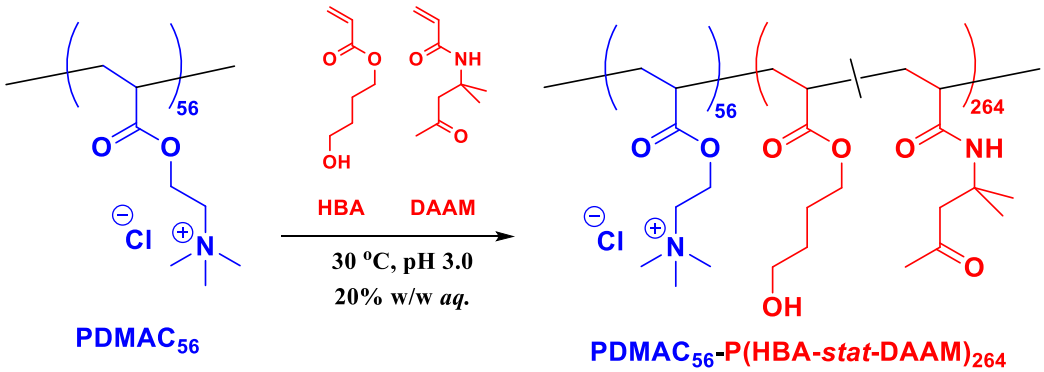

Figure 1.31 Synthesis of $PDMAC_{56}$-P(HBA-*stat*-DAAM)$_{264}$ diblock copolymer nano-objects by RAFT aqueous dispersion polymerisation of a binary mixture of HBA and DAAM using a $PDMAC_{56}$ precursor.[65]

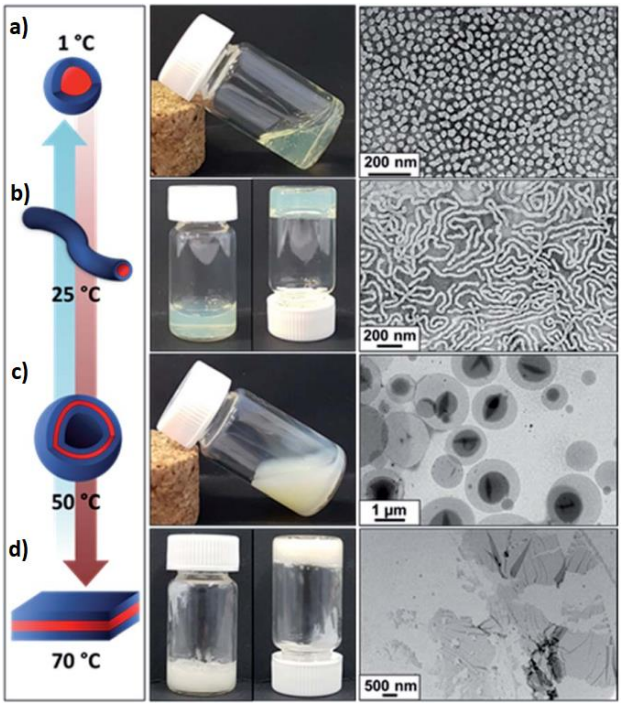

Figure 1.32 Schematic representation of the thermally reversible morphological transitions that occur for a 20% w/w aqueous dispersion of $PDMAC_{56}$–P(HBA-*stat*-DAAM)$_{264}$ on varying the temperature from 1 to 70°C. Cartoon, digital and TEM images show the change in the aqueous dispersion at different temperatures: a) spheres at 1°C, b) worms at 25°C, c) vesicles at 50°C and d) lamellae at 70°C. Reproduced from Byard et al..[65]

It is usually desirable to have core-forming blocks with a relatively low glass transition temperature (T_g) to ensure high chain mobility. Weakly hydrophobic core-forming blocks such as PHPMA or PHBA are plasticised by water, which leads to thermoresponsive behaviour. During PISA, the core-forming block is solvated by unreacted monomer and this swelling enhances chain mobility.[152,153]

1.4.3 Covalent Stabilisation (Intraparticle Crosslinking)

An issue that may arise with diblock copolymer nanoparticles is their colloidal stability when exposed to changes in environment. Addition of surfactants (or good solvents for both blocks) or changes to temperature or pH may result in nanoparticle dissociation to form molecularly-dissolved chains. In principle, covalent stabilisation can stabilise the nanoparticles, which requires the addition of a suitable cross-linker to confine the crosslinking to intraparticle rather than interparticle crosslinking.[125,154]

For example, block copolymer nanoparticles can be stabilised by adding a suitable third comonomer, such as ethylene glycol dimethacrylate (EGDMA).[153,155] For example, Armes and co-workers used a small amount of EGDMA as a third block in PGMA-PHPMA syntheses and demonstrated that the resulting morphologies were stable under high shear conditions when conducting emulsification with an oil to form Pickering emulsions.[156] The same group showed that EGDMA-crosslinked vesicles contained nanodomains within their membranes.[157] A similar vesicle morphology was obtained when conducting post-polymerisation crosslinking using epoxy−amine chemistry.[158] In each case, the initial linear PGMA-PHPMA chains are covalently linked together by the EGDMA comonomer to form 'star-like' copolymers.[157] **Figure 1.33** shows a selection of different cross-linkers used with aqueous PISA formulations.

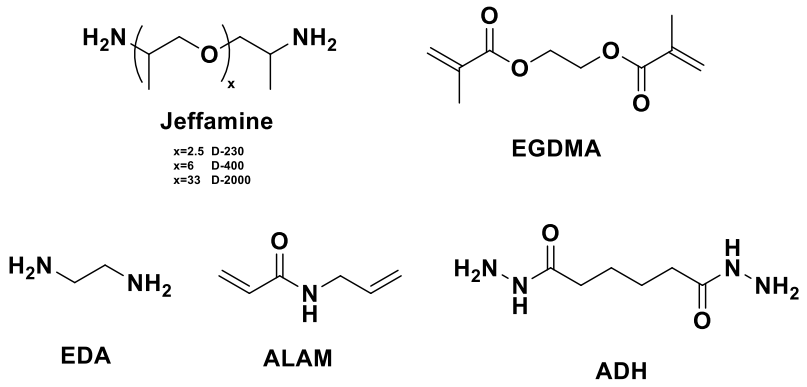

Figure 1.33 Chemical structures of various cross-linkers that have been used to stabilise nanoparticles prepared by RAFT aqueous dispersion polymerisation: poly(propylene glycol) bis(2-aminopropyl ether) (Jeffamine),[159] ethylene glycol dimethacrylate (EGDMA),[156] ethylenediamine (EDA),[160] allyl acrylamide (ALAM),[161] adipic acid dihydrazide (ADH).[147]

An example of a post-polymerisation crosslinking of diblock copolymers was reported by Byard et al..[147] After synthesising $PDMAC_{58}$-$PDAAM_{230}$ vesicles as 20% w/w aqueous dispersions, adipic acid dihydrazide (ADH) was added (DAAM/ADH molar ratio = 10). The reagent's hydrazide groups can react with the pendent ketone groups on the PDAAM chains via nucleophilic substitution to form hydrazone linkages. By monitoring the attenuation of the PDAAM ketone IR band at around 1716 cm^{-1}, the extent of crosslinking could be estimated.

The ADH-modified vesicles became resistant to methanol dissolution once a sufficient degree of crosslinking had been achieved.[147]

1.4.4 RAFT End-Group Removal

For commercial applications, it is usually desirable to remove RAFT chain-ends due to their inherent colour, malodour and toxicity. This can be achieved by thermal treatment or by addition of excess radicals or by using nucleophiles.[162,163] Jesson et al. used H_2O_2 to remove RAFT end-groups from $PGMA_x$-$PHPMA_y$ spheres, worms and vesicles within 8 h at 70°C, see **Figure 1.34**.[164] The rate of end-group removal depended on the H_2O_2 concentration and the nature of the RAFT chain-end, with dithiobenzoates being removed more readily than trithiocarbonates.

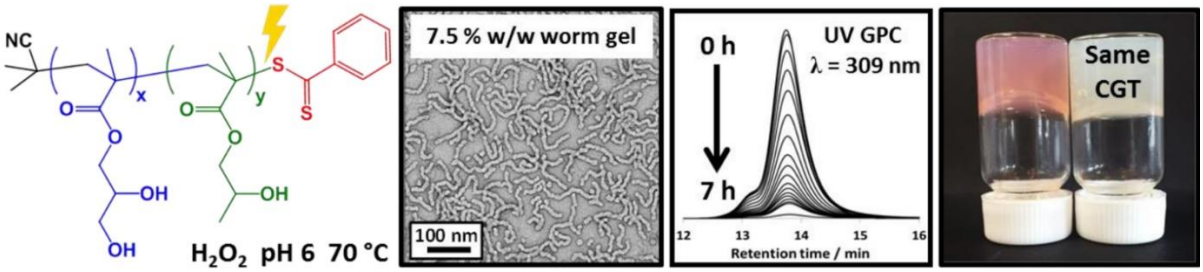

Figure 1.34 Addition of H_2O_2 enables end-group removal from diblock copolymer nano-objects in aqueous media. There is minimal change in copolymer morphology as the absorbance from the dithiobenzoate end-groups is reduced over time.[164]

Spectrophotometry was used to monitor the reduction of an absorption band at 309 nm over time. Both dithiobenzoate and trithiocarbonate RAFT end-groups exhibit this UV band, which has been assigned to a π-π* transition.[165] A much weaker visible absorption band (λ_{max} = 443 nm for trithiocarbonates or λ_{max} = 512 nm for dithiobenzoates) corresponding to a forbidden n-π* transition can also be used for this purpose.[166,165] This approach can be more convenient because it prevents the problem of signal saturation at higher copolymer concentrations.[167] The resulting diblock copolymer worm gel exhibited the same gel modulus and critical gelation temperature after chain-end removal.

1.5 Hydrophilic Block Copolymer Nanoparticles

1.5.1 Colloidal Stability in Highly Salty Aqueous Media

Recently, there has been considerable interest in identifying polymer nanoparticles that remain stable in the presence of high salt concentrations.[57,168–170] Polyelectrolytes confer electrosteric stabilisation to nanoparticles rather than merely steric stabilisation which means they are usually more salt-tolerant than their non-ionic counterparts, as explained in **Section 1.3.7**. Bagaria et al. showed that anionic polyelectrolytic chains consisting of poly(2-acrylamido-2-methylpropanesulfonic acid, sodium salt -*stat*-acrylic acid) (PAMPS-*stat*-PAA), could be used to stabilise iron oxide nanoparticles when adsorbed to their surface in concentrated brine.[171] The nanoparticles remained colloidally stable in 10% w/w brine at 90°C for up to 1 month with no significant change to the particle hydrodynamic diameter.[171]

Poly(2-(acryloyloxy)ethyltrimethylammonium chloride) (PATAC) was chain-extended via RAFT aqueous dispersion polymerisation of diacetone acrylamide (DAAM) by Byard et al., who reported excellent salt tolerance for the resulting PATAC-PDAAM nanoparticles in the presence of 3.8 M ammonium sulfate. Furthermore, such nanoparticles remained resistant to flocculation when stored in 3.0 M $(NH_4)_2SO_4$ for 115 days. The same team also used a binary mixture of PATAC and PDMAC stabiliser blocks to compare how varying the mole fraction of cationic PATAC affected the colloidal stability. On reducing the effective charge density of the steric stabiliser chains, they were able to overcome the restriction of kinetically-trapped spheres and access a range of higher order morphologies. Reasonably good ammonium sulfate salt tolerance was conferred by these binary stabiliser nanoparticles (e.g. up to 2.0 M ammonium sulfate for worms), but they proved to be less tolerant than those prepared with pure PATAC stabiliser blocks, as shown in **Figure 1.35**.[57]

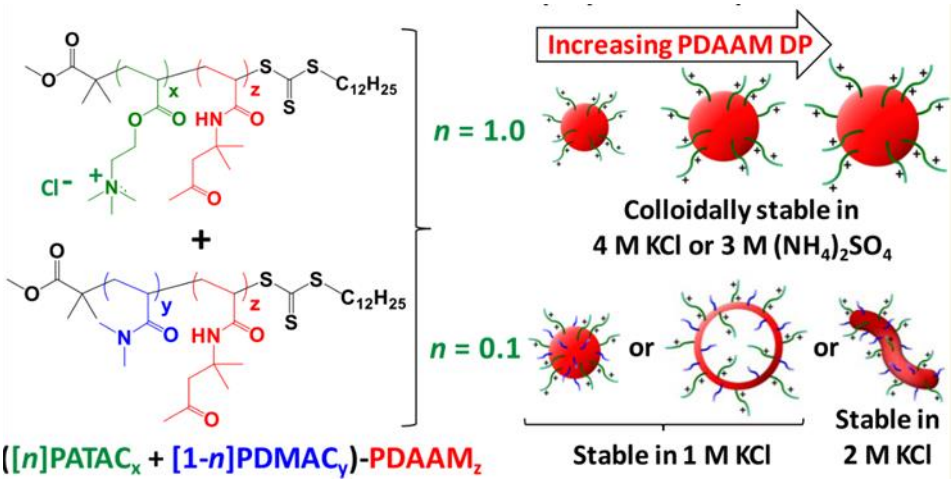

Figure 1.35 $PATAC_x$-$PDAAM_z$ and ($0.1PATAC_x$ + $0.9PDMAC_y$)-$PDAAM_z$ diblock copolymers assembled into kinetically-trapped spheres in the former case and a series of tunable morphologies in the latter case. The colloidal stability of these nano-objects were examined by the addition of salt post-polymerisation. Reproduced from Byard et al.[57]

1.5.2 Synthesis in Highly Salty Aqueous Media

A selection of cationic polyacrylamides were prepared by Huang et al. via statistical copolymerisation of METAC with acrylamide (AM) in aqueous media in the presence of a suitable chain transfer agent, as shown in **Figure 1.36**.[168] This approach enabled a specific degree of cationic character of the stabiliser block to be targeted by controlling the comonomer ratio. Subsequently, these P(METAC-*stat*-AM)$_{360}$ precursors were used for RAFT aqueous dispersion polymerisation of acrylamide in 2.8 M ammonium sulfate to produce a series of P(METAC-*stat*-AM)$_{360}$-*b*-PAM_{600} nanoparticles. This specific salt concentration was selected because AM remains water-miscible under such conditions, but the growing PAM chains become insoluble at some critical DP. If the salt concentration is too low, only RAFT solution polymerisation occurs. On the other hand, if it is too high the colloidal stability of the final nanoparticles may be compromised.[172] Diblock copolymer particles were prepared at 13% solids with an overall copolymer DP of up to 1,059 (MW ≈ 100 kDa) with monomer conversions varying between 57 and 97%. Molecular weights were in surprisingly good agreement with both theoretical values and those obtained via aqueous GPC using PEO calibration standards. M_w/M_n values ranged between 1.10 and 1.30; this is unusually low but

perhaps understandable given the relatively low molecular weights targeted and the incomplete monomer conversions achieved. When compared to the analogous polymer chains synthesised via RAFT solution polymerisation, a thirty-fold reduction in solution viscosity was achieved.[168]

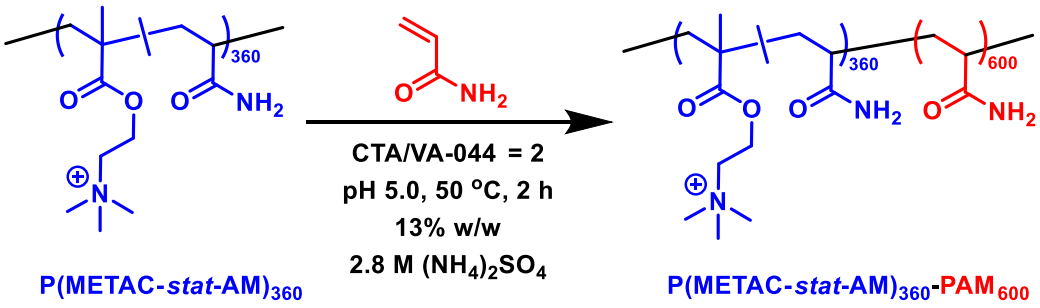

Figure 1.36 P(METAC-*stat*-AM)$_{360}$-PAM$_{600}$ diblock copolymers prepared in highly salty media as reported by Huang et al.[168]

Similarly, Bai et al. prepared a series of PAMPS$_x$ precursors using a symmetric dicarboxylic acid-based trithiocarbonate chain transfer agent.[169,173] Subsequent chain extension shown in **Figure 1.37** via RAFT aqueous dispersion polymerisation using a statistical mixture of AM and AMPS in 2.3 M ammonium sulfate enabled preparation of copolymers with M_n values of ~ 1 MDa. Higher intrinsic viscosities were measured when such copolymerisations were conducted at lower temperatures and when increasing the target solids concentration up to 22.5%. The proposed particle formation mechanism suggested that polymer-rich regions, rather than nuclei, are formed during phase separation that break up into smaller particles during mechanical stirring.[169]

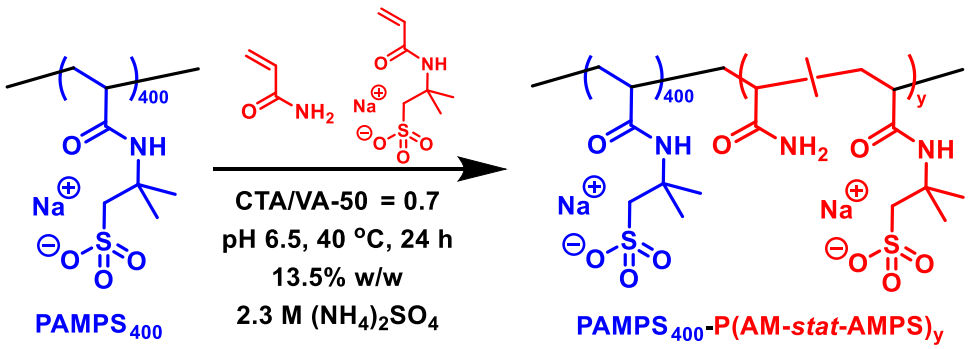

Figure 1.37 PAMPS$_{400}$-P(AM-*stat*-AMPS)$_y$ diblock copolymers synthesised in highly salty media as reported by Bai et al..[169]

1.5.3 Polymer and Colloid Stability in Acidic Aqueous Media

If RAFT polymerisations are conducted in aqueous media above pH 7, it is well known that this increases their susceptibility to RAFT end-group hydrolysis.[174,175] Conversely, end-group hydrolysis is not observed at pH 2.[46,176] The rate of hydrolysis of dithiobenzoate RAFT agents is faster at higher temperatures, and such species are more susceptible to hydrolytic degradation than trithiocarbonates.[164,176] Polymer particles bearing either cationic or anionic charge are colloidally stable due to charge or electrosteric stabilisation. For strong acid or quaternary ammonium groups, this means that colloidal stability is maintained regardless of the solution pH. In contrast, if carboxylic acid or amine groups are involved, particle flocculation usually occurs when such anionic or cationic charge is lost after adjusting the solution pH.

North et al. reported the pH-responsive behaviour of $PMAA_{50}$-$PHPMA_{237}$ nanoparticles prepared via RAFT aqueous dispersion polymerisation of HPMA, as shown in **Figure 1.38**.[177] Large polydisperse spheres were obtained at pH 5.5, but a change to pH 10 led to relatively small spheres being formed. This is because the PMAA stabiliser block became more anionic under such conditions strengthening its electrosteric stabilisation. These spheres increased in size at higher temperature and formed weakly anisotropic worms at 50°C. On the other hand, the dispersion became much more turbid below pH 6.3, with the nanoparticles becoming colloidally unstable. This was attributed to the loss of anionic surface charge via protonation of the PMAA stabiliser block, which led to nanoparticle flocculation.[177]

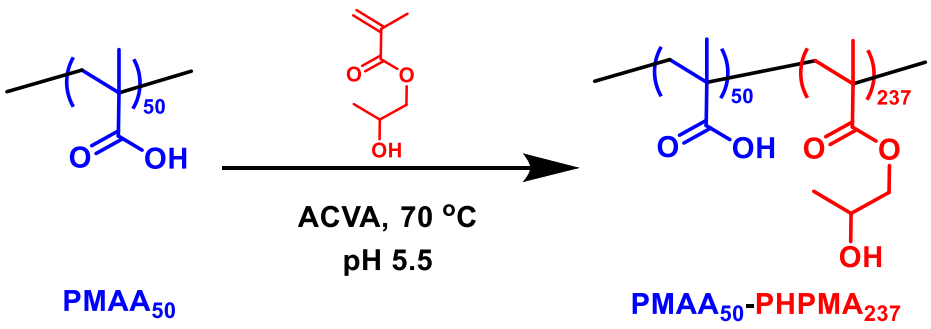

Figure 1.38 Synthesis of $PMAA_{50}$-$PHPMA_{237}$ diblock copolymer nano-objects via RAFT aqueous dispersion polymerisation of HPMA as reported by North et al.[177]

1.5.4 Synthesis in Acidic Aqueous Media

The Armes group reported that doubly pH-responsive poly(2-(diethylamino)ethyl methacrylate)-poly(benzyl methacrylate-*stat*-methacrylic acid) ($PDEA_{88}$-P(BzMA-*stat*-$MAA)_x$) diblock copolymers exhibit so-called 'schizophrenic' self-assembly behaviour. Such diblock copolymers can be prepared directly in the form of sterically-stabilised nanoparticles via aqueous PISA at low pH by chain-extending the protonated cationic precursor (PDEA) with a statistical mixture of benzyl methacrylate (BzMA) and methacrylic acid (MAA).[178] Under such conditions, the protonated PDEA block acts as a cationic steric stabiliser and the neutral P(BzMA-*stat*-$MAA)_x$ block forms the hydrophobic micelle core. On raising the solution pH, the MAA repeat units become ionised and hence the P(BzMA-*stat*-$MAA)_x$ chains now act as an anionic stabiliser block, while the deprotonated PDEA chains form the hydrophobic micelle cores, as shown in **Figure 1.39**.[178]

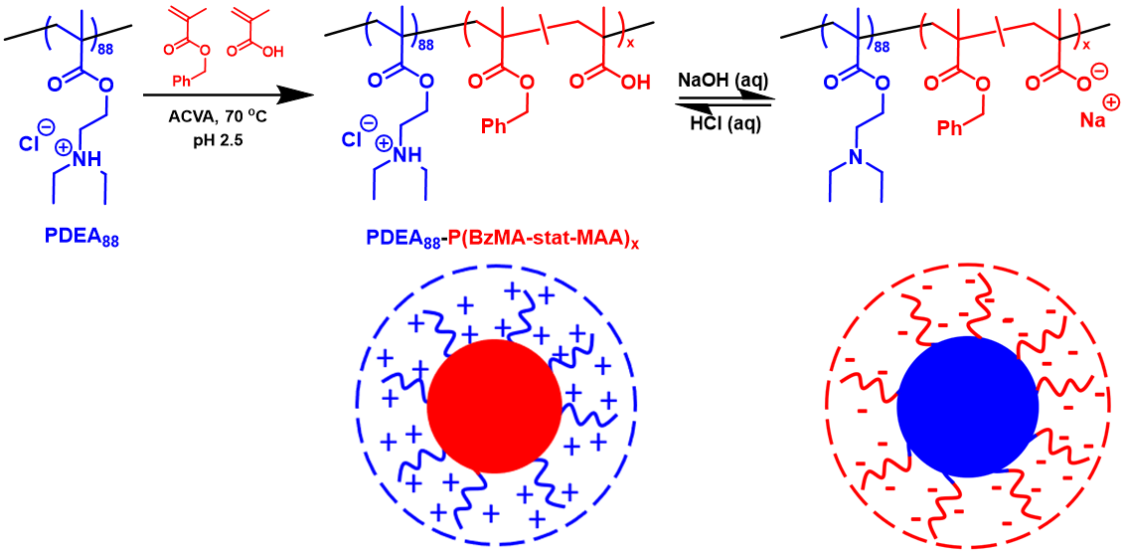

Figure 1.39 Schematic cartoon depicting the schizophrenic behaviour exhibited by $PDEA_{88}$-P(BzMA-*stat*-$MAA)_x$ diblock copolymers. Cationic PCEA-core nanoparticles are formed at low pH and anionic PDEA core nanoparticles are formed at high pH.[178]

A subsequent study by North and Armes focused on doubly pH-responsive poly(2-(diethylamino)ethyl methacrylate)-poly(2-carboxyethyl acrylate) (PDEA–PCEA) diblock

copolymers prepared by RAFT aqueous dispersion polymerisation of CEA at pH 2.[179] In this case, the weak polyelectrolyte nature of each block led to the formation of an isoelectric point (IEP) at which there is no net particle surface charge. At this critical pH, the particles become flocculated, with redispersion being observed on adjusting the solution pH either above or below the IEP, as shown in **Figure 1.40**.[179]

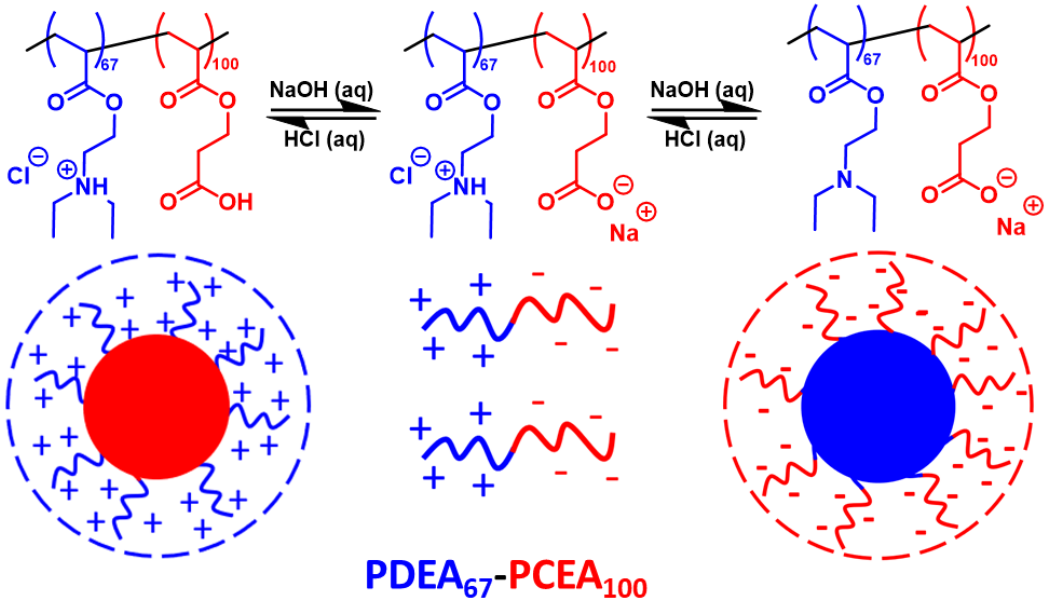

Figure 1.40 Schematic cartoon depicting the schizophrenic behaviour exhibited by a $PDEA_{67}$–$PCEA_{100}$ diblock copolymer. Cationic PCEA-core nanoparticles are formed at low pH, whereas anionic PDEA cores are formed at high pH. At intermediate solution pH, macroscopic precipitation occurs at the IEP.[179]

Other research groups have also incorporated ionisable repeat units into the hydrophobic core block when conducting RAFT PISA. For example, Hong et al.[180] synthesised diblock copolymer vesicles containing the pH-sensitive comonomer 2-(diisopropylamino)ethyl methacrylate (DIPEMA) in a 80/20 w/w ethanol/water mixture. Such vesicles were loaded with Rhodamine B dye and then transferred to aqueous solution using dialysis. Vesicle dissociation occurred upon adjusting the solution to pH 4.0, owing to protonation of the DIPEMA units within the membrane, causing dye release.

Conversely, Rieger et al.[181] synthesised poly(*N*,*N*-dimethylacrylamide)$_{36}$-poly(*N*-cyanomethyl acrylamide-*stat*-acrylic acid)$_x$ [PDMAC$_{36}$-*b*-P(CMAM-*stat*-AA)$_x$] via RAFT PISA at pH 1.5, as shown in **Figure 1.41**. The core block contained ≤ 20 mol% of the pH-sensitive AA comonomer. CMAM was selected as a comonomer because its corresponding homopolymer exhibits an upper critical solution temperature (UCST) – such thermoresponsive behaviour had been hitherto difficult to introduce into PISA formulations.[182] These copolymers can exist either as self-assembled nanostructures at low pH or as molecularly-dissolved unimers at high pH owing to ionisation of the AA repeat units. Moreover, such copolymers can be designed to be both pH-responsive and thermoresponsive.[181]

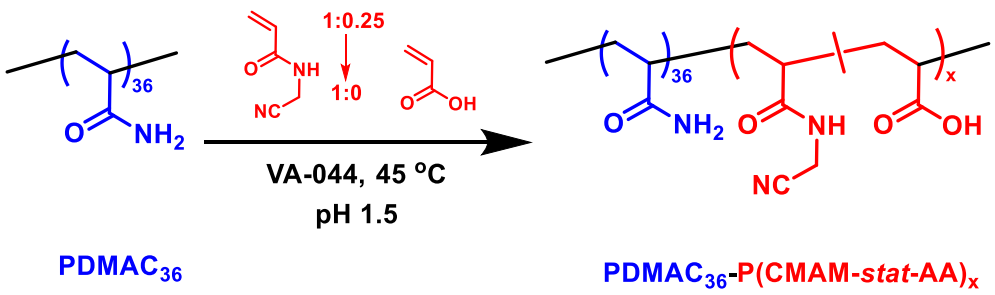

Figure 1.41 PDMAC$_{36}$-P(CMAM-*stat*-AA)$_x$ diblock copolymer nanoparticles synthesised in their neutral form as reported by Rieger et al.[181]

1.6 Ultra High Molecular Weight (UHMW) Polymers

1.6.1 Synthetic Strategies

An interesting synthetic route to ultrahigh molecular weight (UHMW) polyacrylamide (PAM) was reported by Destarac and co-workers via RAFT solution polymerisation of acrylamide using a low-temperature redox initiator, as shown in **Figure 1.42**.[183] The relatively low reaction temperature, unusually high k_p/k_t ratio, high monomer concentration, absence of chain transfer to solvent and an optimised initiation profile with a low flux of radicals were considered to be key parameters for such formulations. A relatively short water-soluble precursor comprising either PAM$_7$ or PDMAC$_7$ was prepared to ensure aqueous solubility of

the xanthate-based RAFT agent. Subsequent chain extension with the corresponding monomer (AM or DMAC) via RAFT solution (gel) polymerisation dramatically increased the solution viscosity. PAM homopolymers up to DP 42,000 and PDMAC homopolymers up to DP 30,000 were synthesised at full monomer conversion within two hours. The theoretical M_n values for these polymers is 3 MDa, but the reported values measured via aqueous and DMF GPC respectively are considerably lower. It is expected that this may be due in part to the resolution of the GPC columns, but more significantly chain transfer reactions leading to new chain growth during the polymerisation. Refractive index and SLS GPC detector used: $PAM_{42,000}$ (M_n = 1.27 MDa; Đ = 1.32) and $PDMAC_{30,000}$ (M_n = 1.04 MDa; Đ = 1.06).

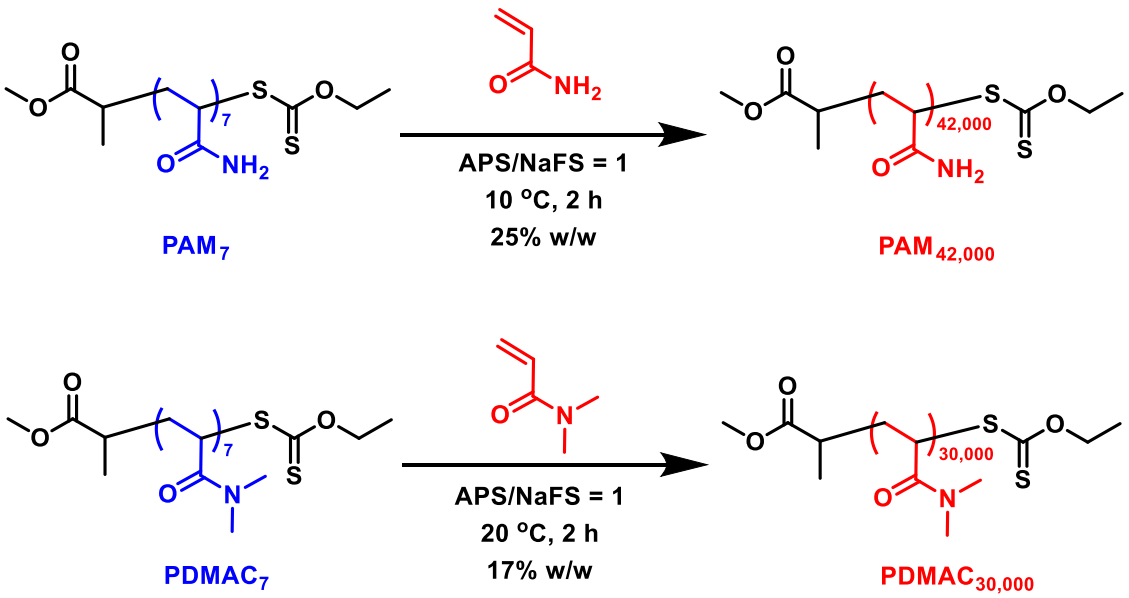

Figure 1.42 $PAM_{42,000}$ and $PDMAC_{30,000}$ polymers prepared at low temperature by aqueous solution gel polymerisation, as reported by Destarac et al.[183]

UHMW PDMAC homopolymers have been synthesised by Sumerlin and co-workers via RAFT photoiniferter polymerisation at 35°C, as shown in **Figure 1.43**.[184] Iniferters induce radical polymerisation to produce polymers bearing an iniferter fragment at each chain-end with minimal bimolecular termination and other transfer reactions.[185,186] A trithiocarbonate and a xanthate RAFT agent were used in turn as iniferters using UV irradiation (λ = 365 nm). An incident wavelength which coincides well with the forbidden n–π* transition has been reported

to result in a faster rate of homolytic cleavage.[184,187,188] The n–π* absorbance wavelength for a xanthate is ≈ 360 nm and a trithiocarbonate is ≈ 443 nm. Hence the photolytic cleavage of xanthates at this wavelength is much more efficient and the experimental M_n data do not significantly exceed theoretical values. This suggests that degenerative chain transfer plays an important role in the consumption of the small-molecule iniferter during the early stages of the reaction.[184]

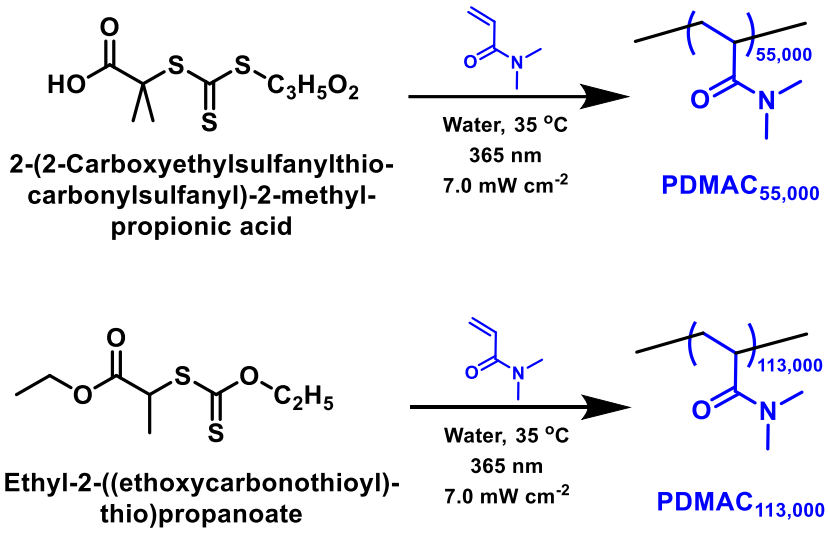

Figure 1.43 $PDMAC_x$ homopolymer synthesised by UV-initiated RAFT solution polymerisation at 35°C using a RAFT iniferter as reported by Sumerlin et al.[184]

More recently, Sumerlin's group has developed an inverse miniemulsion (water-in-oil) polymerisation strategy using a surfactant and a RAFT photoiniferter for the synthesis of UHMW polymers in the form of low-viscosity aqueous droplets.[189] A continuous flow system for the synthesis of UHMW PDMAC or poly(*N*-acryloylmorpholine) (PNAM) provided a much faster rate of polymerisation compared to a batch inverse miniemulsion system.[190] Moreover, good agreement between the theoretical and GPC (light scattering detector) M_n values was observed up to 1 MDa. However, up to a five-fold difference was noted for higher M_n values, with > 99% monomer conversion achieved for all syntheses.[189,190]

While the above-mentioned strategies are undoubtedly very successful for the well-controlled synthesis of UHMW polymers, the resulting highly viscous polymer gels are

impractical for industrial applications. Furthermore, while the inverse miniemulsion strategy is certainly a low-viscosity synthesis, an oil continuous phase is required. This is both economically and environmentally undesirable and post-polymerisation steps are required to remove both excess surfactant and the oil.

1.6.2 Viscosity Modification

Both naturally-derived and synthetic water-soluble polymers are used as viscosity modifiers for a range of commercial applications.[191] These include poly(vinyl alcohol) in ophthalmic products, xanthan gum in toothpaste[192], carrageenan in food products such as ice cream[193], hydrolysed polyacrylamide (a statistical copolymer of acrylamide and acrylic acid) in enhanced oil recovery[194] and cellulose derivatives in latex paints.[195] BASF sells polymeric thickeners in several of their business divisions, including Nutrition & Care, Oilfield and Materials (e.g. paper manufacture).[196–198]

The thickening effect of a polymer in solution depends on its molecular weight. The solution viscosity (η) is governed by the number of chain entanglements, which depend in turn on the polymer concentration and MW. For low MW species, the zero-shear viscosity (η_0) is directly proportional to the mass. However, a power-law relationship between η_0 and MW is observed for higher MW polymers with a numerical exponent of 3.4, as shown in the Mark-Houwink relationship (**Equation 1.20**).[199] M_v is usually comparable within 10% to M_w.[200]

$$\eta_0 = K[DP]^{3.4} \qquad \textbf{(1.20)}$$

When plotting log(η_0) against log MW, Bueche theory predicts that the characteristic change in gradient indicates the critical MW, which corresponds to the average MW spacing between entanglement points.[201] This is shown in **Figure 1.44** for polydimethylsiloxane (PDMS), polyisobutylene (PIB), polyethylene (PE), polybutadiene (PB), poly(methyl methacrylate) (PMMA), poly(ethylene glycol) (PEG), poly(vinyl acetate) (PVAC), and polystyrene (PS).

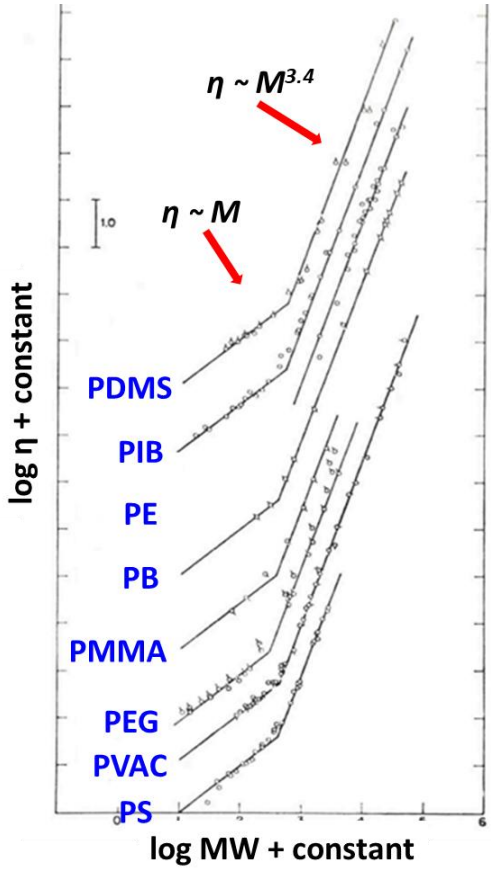

Figure 1.44 Bueche theory predicts that the critical MW of each stated polymer corresponds to the change in gradient for a plot of log(η_0) against log MW. Above this critical MW, the solution viscosity is much more strongly dependent on the polymer MW owing to a higher number of chain entanglements.[201,202]

Many commercial UHMW water-soluble polymers are prepared by FRP, which affords either homopolymers or statistical copolymers with broad MWDs.[203] Lubrizol manufactures a range of *Carbopol* products which comprise crosslinked PAA microgels. Such polymers provide effective rheology modification (solution thickening) for a range of applications, including laundry detergents, surface cleaners and batteries. *Carbopol* products generally exist as powders, though emulsion formulations are also available.[204] *Alcomer* powders made by BASF are marketed as dewatering additives for the oilfield sector. They can clarify dilute drilling fluids by promoting aggregation of colloidal particles in such suspensions. These powders contain both low molecular weight cationic coagulants and high molecular weight non-ionic, anionic, and cationic flocculants.[205] FRP syntheses can also be conducted via

suspension or inverse emulsion (water-in-oil) polymerisation, which remain low-viscosity fluids even at high solids. However, as discussed in **Section 1.6.1,** the resulting copolymers require post-polymerisation processing.[172,189,191]

1.6.3 pH, Temperature and Dilution-Triggered Thickening

Unlike FRP, living polymerisation methods enable the synthesis of low dispersity block copolymers which offer distinct commercial advantages for viscosity modification applications. In particular, RAFT aqueous dispersion polymerisation enables the preparation of diblock copolymer nanoparticles via a low-viscosity route at high solids. To solubilise such low-viscosity dispersions, the solution temperature, pH or salt concentration can be adjusted.[206,207] For example, copolymers that dissolve on switching the solution pH, as discussed in **Section 1.5.4**, can be prepared by these methods. If their MW and solids content are sufficiently high, then a corresponding increase in solution viscosity can be expected.

Cunningham et al. exploited the LCST behaviour of PNMEP to prepare aqueous dispersions of particles at 25% w/w solids using either a $PGMA_{63}$ or a $PMAA_{85}$ precursor, as shown in **Figure 1.45**.[206] PNMEP exhibits an LCST of around 55°C in aqueous solution for DPs above 400. Thus, when targeting a sufficiently high core-forming block DP, these diblock copolymer chains form PNMEP-core particles at their synthesis temperature of 70°C but undergo molecular dissolution on cooling to 20°C. A series of $PGMA_{63}$-$PNMEP_x$ (x = 100 – 6,000) and $PMAA_{85}$-$PNMEP_x$ (x = 300 – 4,000) particles were prepared by RAFT aqueous dispersion polymerisation of NMEP at 70°C. The weakly hydrophobic nature of the PNMEP chains resulted in a high degree of core hydration, producing relatively large particles (~ 1 μm). Variable temperature ^{1}H NMR studies confirmed that the PNMEP chains became substantially dehydrated at 70°C and fully hydrated on cooling to 20°C. Particle dissociation occurs when cooled, which results in the formation of a highly viscous aqueous solution.[206]

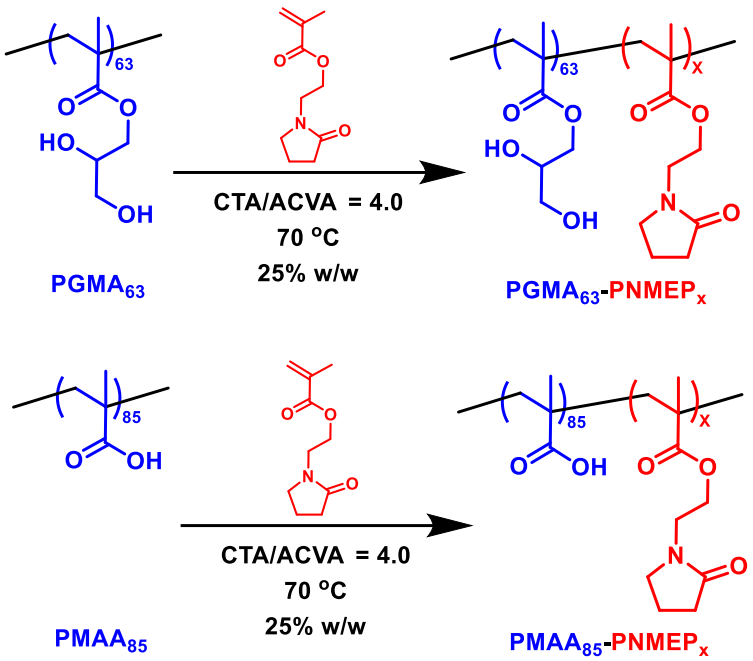

Figure 1.45 Synthesis of low-viscosity $PGMA_{63}$-$PNMEP_x$ and $PMAA_{85}$-$PNMEP_x$ particles via RAFT aqueous dispersion polymerisation of NMEP.[206]

Byard et al. sought to exploit the salt-dependent aqueous solubility of PDMAC to prepare colloidal dispersions of diblock copolymer particles at high solids.[207] DMAC monomer remains water-miscible in the presence of 4.0 M ammonium sulfate, whereas PDMAC is only soluble up to 1.0 M ammonium sulfate. Thus, $PATAC_{100}$-$PDMAC_y$ nanoparticles were prepared at 40% w/w solids via RAFT aqueous dispersion polymerisation of DMAC in the presence of 2.0 M ammonium sulfate, as shown in **Figure 1.46**. To avoid the formation of monomer droplets, it was necessary to slowly drip-feed the DMAC to ensure a true dispersion polymerisation. A relatively high DMAC conversion (>90%) was achieved up to a target DP of 10,000, but unfortunately this aqueous PISA formulation proved to be poorly reproducible and aqueous GPC analysis indicated a bimodal MWD. Nevertheless, four-fold dilution of such turbid free-flowing aqueous dispersions with deionised water led to *in situ* particle dissociation and the formation of a transparent highly viscous solution. Rheology was used to assess the thickening behaviour exhibited by such double-hydrophilic diblock copolymers by comparing

the solution viscosity of the final water-soluble polymer solutions with that of the original particle dispersions prior to dilution.[207]

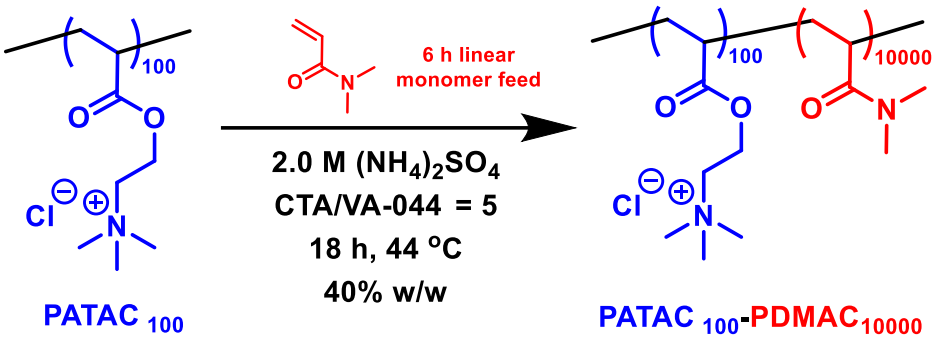

Figure 1.46 Synthesis of $PATAC_{100}$-$PDMAC_{10000}$ particles via RAFT aqueous dispersion polymerisation, as reported by Byard.[207]

Perhaps surprisingly, the studies by Huang et al.[168] and Bai et al.[169] discussed in **Section 1.5.2** do not consider the solubilisation of salt-stabilised polymer nanoparticles by a dilution-triggered thickening effect for UHMW polymers, despite the latter group preparing polymers with M_n ~ 1 MDa.

1.7 Thesis Aims and Outline

The primary aim of this Thesis is to investigate the use of RAFT aqueous dispersion polymerisation formulations to conduct PISA syntheses at 10-30% w/w solids while targeting the highest possible core-forming block DPs. The steric stabiliser block should remain water-soluble while the core-forming block should be tunably soluble or insoluble depending on either the salt concentration or the solution pH.

In **Chapter 2,** preliminary monomer miscibility and homopolymer solubility studies are conducted to identify appropriate steric stabiliser and core-forming blocks for various concentrations of ammonium sulfate. Subsequently, UHMW PATAC-PDMAC particles are synthesised in 2.0 M ammonium sulfate and the behaviour of such salt-responsive diblock copolymers is evaluated. This work extends that originally undertaken by Dr. S. J. Byard during her BASF-sponsored PhD project.[207] In **Chapter 3,** a zwitterionic PMPC steric stabiliser block

that is known to remain water-soluble even at very high salt concentration is chain-extended with DMAC to generate a series of diblock copolymer particles, which are characterised using ^{1}H NMR spectroscopy, aqueous gel permeation chromatography (GPC), dynamic light scattering (DLS), small angle X-ray scattering (SAXS), optical microscopy (OM), rheology and aqueous electrophoresis (Zeta potential). In **Chapter 4,** an anionic PNaAc stabiliser block is used as a precursor for the chain extension of some commodity water-miscible monomers (acrylamide, *N*,*N*-dimethylacrylamide and acrylonitrile). This formulation requires 3.0 M ammonium sulfate to produce a colloidal dispersion of sterically-stabilised particles. In **Chapter 5,** a new wholly non-ionic diblock copolymer system is devised based on a PHEAC steric stabiliser and a PNAM core-forming block. This aqueous PISA formulation requires a relatively low salt concentration to produce particles. Moreover, the resulting PHEAC-PNAM diblock copolymer chains can be analysed using DMF GPC, which aids analysis. In **Chapter 6,** an anionic PAMPS precursor is chain- extended with a pH-sensitive carboxylic acid-based monomer (CEA) at pH 2.5. Under such conditions, the resulting PCEA chains are below their pK_a so they are grown in their neutral hydrophobic form. Raising the solution pH leads to ionisation and hence molecular dissolution of an anionic polyelectrolyte.

1.8 References

1 H. Staudinger, 'Über Polymerisation', *Berichte der Dtsch. Chem. Gesellschaft*, 1920, **53**, 1073–1085.

2 W. H. Carothers, 'Studies on polymerization and ring formation. I. An introduction to the general theory of condensation polymers', *J. Am. Chem. Soc.*, 1929, **51**, 2548–2559.

3 R. Geyer, in *Plastic Waste and Recycling*, ed. T. M. Letcher, Elsevier, Santa Barbara, 2020, pp. 13–32.

4 P. Rikhter, I. Dinc, Y. Zhang, T. Jiang, B. Miyashiro, S. Walsh, R. Wang, Y. Dinh and S. Suh, *Life Cycle Environmental Impacts of Plastics: A Review*, NIST, US Dept of Commerce, 2022.

5 G. Odian, in *Principles of Polymerization*, Wiley, Hoboken, NJ, USA, 2004, pp. 1–38.

6 S. Penczek and G. Moad, 'Glossary of terms related to kinetics, thermodynamics, and mechanisms of polymerization (IUPAC Recommendations 2008)', *Pure Appl. Chem.*, 2008, **80**, 2163–2193.

7 U. W. Jenkins, A. D.; Kratochvíl, P.; Stepto, R. F. T.; Suter, 'International , Union of Pure Glossary of Basic Terms in Polymer', *Pure Appl. Chem.*, 1996, **68**, 2287–2311.

8 R. F. T. Stepto, 'Dispersity in polymer science (IUPAC Recommendations 2009)', *Pure Appl. Chem.*, 2009, **81**, 351–353.

9 J. M. G. Cowie and V. Arrighi, *Polymers*, CRC Press, Boca Raton, 2007.

10 R. J. Young and P. A. Lovell, *Introduction to Polymers*, CRC Press, Boca Raton, 2011.

11 M. S. Chisholm, I. K. Martin and A. T. Slark, 'Facile and cost-effective branched acrylic copolymers from multifunctional comonomers and multifunctional chain transfer agents', *Polym. Chem.*, 2015, **6**, 7333–7341.

12 N. M. Ahmad, B. Charleux, C. Farcet, C. J. Ferguson, S. G. Gaynor, B. S. Hawkett, F. Heatley, B. Klumperman, D. Konkolewicz, P. A. Lovell, K. Matyjaszewski and R. Venkatesh, 'Chain transfer to polymer and branching in controlled radical polymerizations of n-butyl acrylate', *Macromol. Rapid Commun.*, 2009, **30**, 2002–2021.

13 K. Liang and R. A. Hutchinson, 'Solvent effects in semibatch free radical copolymerization of 2-hydroxyethyl methacrylate and styrene at high temperatures', *Macromol. Symp.*, 2013, **325**–**326**, 203–212.

14 E. Laurent, R. Szweda and J. Lutz, in *Macromolecular Engineering*, Wiley, Weinheim, Germany, 2022, pp. 1–34.

15 A. Rudin and P. Choi, in *The Elements of Polymer Science & Engineering*, Elsevier, North York, ON, 3rd edn., 2013, pp. 341–389.

16 K. Matyjaszewski, Y. Gnanou and L. Leibler, *Macromolecular Engineering*, Wiley, Weinheim, Germany, 2007.

17 C. K. Luscombe, G. Moad, R. C. Hiorns, R. G. Jones, D. J. Keddie, J. B. Matson, J. Merna, T. Nakano, G. T. Russell and P. D. Topham, 'A brief guide to polymerization terminology (IUPAC Technical Report)', *Pure Appl. Chem.*, 2022, **94**, 1079–1084.

18 G. Moad and D. H. Solomon, in *The Chemistry of Radical Polymerization*, Elsevier, Kidlington, UK, 2005, pp. 11–48.

19 G. Odian, *Principles of Polymerization*, John Wiley & Sons, Inc., Hoboken, NJ, USA, 4th edn., 2004.

20 W. A. Braunecker and K. Matyjaszewski, 'Controlled/living radical polymerization: Features, developments, and perspectives', *Prog. Polym. Sci.*, 2007, **32**, 93–146.

21 I. Bannister, N. C. Billingham, S. P. Armes, S. P. Rannard and P. Findlay, 'Development of branching in living radical copolymerization of vinyl and divinyl monomers', *Macromolecules*, 2006, **39**, 7483–7492.

22 J.-P. Montheard, M. Chatzopoulos and D. Chappard, '2-Hydroxyethyl Methacrylate (HEMA): Chemical Properties and Applications in Biomedical Fields', *J. Macromol. Sci. Part C Polym. Rev.*, 1992, **32**, 1–34.

23 C. . H. Bamford, R. . W. Dyson and G. . C. Eastmond, 'Network formation IV. The nature of the termination reaction in free-radical polymerization', *Polymer*, 1969, **10**, 885–899.

24 O. F. Olaj, J. W. Breitenbach and B. Wolf, 'Untersuchungen über Molekulargewichtsverteilungen von Hochpolymeren, 6. Mitt.: Zum Problem des Disproportionierungsabbruchs bei der gestarteten Polymerisation des Styrols', *Monatshefte für Chemie und verwandte Teile anderer Wissenschaften*, 1964, **95**, 1646–1655.

25 K. C. Berger and G. Meyerhoff, 'Disproportionierung und kombination als abbruchmechanismen bei der radikalischen polymerisation von styrol, 1.Versuche mit 14C-markierten 2,2′-azoisobutyronitril', *Die Makromol. Chemie*, 1975, **176**, 1983–2003.

26 F. S. Dainton, 'Atoms and radicals in aqueous media. The tilden lecture, delivered before the chemical

society at Burlington House on February 15th, 1981, and at the university college, Hull, on March Ist, 1951', *J. Chem. Soc.*, 1952, **104**, 1533.

27 R. G. R. Bacon, 'The initiation of polymerisation processes by redox catalysts', *Quart. Rev. Chem. Soc.*, 1955, **9**, 287–310.

28 J. H. Baxendale, M. G. Evans and C. S. Park, 'The mechanism and kinetics of the initiation of polymerisation by systems containing hydrogen peroxide', *Trans. Faraday Soc.*, 1946, **42**, 155.

29 D. J. Lamb, C. M. Fellows and R. G. Gilbert, 'Radical entry mechanisms in redox-initiated emulsion polymerizations', *Polymer*, 2005, **46**, 7874–7895.

30 R. P. Quirk and B. Lee, 'Experimental Criteria for Living Polymerizations', *Polym. Int.*, 1992, **27**, 359–367.

31 J. Chiefari, R. T. A. Mayadunne, C. L. Moad, Graeme Moad, E. Rizzardo, A. Postma and S. H. Thang, 'Thiocarbonylthio Compounds (SC(Z)S−R) in Free Radical Polymerization with Reversible Addition-Fragmentation Chain Transfer (RAFT Polymerization). Effect of the Activating Group Z', *Macromolecules*, 2003, **66**, 2273–2283.

32 A. D. Jenkins, R. G. Jones and G. Moad, 'Terminology for reversible-deactivation radical polymerization previously called "controlled" radical or "living" radical polymerization (IUPAC Recommendations 2010)', *Pure Appl. Chem.*, 2009, **82**, 483–491.

33 M. Szwarc, M. Levy and R. Milkovich, 'Polymerization initiated by electron transfer to monomer. A new method of formation of block polymers', *J. Am. Chem. Soc.*, 1956, **78**, 2656–2657.

34 N. Hadjichristidis, M. Pitsikalis, S. Pispas and H. Iatrou, 'Polymers with complex architecture by living anionic polymerization', *Chem. Rev.*, 2001, **101**, 3747–3792.

35 K. Matyjaszewski and T. P. Davis, *Handbook of Radical Polymerization*, John Wiley & Sons, Inc., Hoboken, NJ, USA, 2002.

36 A. D. Jenkins, R. G. Jones and G. Moad, 'Terminology for reversible-deactivation radical polymerization previously called "controlled" radical or "living" radical polymerization (IUPAC Recommendations 2010)', *Pure Appl. Chem.*, 2009, **82**, 483–491.

37 S. Penczek and G. Moad, 'Glossary of terms related to kinetics, thermodynamics, and mechanisms of polymerization (IUPAC Recommendations 2008)', *Pure Appl. Chem.*, 2008, **80**, 2163–2193.

38 R. B. Grubbs, 'Nitroxide-mediated radical polymerization: Limitations and versatility', *Polym. Rev.*, 2011, **51**, 104–137.

39 N. P. Truong, G. R. Jones, K. G. E. Bradford, D. Konkolewicz and A. Anastasaki, 'A comparison of RAFT and ATRP methods for controlled radical polymerization', *Nat. Rev. Chem.*, 2021, **5**, 859–869.

40 J. Chiefari, Y. K. (Bill) Chong, F. Ercole, J. Krstina, J. Jeffery, T. P. T. T. Le, R. T. A. A. Mayadunne, G. F. Meijs, C. L. Moad, G. Moad, E. Rizzardo and S. H. Thang, 'Living Free-Radical Polymerization by Reversible Addition−Fragmentation Chain Transfer: The RAFT Process', *Macromolecules*, 1998, **31**, 5559–5562.

41 K. Matyjaszewski, 'Discovery of the RAFT Process and Its Impact on Radical Polymerization', *Macromolecules*, 2020, **53**, 495–497.

42 G. Moad, E. Rizzardo and S. H. Thang, 'Toward Living Radical Polymerization', *Acc. Chem. Res.*, 2008, **41**, 1133–1142.

43 G. Moad, E. Rizzardo and S. H. Thang, 'Radical addition–fragmentation chemistry in polymer synthesis', *Polymer*, 2008, **49**, 1079–1131.

44 G. Moad, E. Rizzardo and S. H. Thang, 'Living Radical Polymerization by the RAFT Process - A Second Update', *Aust. J. Chem.*, 2009, **62**, 1402.

45 G. Moad, E. Rizzardo and S. H. Thang, 'Living Radical Polymerization by the RAFT Process – A Third Update', *Aust. J. Chem.*, 2012, **65**, 985.

46 C. Barner-Kowollik, *Handbook of RAFT Polymerization*, Wiley, Darmstadt, 2008.

47 S. W. Prescott, M. J. Ballard, E. Rizzardo and R. G. Gilbert, 'Successful use of RAFT techniques in seeded emulsion polymerization of styrene: Living character, RAFT agent transport, and rate of polymerization', *Macromolecules*, 2002, **35**, 5417–5425.

48 M. Lansalot, T. P. Davis and J. P. A. Heuts, 'RAFT miniemulsion polymerization: Influence of the structure of the RAFT agent', *Macromolecules*, 2002, **35**, 7582–7591.

49 K. Parkatzidis, N. P. Truong, M. N. Antonopoulou, R. Whitfield, D. Konkolewicz and A. Anastasaki, 'Tailoring polymer dispersity by mixing chain transfer agents in PET-RAFT polymerization', *Polym. Chem.*, 2020, **11**, 4968–4972.

50 B. Tilottama, K. Manojkumar, P. M. Haribabu and K. Vijayakrishna, 'A short review on RAFT polymerization of less activated monomers', *J. Macromol. Sci. Part A Pure Appl. Chem.*, 2022, **59**, 180–201.

51 S. Perrier and P. Takolpuckdee, 'Macromolecular design via reversible addition-fragmentation chain transfer (RAFT)/xanthates (MADIX) polymerization', *J. Polym. Sci. Part A Polym. Chem.*, 2005, **43**, 5347–5393.

52 A. Goto and T. Fukuda, 'Kinetics of living radical polymerization', *Prog. Polym. Sci.*, 2004, **29**, 329–385.

53 M. J. Monteiro and H. De Brouwer, 'Intermediate radical termination as the mechanism for retardation in reversible addition-fragmentation chain transfer polymerization', *Macromolecules*, 2001, **34**, 349–352.

54 C. Barner-Kowollik, J. F. Quinn, D. R. Morsley and T. P. Davis, 'Modeling the reversible addition-fragmentation chain transfer process in cumyl dithiobenzoate-mediated styrene homopolymerizations: Assessing rate coefficients for the addition-fragmentation equilibrium', *J. Polym. Sci. Part A Polym. Chem.*, 2001, **39**, 1353–1365.

55 S. Perrier, C. Barner-Kowollik, J. F. Quinn, P. Vana and T. P. Davis, 'Origin of inhibition effects in the reversible addition fragmentation chain transfer (RAFT) polymerization of methyl acrylate', *Macromolecules*, 2002, **35**, 8300–8306.

56 M. S. Donovan, A. B. Lowe, B. S. Sumerlin and C. L. McCormick, 'Raft polymerization of N,N-dimethylacrylamide utilizing novel chain transfer agents tailored for high reinitiation efficiency and structural control', *Macromolecules*, 2002, **35**, 4123–4132.

57 S. J. Byard, A. Blanazs, J. F. Miller and S. P. Armes, 'Cationic Sterically Stabilized Diblock Copolymer Nanoparticles Exhibit Exceptional Tolerance toward Added Salt', *Langmuir*, 2019, **35**, 14348–14357.

58 P. Saindane and R. N. Jagtap, 'RAFT copolymerization of amphiphilic poly (ethyl acrylate-b-acrylicacid) as wetting and dispersing agents for water borne coating', *Prog. Org. Coatings*, 2015, **79**, 106–114.

59 S. Perrier, '50th Anniversary Perspective: RAFT Polymerization - A User Guide', *Macromolecules*, 2017, **50**, 7433–7447.

60 A. Feldermann, M. L. Coote, M. H. Stenzel, T. P. Davis and C. Barner-Kowollik, 'Consistent Experimental and Theoretical Evidence for Long-Lived Intermediate Radicals in Living Free Radical Polymerization', *J. Am. Chem. Soc.*, 2004, **126**, 15915–15923.

61 L. Martin, G. Gody and S. Perrier, 'Preparation of complex multiblock copolymers via aqueous RAFT polymerization at room temperature', *Polym. Chem.*, 2015, **6**, 4875–4886.

62 I. de F. A. Mariz, J. R. Leiza and J. C. De la Cal, 'Competitive particle growth: A tool to control the particle size distribution for the synthesis of high solids content low viscosity latexes', *Chem. Eng. J.*, 2011, **168**, 938–946.

63 X. Tian, J. Ding, B. Zhang, F. Qiu, X. Zhuang and Y. Chen, 'Recent Advances in RAFT Polymerization: Novel Initiation Mechanisms and Optoelectronic Applications', *Polymers*, 2018, **10**, 318.

64 L. Martin, G. Gody and S. Perrier, 2018, pp. 57–79.

65 S. J. Byard, C. T. O'Brien, M. J. Derry, M. Williams, O. O. Mykhaylyk, A. Blanazs and S. P. Armes, 'Unique aqueous self-assembly behavior of a thermoresponsive diblock copolymer', *Chem. Sci.*, 2020, **11**, 396–402.

66 O. J. Deane, J. R. Lovett, O. M. Musa, A. Fernyhough and S. P. Armes, 'Synthesis of Well-Defined Pyrrolidone-Based Homopolymers and Stimulus-Responsive Diblock Copolymers via RAFT Aqueous Solution Polymerization of 2-(N-Acryloyloxy)ethylpyrrolidone', *Macromolecules*, 2018, **51**, 7756–7766.

67 G. M. Whitesides and B. Grzybowski, 'Self-assembly at all scales', *Science*, 2002, **295**, 2418–2421.

68 J. N. Israelachvili, D. J. Mitchell and B. W. Ninham, 'Theory of self-assembly of hydrocarbon amphiphiles into micelles and bilayers', *J. Chem. Soc. Faraday Trans. 2 Mol. Chem. Phys.*, 1976, **72**, 1525–1568.

69 J. N. Israelachvili, in *Intermolecular and Surface Forces*, Elsevier, Online, 2011, pp. 503–576.

70 A. Blanazs, S. P. Armes and A. J. Ryan, 'Self-assembled block copolymer aggregates: From micelles to vesicles and their biological applications', *Macromol. Rapid Commun.*, 2009, **30**, 267–277.

71 S. L. Canning, G. N. Smith and S. P. Armes, 'A Critical Appraisal of RAFT-Mediated Polymerization-Induced Self-Assembly', *Macromolecules*, 2016, **49**, 1985–2001.

72 P. J. Flory, 'Thermodynamics of High Polymer Solutions', *J. Chem. Phys.*, 1942, **10**, 51–61.

73 M. L. Huggins, 'Theory of Solutions of High Polymers', *J. Am. Chem. Soc.*, 1942, **64**, 1712–1719.

74 M. Lazzari, G. Liu and S. Lecommandoux, *Block Copolymers in Nanoscience*, Wiley, 2006.

75 Y. Mai and A. Eisenberg, 'Self-assembly of block copolymers', *Chem. Soc. Rev.*, 2012, **41**, 5969–5985.

76 G. H. Fredrickson and F. S. Bates, 'Dynamics of Block Copolymers: Theory and Experiment', *Annu. Rev. Mater. Sci.*, 1996, **26**, 501–550.

77 F. S. Bates, 'Polymer-Polymer Phase Behavior', *Science*, 1991, **251**, 898–905.

78 L. Leibler, 'Theory of Microphase Separation in Block Copolymers', *Macromolecules*, 1980, **13**, 1602–1617.

79 Z. Gao and A. Eisenberg, 'A Model of Micellization for Block Copolymers in Solutions', *Macromolecules*, 1993, **26**, 7353–7360.

80 Z. Gao, S. K. Varshney, S. Wong and A. Eisenberg, 'Block Copolymer "Crew-Cut" Micelles in Water', *Macromolecules*, 1994, **27**, 7923–7927.

81 L. Zhang and A. Eisenberg, 'Multiple morphologies of "crew-cut" aggregates of polystyrene-b-

poly(acrylic acid) block copolymers', *Science*, 1995, **268**, 1728–1731.

82 K. Yu, L. Zhang and A. Eisenberg, 'Novel morphologies of "crew-cut" aggregates of amphiphilic diblock copolymers in dilute solution', *Langmuir*, 1996, **12**, 5980–5984.

83 H. Shamsijazeyi, C. A. Miller, M. S. Wong, J. M. Tour and R. Verduzco, 'Polymer-coated nanoparticles for enhanced oil recovery', *J. Appl. Polym. Sci.*, 2014, **131**, 1–13.

84 S. Creutz, R. Jérôme, G. M. P. Kaptijn, A. W. Van Der Werf and J. M. Akkerman, 'Design of polymeric dispersants for waterborne coatings', *J. Coatings Technol.*, 1998, **70**, 41–46.

85 C. de las H. Alarcón, S. Pennadam and C. Alexander, 'Stimuli responsive polymers for biomedical applications', *Chem. Soc. Rev.*, 2005, **34**, 276–285.

86 B. Perlatti, P. L. de Souza Bergo, M. F. das G. Fernandes da Silva, J. Batista and M. Rossi, in *Insecticides - Development of Safer and More Effective Technologies (ch 20)*, InTechOpen, Online, 2013.

87 M. Okubo, *Polymer Particles*, Springer Berlin Heidelberg, Berlin, Heidelberg, 2005, vol. 175.

88 D. H. Napper and A. Netschey, 'Studies of the steric stabilization of colloidal particles', *J. Colloid Interface Sci.*, 1971, **37**, 528–535.

89 D. H. Napper, 'Steric stabilization', *J. Colloid Interface Sci.*, 1977, **58**, 390–407.

90 T. F. Tadros, *Basic Principles of Interface Science and Colloid Stability*, Walter de Gruyter GmbH, Berlin, 2017.

91 J. N. Israelachvili, in *Intermolecular and Surface Forces*, Elsevier, Online, 2011, pp. 577–616.

92 M. Gouy, 'Sur la constitution de la charge électrique à la surface d'un électrolyte', *J. Phys. Théorique Appliquée*, 1910, **9**, 457–468.

93 D. L. Chapman, 'LI. A contribution to the theory of electrocapillarity', *London, Edinburgh, Dublin Philos. Mag. J. Sci.*, 1913, **25**, 475–481.

94 O. Stern, 'Zur Theorie der Elektrolytischen Doppelschicht', *Zeitschrift für Elektrochemie und Angew. Phys. Chemie*, 1924, **30**, 508–516.

95 D. C. Grahame, 'The Electrical Double Layer and the Theory of Electrocapillarity.', *Chem. Rev.*, 1947, **41**, 441–501.

96 L. Landau and B. Derjaguin, 'Theory of Stability of Highly Charged Lyophobic Sols and Adhesion of Highly Charged Particles in Solutions of Electrolytes', *Z. Eksp. I Teor. Fiz.*, 1945, **15**, 663–682.

97 E. J. W. Verwey and J. T. G. Overbeek, *Theory of the stability of lyophilic colloids*, Elsevier, Amsterdam, 1948.

98 M. Daoud and C. E. Williams, *Soft Matter Physics*, Springer Berlin Heidelberg, Berlin, Heidelberg, 1999.

99 A. G. Goicochea, M. A. B. Altamirano, R. Lopez-Esparza, M. A. Waldo-Mendoza and E. Perez, 'On the computational modeling of the viscosity of colloidal dispersions and its relation with basic molecular interactions', *Eur. J. Phys.*, 2015, **36**, 055032.

100 A. Cardellini, M. Fasano, M. Bozorg Bigdeli, E. Chiavazzo and P. Asinari, 'Thermal transport phenomena in nanoparticle suspensions', *J. Phys. Condens. Matter*, 2016, **28**, 483003.

101 H. Schulze, 'Schwefelarsen in wässriger Lösung', *J. für Prakt. Chemie*, 1882, **25**, 431–452.

102 W. B. Hardy, 'A preliminary investigation of the conditions which determine the stability of irreversible hydrosols', *Proc. R. Soc. London*, 1900, **66**, 110–125.

103 G. Trefalt, I. Szilágyi and M. Borkovec, 'Schulze-Hardy rule revisited', *Colloid Polym. Sci.*, 2020, **298**,

961–967.

104 T. Oncsik, A. Desert, G. Trefalt, M. Borkovec and I. Szilagyi, 'Charging and aggregation of latex particles in aqueous solutions of ionic liquids: Towards an extended Hofmeister series', *Phys. Chem. Chem. Phys.*, 2016, **18**, 7511–7520.

105 J. L.-M. Poiseuille, 'Experimental Investigations on the Flow of Liquids in Tubes of Very Small Diameter', *Ann. Chim. Phys.*, 1847, **21**, 76.

106 G. Jones and M. Dole, 'The Viscosity of Aqueous Solutions of Strong Electrolytes with Special Reference to Barium Chloride', *J. Am. Chem. Soc.*, 1929, **51**, 2950–2964.

107 K. P. Gregory, G. R. Elliott, H. Robertson, A. Kumar, E. J. Wanless, G. B. Webber, V. S. J. Craig, G. G. Andersson and A. J. Page, 'Understanding specific ion effects and the Hofmeister series', *Phys. Chem. Chem. Phys.*, 2022, **24**, 12682–12718.

108 K. Wynne, 'The Mayonnaise Effect', *J. Phys. Chem. Lett.*, 2017, **8**, 6189–6192.

109 J. R. Lovett, N. J. Warren, L. P. D. Ratcliffe, M. K. Kocik and S. P. Armes, 'pH-responsive non-ionic diblock copolymers: Ionization of carboxylic acid end-groups induces an order-order morphological transition', *Angew. Chemie - Int. Ed.*, 2015, **54**, 1279–1283.

110 J. R. Lovett, N. J. Warren, S. P. Armes, M. J. Smallridge and R. B. Cracknell, 'Order–Order Morphological Transitions for Dual Stimulus Responsive Diblock Copolymer Vesicles', *Macromolecules*, 2016, **49**, 1016–1025.

111 N. J. W. Penfold, J. R. Lovett, N. J. Warren, P. Verstraete, J. Smets and S. P. Armes, 'PH-Responsive non-ionic diblock copolymers: Protonation of a morpholine end-group induces an order-order transition', *Polym. Chem.*, 2016, **7**, 79–88.

112 N. J. W. Penfold, J. R. Lovett, P. Verstraete, J. Smets and S. P. Armes, 'Stimulus-responsive non-ionic diblock copolymers: Protonation of a tertiary amine end-group induces vesicle-to-worm or vesicle-to-sphere transitions', *Polym. Chem.*, 2017, **8**, 272–282.

113 P. Biais, P. Beaunier, F. Stoffelbach and J. Rieger, 'Loop-stabilized BAB triblock copolymer morphologies by PISA in water', *Polym. Chem.*, 2018, **9**, 4483–4491.

114 R. R. Gibson, S. P. Armes, O. M. Musa and A. Fernyhough, 'End-group ionisation enables the use of poly(: N -(2-methacryloyloxy)ethyl pyrrolidone) as an electrosteric stabiliser block for polymerisation-induced self-assembly in aqueous media', *Polym. Chem.*, 2019, **10**, 1312–1323.

115 D. L. Beattie, O. J. Deane, O. O. Mykhaylyk and S. P. Armes, 'RAFT aqueous dispersion polymerization of 4-hydroxybutyl acrylate: Effect of end-group ionization on the formation and colloidal stability of sterically-stabilized diblock copolymer nanoparticles', *Polym. Chem.*, 2022, **13**, 655–667.

116 O. J. Deane, J. Jennings, T. J. Neal, O. M. Musa, A. Fernyhough and S. P. Armes, 'Synthesis and Aqueous Solution Properties of Shape-Shifting Stimulus-Responsive Diblock Copolymer Nano-Objects', *Chem. Mater.*, 2021, **33**, 7767–7779.

117 D. H. Napper, *Polymeric Stabilization of Colloidal Dispersions*, Academic Press, London, 1983.

118 M. B. Einarson and J. C. Berg, 'Electrosteric stabilization of colloidal latex dispersions', *J. Colloid Interface Sci.*, 1993, **155**, 165–172.

119 J. Cesarano, I. A. Aksay and A. Bleier, 'Stability of Aqueous alpha-Al2O3 Suspensions with Poly(methacrylic acid) Polyelectrolyte', *J. Am. Ceram. Soc.*, 1988, **71**, 250–255.

120 N. J. Warren and S. P. Armes, 'Polymerization-induced self-assembly of block copolymer nano-objects via RAFT aqueous dispersion polymerization', *J. Am. Chem. Soc.*, 2014, **136**, 10174–10185.

121 M. J. Derry, L. A. Fielding and S. P. Armes, 'Industrially-relevant polymerization-induced self-assembly formulations in non-polar solvents: RAFT dispersion polymerization of benzyl methacrylate', *Polym. Chem.*, 2015, **6**, 3054–3062.

122 M. J. Derry, L. A. Fielding and S. P. Armes, 'Polymerization-induced self-assembly of block copolymer nanoparticles via RAFT non-aqueous dispersion polymerization', *Prog. Polym. Sci.*, 2016, **52**, 1–18.

123 J. Rieger, G. Osterwinter, C. Bui, F. Stoffelbnach and B. Charleux, 'Surfactant-free controlled/living radical emulsion (Co)polymerization of n-butyl acrylate and methyl methacrylate via RAFT using amphiphilic polyethylene oxide-based trithiocarbonate chain transfer agents', *Macromolecules*, 2009, **42**, 5518–5525.

124 A. Blanazs, J. Madsen, G. Battaglia, A. J. Ryan and S. P. Armes, 'Mechanistic insights for block copolymer morphologies: How do worms form vesicles?', *J. Am. Chem. Soc.*, 2011, **133**, 16581–16587.

125 N. J. W. Penfold, J. Yeow, C. Boyer and S. P. Armes, 'Emerging Trends in Polymerization-Induced Self-Assembly', *ACS Macro Lett.*, 2019, **8**, 1029–1054.

126 C. J. Ferguson, R. J. Hughes, B. T. T. Pham, B. S. Hawkett, R. G. Gilbert, A. K. Serelis and C. H. Such, 'Effective ab initio emulsion polymerization under RAFT control', *Macromolecules*, 2002, **35**, 9243–9245.

127 J. T. Sun, C. Y. Hong and C. Y. Pan, 'Formation of the block copolymer aggregates via polymerization-induced self-assembly and reorganization', *Soft Matter*, 2012, **8**, 7753–7767.

128 J. Rieger, F. Stoffelbach, C. Bui, D. Alaimo, C. Jérôme and B. Charleux, 'Amphiphilic poly(ethylene oxide) macromolecular RAFT agent as a stabilizer and control agent in ab initio batch emulsion polymerization', *Macromolecules*, 2008, **41**, 4065–4068.

129 X. Zhang, S. Boissé, W. Zhang, P. Beaunier, F. D'Agosto, J. Rieger, B. Charleux, F. D'Agosto, J. Rieger and B. Charleux, 'Well-Defined Amphiphilic Block Copolymers and Nano-objects Formed in Situ via RAFT-Mediated Aqueous Emulsion Polymerization', *Macromolecules*, 2011, **44**, 4149–4158.

130 W. Zhang, F. D'Agosto, O. Boyron, J. Rieger and B. Charleux, 'Toward a Better Understanding of the Parameters that Lead to the Formation of Nonspherical Polystyrene Particles via RAFT-Mediated One-Pot Aqueous Emulsion Polymerization', *Macromolecules*, 2012, **45**, 4075–4084.

131 Z. An, Q. Shi, W. Tang, C. K. Tsung, C. J. Hawker and G. D. Stucky, 'Facile RAFT precipitation polymerization for the microwave-assisted synthesis of well-defined, double hydrophilic block copolymers and nanostructured hydrogels', *J. Am. Chem. Soc.*, 2007, **129**, 14493–14499.

132 M. Heskins and J. E. Guillet, 'Solution Properties of Poly(N-isopropylacrylamide)', *J. Macromol. Sci. Part A - Chem.*, 1968, **2**, 1441–1455.

133 S. Qin, Y. Geng, D. E. Discher and S. Yang, 'Temperature-Controlled Assembly and Release from Polymer Vesicles of Poly(ethylene oxide)-block- poly(N-isopropylacrylamide)', *Adv. Mater.*, 2006, **18**, 2905–2909.

134 M. Lansalot and J. Rieger, 'Polymerization-Induced Self-Assembly', *Macromol. Rapid Commun.*, 2019, **40**, 1–3.

135 S. L. Canning, G. N. Smith and S. P. Armes, 'A Critical Appraisal of RAFT-Mediated Polymerization-

Induced Self-Assembly', *Macromolecules*, 2016, **49**, 1985–2001.

136 Y. Li and S. P. Armes, 'RAFT Synthesis of Sterically Stabilized Methacrylic Nanolatexes and Vesicles by Aqueous Dispersion Polymerization', *Angew. Chemie*, 2010, **122**, 4136–4140.

137 A. Blanazs, A. J. Ryan and S. P. Armes, 'Predictive phase diagrams for RAFT aqueous dispersion polymerization: Effect of block copolymer composition, molecular weight, and copolymer concentration', *Macromolecules*, 2012, **45**, 5099–5107.

138 R. Verber, A. Blanazs and S. P. Armes, 'Rheological studies of thermo-responsive diblock copolymer worm gels', *Soft Matter*, 2012, **8**, 9915–9922.

139 M. K. Kocik, O. O. Mykhaylyk and S. P. Armes, 'Aqueous worm gels can be reconstituted from freeze-dried diblock copolymer powder', *Soft Matter*, 2014, **10**, 3984–3992.

140 S. Jain, 'On the Origins of Morphological Complexity in Block Copolymer Surfactants', *Science.*, 2003, **300**, 460–464.

141 N. J. Warren, M. J. Derry, O. O. Mykhaylyk, J. R. Lovett, L. P. D. Ratcliffe, V. Ladmiral, A. Blanazs, L. A. Fielding and S. P. Armes, 'Critical Dependence of Molecular Weight on Thermoresponsive Behavior of Diblock Copolymer Worm Gels in Aqueous Solution', *Macromolecules*, 2018, **51**, 8357–8371.

142 M. Williams, N. J. W. Penfold, J. R. Lovett, N. J. Warren, C. W. I. Douglas, N. Doroshenko, P. Verstraete, J. Smets and S. P. Armes, 'Bespoke cationic nano-objects: Via RAFT aqueous dispersion polymerisation', *Polym. Chem.*, 2016, **7**, 3864–3873.

143 S. Sugihara, A. Blanazs, S. P. Armes, A. J. Ryan and A. L. Lewis, 'Aqueous dispersion polymerization: A new paradigm for in situ block copolymer self-assembly in concentrated solution', *J. Am. Chem. Soc.*, 2011, **133**, 15707–15713.

144 L. A. Fielding, M. J. Derry, V. Ladmiral, J. Rosselgong, A. M. Rodrigues, L. P. D. Ratcliffe, S. Sugihara and S. P. Armes, 'RAFT dispersion polymerization in non-polar solvents: Facile production of block copolymer spheres, worms and vesicles in n-alkanes', *Chem. Sci.*, 2013, **4**, 2081–2087.

145 J. Tan, D. Liu, Y. Bai, C. Huang, X. Li, J. He, Q. Xu and L. Zhang, 'Enzyme-Assisted Photoinitiated Polymerization-Induced Self-Assembly: An Oxygen-Tolerant Method for Preparing Block Copolymer Nano-Objects in Open Vessels and Multiwell Plates', *Macromolecules*, 2017, **50**, 5798–5806.

146 D. Zhou, S. Dong, R. P. Kuchel, S. Perrier and P. B. Zetterlund, 'Polymerization induced self-assembly: tuning of morphology using ionic strength and pH', *Polym. Chem.*, 2017, **8**, 3082–3089.

147 S. J. Byard, M. Williams, B. E. McKenzie, A. Blanazs and S. P. Armes, 'Preparation and Cross-Linking of All-Acrylamide Diblock Copolymer Nano-Objects via Polymerization-Induced Self-Assembly in Aqueous Solution', *Macromolecules*, 2017, **50**, 1482–1493.

148 J. C. Foster, S. Varlas, B. Couturaud, J. R. Jones, R. Keogh, R. T. Mathers and R. K. O'Reilly, 'Predicting Monomers for Use in Polymerization-Induced Self-Assembly', *Angew. Chemie - Int. Ed.*, 2018, **57**, 15733–15737.

149 W. Zhou, Q. Qu, Y. Xu and Z. An, 'Aqueous polymerization-induced self-assembly for the synthesis of ketone-functionalized nano-objects with low polydispersity', *ACS Macro Lett.*, 2015, **4**, 495–499.

150 A. Blanazs, A. J. Ryan and S. P. Armes, 'Predictive phase diagrams for RAFT aqueous dispersion polymerization: Effect of block copolymer composition, molecular weight, and copolymer concentration', *Macromolecules*, 2012, **45**, 5099–5107.

151 C. György, S. J. Hunter, C. Girou, M. J. Derry and S. P. Armes, 'Synthesis of poly(stearyl methacrylate)-poly(2-hydroxypropyl methacrylate) diblock copolymer nanoparticles via RAFT dispersion polymerization of 2-hydroxypropyl methacrylate in mineral oil', *Polym. Chem.*, 2020, **11**, 4579–4590.

152 Y. Pei, A. B. Lowe and P. J. Roth, 'Stimulus-Responsive Nanoparticles and Associated (Reversible) Polymorphism via Polymerization Induced Self-assembly (PISA)', *Macromol. Rapid Commun.*, 2017, **38**, 1–14.

153 J. Rieger, 'Guidelines for the Synthesis of Block Copolymer Particles of Various Morphologies by RAFT Dispersion Polymerization', *Macromol. Rapid Commun.*, 2015, **36**, 1458–1471.

154 R. K. O'Reilly, C. J. Hawker and K. L. Wooley, 'Cross-linked block copolymer micelles: Functional nanostructures of great potential and versatility', *Chem. Soc. Rev.*, 2006, **35**, 1068–1083.

155 N. Sanson and J. Rieger, 'Synthesis of nanogels/microgels by conventional and controlled radical crosslinking copolymerization', *Polym. Chem.*, 2010, **1**, 965–977.

156 K. L. Thompson, C. J. Mable, A. Cockram, N. J. Warren, V. J. Cunningham, E. R. Jones, R. Verber and S. P. Armes, 'Are block copolymer worms more effective Pickering emulsifiers than block copolymer spheres?', *Soft Matter*, 2014, **10**, 8615–8626.

157 P. Chambon, A. Blanazs, G. Battaglia and S. P. Armes, 'Facile synthesis of methacrylic ABC triblock copolymer vesicles by RAFT aqueous dispersion polymerization', *Macromolecules*, 2012, **45**, 5081–5090.

158 P. Chambon, A. Blanazs, G. Battaglia and S. P. Armes, 'How does cross-linking affect the stability of block copolymer vesicles in the presence of surfactant?', *Langmuir*, 2012, **28**, 1196–1205.

159 J. Chen, C. E. Frazier and K. J. Edgar, 'In situ forming hydrogels based on oxidized hydroxypropyl cellulose and Jeffamines', *Cellulose*, 2021, **28**, 11367–11380.

160 S. Dacrory, 'Development of mesoporous foam based on dicarboxylic cellulose and graphene oxide for potential oil/water separation', *Polym. Bull.*, 2022, **79**, 9563–9574.

161 Q. Qu, G. Liu, X. Lv, B. Zhang and Z. An, 'In Situ Cross-Linking of Vesicles in Polymerization-Induced Self-Assembly', *ACS Macro Lett.*, 2016, **5**, 316–320.

162 H. Willcock and R. K. O'Reilly, 'End group removal and modification of RAFT polymers', *Polym. Chem.*, 2010, **1**, 149–157.

163 P. Alagi, N. Hadjichristidis, Y. Gnanou and X. Feng, 'Fast and Complete Neutralization of Thiocarbonylthio Compounds Using Trialkylborane and Oxygen: Application to Their Removal from RAFT-Synthesized Polymers', *ACS Macro Lett.*, 2019, **8**, 664–669.

164 C. P. Jesson, C. M. Pearce, H. Simon, A. Werner, V. J. Cunningham, J. R. Lovett, M. J. Smallridge, N. J. Warren and S. P. Armes, 'H2O2 enables convenient removal of RAFT end-groups from block copolymer nano-objects prepared via polymerization-induced self- assembly in water', *Macromolecules*, 2017, **50**, 182–191.

165 K. Skrabania, A. Miasnikova, A. M. Bivigou-Koumba, D. Zehm and A. Laschewsky, 'Examining the UV-vis absorption of RAFT chain transfer agents and their use for polymer analysis', *Polym. Chem.*, 2011, **2**, 2074–2083.

166 E. J. Cornel, S. Van Meurs, T. Smith, P. S. O'Hora and S. P. Armes, 'In Situ Spectroscopic Studies of Highly Transparent Nanoparticle Dispersions Enable Assessment of Trithiocarbonate Chain-End Fidelity

during RAFT Dispersion Polymerization in Nonpolar Media', *J. Am. Chem. Soc.*, 2018, **140**, 12980–12988.

167 E. J. Cornel, S. Van Meurs, T. Smith, P. S. O'Hora and S. P. Armes, 'In Situ Spectroscopic Studies of Highly Transparent Nanoparticle Dispersions Enable Assessment of Trithiocarbonate Chain-End Fidelity during RAFT Dispersion Polymerization in Nonpolar Media', *J. Am. Chem. Soc.*, 2018, **140**, 12980–12988.

168 B. Huang, J. Jiang, M. Kang, P. Liu, H. Sun, B. G. Li and W. J. Wang, 'Synthesis of block cationic polyacrylamide precursors using an aqueous RAFT dispersion polymerization', *RSC Adv.*, 2019, **9**, 12370–12383.

169 S. Bai, Y. Wang, B. Liu, Y. Zhu and R. Guo, 'Dispersion copolymerization of acrylamide and sodium 2-acrylamido-2-methylpropanesulfonate in aqueous salt solution stabilized with a macro-RAFT agent', *Colloids Surfaces A Physicochem. Eng. Asp.*, 2018, **553**, 446–455.

170 H. Park, S. Lim, J. Yang, C. Kwak, J. Kim, J. Kim, S. S. Choi, C. Bin Kim and J. Lee, 'A Systematic Investigation on the Properties of Silica Nanoparticles "Multipoint"-Grafted with Poly(2-acrylamido-2-methylpropanesulfonate- co -acrylic Acid) in Extreme Salinity Brines and Brine–Oil Interfaces', *Langmuir*, 2020, **36**, 3174–3183.

171 H. G. Bagaria, K. Y. Yoon, B. M. Neilson, V. Cheng, J. H. Lee, A. J. Worthen, Z. Xue, C. Huh, S. L. Bryant, C. W. Bielawski and K. P. Johnston, 'Stabilization of iron oxide nanoparticles in high sodium and calcium brine at high temperatures with adsorbed sulfonated copolymers', *Langmuir*, 2013, **29**, 3195–3206.

172 J. Lu, B. Peng, M. Li, M. Lin and Z. Dong, 'Dispersion polymerization of anionic polyacrylamide in an aqueous salt medium', *Pet. Sci.*, 2010, **7**, 410–415.

173 Y. Zhang, X. Li, X. Ma, S. Bai, J. Zhang and R. Guo, 'Critical phase separation concentration of acrylamide and 2-acrylamido-2-methylpropanesulfonate copolymers in ammonium sulfate aqueous solution and its influence factors', *Colloids Surfaces A Physicochem. Eng. Asp.*, 2020, **590**, 124485.

174 C. L. McCormick and A. B. Lowe, 'Aqueous RAFT polymerization: Recent developments in synthesis of functional water-soluble (Co)polymers with controlled structures', *Acc. Chem. Res.*, 2004, **37**, 312–325.

175 D. B. Thomas, A. J. Convertine, R. D. Hester, A. B. Lowe and C. L. McCormick, 'Hydrolytic Susceptibility of Dithioester Chain Transfer Agents and Implications in Aqueous RAFT Polymerizations', *Macromolecules*, 2004, **37**, 1735–1741.

176 M. Mertoglu, A. Laschewsky, K. Skrabania and C. Wieland, 'New water soluble agents for reversible addition-fragmentation chain transfer polymerization and their application in aqueous solutions', *Macromolecules*, 2005, **38**, 3601–3614.

177 S. M. North and S. P. Armes, 'Aqueous solution behavior of stimulus-responsive poly(methacrylic acid)-poly(2-hydroxypropyl methacrylate) diblock copolymer nanoparticles', *Polym. Chem.*, 2020, 2147–2156.

178 S. L. Canning, T. J. Neal and S. P. Armes, 'pH-Responsive Schizophrenic Diblock Copolymers Prepared by Polymerization-Induced Self-Assembly', *Macromolecules*, 2017, **50**, 6108–6116.

179 S. M. North and S. P. Armes, 'One-pot synthesis and aqueous solution properties of pH-responsive schizophrenic diblock copolymer nanoparticles prepared via RAFT aqueous dispersion polymerization',

Polym. Chem., 2021, **12**, 5842–5850.

180 X. F. Xu, C. Y. Pan, W. J. Zhang and C. Y. Hong, 'Polymerization-Induced Self-Assembly Generating Vesicles with Adjustable pH-Responsive Release Performance', *Macromolecules*, 2019, **52**, 1965–1975.

181 N. Audureau, F. Coumes, J. M. Guigner, C. Guibert, F. Stoffelbach and J. Rieger, 'Dual Thermo- and pH-Responsive N-Cyanomethylacrylamide-Based Nano-Objects Prepared by RAFT-Mediated Aqueous Polymerization-Induced Self-Assembly', *Macromolecules*, 2022, **55**, 10993–11005.

182 A. Asadujjaman, B. Kent and A. Bertin, 'Phase transition and aggregation behaviour of an UCST-type copolymer poly(acrylamide-co-acrylonitrile) in water: effect of acrylonitrile content, concentration in solution, copolymer chain length and presence of electrolyte', *Soft Matter*, 2017, **13**, 658–669.

183 E. Read, A. Guinaudeau, D. J. Wilson, A. Cadix, F. Violleau and M. Destarac, 'Low temperature RAFT/MADIX gel polymerisation: Access to controlled ultra-high molar mass polyacrylamides', *Polym. Chem.*, 2014, **5**, 2202–2207.

184 R. N. Carmean, T. E. Becker, M. B. Sims and B. S. Sumerlin, 'Ultra-High Molecular Weights via Aqueous Reversible-Deactivation Radical Polymerization', *Chem*, 2017, **2**, 93–101.

185 T. Otsu and M. Yoshida, 'Role of initiator-transfer agent-terminator (iniferter) in radical polymerizations: Polymer design by organic disulfides as iniferters', *Die Makromol. Chemie, Rapid Commun.*, 1982, **3**, 127–132.

186 T. Otsu, 'Iniferter concept and living radical polymerization', *J. Polym. Sci. Part A Polym. Chem.*, 2000, **38**, 2121–2136.

187 J. D. Coyle and H. A. J. Carless, 'Selected aspects of photochemistry. I Photochemistry of carbonyl compounds', *Chem. Soc. Rev.*, 1972, **1**, 465.

188 N. J. Turro, V. Ramamurthy and J. C. Scaiano, *Modern Molecular Photochemistry of Organic Molecules*, University Science Books, Melville, NY, 2012, vol. 88.

189 R. A. Olson, M. E. Lott, J. B. Garrison, C. L. G. Davidson, L. Trachsel, D. I. Pedro, W. G. Sawyer and B. S. Sumerlin, 'Inverse Miniemulsion Photoiniferter Polymerization for the Synthesis of Ultrahigh Molecular Weight Polymers', *Macromolecules*, 2022, **55**, 8451–8460.

190 C. L. G. Davidson, M. E. Lott, L. Trachsel, A. J. Wong, R. A. Olson, D. I. Pedro, W. G. Sawyer and B. S. Sumerlin, 'Inverse Miniemulsion Enables the Continuous-Flow Synthesis of Controlled Ultra-High Molecular Weight Polymers', *ACS Macro Lett.*, 2023, 1224–1230.

191 K. Halake, M. Birajdar, B. S. Kim, H. Bae, C. C. Lee, Y. J. Kim, S. Kim, H. J. Kim, S. Ahn, S. Y. An and J. Lee, 'Recent application developments of water-soluble synthetic polymers', *J. Ind. Eng. Chem.*, 2014, **20**, 3913–3918.

192 V. G. Kadajji and G. V. Betageri, 'Water soluble polymers for pharmaceutical applications', *Polymers*, 2011, **3**, 1972–2009.

193 J. Necas and L. Bartosikova, 'Carrageenan: a review', *Vet. Med. (Praha).*, 2013, **58**, 187–205.

194 B. L. B. de Lima, N. do N. Marques, M. A. Villetti and R. C. Balaban de, 'HPAM-g-PEOPPO: Rheological modifiers in aqueous media of high temperature and high ionic strength', *J. Appl. Polym. Sci.*, 2019, **136**, 1–10.

195 Water Soluble Hydroxyethyl Methyl Cellulose Ether Thickener for Latex Paint, 3709876, *United States Pat. Off.*, 1973.

196 M. A. Nilsson, R. Kulkarni, L. Gerberich, R. Hammond, R. Singh, E. Baumhoff and J. P. Rothstein, 'Effect of fluid rheology on enhanced oil recovery in a microfluidic sandstone device', *J. Nonnewton. Fluid Mech.*, 2013, **202**, 112–119.

197 R. Ettl, V. Schädler and N. Willenbacher, 'Runnability and flow-induced aggregation of paper coating suspensions', *Nord. Pulp Pap. Res. J.*, 2000, **15**, 509–514.

198 A. Guyot, F. Chu, M. Schneider, C. Graillat and T. F. McKenna, 'High solid content latexes', *Prog. Polym. Sci.*, 2002, **27**, 1573–1615.

199 H. A. Barnes, *Handbook of Elementary Rheology (1st Ed.)*, The University of Wales Institute of Non-Newtonian Fluid Mechanics, Aberystwyth, 1st edn., 2000.

200 J. W. Gooch, in *Encyclopedic Dictionary of Polymers*, Springer, New York, 2011, pp. 799–799.

201 J. D. Ferry, *Viscoelastic Properties of Polymers (2nd Ed.)*, John Wiley & Sons, New York, 2nd edn., 1970.

202 G. C. Berry and T. G. Fox, in *Fortschritte der Hochpolymeren-Forschung*, Springer-Verlag, Berlin/Heidelberg, 1968, pp. 261–357.

203 W. L. Whipple and H. Zheng, in *Monitoring Polymerization Reactions*, John Wiley & Sons, Hoboken, NJ, 2014, pp. 381–394.

204 Lubrizol: Carbopol, https://www.lubrizol.com/Home-Care/Products/Carbopol-Polymers.

205 BASF: Alcomer, https://energy-resources.basf.com/global/en/oilfield-chemicals/applications/drilling/dewatering-agents.html.

206 V. J. Cunningham, M. J. Derry, L. A. Fielding, O. M. Musa and S. P. Armes, 'RAFT aqueous dispersion polymerization of N-(2-(methacryloyloxy)ethyl)pyrrolidone: A convenient low viscosity route to high molecular weight water-soluble copolymers', *Macromolecules*, 2016, **49**, 4520–4533.

207 S. J. Byard, Synthesis and Characterisation of Stimulus-responsive Diblock Copolymer Nano-objects Prepared by RAFT Aqueous Dispersion Polymerisation, PhD Thesis, University of Sheffield, 2019.

Chapter 2: Synthesis and Evaluation of Polymers for use in Highly Salty Aqueous Dispersion Polymerisation

2.1 Introduction

In this Chapter, various polymers are evaluated for their suitability in developing new RAFT aqueous dispersion polymerisation formulations in highly salty media. In principle, such syntheses should enable the preparation of high molecular weight water-soluble diblock copolymers in the form of low-viscosity aqueous dispersions of sterically-stabilised particles. Suitable formulations were identified by evaluating the aqueous solubility of monomers and their corresponding homopolymers across a range of ammonium sulfate concentrations to determine the critical salt concentration required for either immiscibility (monomers) or insolubility (homopolymers).

A relevant patent application was filed by Destarac on behalf of Rhodia (now Solvay) in 2013.[1] It covers the production of homogeneous 'water-in-water' dispersions at high solids, but which are nevertheless fluid and stable to aid transportation, manipulation and storage. The patent covers RAFT polymerisation to prepare polyelectrolytes of up to 20 $\times 10^6$ g mol^{-1} at up to 50% w/w solids in salty media. However, this claim is an extrapolation from the example formulations given which have reported M_w values $\leq 380 \times 10^3$ g mol^{-1} for $PAMPS_{67}$-P($AA_{0.3x}$-*stat*-$AM_{0.7x}$) copolymers where x < 1,000 and solids contents < 20% w/w. (n.b. solids contents calculated and used throughout this Thesis compare mass of reagents against combined mass of water and salt). Subsequent dilution of polymer particles with water leads to molecular dissolution, which produces an increase in solution viscosity. Two main drawbacks are noted for the traditional synthesis of such polymers via traditional free radical aqueous dispersion polymerisation: high viscosity and poor colloidal stability. In practice, the maximum solids content and DP are limited and the final copolymer chains exhibit a broad MWD. Moreover, colloidal instability can cause sedimentation or caking, particularly during the storage and transport of such dispersions.[1]

In this Thesis, cationic, zwitterionic and anionic polyelectrolytes are evaluated as putative salt-tolerant steric stabilisers. In addition, a suitable non-ionic steric stabiliser is identified for the first time. In all cases, the salt-intolerant block is prepared in its non-ionic form. The cost and commercial availability of each vinyl monomer is considered along with less energy-intensive reaction conditions (e.g. low temperature) and minimisation of the salt concentration and RAFT CTA. Ideally, the latter organosulfur reagent should be present in ppm quantities to minimise its cost, malodour and intrinsic colour. An important aspect of this project is to establish the practical upper limit for the solids content and copolymer DP while achieving very high monomer conversion and efficient chain extension of the steric stabiliser precursor.

2.2 Experimental

2.2.1 Materials

Acrylic acid (AA; ≥ 99%; purified with acidic alumina), acidic alumina, basic alumina, 2-acrylamido-2-methylpropanesulfonic acid, sodium salt (AMPS; 50% w/w aqueous solution), *N*,*N*-dimethylacrylamide (DMAC; ≥ 99%), 2-hydroxyethyl acrylamide (HEAC; ≥ 96%), hydroxymethyl methacrylamide (HMMAC; 55% w/w aqueous solution), methacrylic acid (MAA; ≥ 99%), 2-*N*-morpholinoethyl methacrylate* (MEMA; ≥ 95%), N-acryloylmorpholine* (NAM; ≥ 97%), 4,4'-azobis(4-cyanopentanoic acid) (ACVA; ≥ 98%), formic acid (≥ 96%), monosodium phosphate (≥ 99%), sodium bicarbonate, sodium hydride, sodium nitrate, TRIZMA (≥ 99.8%), TRIZMA•HCl (≥ 99%), 1-butanethiol (> 98.5%), 2-phenylethanethiol (≥ 98%), 2-methyl-2-bromopropanoic acid (≥ 98%), carbon disulfide (anhydrous; 99%), iodine (≥ 99.8%) and deuterium oxide (D_2O; ≥ 99.9% D) were sourced from Sigma Aldrich (Merck; UK). Acrylamide (AM), sodium thiosulfate pentahydrate (≥ 99%), triethylamine (≥ 99%) and ethanoic acid (100%) were sourced from VWR (UK). Hydrochloric acid (HCl; 37% w/w in water), magnesium sulfate (anhydrous; 99.5%), diethyl ether (≥ 99%)

and ethyl acetate (≥ 99%) were sourced from Fisher Scientific (UK). 2-(Acryloyloxy)ethyl trimethylammonium chloride (ATAC; 80% w/w aqueous solution), 2-(methacryloyloxy)ethyl trimethylammonium chloride (METAC; 75% w/w aqueous solution), 2-(acryloxyethyl)benzyldimethylammonium chloride (BzDA; 80% w/w aqueous solution; purified using an activated charcoal column) and 2-(methacryloxyethyl)benzyldimethyl-ammonium chloride (BzDMA; 80% w/w aqueous solution) were provided by BASF (Ludwigshafen, Germany). 2-(*N*-(Acryloyloxy)ethyl pyrrolidone) (NAEP; 95%) was kindly provided by Ashland Specialty Ingredients (Cherry Hill, NJ, USA). 2,2'-Azobis(2-(2-imidazolin-2-yl)propane)dihydrochloride (VA-044; ≥ 98%) was sourced from Fluorochem. d_2-dichloromethane (CD_2Cl_2; ≥ 99.8% D) was sourced from Cambridge Isotopes Laboratories (Cambridge, UK). Sodium hydroxide (≥ 98%) and ammonium sulfate (> 98%) was sourced from Thermo Fisher Scientific (UK). PEO standards were sourced from Agilent/PSS (UK). 2-(Methacryloyloxy)ethyl phosphorylcholine (MPC) was kindly donated by Biocompatibles (UK). Glycerol monomethacrylate (GMA; 99.8%; < 0.06 mol % dimethacrylate impurity) was kindly donated by GEO Specialty Chemicals (UK). 2-Hydroxyethyl methacrylamide* (HEMAC; ≥ 96%) was sourced from Apollo Scientific (UK) while *N*-(2-hydroxypropyl) methacrylamide* (HPMAC; ≥ 95%) was sourced from Polysciences Inc (USA). Monomers marked with an asterisk (*) were purified using a basic alumina column prior to use. Unless otherwise stated, all solvents were purchased from Fisher Scientific (UK) and were used as received. Deionised water was used for all experiments.

2.2.2 Characterisation Techniques

Nuclear Magnetic Resonance (NMR) Spectroscopy

All ^{1}H NMR spectra were recorded at 25°C using a 400 MHz Bruker Avance-400 spectrometer with 64 scans being averaged per spectrum. Approximately 30 mg of (co)polymer was dissolved in 1 mL of either D_2O or CD_2Cl_2. Spectra were analysed using TopSpin software. Monomer conversions were determined from ^{1}H NMR spectra by comparing the integrated intensities of monomer vinyl signals (5.5 – 7.0 ppm) to that of the corresponding polymer backbone methine signal (2.4 – 2.7 ppm).

Mass Spectrometry

Mass spectra were recorded for RAFT CTAs using an Agilent 1260 Infinity liquid chromatography set-up and an Agilent 6530 Q-ToF mass spectrometer (LC-MS) in positive electrospray ionisation (ESI+) mode with an aqueous eluent containing 0.1% w/w formic acid and 0.05% NaOH. Ionisation results in adduct ions forming with very little fragmentation. Qualitative analysis enabled identification of the molecular parent ion and its corresponding sodium adduct (MH^+ and MNa^+).

Aqueous Gel Permeation Chromatography (GPC) with Multi Angle Laser Light Scattering (MALLS)

The Agilent 1260 Infinity GPC set-up comprises a pump, a degasser, a guard column, three PL-Aquagel Mixed-H, OH-30 and OH-40 columns connected in series, a Dawn Helios II multi-angle laser light scattering (MALLS) detector (Wyatt Technology Corp., USA), an Optilab T-rEX differential refractometer (Wyatt Technology Corp., USA) and a refractive index (RI) detector. GPC curves were recorded with a column and detector temperature of 30°C using a flow rate of 0.8 mL min^{-1}. The eluent was selected according to the nature of the copolymer samples. Eluent 1 comprised 0.50 M CH_3COOH and 0.30 M NaH_2PO_4 at pH 3.0 and was used

to analyse PATAC-PDMAC copolymers. Eluent 2 comprised 0.2 M $NaNO_3$ and 0.05 M TRIZMA/ TRIZMA•HCl buffer at pH 7.0 and was used to analyse PMPC-PDMAC copolymers. Eluent 3 comprised 0.1 M $NaNO_3$, 0.02 M TEA and 0.05 M $NaHCO_3$ at pH 8.0 and was used to analyse PNaAc-P(AM-*stat*-DMAC) and PAMPS-PCEA copolymers. Eluent 4 comprised 70% v/v 0.2 M $NaNO_3$ and 0.01 M NaH_2PO_4 at pH 7.0 plus 30% v/v methanol and was used to analyse PAMPS-PNaAc copolymers.

Calibration of the RI detector was achieved using nine near-monodisperse poly(ethylene oxide) standards (2.1 – 969 kDa) and data were analysed using Agilent Technologies GPC/SEC software. The MALLS instrument was equipped with a 130 mW linearly polarised gallium arsenide laser source operating at 658 mm and 18 detectors placed at angles ranging from 22.5° to 147°. The absolute weight-average molecular weight (M_w) was determined for each diblock copolymer via analysis on Astra 7 software according to MALLS and Zimm formalisms. The differential refractometer was used as a concentration detector in online mode. In offline mode, it was used to determine the dn/dc value for copolymers dissolved in the GPC eluent at pH 8. Copolymer solutions of varying concentration were injected consecutively (lowest concentration first) into the instrument at the same flow rate used for the online mode experiments using a syringe pump. A linear calibration plot of refractive index versus copolymer concentration enables a dn/dc value to be calculated directly from the gradient. Hence the copolymer concentrations used for the online mode measurements can be calculated.

UV Absorption Spectroscopy

Spectra were recorded between 200 and 400 nm at 20°C using a PC-controlled UV-1800 spectrophotometer at 20°C and a 1 cm path length quartz cell. A Beer-Lambert curve was constructed using a series of four or five CTA concentrations in either methanol or water. The absorption maximum at 306 – 310 nm assigned to the π-π* transition for the trithiocarbonate group was used for the calibration plot and the concentration range was selected such that the

absorbance remained less than 1.1. The molar extinction coefficient was calculated for each CTA to enable quantitative determination of homopolymer DPs.[2]

Dynamic Light Scattering (DLS)

Analysis was performed using a Malvern Zetasizer Nano ZS instrument equipped with a 4 mW He–Ne 633 nm laser and an avalanche photodiode detector. The instrument was configured to automatically determine the optimum experimental duration and optical attenuation. Back-scattered light was detected at 173° and measurements were conducted at a copolymer concentration of 0.05% w/w at 20 °C using a 10 mm path length quartz cuvette. Malvern Zetasizer software v7.11 was used to calculate the z-average hydrodynamic diameters (D_z) via the Stokes-Einstein equation, which assumes perfectly monodisperse, non-interacting spherical particles. Data were averaged over at least three consecutive runs with a minimum of ten measurements being recorded for each run. The viscosity of 2.0 M ammonium sulfate is 1.510 Pa s and the refractive index is 1.370 and the viscosity of 3.0 M ammonium sulfate is 2.030 Pa s and the refractive index is 1.384.[3]

Optical Microscopy (OM)

A 0.1% w/w dispersion was prepared and a single drop from a pipette was applied to a glass microscope slide which was subsequently covered with a glass slide cover. Images were recorded at x400 magnification using a Cole-Parmer bifocal compound microscope equipped with a Moticam-BTW digital camera. The focus, brightness, and contrast were adjusted and the acquired images were processed using *ImageJ* software.

Rotational Rheology

An MCR 502 rheometer (Anton Paar, Graz, Austria) equipped with a concentric cylinder measuring set geometry (CC27) was used for rotational rheology experiments. Measurements were performed at 20°C and shear sweeps were conducted from 0.05 s^{-1} to 500 s^{-1} with 51

measurements across the logarithmic shear rate ramp, with each measurement requiring 1 to 45 s (longer measurement times for lower shear rates to ensure steady state reached). Approximately 10 mL of each copolymer dispersion (or solution) was used for each measurement. An overall measurement time of approximately ten minutes was required for each sample.

2.2.3 Synthesis of 4-Cyano-4-(2-phenylethanesulfanylthiocarbonyl)sulfanyl-pentanoic acid (PETTC)

The synthetic protocol used to prepare PETTC is based on a prior study by Armes and co-workers.[4,5] 2-Phenylethanethiol (37.21 g, 269 mmol) was added dropwise to a stirred suspension of sodium hydride (60% in oil, 11.4 g, 286 mmol) in diethyl ether (350 mL) in a 1 L round-bottom flask at 5°C. Evolution of hydrogen was observed and the initial grey suspension formed a white slurry of sodium phenylethanethiolate over an hour. Carbon disulfide (13.8 g, 277 mmol) was added dropwise and a yellow precipitate of sodium 2-phenylethanetrithiocarbonate formed, which was collected via filtration. To a suspension of sodium 2-phenylethanetrithiocarbonate (44.7 g, 189 mmol) in diethyl ether (700 mL), solid iodine (34.5 g, 137 mmol) was added. The reaction mixture was stirred for 60 min at 20°C, and the resulting precipitate of sodium iodide was removed via filtration. The brown filtrate was washed with a saturated solution of sodium thiosulfate (4 × 250 mL), dried using magnesium sulfate, and solvent was removed under reduced pressure (rotary evaporator) to afford bis-(2-phenylethanesulfanylthiocarbonyl)disulfide as an orange solid (~100% yield). A solution of bis-(2-phenylethanesulfanylthiocarbonyl)disulfide (20.0 g, 46 mmol) and 4,4′-azobis(4-cyanovaleric acid) (20 g, 71.3 mmol) in ethyl acetate (450 mL) was purged with nitrogen for 30 min before being refluxed under a dry nitrogen atmosphere for 15 h. The resulting solution was washed with water (5 × 300 mL), dried over magnesium sulfate and solvent was removed under reduced pressure. The remaining sticky orange residue was purified using silica column

chromatography (5% methanol in ethyl acetate mobile phase), which yielded 4-cyano-4-(2-phenylethanesulfanylthiocarbonyl)sulfanylpentanoic acid (PETTC) as a yellow solid (63.2 g, 84%), m/z = 340 (M^+), δ_H(400 MHz; CD_2Cl_2; Me_4Si) 1.9 (3 H, s, Me), 2.5 (2 H, m, CH_2), 2.7 (2 H, t, CH_2), 3.0 (2 H, t, CH_2), 3.7 (2 H, t, CH_2), 7.3 (5 H, C_5H_5).

2.2.4 Synthesis of S-butyl-S′-(α,α′-dimethyl-α″-acetic acid)trithiocarbonate (BDMAT)

The synthetic protocol for the preparation of BDMAT is based on prior studies by Lai et al. and Bray et al..[6,7] 1-Butanethiol (24 mL), acetone (12 mL) and 5 M NaOH (44 mL) were added to a 500 mL round-bottom flask and stirred at 20°C for 25 min to produce a light pink solution. Addition of carbon disulfide (15 mL) produced an orange solution, which was stirred for a further 30 min before being immersed in an ice bath. 2-Methyl-2-bromopropanoic acid (38.4 g) was heated to 50°C to produce a molten liquid, which was slowly dripped into the flask. The reaction solution turned yellow, the flask was removed from the ice bath and its contents were poured into an aqueous solution of 5 M NaOH (44 mL); the resulting solution was stirred overnight at 20°C. After 20 h, the reaction mixture was diluted with water (200 mL) and washed four times with hexane (4 x 200 mL). The orange aqueous phase was cooled with the aid of an ice bath and 1.0 M HCl (230 mL) was slowly added to adjust the solution to pH 3. The resulting yellow precipitate was isolated, washed with water and dissolved in chloroform (200 mL). After drying with $MgSO_4$ and removing the solvent under vacuum, the product was a viscous orange liquid that crystallised to form a yellow solid when poured into a glass vial (20.7 g, 37%), m/z 253 (M^+), δ_H(400 MHz; CD_2Cl_2; Me_4Si) 1.0 (3 H, t, Me), 1.7 (10 H, s,q,q, CH_3, CH_2, CH_2), 3.4 (2 H, t, CH_2).

2.2.5 Synthesis of PATAC Precursor via RAFT Solution Polymerisation of ATAC at 56°C

2-(Acryloyloxyethyl)trimethylammonium chloride (ATAC; 41.35 g; 80% w/w aqueous solution, 171 mmol), 4-cyano-4-(2-phenylethanesulfanylthiocarbonyl)sulfanylpentanoic acid

(PETTC; 290 mg, 854 μmol), *α,α′*-azodiisobutyramidine dihydrochloride (AIBA, 46.3 mg, 171 μmol) and methanol (41.9 g) were weighed into a 250 mL round-bottom flask equipped with a magnetic flea and the resulting reaction solution was degassed using a stream of nitrogen gas for 45 min at 20°C. The sealed flask was immersed in an oil bath set at 56°C and the ensuing polymerisation was allowed to proceed for 2 h, achieving 97% ATAC conversion. The polymer solution was purified by dialysis against water for three days to remove unreacted monomer and then freeze-dried overnight. The mean degree of polymerisation was determined to be 242 ± 1, as judged by end-group analysis using UV spectroscopy at the absorption maximum of 306 nm. Aqueous GPC analysis indicated an M_n of 32.7 kg mol^{-1} and an M_w/M_n of 1.58.

2.2.6 Summary of Polymer Precursor Syntheses via RAFT Solution Polymerisation

The reaction conditions for the polymer syntheses of all homopolymers which underwent solubility testing are shown in **Table 2.1**.

Monomer	Initiator	Solvent	RAFT Agent	Temperature / °C	Time / h	Target Polymer DP	Conversion / %	Actual Polymer DP
AA	VA-044	Water	BDMAT	44	1.5	200	95	258
AMPS	T-21S	Water/PBS	BDMAT	90	2.5	250	99	250
AM	VA-044	Water	BM1433	46	18	500	92	495
ATAC	AIBA	Methanol	PETTC	56	2	200	97	242
BzDA	VA-044	Water	BDMAT	48	6	100	99	115
BzDMA	ACVA	Methanol	PETTC	70	6	100	98	126
DMAC	VA-044	Water/PBS	BDMAT	48	4	500	95	515
GMA	ACVA	Water	PETTC	70	5	200	83	162
HEAC	VA-044	Water	BM1433	46	3	300	89	216
HEMAC	VA-044	Water	BM1433	46	3	200	75	187
HMMAC	VA-044	Water	BM1433	46	3	350	64	222
HPMAC	VA-044	Water	BM1433	46	3	200	81	257
MAA	ACVA	Water	PETTC	70	5	200	79	150
METAC	VA-044	Water	BDMAT	46	4	250	91	235
MEMA	VA-044	Water	BDMAT	48	2	120	54	67
MPC	ACVA	Methanol	PETTC	75	3.5	120	75	139
NAM	VA-044	Water	BM1433	46	18	500	78	520
NAEP	KPS/AsAc	Water	DDMAT	30	0.5	100	50	75

Table 2.1 Summary of reaction conditions for the synthesis of a range of homopolymers used in subsequent solubility testing. (The PAA_{258} and $PNaAc_{258}$ polymers are only different by the pH at which they were tested).

Each polymer has been prepared using a trithiocarbonate RAFT agent, and has been purified by dialysis in water for at least 48 hours.

2.2.7 Core-Forming Monomer Solubility Testing

The protocol for evaluating the aqueous solubility of various vinyl monomers and their corresponding homopolymers was as follows. 2% w/w aqueous solutions containing zero to 4.0 M ammonium sulfate were prepared in sealed glass vials at pH 5.5. Each vial was shaken and allowed to stand for 2 h at either 20°C or 30°C followed by visual inspection to determine whether complete dissolution had occurred. Exceptionally, AA/PAA/MAA/PMAA and NaAc/PNaAc were examined at pH 8.0 and pH 2.0, respectively.

2.2.8 Synthesis of PATAC-PDMAC Diblock Copolymer Spheres via RAFT Dispersion / Emulsion Polymerisation

A typical protocol for the synthesis of $PATAC_{242}$-$PDMAC_{5000}$ spheres at 20% w/w solids was conducted as follows. $PATAC_{242}$ (0.09 g, 1.91 μmol), DMAC (0.941 g, 9.53 mmol) and an aqueous solution of 2.0 M $(NH_4)_2SO_4$ (3.93 g) were added together in a small glass vial equipped with a magnetic flea and stirred while degassing using a stream of N_2 gas for 30 min at 20°C. Separately, VA-044 initiator (0.64 μmol, 0.206 g, 0.1% in 2.0 M $(NH_4)_2SO_4$) was degassed and added just prior to immersion of the glass vial in an oil bath set at 46°C. The polymerisation was allowed to proceed for 18 h, then quenched by exposure to air with concomitant cooling to 20°C. The DMAC monomer conversion was determined to be 99% by ^{1}H NMR spectroscopy.

2.2.9 Synthesis of Diblock Copolymer Spheres via RAFT Dispersion Polymerisation using Monomer-Starved Conditions

A typical protocol for the synthesis of $PATAC_{242}$-$PDMAC_{5000}$ spheres at 30% w/w solids using a monomer-starved feed was conducted as follows. $PATAC_{242}$ (0.252 g, 5.3 μmol), and an aqueous solution of 2.0 M $(NH_4)_2SO_4$ (6.14 g) were added in turn to a 25 mL round-bottom flask. The resulting aqueous solution was stirred and degassed using a stream of N_2 gas for 30

min at 20°C. Separately, excess DMAC monomer and a 0.1% w/w solution of VA-044 initiator in 2.0 M $(NH_4)_2SO_4$ were degassed for 20 min. The round-bottom flask was immersed into an oil bath set at 46°C and the initiator solution (0.57 mL, 1.77 μmol, $[PATAC_{242}]$/VA-044 molar ratio = 3) was added. At the same time, DMAC (2.73 mL, 26.5 mmol) was loaded into a 3.0 mL syringe and attached to a syringe pump with the needle bent to pass through the airtight seal and just above the reaction solution within the flask. The pump was switched on and the monomer was slowly added to the reaction solution over a three hour period at a rate of 0.87 mL h^{-1}. The polymerisation was allowed to proceed for 18 h and then quenched by exposure to air with concomitant cooling to 20°C. The DMAC monomer conversion was determined to be 99% by ^{1}H NMR spectroscopy.

2.3 Results and Discussion

2.3.1 Synthesis and Selection of CTAs

4-Cyano-4-(2-phenylethanesulfanylthiocarbonyl)sulfanylpentanoic acid (PETTC) RAFT agent was synthesised in 84% yield. A previously reported protocol was used,[4,5] as outlined in **Scheme 2.1**. Purification was achieved using silica column chromatography (mobile phase: 10:1 v/v ethyl acetate/methanol) to remove impurities.

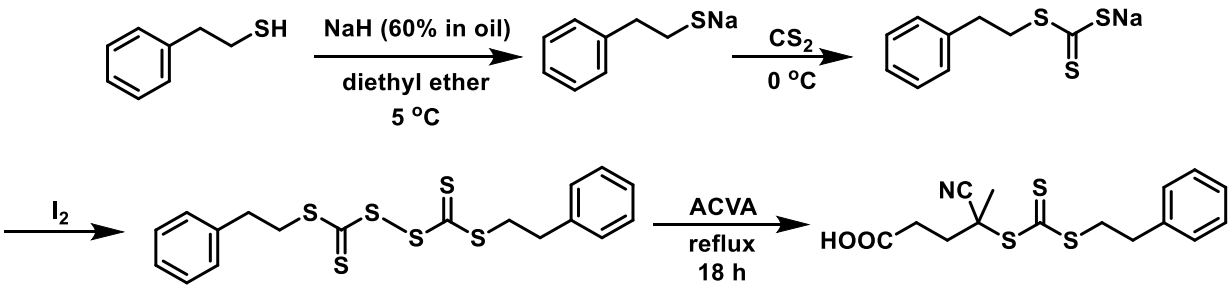

Scheme 2.1 Four-step synthesis of the PETTC RAFT agent. Initial deprotonation of 2-phenylethanethiol, carbon disulfide insertion to form a sodium carbotrithioate salt, oxidation with iodine to generate bis(thioacyl)disulfide and finally decomposition with ACVA to form crude PETTC. Adapted from prior studies by Jones and Rymaruk et al..[4,5]

The PETTC ^{1}H NMR spectrum (**Figure 2.1**) and the mass spectrum (**Figure 2.2**) were consistent with the desired product. In addition to the primary peak at 9.5 minutes, there is a smaller elution peak at 5.5 minutes present in the preparative HPLC, and is likely to be some of the remaining starting material used for the PETTC synthesis. The positive electrospray ionisation (ESI+) method results in the production of the sodium adduct product hence the additional peaks between m/z 362 and 364.

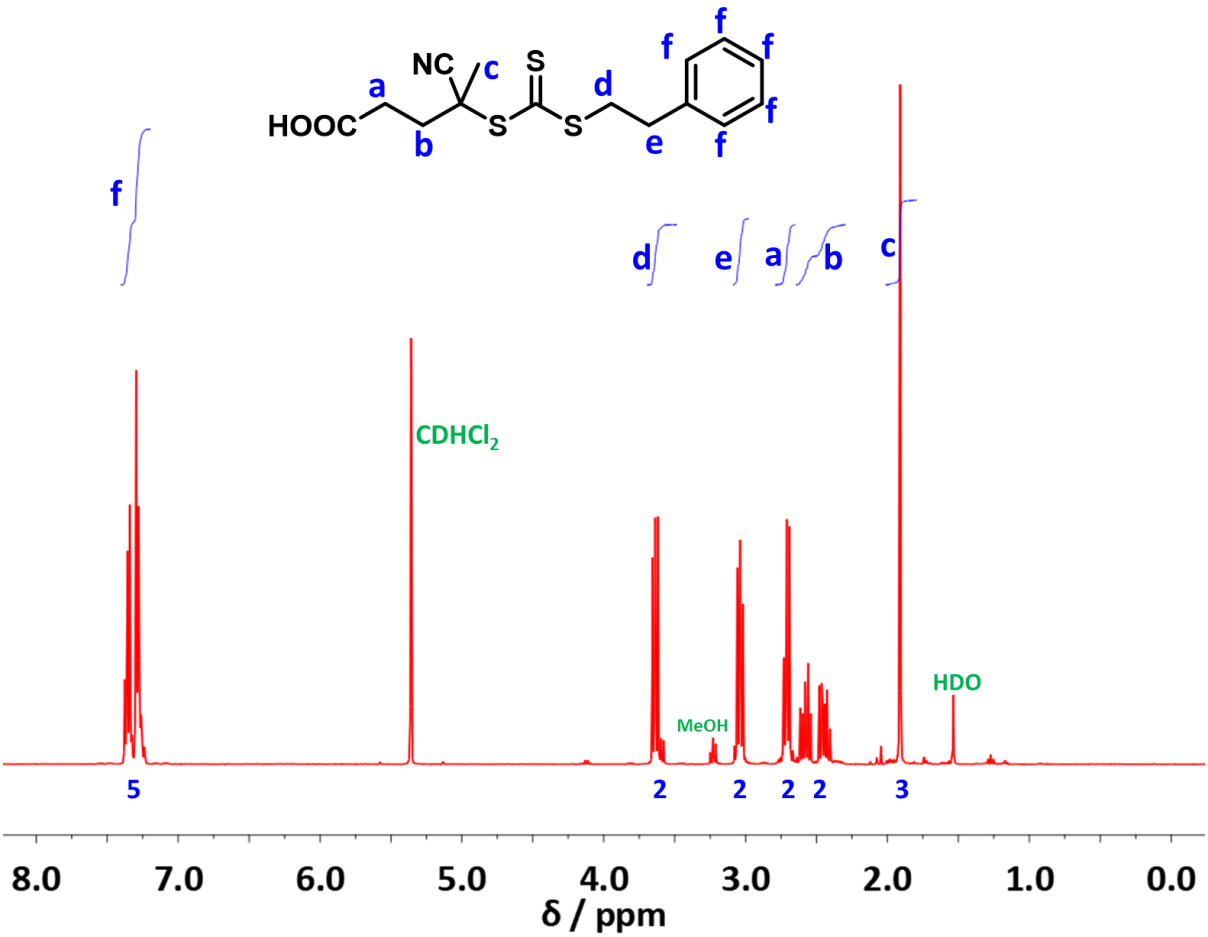

Figure 2.1 Annotated ^{1}H NMR spectrum of PETTC in CD_2Cl_2.

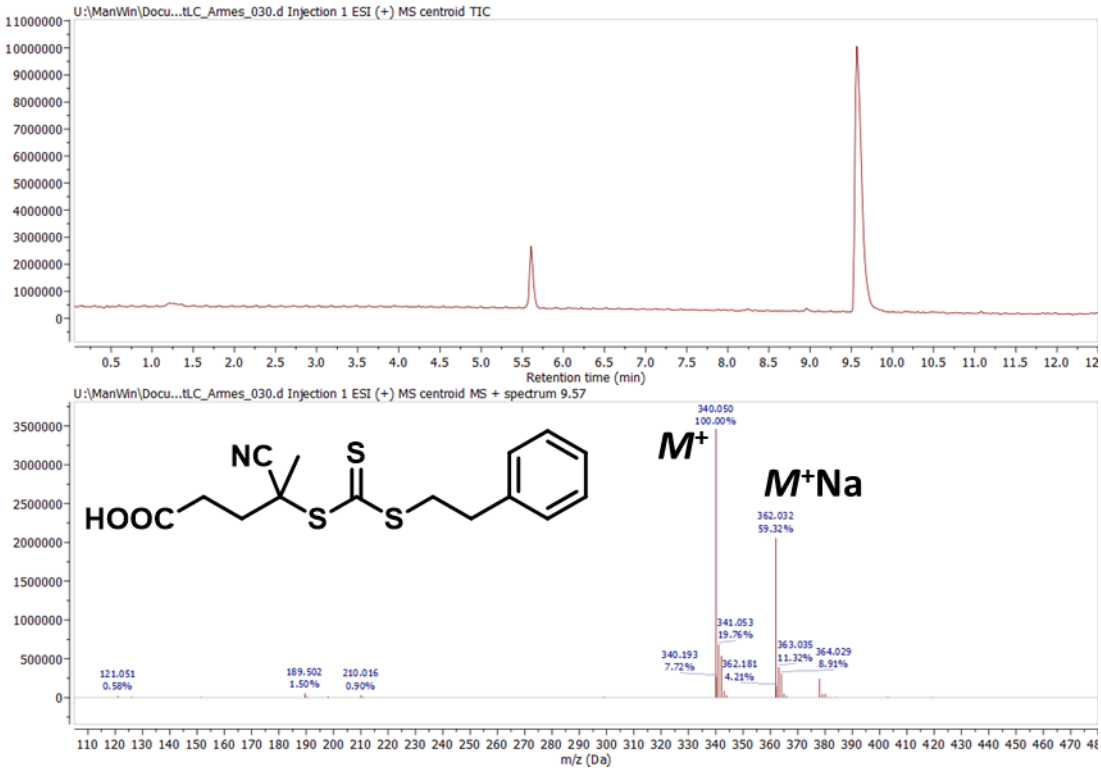

Figure 2.2 HPLC and ESI+ mass spectrum of PETTC.

S-Butyl-S′-(α,α′-dimethyl-α′′-acetic acid)trithiocarbonate (BDMAT) RAFT agent was synthesised in 37% yield. A previously reported protocol was used,[6,7] as outlined in **Scheme 2.2**. The product was purified by repeated washes with water and hexane.

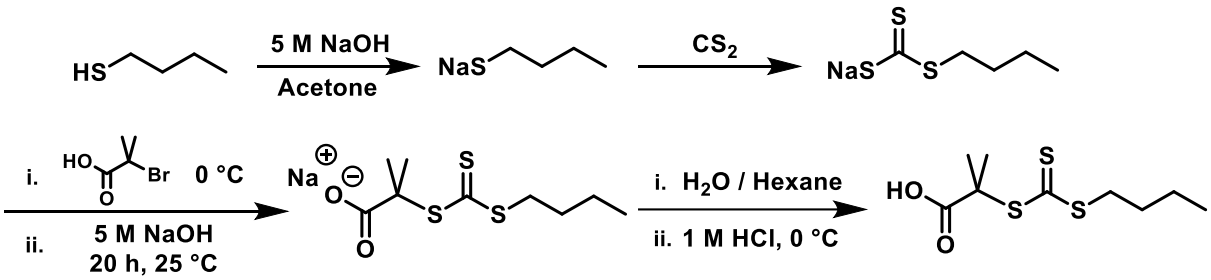

Scheme 2.2 Four-step synthesis of BDMAT RAFT agent. Initial deprotonation of 1-butanethiol, carbon disulfide insertion to form a sodium carbotrithioate salt, nucleophilic substitution using 2-methyl-2-bromopropanoic acid and carboxylate protonation to form crude BDMAT. Based on the reports by Lai et al. and Bray et al..[6,7]

The BDMAT ^{1}H NMR spectrum (**Figure 2.3**) and the mass spectrum (**Figure 2.4**) were consistent with the desired product.

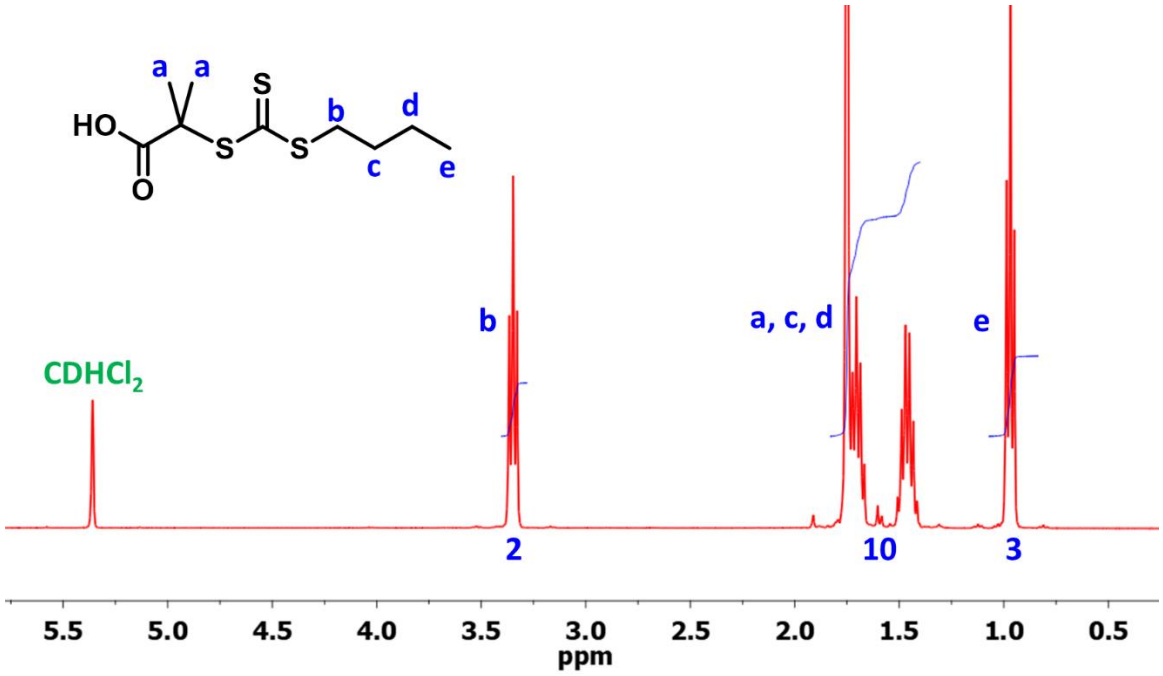

Figure 2.3 Annotated ^{1}H NMR spectrum of BDMAT in CD_2Cl_2.

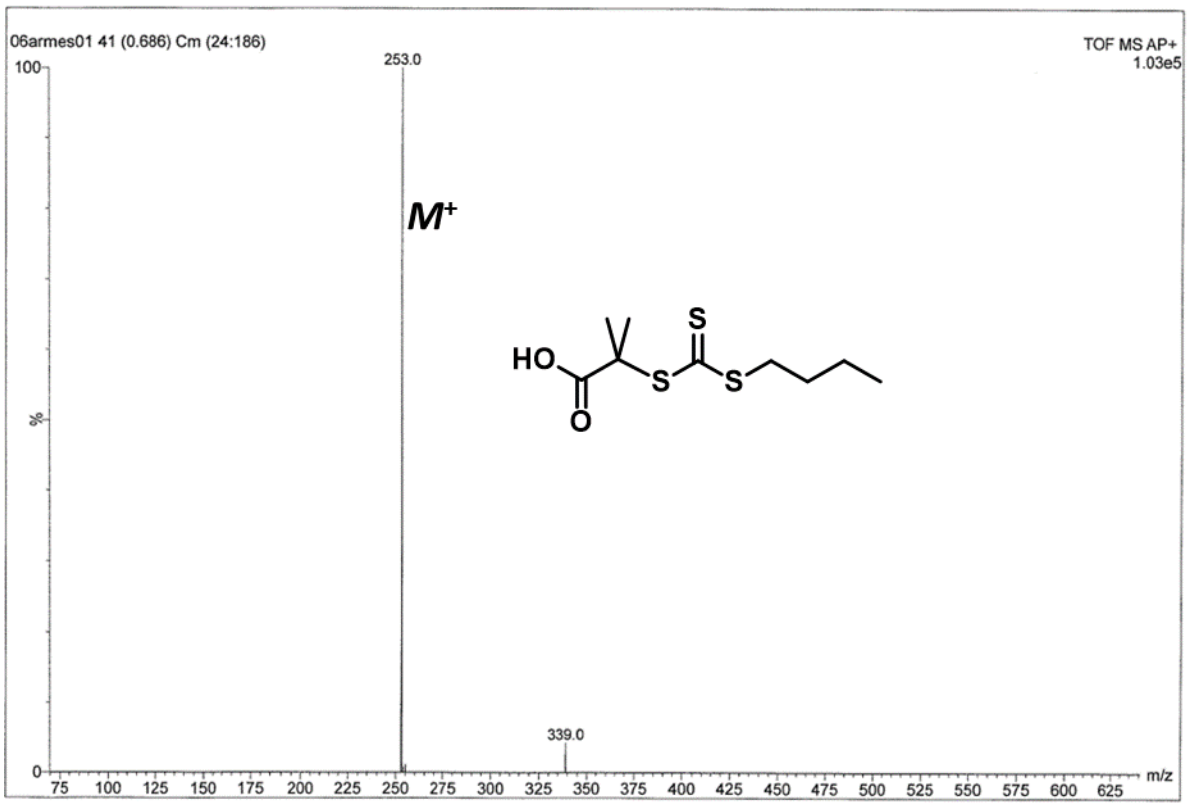

Figure 2.4 ESI+ mass spectrum of BDMAT.

BDMAT has been reported by Bray et al.,[7,8] who drew attention to its higher aqueous solubility relative to the dodecyl variant used by Byard et al.[9,10] More specifically, DDMAT is only soluble in water at 90°C, whereas BDMAT is soluble in water at 20°C (but slow dissolution is observed below 40°C). The latter reagent is more suitable for use in wholly aqueous formulations. Diacid trithiocarbonate RAFT agents such as 4-((((2-carboxyethyl)-thio)carbonothioyl)thio)-4-cyanopentanoic acid (BM1433) are also known to have relatively high aqueous solubility.

2.3.2 Homopolymer Synthesis

Homopolymers were mostly prepared using water-soluble azo-initiators such as VA-044 ($t_{1/2}$ = 44°C) at 44 – 48°C, AIBA ($t_{1/2}$ = 56°C) at 56°C or ACVA ($t_{1/2}$ = 70°C) at 70 – 75°C. Preparation of $PAMPS_{250}$ used the peroxy-initiator T-21S at 90°C and $PNAEP_{75}$ used a low temperature redox initiator pair. There is a wide range of homopolymer DPs targeted and obtained which is not expected to have a significant effect on the solubility measurements, provided they are sufficiently large so they are representative of longer polymer chains.

The temperature probe connected to the heating element was positioned close to the edge of the oil bath. A thermometer was used to corroborate the oil bath temperature, although the reaction mixture has an estimated uncertainty of ± 2°C. After purification of each homopolymer precursor by dialysis, its mean DP was determined by comparing one of the polymer signals, for example the carbon backbone at 1.0 – 3.0 ppm, relative to the distinctive BDMAT methyl signal at 1.0 ppm or the aromatic proton signal at 7.2 ppm for PETTC. However, the experimental error associated with such DP values is relatively high. Hence UV spectroscopy was employed to determine the polymer DP more precisely by constructing a linear calibration curve based on the Beer-Lambert relation, as shown in **Figure 2.5**.

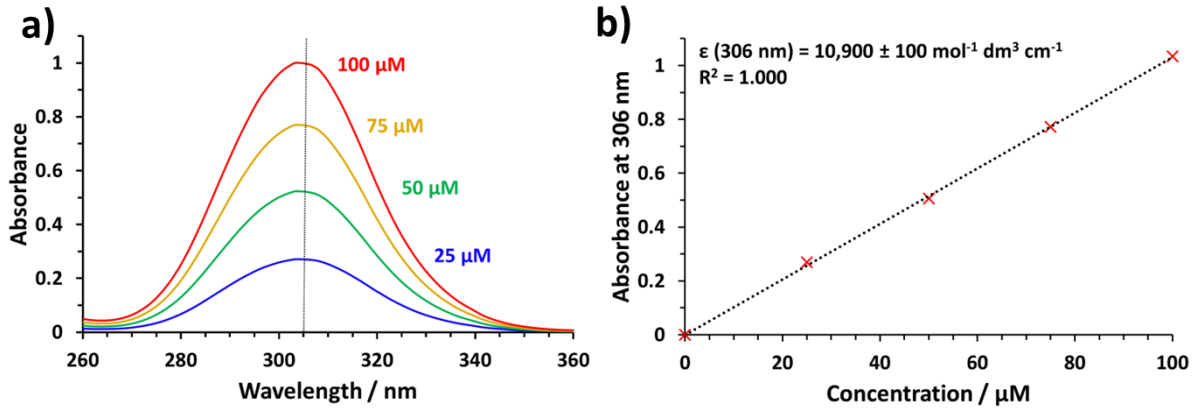

Figure 2.5 (a) UV absorption spectra recorded for a sereis of methanolic solutions of 4-cyano-4-(2-phenylethanesulfanylthiocarbonyl)sulfanylpentanoic acid (PETTC) ranging from 0 µM to 100 µM. (b) Beer-Lambert calibration plot constructed for PETTC in methanol to calculate its molar extinction coefficient (ε) at the absorption maximum of 306 nm.

Organosulfur RAFT agents usually have two UV absorption bands, with the strong and allowed π–π* transition that produces an absorption maximum at around 306 nm being selected to construct the linear calibration plot for the polymer DP determination.

2.3.3 Solubility Testing

Eighteen monomers (**Scheme 2.3**) and their corresponding homopolymers were investigated using the aqueous solubility protocols outlined in **Section 2.2.6**. Most homopolymers became water-insoluble as the ammonium sulfate concentration was increased but the minimum critical concentration required for insolubility varied significantly depending on the chemical structure. Such information enabled identification of relatively salt-tolerant polymers that should act as suitable steric stabilisers. Similarly, particularly salt-intolerant polymers were judged to be suitable core-forming blocks for the intended RAFT aqueous dispersion polymerisation syntheses. A few vinyl monomers proved to be water-immiscible at the pH values and temperatures investigated. These were judged unsuitable for aqueous dispersion polymerisation formulations, but it is possible that they might be amenable to aqueous emulsion polymerisation formulations. However, this avenue was not pursued in this Thesis.

The eighteen vinyl monomers were acrylic acid (**AA**), 2-acrylamido-2-methylpropanesulfonic acid, sodium salt (**AMPS**), acrylamide (**AM**), 2-(acryloyloxy)ethyl trimethylammonium chloride (**ATAC**), 2-(acryloxyethyl)benzyldimethylammonium chloride (**BzDA**), 2-(methacryloxyethyl)benzyl-dimethylammonium chloride (**BzDMA**), *N*,*N*-dimethyl acrylamide (**DMAC**), glycerol monomethacrylate (**GMA**), 2-hydroxyethyl acrylamide (**HEAC**), 2-hydroxyethyl methacrylamide (**HEMAC**), hydroxymethyl methacrylamide (**HMMAC**), *N*-(2-hydroxypropyl) methacrylamide (**HPMAC**), methacrylic acid (**MAA**), 2-(methacryloyloxy)ethyl trimethylammonium chloride (**METAC**), 2-*N*-morpholinoethyl methacrylate (**MEMA**), 2-(methacryloyloxy)ethyl phosphorylcholine (**MPC**), sodium acrylate (**NaAc**), *N*-(acryloyl)morpholine (**NAM**) and 2-(*N*-(acryloyloxy)ethyl pyrrolidone) (**NAEP**). This series includes hydrophilic acrylates, methacrylates, acrylamides and methacrylamides.

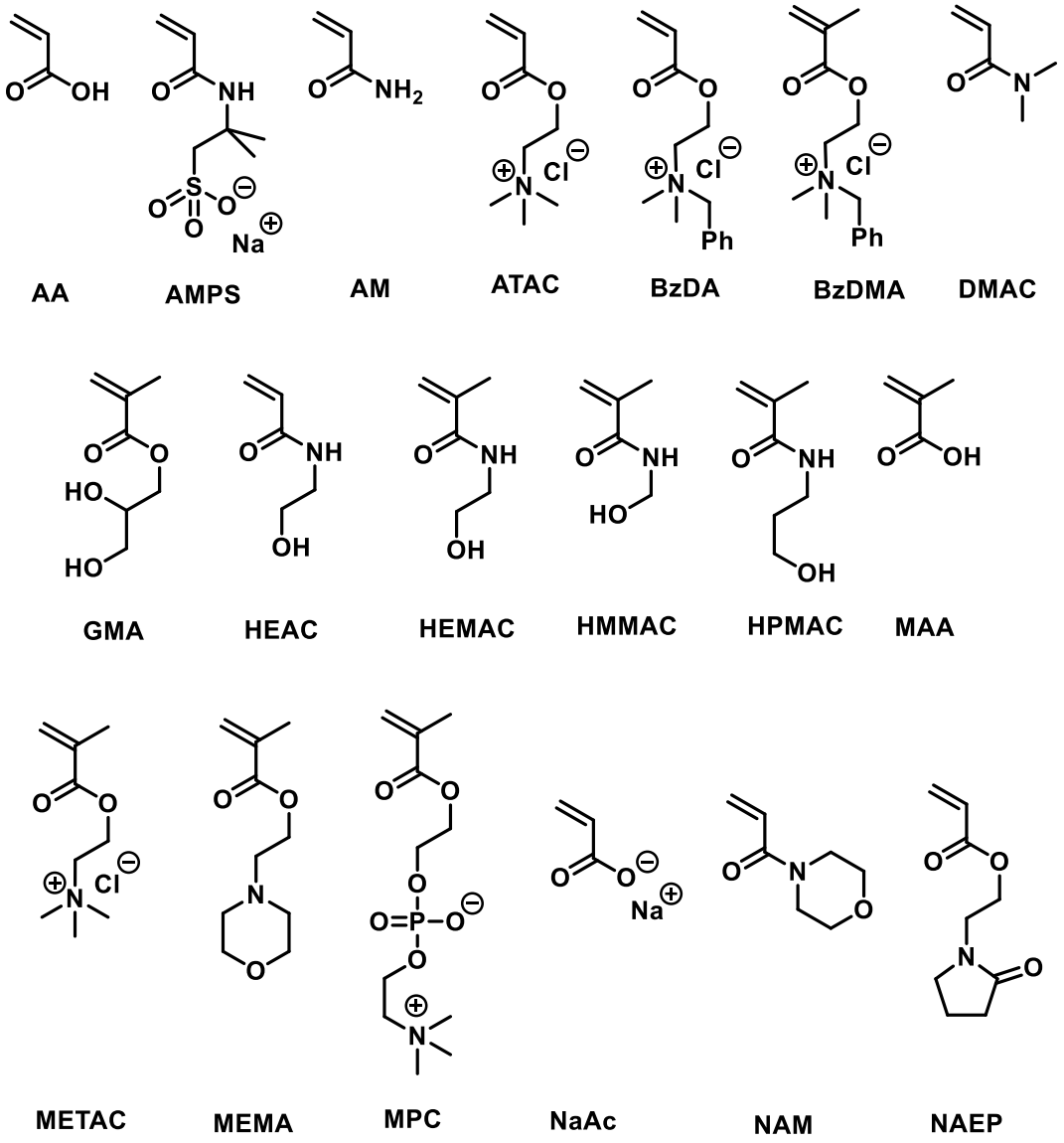

Scheme 2.3 Chemical structures of hydrophilic monomers evaluated for their use in RAFT aqueous dispersion polymerisation syntheses conducted in highly salty media.

Aqueous solubility data are reported over a wide range of ammonium sulfate concentrations, see **Table 2.2** for the monomer data and **Table 2.3** for the corresponding homopolymer data. These visual inspection studies were conducted at 20°C, although most RAFT aqueous dispersion polymerisation syntheses reported in this Thesis were conducted between 30°C and 46°C. Nevertheless, the tabulated data can be used to infer suitable polymer formulations. Ideally, there should be a large difference between the critical minimum salt concentration required to salt out the core-forming block and that required to salt out the steric stabiliser.

With the notable exceptions of acrylic acid and methacrylic acid, most of the vinyl monomers are either non-ionic or permanently ionic species. The pK_a values for acrylic acid and methacrylic acid are 4.25[3] and 4.65,[3] respectively. However, the reported pK_a for poly(acrylic acid) has been reported to be between 6.22 and 6.60 by some authors[11,12] and between 4.28 and 4.55 by others[13,14]. The latter values are expected to be better representative of the actual value as Rimmer et al. have taken into account the theory reported by Kern, Katchalsky, Gillis and Spitnik that the course of the neutralisation of a polymeric acid may be represented by an equation of the form:[13,15–17]

$$pH = pK_a + kf^{\frac{1}{3}} - log\left(\frac{1-f}{f}\right)$$

where *k* is a constant and *f* is the degree of ionisation. This formula shows that in contrast to low molecular weight acids, which have a well-defined acid dissociation constant, polyacids exhibit a mean value that depends on the degree of ionisation. The apparent pK_a value is usually taken to be based on the solution pH at 50% neutralisation (f = 0.5).[11,14] Therefore, solubility tests were conducted at both acidic and basic pH, which correspond to the fully protonated and deprotonated forms, respectively. NaAc/PNaAc was examined at pH 8.0 to ensure complete ionisation of the carboxylic acid groups, whereas both AA/PAA and MAA/PMAA were evaluated at pH 2.0 to ensure complete protonation of the carboxylic acid groups.

	Aqueous $(NH_4)_2SO_4$ solution / mol dm^{-3}									Critical Solubility Concentration / mol dm^{-3}
	0.0	0.5	1.0	1.5	2.0	2.5	3.0	3.5	4.0	
AA (pH 2)	S	S	S	S	S	S	S	S	S	-
AMPS	S	S	S	S	S	S	S	S	S	-
AM	S	S	S	S	S	S	S	S	S	-
ATAC	S	S	S	S	S	S	S	S	S	-
BzDA	S	S	S	S	S	S	S	S	I	3.8
BzDMA	S	S	S	S	S	S	S	S	I	3.6
DMAC	S	S	S	S	S	S	S	S	I	3.8
GMA	S	S	S	S	S	S	I	I	I	2.6
HEAC	S	S	S	S	S	S	S	S	I	3.8
HEMAC	S	S	S	S	S	S	S	S	I	3.7
HMMAC	S	S	S	S	S	S	S	S	S	-
HPMAC	S	S	S	S	S	S	S	S	S	-
MAA (pH 2)	S	S	S	S	S	S	S	S	S	-
METAC	S	S	S	S	S	S	S	S	S	-
MEMA	S	S	S	S	I	I	I	I	I	1.6
MPC	S	S	S	S	S	S	S	S	S	-
NaAc (pH 8)	S	S	S	S	S	S	S	S	S	-
NAM	S	S	S	S	S	S	I	I	I	2.8
NAEP	S	S	S	S	S	I	I	I	I	2.3

Table 2.2 Aqueous solubility data obtained for a range of hydrophilic vinyl monomers at 2% w/w, 20°C and pH 5.5, unless otherwise stated. **S** denotes solubility and **I** denotes insolubility; an estimated critical ammonium sulfate concentration for (in)solubility is also provided.

Each vinyl monomer proved to be water-miscible up to 1.5 M ammonium sulfate. The highest ammonium sulfate concentration investigated was 4.0 M, which corresponds to a 42.7% w/w solution. Compared to pure deionised water, this solution has a density of 1.24 g cm^{-3} and a viscosity of 2.77 mPa s.[3]

	Aqueous $(NH_4)_2SO_4$ solution / mol dm^{-3}									Critical Solubility Concentration / mol dm^{-3}
	0.0	0.5	1.0	1.5	2.0	2.5	3.0	3.5	4.0	
PAA (pH 2)	S	S	S	S	S	S	I	I	I	**2.8**
PAMPS	S	S	S	S	S	S	S	S	S	**-**
PAM	S	S	S	S	S	I	I	I	I	**2.1**
PATAC	S	S	S	S	S	S	S	S	S	**-**
PBzDA	S	S	S	S	I	I	I	I	I	**1.9**
PBzDMA	S	S	S	S	S	S	I	I	I	**2.7**
PDMAC	S	S	S	I	I	I	I	I	I	**1.1**
PGMA	S	S	S	S	I	I	I	I	I	**1.9**
PHEAC	S	S	S	S	I	I	I	I	I	**1.8**
PHEMAC	S	S	S	S	I	I	I	I	I	**1.8**
PHMMAC	S	S	S	S	S	I	I	I	I	**2.2**
PHPMAC	S	S	S	S	I	I	I	I	I	**1.9**
PMAA (pH 2)	S	S	S	S	S	S	I	I	I	**2.8**
PMETAC	S	S	S	S	S	S	S	S	S	**-**
PMEMA	S	I	I	I	I	I	I	I	I	**0.4**
PMPC	S	S	S	S	S	S	S	S	S	**-**
PNaAc (pH 8)	S	S	S	S	S	S	S	S	S	**-**
PNAM	S	S	I	I	I	I	I	I	I	**0.6**
PNAEP	S	S	I	I	I	I	I	I	I	**0.5**

Table 2.3 Aqueous solubility data obtained for a range of hydrophilic homopolymers at 2% w/w, 20°C and pH 5.5, unless otherwise stated. **S** denotes solubility and **I** denotes insolubility; an estimated critical ammonium sulfate concentration for (in)solubility is also provided.

Zwitterionic PMPC is known to be highly tolerant of added salt: it remains soluble in the presence of 5 M NaCl.[18] The other highly salt-tolerant homopolymers listed in **Table 2.3** are anionic (PAMPS and PNaAc) and cationic (PATAC, PMETAC) polyelectrolytes. In principle, such homopolymers can confer colloidal stability even in highly saline media via an electrosteric mechanism.[19,20] On the other hand, the most salt-intolerant homopolymers are PMEMA, PNAM and PNAEP which each become water-insoluble in the presence of less than 1.0 M ammonium sulfate.

2.3.4 Homopolymer Chain Extensions

Once suitable steric stabiliser and core-forming blocks have been selected, the data provided in **Table 2.3** can be used to infer an ammonium sulfate concentration that should cause *in situ* self-assembly once a critical core-forming block DP has been attained. A few fully cationic diblock copolymers were prepared using either PATAC or PMETAC as the steric stabiliser to

target a PBzDA or PBzDMA core-forming block in 2.0 M and 3.0 M ammonium sulfate respectively. In principle, such formulations should be amenable to aqueous GPC analysis. Unfortunately, the hydrophobic nature of the pendent benzyl group in the PBzDA or PBzMA block leads to adsorption on the GPC column when using an aqueous eluent. Therefore, these experiments lack convincing polymer characterisation data and are not reported in this Thesis.

2.3.5 PATAC-PDMAC Diblock Copolymer Synthesis

Visual inspection confirmed that the $PATAC_{242}$ precursor remains water-soluble up to 4.0 M ammonium sulfate at 20°C. In contrast, $PDMAC_{500}$ homopolymer proved to be water-soluble in the presence of 1.0 M ammonium sulfate but becomes insoluble at 2.0 M ammonium sulfate. Furthermore, DMAC monomer remains water-miscible in the presence of 2.0 M ammonium sulfate and only becomes water-immiscible at 3.0 M ammonium sulfate. In view of these observations (summarised in **Table 2.4**), an ammonium sulfate concentration of 2.0 M was selected for trial RAFT aqueous dispersion polymerisation syntheses.

Additive	Aqueous $(NH_4)_2SO_4$ solution / mol dm^{-3}				
	0	1.0	2.0	3.0	4.0
ATAC monomer	Soluble	Soluble	Soluble	Soluble	Soluble
$PATAC_{242}$	Soluble	Soluble	Soluble	Soluble	Soluble
DMAC monomer	Soluble	Soluble	Soluble	Soluble	Insoluble
$PDMAC_{500}$	Soluble	Soluble	Insoluble	Insoluble	Insoluble

Table 2.4 Aqueous solubility of ATAC monomer, $PATAC_{242}$ homopolymer, DMAC monomer and $PDMAC_{500}$ homopolymer at 2.0% w/w solids in the presence of zero to 4.0 M ammonium sulfate as judged by visual inspection at pH 5.5 and 20°C.

Accordingly, the RAFT aqueous dispersion polymerisation of DMAC using a salt-tolerant poly(2-(acryloyloxy)ethyl trimethylammonium chloride) (PATAC) precursor in the presence of 2.0 M ammonium sulfate was conducted under the conditions summarised in **Scheme 2.4a**. The final turbid latex dispersion was transformed into a transparent viscous polymer solution after a four-fold dilution using deionised water, see **Scheme 2.4b**.

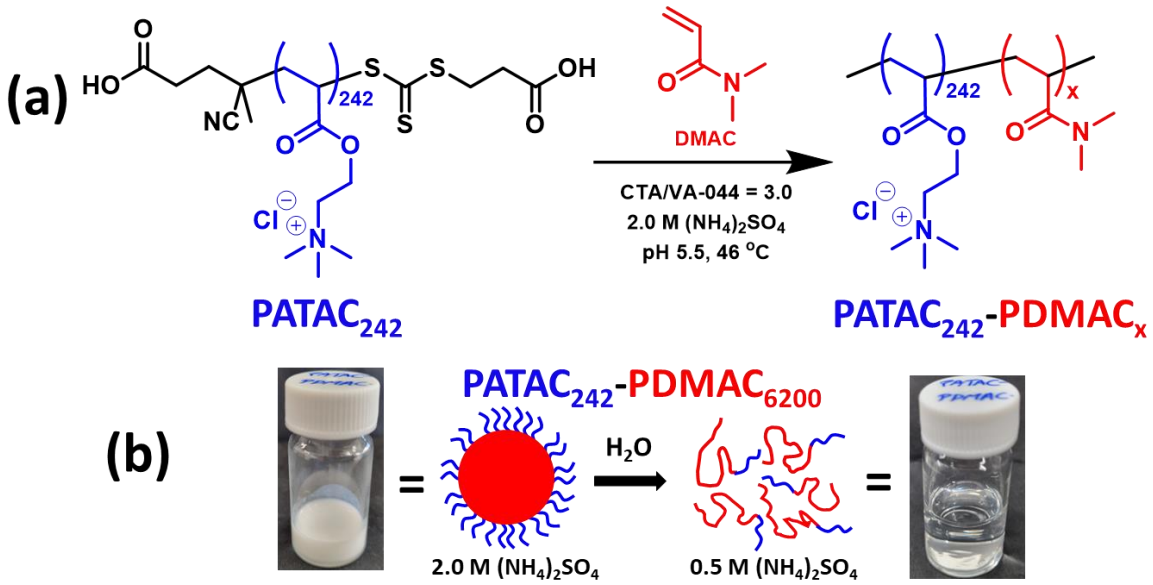

Scheme 2.4 (a) Reaction scheme for the synthesis of $PATAC_{242}$-$PDMAC_x$ diblock copolymer particles via RAFT aqueous dispersion polymerisation of DMAC at 46°C in the presence of 2.0 M ammonium sulfate. Conditions: a $PATAC_{242}$/VA-044 molar ratio of 3.0 was used to target 20% w/w solids. (b) Schematic cartoon and corresponding digital images to illustrate the sterically-stabilised diblock copolymer particles formed in the presence of 2.0 M ammonium sulfate after RAFT aqueous dispersion polymerisation of DMAC. A four-fold dilution of this aqueous dispersion with deionised water reduces the salt concentration and hence causes molecular dissolution of the particles, producing a viscous transparent aqueous solution comprising fully-solvated diblock copolymer chains.

When targeting 10% w/w copolymer solids, consisting of 10 – 7% w/w DMAC with correspondingly 0 – 3% $PATAC_{242}$ (target PDMAC DP ≥ 1,100), the transparent appearance of the solutions indicates they are fully miscible in 2.0 M ammonium sulfate up to 44°C. However, when targeting 11% w/w copolymer solids or higher, a turbid partial emulsion may be formed in 2.0 M ammonium sulfate, particularly when the DMAC concentration is ≥ 10% w/w. The critical insolubility temperature (above which insolubility is observed) for different proportions of $PATAC_{242}$ and PDMAC in an 11% w/w solution are recorded in **Table 2.5**.

$PATAC_{242}$ / % w/w	DMAC / % w/w	Critical insolubility temperature / °C
0	11	16
1	10	40
2	9	53
3	8	67

Table 2.5 Critical insolubility temperature recorded for $PATAC_{242}$ and DMAC monomer mixtures in 2.0 M ammonium sulfate.

Therefore, the DMAC solids content should not exceed 10% w/w, at least for target DPs greater than 1,100, for a true aqueous dispersion polymerisation using $PATAC_{242}$ precursor. However, more concentrated formulations should deliver an enhanced thickening effect, so 20 – 40% w/w DMAC was also explored. This means that the initial reaction mixture contains some fraction of water-immiscible DMAC monomer. Thus such formulations arguably correspond to a RAFT aqueous emulsion polymerisation, rather than a true RAFT aqueous dispersion polymerisation. However, if approximately 50% of the DMAC monomer remains water-soluble, then it is likely that the latter nomenclature is a more accurate description, at least in terms of the kinetics of polymerisation.

^{1}H NMR spectra for ATAC and DMAC monomers and their corresponding purified $PATAC_{242}$ and $PDMAC_{500}$ homopolymers are shown in **Figure 2.6**. In addition, a $PATAC_{242}$-$PDMAC_{1000}$ diblock copolymer has been included: its PDMAC backbone (f' and g') and dimethyl (h') proton signals are readily identifiable. The PATAC oxymethylene (c'), azamethylene (d') and trimethyl (e') protons are also present, albeit at significantly lower intensities.

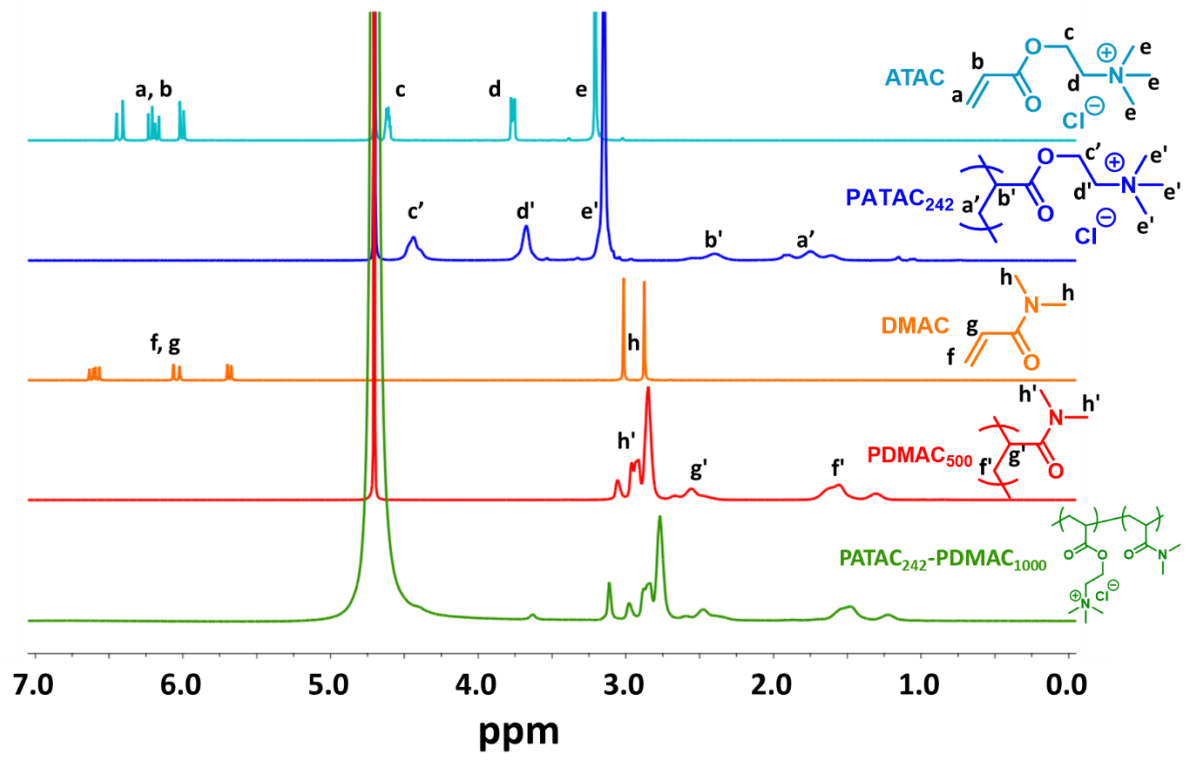

Figure 2.6 ^{1}H NMR spectra recorded in D_2O for ATAC, $PATAC_{242}$, DMAC, $PDMAC_{500}$ and a $PATAC_{242}$-$PDMAC_{1000}$ homopolymer.

When ammonium sulfate is dissolved in water, a buffer equilibrium is established between the ammonium cation and ammonia. This equilibrium is pH dependent, so addition of acid shifts it in favour of the ammonium cation, and addition of base shifts it in favour of ammonia: $NH_4^+(aq) + H_2O\,(aq) \rightleftharpoons NH_3\,(aq) + H_3O^+\,(l)$.

The ^{1}H NMR spectra recorded for pure ammonium sulfate solutions and molecularly-dissolved PATAC-PDMAC diblock copolymers containing just 0.2 M ammonium sulfate, these are shown in **Figure 2.7**. For the pH 4.8 salt solution (brown spectra), the fast proton exchange results in a broad NH_4^+ peak between 6 – 8 ppm and also broadening of the solvent peak between 4 – 5 ppm. However, when the pH of this solution is modified to be pH 8.2 via addition of NaOH (aq), the NH_4^+ peak disappears completely (green spectra). In this work, ^{1}H NMR spectra of many diblock copolymer samples containing residual salt quantities from dilution with D_2O have been obtained. Notably, the salt signals present on these spectra can

appear in different forms which is attributed to the solution pH and extent of NMR resonance with the ammonium group. The purple spectrum shows a broad signal for NH_4^+, whereas the blue spectrum shows a 1:1:1 triplet at 7.0 ppm (52 Hz, *J*-coupling). This ammonium signal has been identified by other research groups who have developed techniques to selectively monitor it.[21,22] Moreover, some samples slow down the H/D exchange rate on the NMR timescale, so the solvent signal at 4 – 5 ppm is split into two signals for HDO and H_2O.

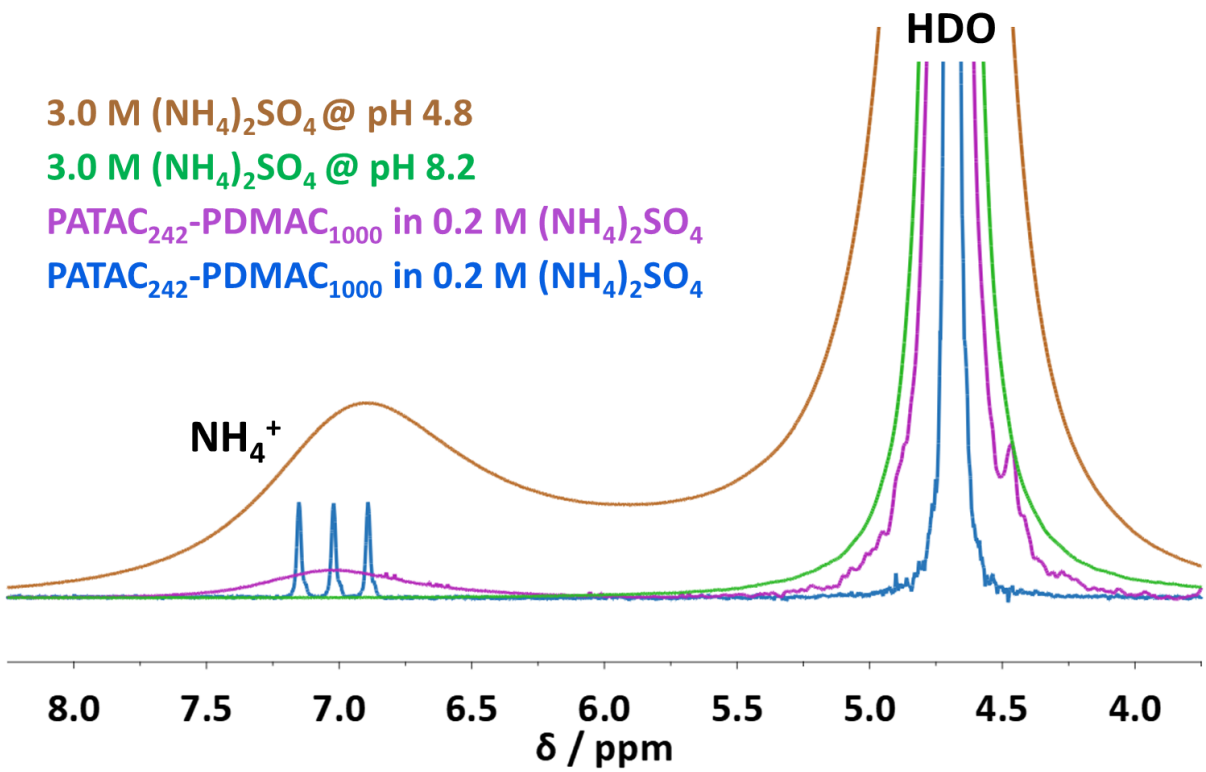

Figure 2.7 Partial ^1H NMR spectra recorded in D_2O for ammonium sulfate (pH 4.8 and pH 8.2) and for two $PATAC_{242}$-$PDMAC_x$ formulations in 0.2 M ammonium sulfate. A broad peak for the NH_4^+ signal is present at around 7.0 ppm for each spectrum except one of the $PATAC_{242}$-$PDMAC_{1000}$ spectra which instead has a 1:1:1 triplet with J-coupling = 52 Hz.

When targeting 20% w/w solids for the $PATAC_{242}$-$PDMAC_x$ formulations, final DMAC conversions typically ranged from 96% to more than 99% for the first six aqueous PISA syntheses shown in **Table 2.6**. However, a significantly lower conversion (58%) was achieved when targeting a DP of 15,000. Thus a target DP of 12,400 probably represents the realistic upper limit for this particular aqueous PISA formulation. For a target PDMAC DP of 1,250, a

low-turbidity dispersion of relatively high viscosity was obtained due to incomplete micellar nucleation. In contrast, lower viscosity dispersions were obtained when targeting higher PDMAC DPs.

PDMAC DP (x)	Conversion[a] / %	NMR M_n[a] / kg mol^{-1}	M_w[b] / kg mol^{-1}	GPC M_n[c] / kg mol^{-1}	M_w / M_n [c]	D_z[d] / nm	PDI[d]
1,250	> 99	171	294	62	2.61	116	0.06
3,000	> 99	344	535	101	2.59	225	0.13
5,000	99	538	1,118	153	2.73	320	0.07
6,200	99	655	1,399	156	2.92	350	0.19
9,300	99	959	1,973	210	2.86	505	0.20
12,400	96	1,227	2,091	253	2.70	1020	0.60
15,000	58	low conversion					

Table 2.6 Summary of a) monomer conversions and polymer masses obtained via ^{1}H NMR spectroscopy, b) M_w determined obtained by aqueous GPC MALLS detector (using Eluent 1, dn/dc = 0.151), c) M_n and M_w/M_n data obtained by aqueous GPC refractive index detector (using Eluent 1; vs. PEO calibration standards) and d) DLS particle size data.

The hydrodynamic z-average particle diameter (D_z) determined by DLS increases monotonically with PDMAC DP. However, higher DLS polydispersities are obtained at higher DPs, indicating progressively broader particle size distributions. In particular, the polydispersity of 0.60 observed for the DP 12,400 entry indicates an extremely broad size distribution. DLS (and other particle sizing techniques which use the Stokes-Einstein equation) can quantify the particle size, but the dynamic viscosity of the diluent must be known. Example data for this is shown in **Table 2.7** and each DLS measurement was performed using the relevant values.

$(NH_4)_2SO_4$ concentration / M	Dynamic viscosity / Pa s	Refractive index
0.5	1.095	1.344
1.0	1.225	1.353
2.0	1.510	1.370
3.0	2.030	1.384

Table 2.7 Summary of dynamic viscosities and refractive indices for various aqueous ammonium sulfate solutions at 20°C.[3] These data were used for DLS analysis.

Various aqueous GPC protocols were evaluated for this series of $PATAC_{242}$-$PDMAC_x$ diblock copolymers. This included varying both the eluent composition and GPC column type. Ultimately, Eluent 1 (see Experimental) was selected as optimal. In a prior study, Byard reported bimodal GPC traces for lower molecular weight PDMAC-based diblock copolymers.[10] Similar observations were made for copolymers with PDMAC DPs below 3000. The GPC curves are shown in **Figure 2.8**: M_n values increase monotonically and reasonable blocking efficiency (or chain extension efficiency) is observed. However, relatively high dispersities are obtained (M_w/M_n = 2.59-2.92), which suggests poorly controlled RAFT polymerisations. This is understandable given the relatively low RAFT agent/initiator molar ratio of 3.0 used in these aqueous PISA syntheses, which is essential to achieve high DMAC conversions.

Furthermore, the GPC M_n values are significantly lower than the corresponding calculated M_n values (after taking into account the final DMAC conversion). This systematic error is attributed to the choice of calibration standards: PEO exhibits a significantly different hydrodynamic volume compared to that of a PATAC-PDMAC diblock copolymer of equivalent molecular weight.

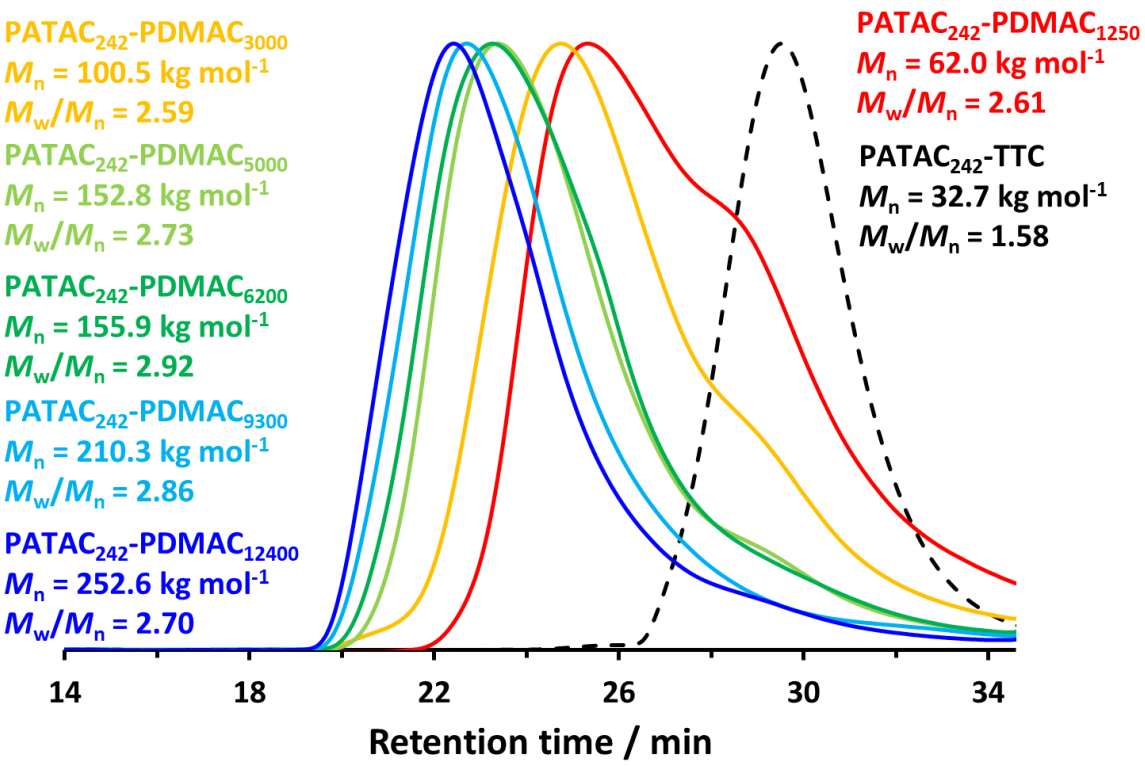

Figure 2.8 Aqueous GPC curves recorded for the $PATAC_{242}$ precursor and a series of $PATAC_{242}$-$PDMAC_x$ diblock copolymers prepared by chain extension via RAFT aqueous dispersion polymerisation of DMAC at 46°C in the presence of 2.0 M ammonium sulfate. M_n values are calculated relative to a series of near-monodisperse PEO calibration standards. Eluent 1 was used which consisted of 0.50 M CH_3COOH and 0.30 M NaH_2PO_4 at pH 3.0.

Inspection of the SLS-derived M_w column in **Table 2.6** indicates a monotonic increase in the weight-average molecular weight (M_w) for the $PATAC_{242}$-$PDMAC_{1250\text{-}12400}$ series. The SLS plots associated with each sample obtained are shown in **Figure 2.9**. Each datapoint corresponds to the light scattering signal at different pre-set angles which have been intensity normalised. The datapoint at zero-angle (the intercept of the trendline), is equal to the reciprocal of the M_w.[23] Only a single concentration has been used to obtain these graphs for each sample, a more accurate determination of M_w can be obtained via a Zimm plot at multiple concentrations. This analysis has been completed for the formulations described in **Chapter 5**.

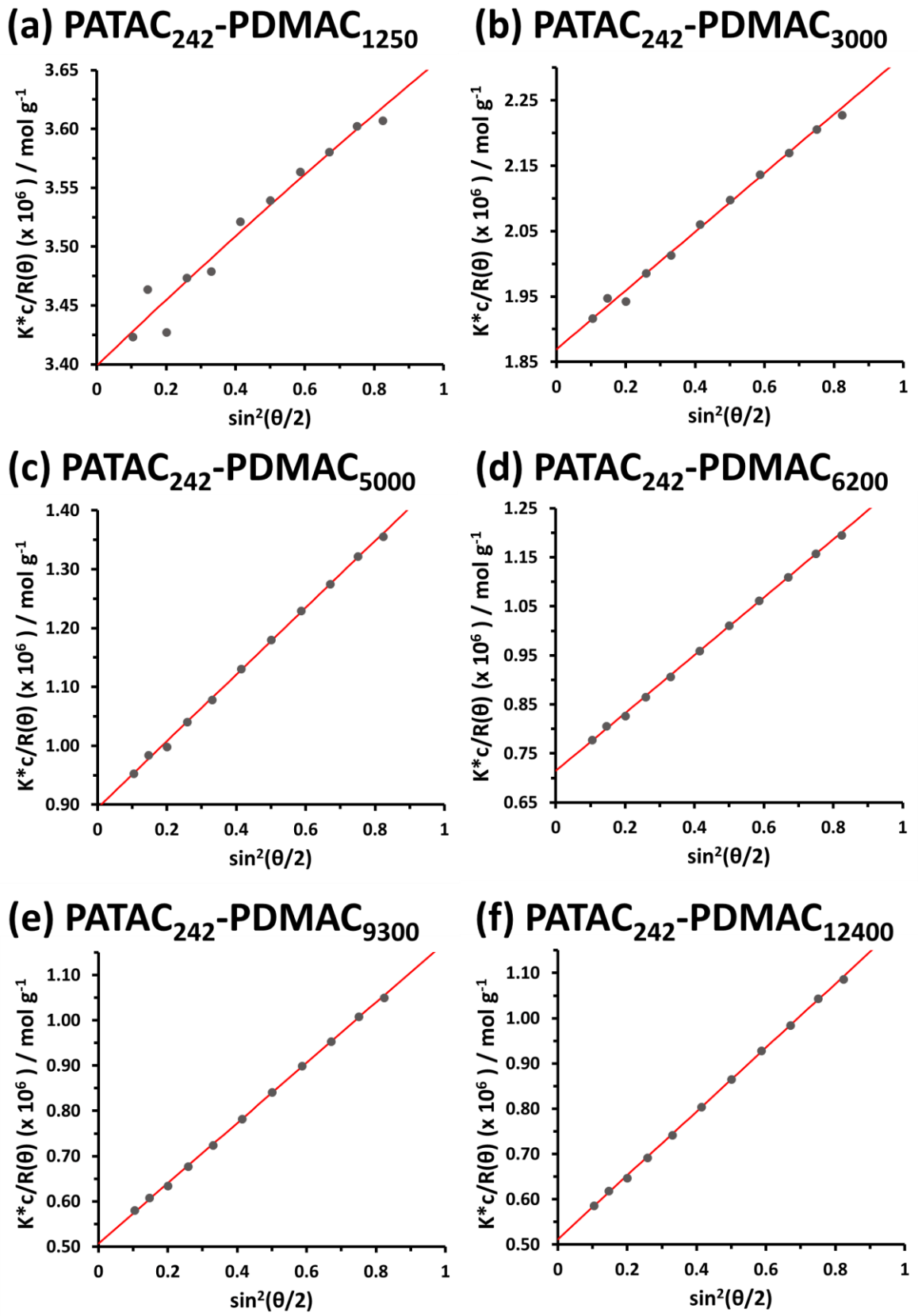

Figure 2.9 SLS plots using the Zimm formalism for light scattering data obtained for $PATAC_{242}$-$PDMAC_{1250\text{-}12400}$ diblock copolymers (in the presence of approximately 0.01 M ammonium sulfate). The weight-average molecular weight (M_w) of these micelles was determined using a MALLS-GPC detector.

Optical microscopy analysis of the $PATAC_{242}$-$PDMAC_{12400}$ formulation confirms the presence of polydisperse spherical particles, see **Figure 2.10**. This is consistent with the relatively high DLS polydispersity obtained for this sample. Given the highly salty nature of the particulate formulation, transmission electron microscopy (TEM) and scanning electron microscopy (SEM) are problematic owing to the excess (non-volatile) salt.

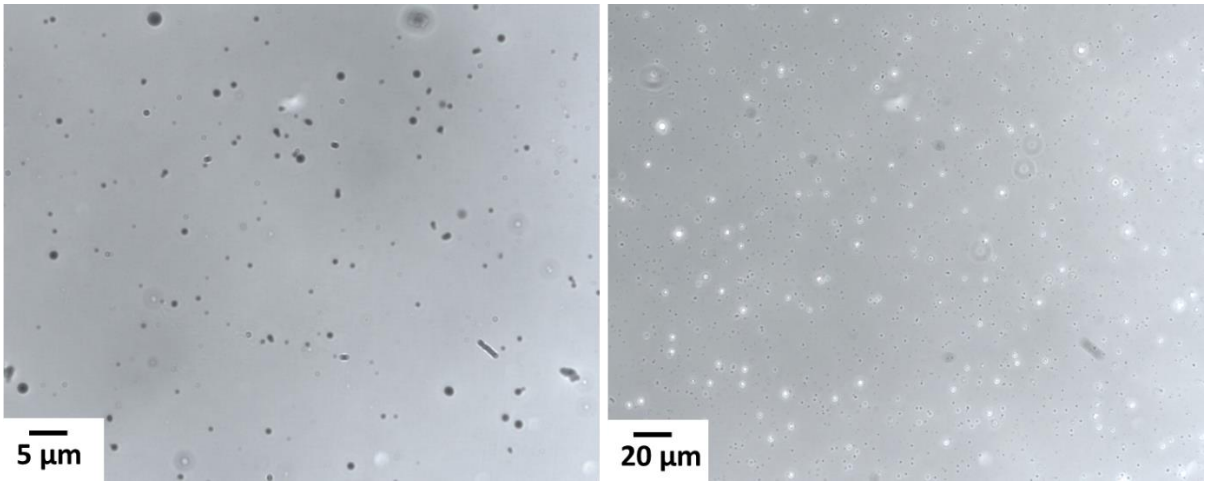

Figure 2.10 Optical microscopy images recorded for $PATAC_{242}$-$PDMAC_{12400}$ particles prepared by RAFT aqueous dispersion polymerisation of DMAC in the presence of 2.0 M ammonium sulfate targeting 20% w/w solids.

Rheology data are shown in **Figure 2.11**. The viscosity of the as-synthesised 20% w/w aqueous diblock copolymer dispersions is relatively low at all shear rates. However, an increase in solution viscosity of one to three orders of magnitude is observed for the corresponding molecularly-dissolved diblock copolymers obtained after a four-fold dilution using deionised water. This demonstrates the principle of dilution-triggered thickening.

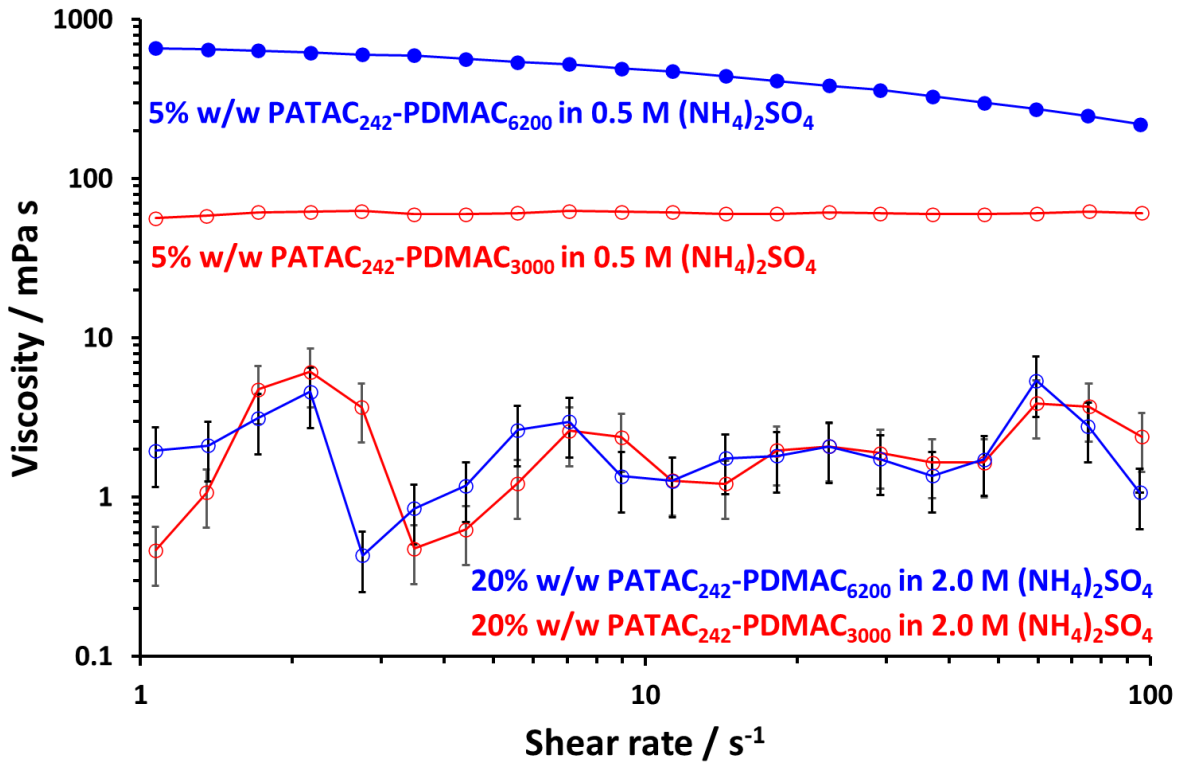

Figure 2.11 Viscosity vs. shear rate data obtained by rotational rheology studies of 20% w/w aqueous *dispersions* of either $PATAC_{242}$-$PDMAC_{3000}$ or $PATAC_{242}$-$PDMAC_{6200}$ particles in 2.0 M ammonium sulfate (open circles) compared to that for 5% w/w aqueous *solutions* of the same two copolymers in the presence of 0.5 M ammonium sulfate (closed circles) formed after a four-fold dilution using deionised water.

After establishing a set of data at 20% w/w solids, further development of the $PATAC_{242}$-$PDMAC_x$ formulation was undertaken. A monomer-starved protocol, whereby the core block monomer is gradually added to the reaction mixture, enables the concentration of unreacted monomer to be kept low while still targeting high solids and DPs. Accordingly, $PATAC_{242}$-$PDMAC_{10000}$ particles were targeted at 40% w/w solids. However, this protocol only resulted in very large polydisperse particles, see **Table 2.8**. Moreover, partial macroscopic precipitation was observed as well as the free-flowing colloidal dispersion. Interestingly, conducting the same formulation with no stirring resulted in complete macroscopic precipitation. Although dispersion polymerisations should not normally require agitation, stirring is essential for this particular system to ensure a homogeneous reaction mixture, otherwise unreacted monomer formed an insoluble surface layer within an hour. Increasing the target PDMAC DP up to

11,000 resulted in macroscopic precipitation, which most likely represents the upper limit DP for this formulation. DMAC monomer was added over 6 h for the DP 10,000 synthesis, with shorter times being used when targeting lower DPs.

PDMAC DP (x)	Solids / % w/w	Conversion[a] / %	M_n[a] / kg mol^{-1}	D_z[b] / nm	PDI[b]
5,000	30	> 99	523	300	0.29
8,000	30	99	832	550	0.15
5,000	40	97	527	500	0.65
10,000[c]	40	99	1031	1850	0.60
10,000[c]	40	**No stirring:** macroscopic precipitation			
11,000[c]	40	macroscopic precipitation			

Table 2.8 Summary of high solids and DP formulations using monomer-starved protocol. Reported with (a) ^{1}H NMR spectroscopy to determine monomer conversion and a calculated M_n based on the conversion, (b) DLS determined values for particle z-average hydrodynamic diameter (D_z) and PDI. (c) An inhomogeneous product formed with at least some precipitate.

A homogeneous portion of the $PATAC_{242}$-$PDMAC_{10000}$ formulation was diluted four-fold with deionised water and a highly viscous free-standing gel was obtained, see **Figure 2.12**. In principle, such formulations offer potential scope for viscosity modification applications. Moreover, the initial dispersion remained colloidally stable for four years, although the 0.50 M copolymer solution became mouldy within six months. The latter problem should be alleviated by addition of a suitable antimicrobial agent (e.g. sodium azide).

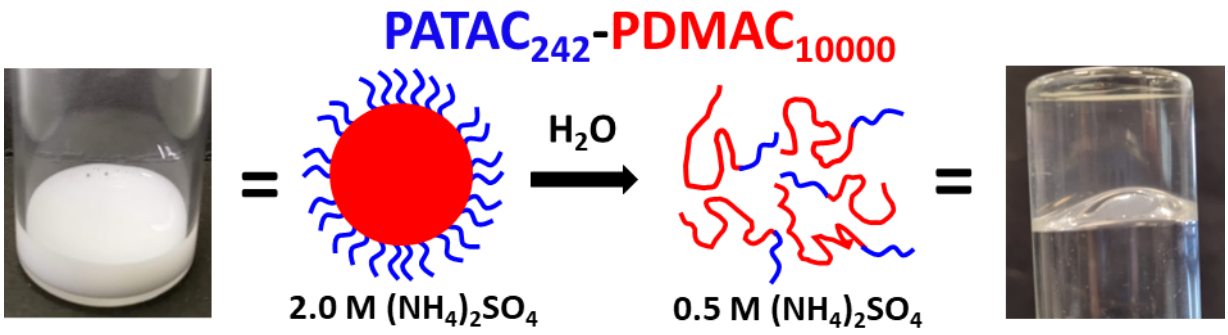

Figure 2.12 Schematic cartoon and corresponding digital images to illustrate the sterically-stabilised $PATAC_{242}$-$PDMAC_{10000}$ diblock copolymer particles formed via RAFT aqueous dispersion polymerisation of DMAC at 40% w/w in the presence of 2.0 M ammonium sulfate. A four-fold dilution of this aqueous dispersion with deionised water lowers the salt

concentration and results in molecular dissolution of the particles to form copolymer chains, with the concomitant formation of a free-standing viscous transparent aqueous solution.

2.4 Conclusions

RAFT solution polymerisation using trithiocarbonates has been used to synthesise a range of hydrophilic homopolymers from the respective vinyl monomers. Aqueous solubility experiments conducted on eighteen water-soluble vinyl monomers and their corresponding homopolymers using a series of ammonium sulfate concentrations enabled identification of suitable reaction conditions for RAFT aqueous dispersion polymerisation using a suitably salt-tolerant homopolymer as an electrosteric stabiliser to grow a salt-intolerant core-forming block. Suitable salt-intolerant polymers include PNAM, PMEMA and PNAEP, which each become water-immiscible in the presence of 0.50 to 1.0 M ammonium sulfate. In contrast, salt-tolerant polymers such as PATAC, PMETAC, PMPC, PNaAc and PAMPS remain water-soluble up to 4.0 M ammonium sulfate. In principle, PHEAC, PAM and PDMAC could be employed either as non-ionic steric stabilisers or core-forming blocks depending on the precise salt concentration.

$PATAC_{242}$-$PDMAC_x$ diblock copolymer particles have been prepared at 20% w/w solids, with high DMAC conversions being achieved when targeting a PDMAC DP of 12,400. Under monomer-starved conditions, a PDMAC DP of 10,000 can be achieved at 40% w/w solids (albeit with partial macroscopic precipitation). Good RAFT control cannot be expected given the relatively low CTA/initiator molar ratio required to ensure a high DMAC conversion. The MALLS data for the $PATAC_{242}$-$PDMAC_{1250\text{-}12400}$ series shows an increase in M_w from 294 – 2,091 kg mol^{-1}. Thus, this strategy for the synthesis of high molecular weight polymers has led to the formation of free-standing highly viscous polymer solutions via a low-viscosity synthetic method.

DLS studies indicate a monotonic increase in the hydrodynamic z-average diameter with increasing PDMAC DP. However, the concomitant increase in DLS polydispersity suggests a gradual loss of control over the particle size distribution. The largest diblock copolymer particles synthesised at 20% w/w could be imaged using optical microscopy.

When using a monomer-starved protocol, efficient stirring is required to ensure uniform mixing of the monomer with the reaction mixture and hence avoid macroscopic precipitation. A four-fold dilution of the final aqueous diblock copolymer dispersion with water lowers the ammonium sulfate concentration from 2.0 M to 0.50 M, which converts the free-flowing turbid dispersion into a highly viscous, free-standing transparent gel. Such dilution-triggered thickening may offer potential applications in the field of viscosity modification.

2.5 References

1 Controlled Radical Polymerization in Water-in-Water Dispersion, M. Destarac, J. D. Wilson, S. Silvia, Rhodia, WO2013132108A1, 2013.

2 K. Skrabania, A. Miasnikova, A. M. Bivigou-Koumba, D. Zehm and A. Laschewsky, 'Examining the UV-vis absorption of RAFT chain transfer agents and their use for polymer analysis', *Polym. Chem.*, 2011, **2**, 2074–2083.

3 R. Weast, *CRC Handbook of Chemistry and Physics*, CRC Press, Boca Raton, Florida, 66th edn., 1985.

4 E. R. Jones, M. Semsarilar, A. Blanazs and S. P. Armes, 'Efficient synthesis of amine-functional diblock copolymer nanoparticles via RAFT dispersion polymerization of benzyl methacrylate in alcoholic media', *Macromolecules*, 2012, **45**, 5091–5098.

5 M. J. Rymaruk, K. L. Thompson, M. J. Derry, N. J. Warren, L. P. D. Ratcliffe, C. N. Williams, S. L. Brown and S. P. Armes, 'Bespoke contrast-matched diblock copolymer nanoparticles enable the rational design of highly transparent Pickering double emulsions', *Nanoscale*, 2016, **8**, 14497–14506.

6 J. T. Lai, D. Filla and R. Shea, 'Functional Polymers from Novel Carboxyl-Terminated Trithiocarbonates as Highly Efficient RAFT Agents', *Macromolecules*, 2002, **35**, 6754–6756.

7 C. Bray, R. Peltier, H. Kim, A. Mastrangelo and S. Perrier, 'Anionic multiblock core cross-linked star copolymers: via RAFT polymerization', *Polym. Chem.*, 2017, **8**, 5513–5524.

8 C. P. Bray, PhD Thesis, University of Warwick, 2018.

9 S. J. Byard, C. T. O'Brien, M. J. Derry, M. Williams, O. O. Mykhaylyk, A. Blanazs and S. P. Armes, 'Unique aqueous self-assembly behavior of a thermoresponsive diblock copolymer', *Chem. Sci.*, 2020, **11**, 396–402.

10 S. J. Byard, Synthesis and Characterisation of Stimulus-responsive Diblock Copolymer Nano-objects

Prepared by RAFT Aqueous Dispersion Polymerisation, PhD Thesis, University of Sheffield, 2019.

11 F. A. Plamper, H. Becker, M. Lanzendörfer, M. Patel, A. Wittemann, M. Ballauff and A. H. E. Müller, 'Synthesis, characterization and behavior in aqueous solution of star-shaped poly(acrylic acid)', *Macromol. Chem. Phys.*, 2005, **206**, 1813–1825.

12 E. V. Piletska, A. R. Guerreiro, M. Romero-Guerra, I. Chianella, A. P. F. Turner and S. A. Piletsky, 'Design of molecular imprinted polymers compatible with aqueous environment', *Anal. Chim. Acta*, 2008, **607**, 54–60.

13 R. Arnold, 'The titration of polymeric acids', *J. Colloid Sci.*, 1957, **12**, 549–556.

14 T. Swift, L. Swanson, M. Geoghegan and S. Rimmer, 'The pH-responsive behaviour of poly(acrylic acid) in aqueous solution is dependent on molar mass', *Soft Matter*, 2016, **12**, 2542–2549.

15 W. Kern, 'Heteropolar molecular colloids. I. Polyacrylic acid, a model of the proteins', *Z. Phys. Chem*, 1938, **181**, 249–282.

16 A. Katchalsky and P. Spitnik, 'Potentiometric titrations of polymethacrylic acid', *J. Polym. Sci.*, 1947, **2**, 432–446.

17 A. Katchalsky and J. Gillis, 'Theory of the potentiometric titration of polymeric acids', *Recl. des Trav. Chim. des Pays-Bas*, 1949, **68**, 879–897.

18 M. Kikuchi, Y. Terayama, T. Ishikawa, T. Hoshino, M. Kobayashi, H. Ogawa, H. Masunaga, J. I. Koike, M. Horigome, K. Ishihara and A. Takahara, 'Chain dimension of polyampholytes in solution and immobilized brush states', *Polym. J.*, 2012, **44**, 121–130.

19 M. B. Einarson and J. C. Berg, 'Electrosteric stabilization of colloidal latex dispersions', *J. Colloid Interface Sci.*, 1993, **155**, 165–172.

20 J. Cesarano, I. A. Aksay and A. Bleier, 'Stability of Aqueous alpha-Al2O3 Suspensions with Poly(methacrylic acid) Polyelectrolyte', *J. Am. Ceram. Soc.*, 1988, **71**, 250–255.

21 A. C. Nielander, J. M. McEnaney, J. A. Schwalbe, J. G. Baker, S. J. Blair, L. Wang, J. G. Pelton, S. Z. Andersen, K. Enemark-Rasmussen, V. Čolić, S. Yang, S. F. Bent, M. Cargnello, J. Kibsgaard, P. C. K. Vesborg, I. Chorkendorff and T. F. Jaramillo, 'A versatile method for ammonia detection in a range of relevant electrolytes via direct nuclear magnetic resonance techniques', *ACS Catal.*, 2019, **9**, 5797–5802.

22 M. Kolen, W. A. Smith and F. M. Mulder, 'Accelerating 1H NMR Detection of Aqueous Ammonia', *ACS Omega*, 2021, **6**, 5698–5704.

23 E. R. Jones, O. O. Mykhaylyk, M. Semsarilar, M. Boerakker, P. Wyman and S. P. Armes, 'How Do Spherical Diblock Copolymer Nanoparticles Grow during RAFT Alcoholic Dispersion Polymerization?', *Macromolecules*, 2016, **49**, 172–181.

Chapter 3: Synthesis of High Molecular Weight Water-Soluble Polymers as Low-Viscosity Latex Particles by RAFT Aqueous Dispersion Polymerisation

Reproduced with permission from [R. J. McBride, J. F. Miller, A. Blanazs, H.-J. Hähnle, and S. P. Armes, *Macromolecules*, 2022, **55**, 7380−7391]

3.1 Introduction

We report the synthesis of sterically-stabilised diblock copolymer particles at 20% w/w solids via reversible addition-fragmentation chain transfer (RAFT) aqueous dispersion polymerisation of *N*,*N*-dimethylacrylamide (DMAC) in highly salty media (2.0 M ammonium sulfate). This is achieved by selecting a well-known zwitterionic water-soluble polymer, poly(2-(methacryloyloxy)ethyl phosphorylcholine) (PMPC), to act as the salt-tolerant soluble precursor block. A relatively high degree of polymerisation (DP) can be targeted for the salt-insoluble PDMAC block, which leads to formation of a turbid free-flowing dispersion by a steric stabilisation mechanism. ^{1}H NMR spectroscopy studies indicate that relatively high DMAC conversions (>99%) can be achieved within a few hours at 30°C. Aqueous GPC analysis indicates high blocking efficiencies and unimodal molecular weight distributions, although dispersities increase monotonically as higher degrees of polymerisation (DPs) are targeted for the PDMAC block. Particle characterisation techniques include dynamic light scattering (DLS) and electrophoretic light scattering (ELS) using a state-of-the-art instrument that enables accurate zeta potential measurements in concentrated salt solution. ^{1}H NMR spectroscopy studies confirm that subsequent dilution using deionised water lowers the background salt concentration and hence causes *in situ* molecular dissolution of the salt-intolerant PDMAC chains, which leads to a substantial thickening effect and the formation of transparent gels. Thus this new polymerisation-induced self-assembly (PISA) formulation enables high molecular weight water-soluble polymers to be prepared in a highly convenient, low-viscosity latex-like form. In principle, such aqueous PISA formulations are highly attractive: there are various commercial applications for high molecular weight water-soluble polymers while the well-known negative aspects of using a RAFT agent (i.e. its cost, colour and malodour) are minimised when targeting such high DPs.

It is well-known that reversible addition-fragmentation chain transfer (RAFT) polymerisation enables the synthesis of a wide range of *functional* vinyl polymers with good control over the molecular weight distribution.[1–4] There are many literature examples of RAFT solution homopolymerisation and in some cases mean degrees of polymerisation (DP) up to (and even beyond) 10,000 have been targeted.[5–7] This latter aspect is interesting for two reasons. Firstly, in the case of water-soluble polymers (e.g. polyacrylamide), such high molecular weights are useful for commercial applications such as flocculants, binders or thickeners.[8–10] Secondly, the main disadvantage of RAFT chemistry is that the chain transfer agent is an organosulfur compound, which is relatively expensive and confers both malodour and colour.[11] Since the mean DP is inversely proportional to the concentration of this RAFT agent,[12] targeting very high DPs minimises the problems associated with its use, which is likely to make a decisive difference to the feasibility of industrial scale-up.[13]

However, the synthesis of high molecular weight water-soluble polymers via RAFT aqueous solution polymerisation leads to extremely viscous reaction mixtures. For example, gel formation was reported by Destarac and co-workers when preparing polyacrylamide with a mean DP of around 10,000.[6] Such gels can be difficult to remove from the reaction vessel after the polymerisation and heat dissipation during polymerisation can become inefficient. In principle, this problem could be addressed by conducting such polymerisations in highly salty media. Under such conditions, the water-soluble polymer chains are ‘salted-out’, which leads to the formation of low-viscosity, free-flowing particulate dispersions, rather than highly viscous or gel-like aqueous solutions.[14] Indeed, this approach is used to prepare high molecular weight polyacrylamide in the form of particles via conventional free radical polymerisation conducted in aqueous solution in the presence of 2.0 M ammonium sulfate.[15–17]

Polymerisation-induced self-assembly (PISA) involves the growth of an insoluble block from a soluble precursor block in a suitable solvent. In the case of an aqueous PISA

formulation, the growing second block becomes water-insoluble while the first block remains water-soluble: the resulting amphiphilic diblock copolymer chains undergo micellar nucleation and ultimately sterically-stabilised diblock copolymer nanoparticles are produced. Depending on the aqueous solubility of the monomer used to generate the hydrophobic block, aqueous PISA formulations involve either RAFT aqueous emulsion polymerisation[18–20] or RAFT aqueous dispersion polymerisation.[21–26] In both cases, the hydrophobic block normally remains insoluble at the end of the polymerisation. However, there are several literature examples in which a temperature switch leads to *in situ* nanoparticle dissolution to yield molecularly-dissolved diblock copolymer chains.[27–29] In principle, a similar approach could involve the synthesis of a salt-intolerant water-soluble polymer in highly salty media to produce low-viscosity particles. Subsequent dilution using pure water would then lower the salt concentration in the aqueous continuous phase, which should lead to molecular dissolution of the high molecular weight copolymer chains within the particle cores and hence a strong thickening effect (see **Scheme 3.1**).

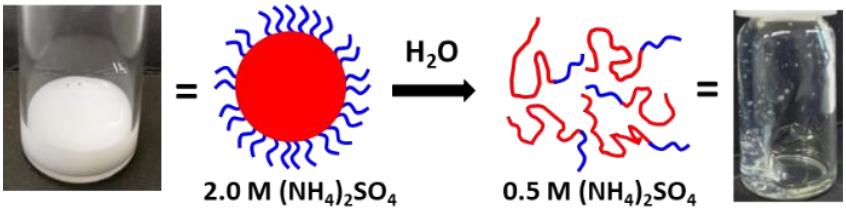

Scheme 3.1 Schematic cartoon and corresponding digital images to illustrate the sterically-stabilised diblock copolymer particles in the presence of 2.0 M ammonium sulfate obtained after RAFT aqueous dispersion polymerisation of a suitable water-soluble monomer to form the 'salted out' red chains. A four-fold dilution with deionised water lowers the salt concentration of the initial aqueous dispersion and results in molecular dissolution of these particles, with the concomitant formation of a highly viscous transparent aqueous solution.

According to well-established principles in colloid science, steric stabilisation is much more likely to be effective than charge stabilisation for such aqueous PISA syntheses.[30–32] Clearly, such formulations would require a steric stabiliser that remains soluble in the presence of substantial amounts of salt in order to confer effective colloidal stabilisation. According to the

literature, suitable salt-tolerant water-soluble polymeric stabilisers are likely to be either certain types of polyelectrolytes[16,17,33,34] or polybetaines.[35–37]

Herein we report the RAFT aqueous dispersion polymerisation of *N*,*N*-dimethylacrylamide (DMAC) in highly salty media using poly(2-(methacryloyloxy)ethyl phosphorylcholine) (PMPC) as a salt-tolerant steric stabiliser. According to the literature, PMPC remains soluble even in the presence of 5.0 M NaCl.[35] The previous chapter has shown that DMAC is a suitable monomer for aqueous dispersion polymerisations and the PATAC stabiliser is being substituted for another highly salt tolerant precursor polymer.

3.2 Experimental

3.2.1 Materials

N,*N*-Dimethylacrylamide (DMAC; ≥ 99%), L-ascorbic acid (AsAc; 99%), 4,4'-azobis(4-cyanopentanoic acid) (ACVA; ≥ 98%), basic alumina, azobis(isobutyl)amidine dihydrochloride (AIBA; ≥ 97%), glacial acetic acid (≥ 99%), sodium phosphate monobasic (≥ 99%), sodium nitrate (≥ 99%), 2-acrylamido-2-methylpropanesulfonic acid, sodium salt (AMPS; 50% w/w in water), phosphate buffered saline (PBS) tablets and deuterium oxide (D_2O; ≥ 99.9% D) were purchased from Sigma Aldrich (Merck; UK). 2-(Methacryloyloxy)ethyl phosphorylcholine (MPC) was kindly donated by Biocompatibles (UK). 2-Ethylhexanoyl tert-butyl peroxide (T-21S; ≥ 97%) was obtained from AkzoNobel (Netherlands). Potassium persulfate (KPS, 99%) and 2,2′-Azobis(2-imidazolinylpropane) dihydrochloride (VA-044, ≥ 98%) was obtained from Fluorochem Ltd (UK). Sodium hydroxide (≥ 98%) and ammonium sulfate (> 98%) were sourced from Thermo Fisher Scientific (UK). PEO standards were sourced from Agilent/PSS (Church Stretton, UK). 2-(Acryloyloxy)ethyl trimethylammonium chloride (ATAC; 80% w/w in water) was donated by BASF (Germany). 4-Cyano-4-(2-phenylethanesulfanylthiocarbonyl)-sulfanylpentanoic acid

(PETTC) was prepared and purified as reported elsewhere[38], as was 2-(((butylthio)-carbonothioyl)-thio)-2-methylpropanoic acid (BDMAT).[39,40] Unless otherwise stated, all solvents and concentrated acids were purchased from Fisher Scientific (UK) and were used as received. Deionised water was used for all experiments.

3.2.2 Characterisation Techniques

Experimental protocols for ^{1}H NMR spectroscopy, UV absorption spectroscopy, DLS, optical microscopy and rotational rheology are described in **Chapter 2**.

Aqueous Gel Permeation Chromatography (GPC)

The Agilent 1260 Infinity GPC set-up comprises a pump, a degasser, a guard column, three PL-Aquagel Mixed-H, OH-30 and OH-40 columns connected in series and a refractive index (RI) detector. GPC curves were recorded with a column and detector temperature of 30°C. All eluents used in this Thesis are reported in the experimental of **Chapter 2**. $PMPC_x$ and its derivative polymers were analysed at 1.0 mL min^{-1} using Eluent 2, which comprised 0.2 M $NaNO_3$ and 0.05 M TRIZMA/ TRIZMA•HCl buffer at pH 7.0. Calibration of the RI detector was achieved using nine near-monodisperse poly(ethylene oxide) standards (2.1 – 969 kDa) and data were analysed using Agilent Technologies GPC/SEC software.

Potentiometric Titration

An acidified aqueous dispersion (25.0 mL) was placed in a 250 mL glass beaker and stirred with a magnetic follower. Titrant solution was passed through a 0.2 µm polyethersulfone syringe filter into a volumetric 50 mL burette, and a standard glass pH electrode was immersed within the aqueous dispersion. A total titrant of 7.0 mL was added in aliquots of no more than 0.5 mL, with smaller aliquots being used where necessary to accurately determine the equivalence point. The apparent pH of the aqueous dispersion was recorded after adding each aliquot, with pH equilibration being achieved within 30 seconds of each addition. All

measurements were performed at 22 ± 1°C. Approximately 0.25 mL of the aqueous dispersion was removed at suitable intervals for subsequent electrophoretic light scattering (ELS) and dynamic light scattering (DLS) analyses. No attempt was made to remove dissolved CO_2 or to prevent its dissolution into the samples. It was assumed that the samples were near to or at the saturation level of dissolved CO_2.

Electrophoretic Light Scattering (ELS)

Electrophoretic mobilities were determined using Next Generation Electrophoretic Light Scattering (NG-ELS) using an instrument provided by Enlighten Scientific LLC (Hillsborough, NC, USA). The functional design and operation of this instrument are based upon the original phase analysis light scattering (PALS) apparatus[41] that employed a crossed-beam optical configuration in contrast to the more common reference beam configuration used in other ELS instruments. The electrode assembly used for the NG-ELS equipment was a variation of that described by Uzgiris.[42] Disposable polystyrene semi-micro cuvettes (4 mm path length; required volume = 0.25 mL) were used as the sample holders. Two identical parallel plate platinised platinum[43] electrodes, placed 4 mm apart, were used to provide the driving voltage. The sample temperature was determined using a miniature NTC-type thermistor placed in direct contact with an ≈ 0.1% w/w aqueous copolymer dispersion. This temperature sensor was positioned at the mid-point between the electrodes and approximately 1 mm above the intersection point of the two laser beams. Temperature control was achieved by placing the sample cuvette in an aluminum block that ensured efficient heat transfer with the (cooler) water circulating through channels within the block. The required water temperature depended on the amount of Joule heating of the sample and hence on both the sample conductivity and the voltage applied across the electrodes. Complex impedance analysis of the electrode waveform was used to quantify electrode polarisation and Joule heating. Mobility measurements were made using sinusoidal electrode signal waveforms with a nominal amplitude of 4.5 V at

frequencies of 64 and 128 Hz. Small adjustments (up to ± 0.3 V) to the amplitude were made prior to data collection to ensure that the sample temperature remained at 25 ± 1°C during each measurement. The scattered light was analysed using both the PALS and the laser Doppler electrophoresis (LDE) methods simultaneously. Data were collected for 1 min and the same data set was used to calculate the electrophoretic mobility using each method. For each sample, five independent measurements were made at each electrode signal frequency, yielding a total of ten measurements per sample from which a mean value was calculated.

Small Angle X-Ray Scattering (SAXS)

SAXS patterns were recorded for 1.0% w/w aqueous copolymer dispersions at Diamond Light Source (station I22, Didcot, UK) using a monochromatic X-ray beam ($\lambda = 0.124$ nm), a 2D Pilatus 2M pixel detector (Dectris, Switzerland) and a q range of 0.02−2.00 nm^{-1} for these experiments. $q = (4\pi \sin \theta)/\lambda$ corresponds to the modulus of the scattering vector and θ is half of the scattering angle. SAXS data were reduced (integrated, normalised, and background-subtracted) using Dawn software supplied by Diamond Light Source. The X-ray scattering intensity for water was used for absolute scale calibration of the scattering patterns with data manipulation on SAXS Utilities. Irena SAS macros for Igor Pro were utilised for modelling.[44]

3.2.3 Synthesis of the $PMPC_{139}$ Precursor via RAFT Solution Polymerisation of 2-(Methacryloyloxy)ethyl phosphorylcholine (MPC) in Methanol at 64°C

PETTC (250 mg, 0.74 mmol), MPC (26.10 g, 88.4 mmol), ACVA (41 mg, 150 µmol), and methanol (49.0 g, corresponding to a 35% w/w solution) were weighed into a 250 mL round-bottom flask charged with a magnetic stirrer and this reaction solution was degassed using nitrogen gas for 45 min at 20°C. The sealed flask was immersed into an oil bath set at 64°C for 210 min and the polymerisation was subsequently quenched by exposing the reaction mixture to air while cooling to 20°C. The final MPC conversion was 75%, as judged by ^{1}H NMR

spectroscopy (calculated by comparing the integrated vinyl signals assigned to MPC monomer at 5.6 – 6.2 ppm to the integrated polymethacrylic backbone signals at 0.6 – 2.4 ppm). The reaction solution was precipitated into a ten-fold excess of acetone. The crude PMPC precursor was redissolved in methanol and the precipitation was repeated. After dissolution using deionised water, the resulting aqueous polymer solution was freeze-dried overnight. The degree of polymerisation was 135 ± 10, as judged by ^{1}H NMR spectroscopy (calculated by comparing the integrated aromatic signals assigned to the RAFT end-group at 7.1 – 7.4 ppm to the integrated polymethacrylic backbone signals at 0.6 – 2.4 ppm). RAFT end-group analysis using UV spectroscopy indicated a mean degree of polymerisation of 139 ± 1 (the Beer−Lambert plot for PETTC is provided previously in **Figure 2.1**). Aqueous GPC analysis indicated an M_n of 17 kg mol^{-1} and an M_w/M_n of 1.18 (see **Section 3.2.2** for eluent and calibration details).

3.2.4 Preparation of 2.0 M Ammonium Sulfate Solution and Redox Initiator Solutions

Ammonium sulfate (26.43 g) was added to a 100 mL volumetric flask, which was subsequently filled with water to obtain a 2.0 M solution. The required molarity, refractive index and dynamic viscosity for an aqueous solution of 2.0 M ammonium sulfate were calculated by interpolation of tabulated solution properties reported at 20°C as recorded in **Table 3.1**.[45] The interpolated dynamic viscosity was estimated to 25°C using the ratio of the dynamic viscosity for water at 20°C and 25°C. The following numerical values for a 2.0 M aqueous solution of ammonium sulfate were used in this study: molality = 2.32 mol kg^{-1}; refractive index = 1.370 and dynamic viscosity = 1.367 x 10^{-3} kg m^{-1} s^{-1}. The relative permittivity of a 2.0 M aqueous solution of ammonium sulfate was assumed to be that for pure water. According to the literature, the addition of salt leads to a lower relative permittivity compared to that of water.[46] However, this systematic error is not considered to be important relative to the likely error incurred when calculating the zeta potential for electrosterically-stabilised nanoparticles[47] (see results and discussion for further details).

$(NH_4)_2SO_4$ concentration / M	Dynamic viscosity / Pa s	Refractive index
0.5	1.095	1.344
1.0	1.225	1.353
2.0	1.510	1.370
3.0	2.030	1.384

Table 3.1 Summary of dynamic viscosities and refractive indices for various aqueous ammonium sulfate solutions at 20°C.[45] These data were used for DLS analysis.

KPS (30.0 mg) was dissolved in an aqueous solution of 2.0 M ammonium sulfate (30 g) to make up a 0.1% w/w KPS stock solution. Similarly, AsAc (30.0 mg) was dissolved in an aqueous solution of 2.0 M ammonium sulfate (30 g) to make up a 0.1% w/w AsAc stock solution. Each stock solution was prepared just prior to use.

3.2.5 Synthesis of $PMPC_{139}$-$PDMAC_x$ Diblock Copolymer Particles via RAFT Aqueous Dispersion Polymerisation of *N,N*-Dimethylacrylamide (DMAC) in 2.0 M Ammonium Sulfate at 30°C

A typical protocol for the synthesis of $PMPC_{139}$-$PDMAC_{5000}$ spheres at 20% w/w solids was conducted as follows. The $PMPC_{139}$ precursor (140 mg, 4.0 µmol), DMAC (1.972 g, 19.9 mmol), KPS (1.0 µmol; 270 mg of a 0.1% w/w aqueous stock solution) and an aqueous solution of 2.0 M ammonium sulfate (8.00 g) were weighed into a 25 mL round-bottom flask charged with a magnetic stirrer and this reaction solution was degassed using nitrogen gas for 30 min at 20°C. The sealed flask was immersed into an oil bath set at 30°C and AsAc (1.0 µmol; 170 mg of a 0.1% w/w aqueous stock solution) was added to initiate the DMAC polymerisation. After 18 h, the polymerisation was subsequently quenched by exposing the reaction mixture to air while cooling to 20°C. The final DMAC conversion was more than 99%, as judged by ^{1}H NMR spectroscopy (as calculated by comparing the integrated vinyl signals assigned to DMAC monomer at 5.6 – 6.7 ppm to the integrated polyacrylamide backbone signals at 1.1 – 2.7 ppm).

Aqueous GPC analysis indicated an M_n of 262 kg mol^{-1} and an M_w/M_n of 1.97 (see **Section 3.2.2** for eluent and calibration details).

3.2.6 Synthesis of $PATAC_{195}$-$PDMAC_{1000}$ Diblock Copolymer Particles via RAFT Solution and Dispersion Polymerisations

See experimental in **Chapter 2**.

3.2.7 Synthesis of $PAMPS_{250}$-$PDMAC_{1000}$ Diblock Copolymer Particles via RAFT Solution and Dispersion Polymerisations

BDMAT (150 mg, 0.59 mmol), AMPS (55% w/w) (61.92 g, 149 mmol), T-21S (25.7 mg, 119 µmol), and 1.0 M PBS (23.5 g, corresponding to a 40% w/w solution) were weighed into a 250 mL round-bottom flask charged with a magnetic stirrer and this reaction solution was degassed using nitrogen gas for 45 min at 20°C. The sealed flask was immersed into an oil bath set at 90°C for 150 min and the polymerisation was subsequently quenched by exposing the reaction mixture to air while cooling to 20°C. The final AMPS conversion was 99%, as judged by ^{1}H NMR spectroscopy (calculated by comparing the integrated vinyl signals assigned to AMPS monomer at 5.6 – 6.2 ppm to the integrated polyacrylic backbone signals at 1.2 – 2.3 ppm). The reaction solution was purified by dialysis over three days with regular water changes. The resulting aqueous polymer solution was freeze-dried overnight. The degree of polymerisation was 250, as judged by ^{1}H NMR spectroscopy (calculated by comparing the integrated methyl signals assigned to the RAFT end-group at 0.8 – 0.9 ppm to the integrated polyacrylic backbone signals at 1.2 – 2.3 ppm). Aqueous GPC analysis indicated an M_n of 28 kg mol^{-1} and an M_w/M_n of 1.35 (see **Section 3.2.2** for eluent and calibration details).

Subsequently, the $PAMPS_{250}$ precursor (220 mg, 3.8 µmol), DMAC (379 mg, 3.82 mmol), VA-044 (1.3 µmol, 344 mg 0.1% of an aqueous stock solution) and an aqueous solution of 2.0 M ammonium sulfate (2.05 g) were weighed into a 10 mL round-bottom flask charged with a

magnetic stirrer and this reaction solution was degassed using nitrogen gas for 30 min at 20°C. The sealed flask was immersed into an oil bath set at 46°C to initiate the DMAC polymerisation. After 18 h, the polymerisation was subsequently quenched by exposing the reaction mixture to air while cooling to 20°C. The final DMAC conversion was more than 99%, as judged by ^{1}H NMR spectroscopy (as calculated by comparing the integrated vinyl signals assigned to DMAC monomer at 5.6 – 6.7 ppm to the integrated polyacrylamide backbone signals at 1.1 – 2.7 ppm). Aqueous GPC analysis indicated an M_n of 74 kg mol^{-1} and an M_w/M_n of 1.54 (see **Section 3.2.2** for eluent and calibration details).

3.2.8 Preparation of Dilute Aqueous Dispersions for DLS and Zeta Potential Studies and Titrants

Aqueous dispersions of $PMPC_{139}$-$PDMAC_{1000}$, $PATAC_{195}$-$PDMAC_{1000}$ and $PAMPS_{250}$-$PDMAC_{1000}$ particles in 2.0 M ammonium sulfate were diluted to 0.1% w/w using 2.0 M ammonium sulfate which had been adjusted to an apparent pH of 3.

A stock titrant solution was prepared gravimetrically comprising an aqueous solution of 1.0 M KOH (22.97 g), deionised water (99.98 g) and ammonium sulfate (30.40 g). Deionised water was filtered through a 0.2 µm polyethersulfone syringe filter prior to use.

3.3 Results and Discussion

The RAFT solution polymerisation of MPC was conducted in methanol at 64°C using a trithiocarbonate-based RAFT agent (PETTC). The mean degree of polymerisation (DP) of the PMPC homopolymer was determined via end-group analysis using UV spectroscopy to be 139 ± 1 based on the Beer Lambert calibration curve shown in **Figure 2.5**. This is larger than the target DP of 120. Aqueous GPC analysis indicated a relatively narrow molecular weight distribution (M_w/M_n = 1.18) for the precursor. However, the PEG calibration standards used for GPC analysis meant that only relative M_n values could be obtained. The RAFT aqueous

dispersion polymerisation of DMAC was conducted in the presence of 2.0 M ammonium sulfate at 30°C using the $PMPC_{139}$ precursor as a salt-tolerant steric stabiliser block, as outlined in **Scheme 3.2**.

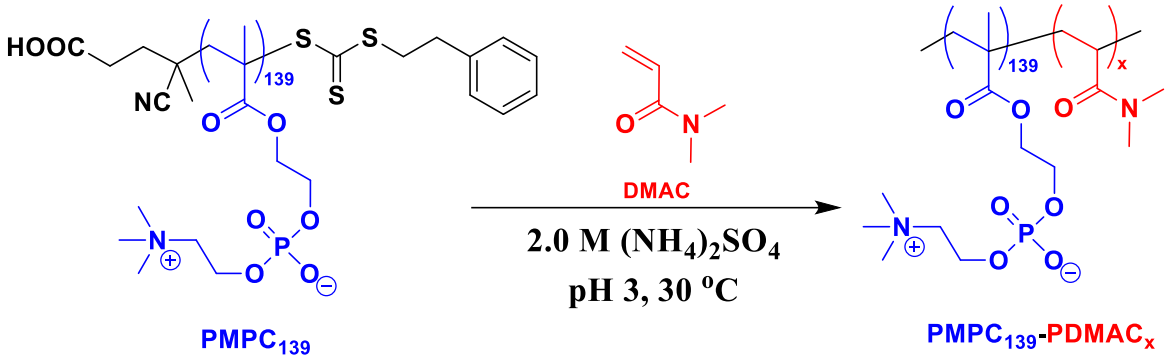

Scheme 3.2 Reaction scheme for the synthesis of $PMPC_{139}$-$PDMAC_x$ (x = 500 to 7,000) diblock copolymer particles via RAFT aqueous dispersion polymerisation of DMAC at 30°C in the presence of 2.0 M ammonium sulfate. Conditions: targeting 20% w/w solids using a $PMPC_{139}$/KPS molar ratio of 4.0 and a [KPS]/[AsAc] molar ratio of 1.0.

PMPC was chosen as the steric stabiliser block because its zwitterionic structure is known to confer aqueous solubility even at 5.0 M NaCl.[35] PDMAC was chosen as the core-forming block because it is a non-ionic water-soluble polymer that becomes water-insoluble in the presence of sufficient salt.[48] Moreover, the resulting PMPC-PDMAC diblock copolymer chains were anticipated to be amenable to aqueous GPC analysis.[49] Inspecting the data presented in **Table 3.2**, using 2.0 M ammonium sulfate should be sufficient to produce an aqueous dispersion polymerisation formulation, since the PMPC precursor and the DMAC monomer are soluble in the aqueous continuous phase and the growing PDMAC chains should become insoluble. Accordingly, the series of aqueous PISA syntheses shown in **Table 3.3** were conducted at 30°C using a well-known low-temperature persulfate/ascorbic acid (KPS/AsAc) redox initiator while targeting 20% w/w solids at pH 3.

Additive	Aqueous $(NH_4)_2SO_4$ solution / mol dm^{-3}				
	0	1.0	2.0	3.0	4.0
MPC monomer	Soluble	Soluble	Soluble	Soluble	Soluble
$PMPC_{139}$	Soluble	Soluble	Soluble	Soluble	Soluble
DMAC monomer	Soluble	Soluble	Soluble	Soluble	Insoluble
$PDMAC_{500}$	Soluble	Soluble	Insoluble	Insoluble	Insoluble

Table 3.2 Aqueous solubility of MPC monomer, $PMPC_{139}$ homopolymer, DMAC monomer and $PDMAC_{500}$ homopolymer at 2.0% w/w solids in the presence of zero to 4.0 M ammonium sulfate as judged by visual inspection at pH 5.5 and 20°C.

The $PMPC_{139}$ precursor afforded colloidally stable dispersions of increasing turbidity when targeting PDMAC DPs ranging from 500 to 6,000. However, precipitation was observed when targeting PDMAC DPs above 6,000 or when the target copolymer concentration was increased to 25% w/w solids. The PDMAC core block DPs were determined relative to that of the stabiliser block by end-group analysis using ^{1}H NMR spectroscopy. Reasonably good agreement (within experimental error) with the target PDMAC DPs was obtained by comparing the integrated methine proton signal on the PDMAC backbone at 2.2 – 2.7 ppm and the $PMPC_{139}$ azamethylene signal at 3.6 ppm. Comparing these NMR-derived M_n values to those determined by GPC analysis suggests a significant systematic error for the latter technique. This is understandable because PEO calibration standards are unlikely to be accurate for the analysis of PDMAC-rich diblock copolymers. Macroscopic precipitation was observed for the attempted synthesis conducted at 30% w/w solids. Essentially full DMAC conversion (> 98%) was obtained for each of these syntheses as judged by ^{1}H NMR spectroscopy studies. Targeting PDMAC DPs ≤ 1,000 produced translucent gels, but lowering the solids concentration led to free-flowing dispersions. These gels are most likely caused by these relatively short PDMAC chains not being fully desolvated in the presence of 2.0 M ammonium sulfate.

There is a systematic increase in particle diameter when targeting higher PDMAC DPs. Similar observations have been reported for various other PISA formulations that produce kinetically-trapped spheres.[33,50,51] Moreover, there is also good evidence that targeting larger

particles (i.e. higher PDMAC DPs) leads to progressive broadening of the particle size distribution.

Solids / w/w %	PDMAC DP (x)	Conversion[a] / %	Calculated for PDMAC block:		GPC M_n[b] / kg mol^{-1}	M_w/M_n[b]	D_z[c] / nm	PDI[c]	Physical Appearance
			DP[a]	M_n[a] / kg mol^{-1}					
20	500	> 99	520	52	31	1.96	70	0.09	Translucent gel
	1,000	> 99	1000	99	62	1.76	98	0.12	Translucent gel
	2,000	> 99	1,980	196	131	1.65	240	0.10	Free-flowing & turbid
	3,000	> 99	3,060	303	150	1.82	253	0.17	Free-flowing & turbid
	4,000	> 99	4,020	398	168	1.97	350	0.27	Free-flowing & turbid
	5,000	> 99	4,910	487	262	1.97	560	0.31	Free-flowing & turbid
	6,000	99	6,090	604	338	2.10	680	0.40	Free-flowing & turbid
	7,000	98	6,630	657	Unstable dispersion				
25	5,000	99	5,110	506	Unstable dispersion				
30	5,000	Macroscopic precipitation							

Table 3.3 Summary of conversion, GPC and DLS data obtained for the RAFT aqueous dispersion polymerisation of DMAC using a $PMPC_{139}$ precursor at 20-30% w/w solids. [a] Determined by ^{1}H NMR spectroscopy (comparison between the integrated vinyl signals assigned to DMAC monomer at 5.6 – 6.7 ppm, the integrated PDMAC methine proton signal at 2.2 – 2.7 ppm and the $PMPC_{139}$ azamethylene signal at 3.6 ppm). [b] Determined by aqueous GPC using a series of near-monodisperse poly(ethylene oxide) calibration standards. [c] D_z denotes z-average hydrodynamic diameter and PDI denotes polydispersity index as determined by DLS according to method 1 (see experimental).

Aqueous GPC data obtained for the series of $PMPC_{139}$-$PDMAC_x$ diblock copolymers shown in **Table 3.3** are summarised in **Figure 3.1**. Unimodal molecular weight distributions are obtained in each case, with a systematic shift to higher M_n observed when targeting higher PDMAC DPs which can also be seen in the normalised GPC traces. However, dispersities are above 1.50, which suggests that imperfect RAFT control is achieved. However, we have reported similar dispersities when targeting relatively high DPs for the core-forming block in other PISA formulations.[52–55] Because M_n values are calculated relative to a series of near-monodisperse poly(ethylene oxide) calibration standards, a significant systematic error is expected in this case. Indeed, the theoretical M_n for $PMPC_{139}$-$PDMAC_{6000}$ is 636 kg mol^{-1}, whereas the experimental GPC value is 338 kg mol^{-1}.

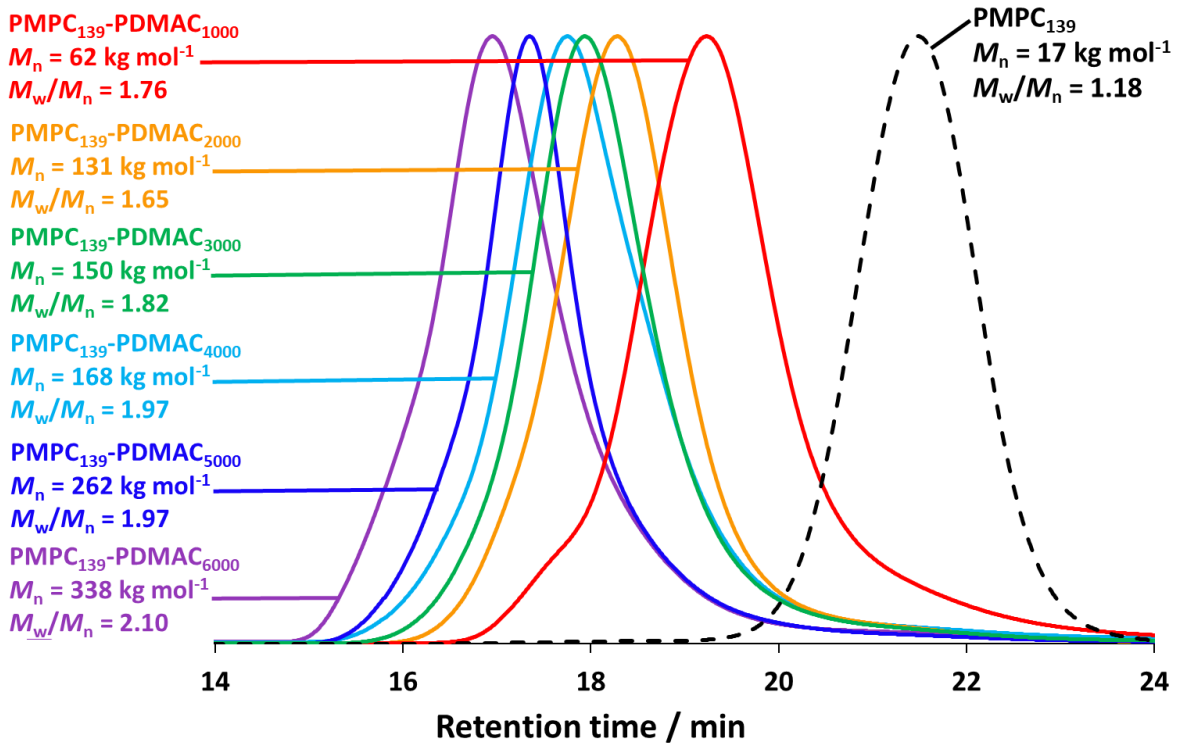

Figure 3.1 Aqueous GPC curves recorded for the $PMPC_{139}$ precursor and a series of $PMPC_{139}$-$PDMAC_x$ diblock copolymers prepared by chain extension via RAFT aqueous dispersion polymerisation of DMAC at 30°C in the presence of 2.0 M ammonium sulfate. M_n values are calculated relative to a series of near-monodisperse PEO calibration standards. Eluent 2 was used which consisted of 0.2 M $NaNO_3$ and 0.05 M TRIZMA/ TRIZMA•HCl buffer at pH 7.0.

Small-angle X-ray scattering (SAXS) was used to characterise selected $PMPC_{139}$-$PDMAC_x$ particles (where x = 1,000 or 3,000), see **Figure 3.2**. A well-established spherical micelle model[56–58] was used to provide a satisfactory data fit to an I(q) vs. q plot. This approach indicated a volume-average diameter (D_v) of 67 ± 8 nm for the $PMPC_{139}$-$PDMAC_{1000}$ and 213 ± 38 nm for $PMPC_{139}$-$PDMAC_{3000}$. As expected, these diameters are somewhat lower than the corresponding z-average diameters reported by DLS (see **Table 3.3**).[59]

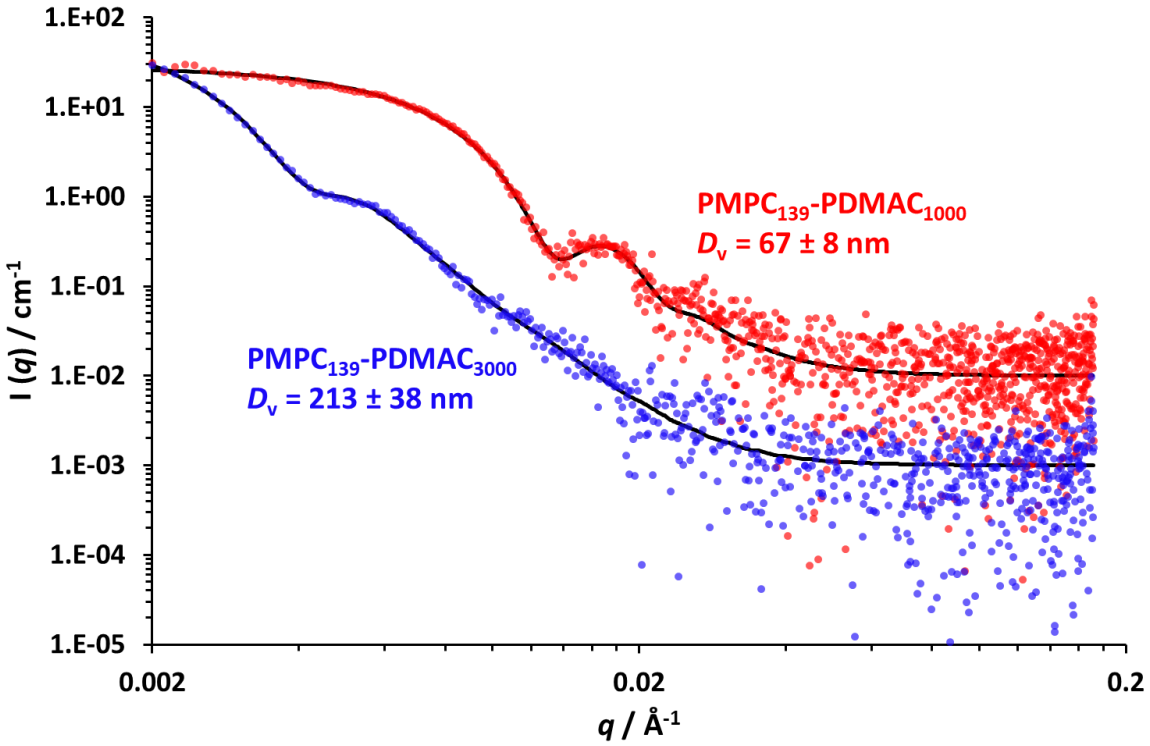

Figure 3.2 SAXS patterns recorded for 1.0% w/w aqueous dispersions of $PMPC_{139}$-$PDMAC_x$ particles (where x = 1,000 or 3,000) at 25°C. The black solid lines denote the data fit obtained using a well-known spherical micelle model.[56–58] D_v denotes the volume-average diameter. The red pattern has been scaled by a factor of ten relative to the blue pattern for the sake of clarity.

^{1}H NMR spectroscopy was used to study the kinetics of the DMAC polymerisation at 30°C when targeting $PMPC_{139}$-$PDMAC_{5000}$ particles at 20% w/w solids (see **Figure 3.3a**). Periodic sampling of the reaction mixture confirmed that a DMAC conversion of 98% was achieved within 2 h under such conditions, while the corresponding linear semi-logarithmic plot indicated first-order kinetics with respect to monomer. Each aliquot taken from the reaction mixture was also subjected to analysis by aqueous GPC (see **Figure 3.3b**). Each GPC curve was unimodal and there was a clear shift in the entire molecular weight distribution towards higher molecular weight, indicating a reasonably high blocking efficiency for the $PMPC_{139}$ precursor and hence well-defined diblock copolymer chains. However, dispersities increase monotonically with monomer conversion and always remained above 1.50.

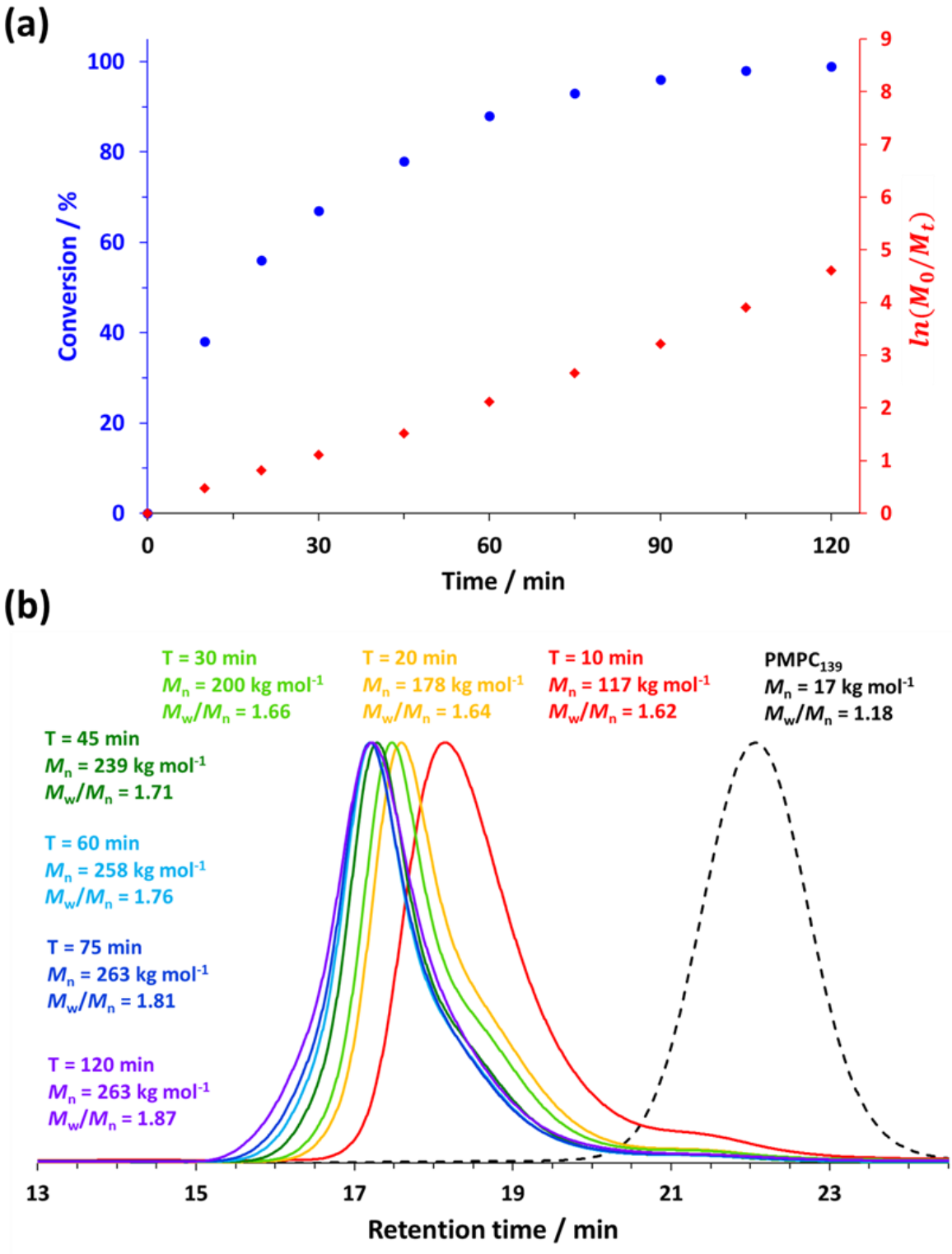

Figure 3.3 (a) Conversion vs. time curve and corresponding semi-logarithmic plot determined by ^{1}H NMR spectroscopy for the RAFT aqueous dispersion polymerisation of DMAC at 30°C in 2.0 M ammonium sulfate when targeting a PDMAC DP of 5,000 at 20% w/w solids. (b) Aqueous GPC curves obtained by periodic sampling of the reaction mixture to monitor the evolution in the molecular weight distribution.

In principle, transmission electron microscopy (TEM) can be used to assign the morphology of diblock copolymer particles prepared via PISA. In practice, the particles prepared herein are unstable with respect to dilution with deionised water (see below). On the other hand, dilution using an aqueous solution of 2.0 M ammonium sulfate is also problematic because this leads to extensive salt crystal formation during TEM grid preparation. In view of these technical problems, we examined the $PMPC_{139}$-$PDMAC_{5000}$ particles by optical microscopy, see **Figure 3.4**. This technique indicates the presence of a population of micron-sized particles but it is insensitive to the submicron-sized particle populations indicated by DLS and SAXS studies.

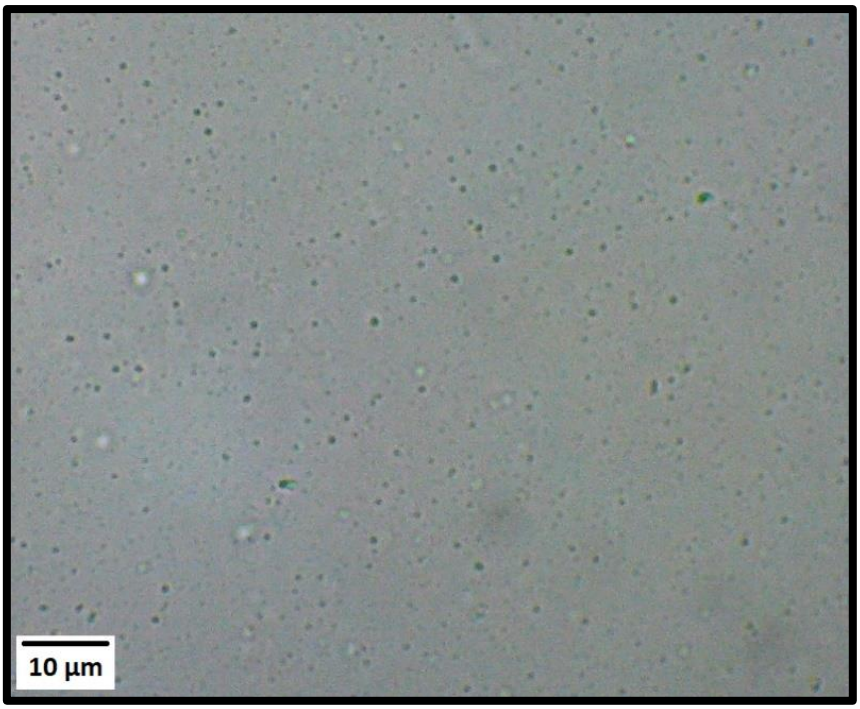

Figure 3.4 Optical microscopy image recorded for $PMPC_{139}$-$PDMAC_{5000}$ particles prepared at 20% w/w solids by RAFT aqueous dispersion polymerisation of DMAC at 30°C in the presence of 2.0 M ammonium sulfate.

^{1}H NMR spectroscopy was employed to investigate the extent of solvation of the core-forming PDMAC block before and after particle dissolution on dilution of a 20% w/w aqueous dispersion with deionised water. Accordingly, $PMPC_{139}$-$PDMAC_{5000}$ particles were prepared in D_2O in the presence of 2.0 M ammonium sulfate using the same reaction conditions as outlined in **Scheme 3.2**. ^{1}H NMR spectra were recorded for the initial aqueous dispersion and

the resulting aqueous solutions after up to a four-fold dilution using D_2O (see **Figure 3.5**). The lower five spectra were normalised to the signal assigned to the two azamethylene protons (–C*H*$_2$N(CH$_3$)$_3$) adjacent to the quaternary amine within the PMPC block, which remains fully solvated at all salt concentrations. The uppermost spectrum was recorded for a PDMAC$_{500}$ homopolymer in D_2O; the signals marked *a* and *b* correspond to the PDMAC backbone and *c* corresponds to the two equivalent pendent methyl groups.

Clearly, signal *a* is almost completely attenuated in the presence of 2.0 M ammonium sulfate. However, this signal becomes much more prominent as the ammonium sulfate concentration is lowered, indicating a much higher degree of hydration for the PDMAC block on dilution. Similar observations were made for signals *b* and *c*. However, the former signal overlaps with other signals, while the latter is only partially suppressed in the presence of 2.0 M ammonium sulfate. The spectra recorded using 0.5 M ammonium sulfate and the pure PDMAC homopolymer were almost identical, which suggests that this polymer is essentially fully solvated at this salt concentration. This indicates that lowering the ammonium sulfate concentration from 2.0 M to 0.5 M via four-fold dilution of the as-synthesised 20% w/w PMPC$_{139}$-PDMAC$_{5000}$ particles using deionised water should be sufficient to cause complete particle dissolution.[48,60]

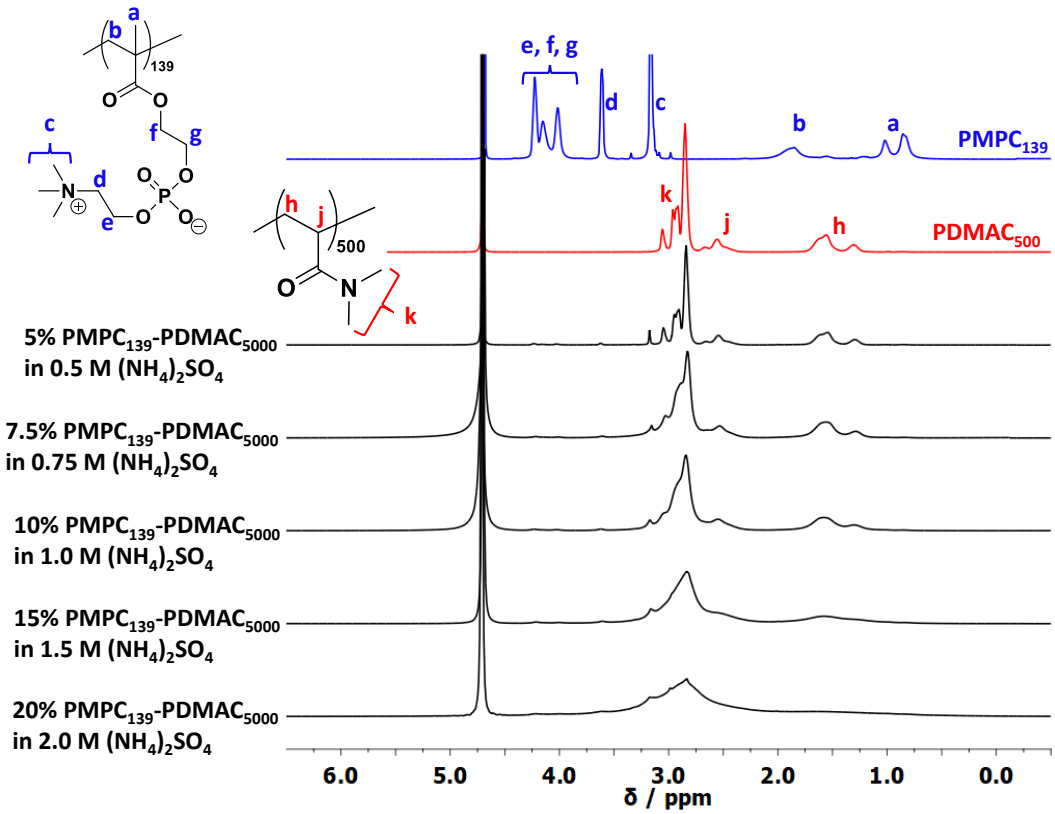

Figure 3.5 ^{1}H NMR spectra recorded for a $PDMAC_{500}$ (red spectrum) and a $PMPC_{139}$ (blue spectrum) homopolymer in the absence of salt, as well as a $PMPC_{139}$-$PDMAC_{5000}$ diblock copolymer prepared at 20% w/w in D_2O in the presence of 2.0 M $(NH_4)_2SO_4$, see lowest black spectrum. As the 20% w/w $PMPC_{139}$-$PDMAC_{5000}$ dispersion is diluted with further D_2O, both the background salt concentration and the copolymer concentration are systematically reduced (see four other black spectra). Just a two-fold dilution of the turbid dispersion is sufficient to cause molecular dissolution of the particles as the PDMAC block becomes solvated in 1.0 M $(NH_4)_2SO_4$. A further two-fold dilution of this transparent solution with D_2O results in $PMPC_{139}$-$PDMAC_{5000}$ chains dissolved in 0.5 M ammonium sulfate for which the PDMAC signals are now indistinguishable from those of $PDMAC_{500}$ homopolymer in water (compare the uppermost black spectrum with the red spectrum).

Rotational rheology experiments were conducted on samples using shear sweeps from 0.05 s^{-1} to 500 s^{-1} at 20°C. The evaluation of the viscosities of a range of 10% w/w aqueous solutions comprising molecularly-dissolved $PMPC_{139}$-$PDMAC_x$ chains in the presence of 1.0 M ammonium sulfate formed by a two-fold dilution of the *as-synthesised* dispersions using deionised water is shown in **Figure 3.6a**. A monotonic increase in solution viscosity is observed at all shear rates when increasing the PDMAC DP for the molecularly-dissolved chains. The viscosity of the aqueous solution remains relatively constant for shear rates ranging from 0.05 to 5.0 s^{-1}, with shear-thinning behavior being observed at higher shear rates. **Figure**

3.6b compares the viscosities of *as-synthesised* 20% w/w aqueous dispersions of $PMPC_{139}$-$PDMAC_x$ particles (where x = 3,000 or 5,000) in 2.0 M ammonium sulfate with the corresponding two 10% w/w aqueous copolymer solutions in 1.0 M ammonium sulfate. Clearly, the viscosity of each dispersion is significantly lower than that of the *more dilute* solution at all shear rates. Moreover, the two dispersions are much more strongly shear-thinning at higher shear, leading to an order of magnitude reduction in viscosity by 5 s^{-1}. Similar behavior has been reported in the literature when comparing colloidal particles with the corresponding solvated copolymer chains.[61,62]

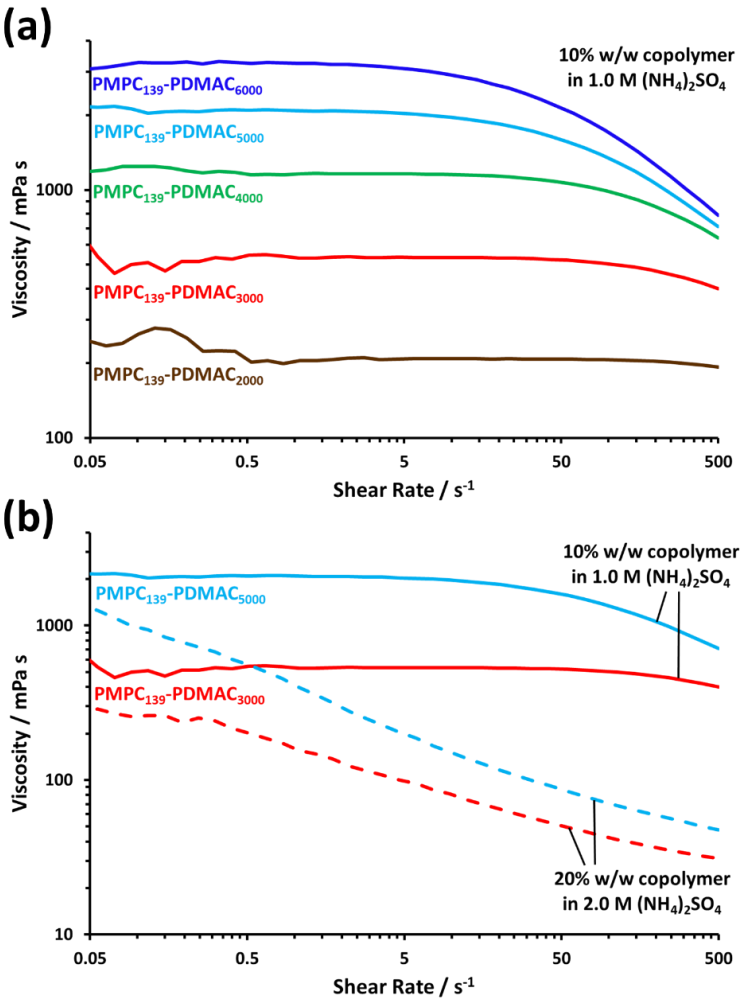

Figure 3.6 (a) Viscosity vs. shear rate data obtained by rotational rheology studies of 10% w/w aqueous solutions of molecularly-dissolved $PMPC_{139}$-$PDMAC_x$ chains in the presence of 1.0 M $(NH_4)_2SO_4$. (b) Viscosity vs. shear rate data obtained by rotational rheology studies of 20% w/w aqueous *dispersions* of either $PMPC_{139}$-$PDMAC_{3000}$ or $PMPC_{139}$-$PDMAC_{5000}$ particles in 2.0 M $(NH_4)_2SO_4$ compared to that for 10% w/w aqueous *solutions* of the same two copolymers in the presence of 1.0 M $(NH_4)_2SO_4$.

Two alternative steric stabilisers were also evaluated for the RAFT aqueous dispersion polymerisation of DMAC conducted in the presence of 2.0 M ammonium sulfate. To complement the zwitterionic nature of the salt-tolerant $PMPC_{139}$ steric stabiliser, we evaluated a cationic polyelectrolyte ($PATAC_{195}$) and an anionic polyelectrolyte ($PAMPS_{250}$), see chemical structures shown in **Scheme 3.3**. Both these polyelectrolytes have been reported to exhibit salt-tolerant behavior.[34,63–65] A PDMAC DP of 1,000 was targeted and ^{1}H NMR spectroscopy studies of the final reaction mixtures confirmed that more than 99% DMAC conversion was obtained in each case.

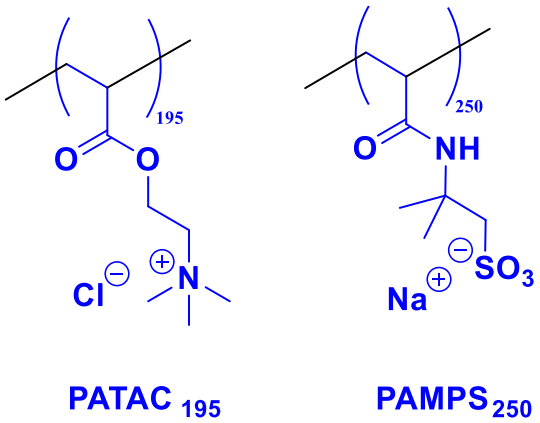

Scheme 3.3 Chemical structures of the cationic $PATAC_{195}$ and anionic $PAMPS_{250}$ precursors used to stabilise PDMAC-rich diblock copolymer particles prepared via RAFT aqueous dispersion polymerisation of DMAC in 2.0 M $(NH_4)_2SO_4$.

It is common practice to estimate the zeta potential of colloidal particles in aqueous solution as a function of pH. However, the correct interpretation of the experimental data for sterically-stabilised particles dispersed in highly salty aqueous media can be problematic for two reasons. First, the relatively high ionic strength reduces the hydrogen ion activity, which affects the accuracy of the glass Ag/AgCl reference electrode typically used to measure the pH. Moreover, additional errors may be incurred owing to a change in the junction potential of such electrodes when in contact with such salty media. Second, the steric stabiliser chains at the particle-liquid interface provide a permeable medium through which the solution phase can flow. If electrical charge arises from the ionic groups within such steric stabiliser chains, the electrokinetic

models commonly used to calculate zeta potential from electrophoretic mobility become invalid.[66] To overcome these technical problems, we used a state-of-the-art instrument to determine apparent zeta potentials for the three types of PDMAC-rich particles prepared in high salt using the $PMPC_{139}$, $PATAC_{195}$ or $PAMPS_{250}$ precursor in turn.

In the present study, the electrophoretic mobility of the particles was measured as a function of the addition of known amounts of KOH. The apparent pH was determined using a glass Ag/AgCl reference electrode without any compensation to offset the effect of the high ionic strength on the electrode response (although a temperature sensor within the electrode assembly did enable temperature compensation). Accordingly, zeta potentials calculated using the Smoluchowski model[67] are denoted as 'apparent zeta potentials'. The hydrodynamic z-average diameter of the particles was also determined in the presence of 2.0 M ammonium sulfate as a function of pH during these measurements.

The apparent zeta potentials determined by electrophoretic light scattering (ELS) for each of these three dispersions as a function of added KOH is shown in **Figure 3.7**. As expected, the electrophoretic footprint for each type of particle is dictated by the chemical nature of the steric stabiliser chains. Thus the cationic $PATAC_{195}$-$PDMAC_{1000}$ particles exhibit positive apparent zeta potentials of +15.8 ± 1.1 mV, whereas the anionic $PAMPS_{250}$-$PDMAC_{1000}$ particles exhibit negative apparent zeta potentials of –25.9 ± 1.5 mV. Finally, the zwitterionic $PMPC_{250}$-$PDMAC_{1000}$ particles exhibit apparent zeta potentials close to zero (+1.1 ± 1.2 mV). Similar observations have been reported for other PMPC-stabilised nano-objects at low salt.[68,69]

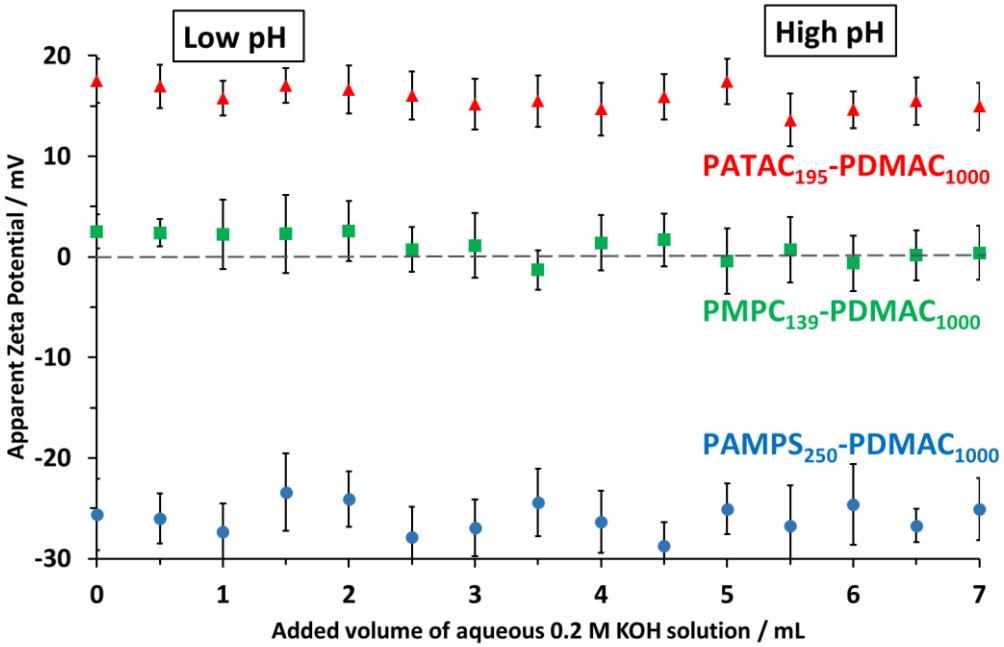

Figure 3.7 Apparent zeta potentials observed on addition of varying volumes of aqueous 0.2 M KOH solution in the presence of 2.0 M ammonium sulfate for 0.1% w/w aqueous dispersions of $PATAC_{195}$-$PDMAC_{1000}$ (red triangles), $PMPC_{139}$-$PDMAC_{1000}$ (green squares) or $PAMPS_{250}$-$PDMAC_{1000}$ (blue circles) particles.

If these particles were hard spheres, the conventional interpretation for such electrophoretic observations is that the $PAMPS_{250}$-$PDMAC_{1000}$ particles possess a sufficiently high anionic zeta potential to prevent aggregation, the $PATAC_{195}$-$PDMAC_{1000}$ particles possess a moderate cationic zeta potential that is likely to retard but not prevent aggregation, while the $PMPC_{250}$-$PDMAC_{1000}$ particles are essentially uncharged and hence likely to be colloidally unstable. However, this is a naïve and incorrect interpretation, not least because the salt-tolerant $PAMPS_{250}$, $PATAC_{195}$, and $PMPC_{139}$ chains confer additional steric stabilisation.[70]

3.3.1 Further Details Regarding Zeta Potential Measurements at High Salt Concentrations

The hydrogen ion activity can be determined by potentiometric acid-base titration using a suitable electrode and standardised aqueous solutions of HCl and KOH in the presence of the relevant electrolyte. Since the hydrogen ion concentration can be determined volumetrically, its apparent value indicated by the reference electrode can be corrected. However, this approach

fails if there is any buffering action due to the presence of electrolyte, which is unfortunately the case for the dispersions investigated herein. In principle, the electrophoretic mobility can be determined at constant pH over a wide range of electrolyte concentration in order to select an appropriate electrokinetic model.[66] However, for the particles described herein this is not possible, because a relatively high ionic strength (e.g. 2.0 M ammonium sulfate) is required to ensure that the core-forming PDMAC chains remain sufficiently dehydrated to maintain particle stability. In this context, it is noteworthy that the hydrodynamic diameters determined by DLS (using method 2, see Experimental) for each dispersion after addition of various volumes of aqueous 0.2 M KOH solution remains relatively constant (see **Figure 3.8**).

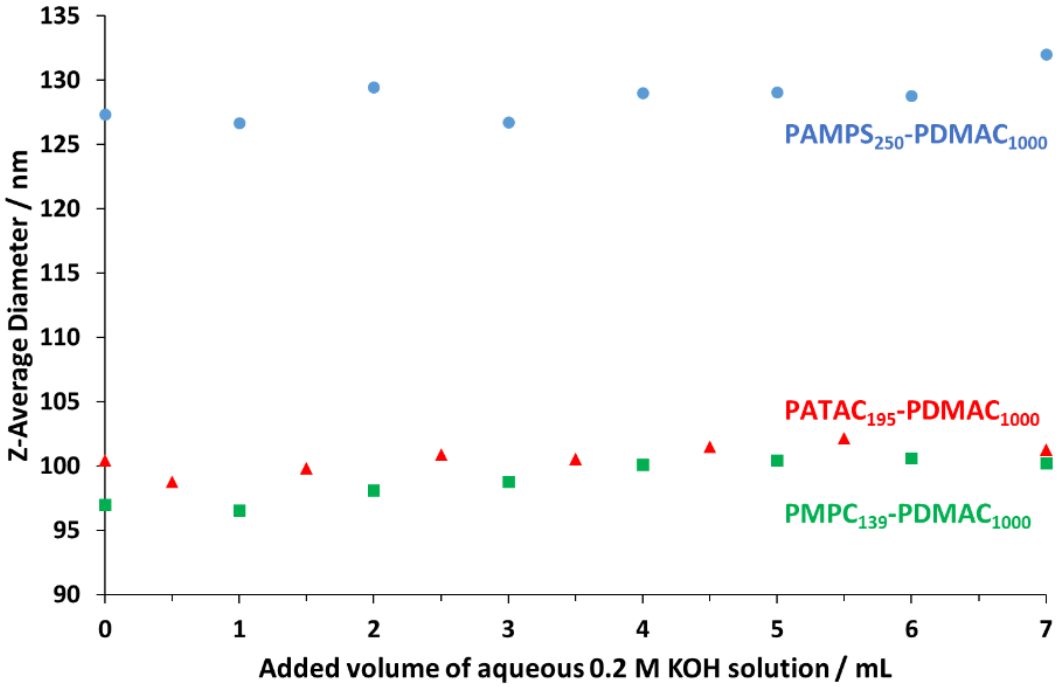

Figure 3.8 DLS z-average hydrodynamic diameter (D_z) determined for three types of PDMAC-core latex particles using method 2 (see Experimental) after dilution to 0.1% w/w using 2.0 M ammonium sulfate and adjustment of the solution pH to an apparent value of pH 3. This was followed by addition of varying volumes of aqueous 0.2 M KOH. Red triangles, green squares and blue circles denote $PATAC_{195}$-$PDMAC_{1000}$, $PMPC_{139}$-$PDMAC_{1000}$ and $PAMPS_{250}$-$PDMAC_{1000}$, respectively.

In order to enable conversion between apparent pH and calculated pH, potentiometric titration curves were obtained for dilute 0.1% w/w aqueous dispersions comprising $PMPC_{139}$-$PDMAC_{1000}$, $PATAC_{195}$-$PDMAC_{1000}$ and $PAMPS_{250}$-$PDMAC_{1000}$ particles (see **Figure 3.9**).

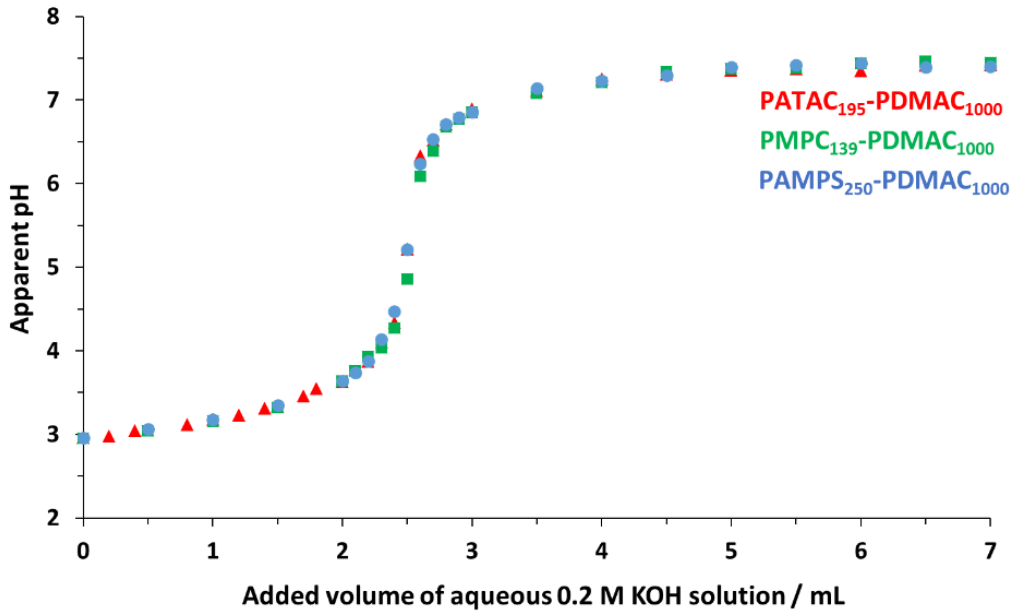

Figure 3.9 Apparent pH recorded for various aqueous dispersions of PDMAC-core latex particles in 2.0 M ammonium sulfate on addition of varying volumes of aqueous 0.2 M KOH. Application of a numerical curve-fitting protocol to these data yielded an approximate equivalence point at an added volume of 0.20 M KOH solution of 2.48 mL. Thus the initial HCl concentration for each dispersion is estimated to be 0.0198 M, which corresponds to a pH of 1.70 under ideal conditions (i.e., a hydrogen activity coefficient of unity). Red triangles, green squares and blue circles denote $PATAC_{195}$-$PDMAC_{1000}$, $PMPC_{139}$-$PDMAC_{1000}$ and $PAMPS_{250}$-$PDMAC_{1000}$, respectively.

A calculated pH value of 1.70 can be compared with the apparent pH of approximately 2.96 determined in the presence of 2.0 M ammonium sulfate. This discrepancy serves to illustrate the influence of such high ionic strength on pH measurements using glass Ag/AgCl reference electrodes. Moreover, the relatively high ionic strength must also be considered when interpreting the electrophoretic mobility (and corresponding apparent zeta potential). Using classical electrical double layer theory, the relationship between electrical charge and electrical potential at the slipping plane is given by:[66]

$$Q_e = 4\pi\varepsilon_0\varepsilon_r a(1 + \kappa a)\zeta \qquad (3.1)$$

where Q_e is the electrical charge at the slipping plane (the electrokinetic charge), ζ is the electrokinetic (zeta) potential which, by definition, is the electrical potential at the slipping plane, ε_0 is the absolute permittivity in vacuo, ε_r is the relative permittivity (or dielectric

constant) of the fluid, $\boldsymbol{a}$ is the particle radius (which is the distance between the particle's true surface and the slipping plane), and $\boldsymbol{\kappa}$ is the Debye-Hückel parameter, as given by:

$$\boldsymbol{\kappa = \left(\frac{2000F^2I}{\varepsilon_0\varepsilon_r RT}\right)^{1/2}} \qquad \textbf{(3.2)}$$

here F is the Faraday constant, R is the ideal gas constant, T is the absolute temperature, and I is the ionic strength (mol dm^{-3}), as given by:

$$\boldsymbol{I = \frac{1}{2}\sum_i c_i z_i^2} \qquad \textbf{(3.3)}$$

where c_i and z_i are the molar concentrations in bulk solution and the valency of ions of type i, respectively.

For a particle whose electrokinetic charge remains constant irrespective of the ionic composition of the bulk phase, **Equation 3.1** indicates that there must be a reduction in zeta potential with increasing ionic strength. The apparent zeta potentials obtained for this study are comparable to those determined for many types of particles dispersed in low ionic strength media (e.g. 0.001 M KCl). Given the hydrodynamic diameters reported above, **Equations 3.2 and 3.3** indicate a κa value of approximately 6.5 to 8.5 in 0.001 M KCl. However, the ionic strength of the aqueous solution of 2.0 M ammonium sulfate used herein is approximately 6.1 M, hence the corresponding κa ranges from 510 to 663. **Equation 3.1** predicts that the zeta potential at this relatively high ionic strength should be reduced to approximately 0.015 of its value at low ionic strength. This is not observed experimentally, which indicates that these particles cannot be described in terms of conventional electrokinetics. This classical theory assumes non-conducting hard spheres with smooth, impenetrable surfaces and a uniform charge distribution located entirely at the surface; it neither accounts for the finite size and hydration of ions at or near the particle surface nor for particles that are permeable towards the

dispersion medium. Clearly, such assumptions are not valid for the particles studied herein. More specifically, the particles are best described as soft spheres and all the charged groups are located within the steric stabiliser layer, which is highly permeable to the surrounding liquid. The Hermans-Fujita model[71,72] considers the flow of liquid through a porous sphere. In the case of a polymer chain, liquid flow is determined by the forces arising from the interaction between the liquid and the monomer repeat units (or segments) when the polymer chain moves in response to an externally applied electric field (as is the case for a polyelectrolyte in solution during an electrophoresis experiment). This model predicts that the electrophoretic mobility for a non-free draining porous particle containing spatially fixed charges tends to a constant finite value with increasing ionic strength, whereas **Equation 3.1** predicts that the electrophoretic mobility tends to zero for hard spheres. Indeed, this has been recently demonstrated experimentally for a globular protein (bovine serum albumin) in aqueous KCl solution using the NG-ELS technique.[66] Ohshima has considered the electrophoretic behavior of charged soft particles (*i.e.*, hard spheres coated with a weakly charged porous polymer layer) on a theoretical basis.[73] This theory incorporates some of the concepts within the Hermans-Fujita model and similarly predicts a non-zero electrophoretic mobility at high ionic strength. The experimental data reported herein support this prediction.

The cationic $PATAC_{195}$-$PDMAC_{1000}$ and zwitterionic $PMPC_{139}$-$PDMAC_{1000}$ particles both exhibit a modest reduction in apparent zeta potential on addition of KOH that is not observed for the anionic $PAMPS_{250}$-$PDMAC_{1000}$ particles (see **Figure 3.7**). There is insufficient information available regarding the configurational properties of the steric stabiliser chains, including their permeability, to provide a satisfactory explanation for the observed reduction in the apparent zeta potential. As indicated above, liquid flow through a permeable network of charged polymer chains depends on the balance of various forces. Since the liquid contains dissolved ions, it is feasible that both the random translational diffusion of the particles and

their electrophoretic mobility depend on the salt concentration. In the present study, ammonium sulfate was preferred over potassium sulfate or sodium sulfate because the former salt possesses significantly higher aqueous solubility. However, the ammonium cation complicates the solution chemistry owing to its buffering action, which involves an equilibrium between ammonium ions and neutral ammonia. Indeed, a distinct ammonia odor was noted at the end of each titration whereas the initial acidic dispersions were odourless.

3.4 Conclusions

We report the synthesis of a range of sterically-stabilised diblock copolymer particles via RAFT aqueous dispersion polymerisation of DMAC in highly salty media. This is achieved by selecting a suitable salt-tolerant water-soluble polymer to act as an effective steric stabiliser. Such stabilisers can possess zwitterionic (e.g. PMPC), cationic (e.g. PATAC) or anionic (e.g. PAMPS) character, which leads to the corresponding diblock copolymer particles exhibiting essentially zero, negative or positive apparent zeta potentials respectively. It is non-trivial to make such aqueous electrophoresis measurements in highly salty media. Indeed, such experiments can only be reliably performed by utilising state-of-the-art instrumentation. Relatively high DPs can be targeted for the salt-insoluble block to ensure that this component dominates the formulation. This approach enables high molecular weight water-soluble polymers to be prepared in a highly convenient low-viscosity form. Subsequent dilution using deionised water lowers the background salt concentration and causes *in situ* molecular dissolution of the particles, which leads to a substantial thickening effect and the formation of highly viscous transparent aqueous solutions. In principle, such aqueous PISA formulations are highly attractive: there are various potential commercial applications for high molecular weight water-soluble polymers while the well-known negative aspects of using RAFT agents (i.e. its cost, colour and malodour) are minimised. For example, the organosulfur content of the

dry $PMPC_{139}$-$PDMAC_{6000}$ diblock copolymer targeted herein is only ≈ 0.015%, which corresponds to just ≈ 31 ppm for a 20% w/w aqueous copolymer dispersion.

3.5 References

1 G. Moad, E. Rizzardo and S. H. Thang, 'Living radical polymerization by the RAFT process', *Aust. J. Chem.*, 2005, **58**, 379–410.

2 G. Moad, E. Rizzardo and S. H. Thang, 'Living radical polymerization by the RAFT process - A first update', *Aust. J. Chem.*, 2006, **59**, 669–692.

3 G. Moad, E. Rizzardo and S. H. Thang, 'Living Radical Polymerization by the RAFT Process - A Second Update', *Aust. J. Chem.*, 2009, **62**, 1402.

4 G. Moad, E. Rizzardo and S. H. Thang, 'Living Radical Polymerization by the RAFT Process – A Third Update', *Aust. J. Chem.*, 2012, **65**, 985.

5 R. N. Carmean, T. E. Becker, M. B. Sims and B. S. Sumerlin, 'Ultra-High Molecular Weights via Aqueous Reversible-Deactivation Radical Polymerization', *Chem*, 2017, **2**, 93–101.

6 E. Read, A. Guinaudeau, D. J. Wilson, A. Cadix, F. Violleau and M. Destarac, 'Low temperature RAFT/MADIX gel polymerisation: Access to controlled ultra-high molar mass polyacrylamides', *Polym. Chem.*, 2014, **5**, 2202–2207.

7 R. N. Carmean, M. B. Sims, C. A. Figg, P. J. Hurst, J. P. Patterson and B. S. Sumerlin, 'Ultrahigh Molecular Weight Hydrophobic Acrylic and Styrenic Polymers through Organic-Phase Photoiniferter-Mediated Polymerization', *ACS Macro Lett.*, 2020, **9**, 613–618.

8 R. H. Pelton and L. H. Allen, 'The effects of some electrolytes on flocculation with a cationic polyacrylamide', *Colloid Polym. Sci.*, 1983, **261**, 485–492.

9 K. A. Klimchuk, M. B. Hocking and S. Lowen, 'Water-soluble acrylamide copolymers. IX. Preparation and characterization of the cationic derivatives of poly(acrylamide-co-N, N-dimethylacrylamide), poly(acrylamide-co-methacrylamide), and poly(acrylamide-co-N-t-butylacrylamide)', *J. Polym. Sci. Part A Polym. Chem.*, 2001, **39**, 2525–2535.

10 A. Guyot, F. Chu, M. Schneider, C. Graillat and T. F. McKenna, 'High solid content latexes', *Prog. Polym. Sci.*, 2002, **27**, 1573–1615.

11 S. Perrier, '50th Anniversary Perspective: RAFT Polymerization - A User Guide', *Macromolecules*, 2017, **50**, 7433–7447.

12 J. Chiefari, Y. K. Chong, F. Ercole, J. Krstina, J. Jeffery, T. P. T. Le, R. T. A. Mayadunne, G. F. Meijs, C. L. Moad, G. Moad, E. Rizzardo and S. H. Thang, 'Living free-radical polymerization by reversible addition - Fragmentation chain transfer: The RAFT process', *Macromolecules*, 1998, **31**, 5559–5562.

13 M. Destarac, 'Industrial development of reversible-deactivation radical polymerization: Is the induction period over?', *Polym. Chem.*, 2018, **9**, 4947–4967.

14 Controlled Radical Polymerization in Water-in-Water Dispersion, M. Destarac, J. D. Wilson, S. Silvia, Rhodia, WO2013132108A1, 2013.

15 Y. M. Wu, Y. P. Wang, Y. Q. Yu, J. Xu and Q. F. Chen, 'Dispersion polymerization of acrylamide with 2-acrylamido-2-methyl-1- propane sulfonate in aqueous solution', *J. Appl. Polym. Sci.*, 2006, **102**, 2379–

2385.

16 A. Guo, Y. Geng, L. Zhao, J. Li, D. Liu and P. Li, 'Preparation of cationic polyacrylamide microsphere emulsion and its performance for permeability reduction', *Pet. Sci.*, 2014, **11**, 408–416.

17 M. S. Cho, K. J. Yoon and B. K. Song, 'Dispersion polymerization of acrylamide in aqueous solution of ammonium sulfate: Synthesis and characterization', *J. Appl. Polym. Sci.*, 2002, **83**, 1397–1405.

18 C. J. Ferguson, R. J. Hughes, B. T. T. Pham, B. S. Hawkett, R. G. Gilbert, A. K. Serelis and C. H. Such, 'Effective ab initio emulsion polymerization under RAFT control', *Macromolecules*, 2002, **35**, 9243–9245.

19 C. J. Ferguson, R. J. Hughes, D. Nguyen, B. T. T. Pham, R. G. Gilbert, A. K. Serelis, C. H. Such and B. S. Hawkett, 'Ab initio emulsion polymerization by RAFT-controlled self-assembly', *Macromolecules*, 2005, **38**, 2191–2204.

20 X. Zhang, S. Boissé, W. Zhang, P. Beaunier, F. D'Agosto, J. Rieger, B. Charleux, F. D'Agosto, J. Rieger and B. Charleux, 'Well-Defined Amphiphilic Block Copolymers and Nano-objects Formed in Situ via RAFT-Mediated Aqueous Emulsion Polymerization', *Macromolecules*, 2011, **44**, 4149–4158.

21 N. J. Warren and S. P. Armes, 'Polymerization-induced self-assembly of block copolymer nano-objects via RAFT aqueous dispersion polymerization', *J. Am. Chem. Soc.*, 2014, **136**, 10174–10185.

22 B. Charleux, G. Delaittre, J. Rieger and F. D'Agosto, 'Polymerization-induced self-assembly: From soluble macromolecules to block copolymer nano-objects in one step', *Macromolecules*, 2012, **45**, 6753–6765.

23 S. Boissé, J. Rieger, K. Belal, A. Di-Cicco, P. Beaunier, M. H. Li and B. Charleux, 'Amphiphilic block copolymer nano-fibers via RAFT-mediated polymerization in aqueous dispersed system', *Chem. Commun.*, 2010, **46**, 1950–1952.

24 F. D'Agosto, J. Rieger and M. Lansalot, 'RAFT-Mediated Polymerization-Induced Self-Assembly', *Angew. Chemie - Int. Ed.*, 2019, 2–27.

25 G. Liu, Q. Qiu, W. Shen and Z. An, 'Aqueous dispersion polymerization of 2-methoxyethyl acrylate for the synthesis of biocompatible nanoparticles using a hydrophilic RAFT polymer and a redox initiator', *Macromolecules*, 2011, **44**, 5237–5245.

26 S. Sugihara, A. H. Ma'Radzi, S. Ida, S. Irie, T. Kikukawa and Y. Maeda, 'In situ nano-objects via RAFT aqueous dispersion polymerization of 2-methoxyethyl acrylate using poly(ethylene oxide) macromolecular chain transfer agent as steric stabilizer', *Polymer (Guildf).*, 2015, **76**, 17–24.

27 Z. An, Q. Shi, W. Tang, C. K. Tsung, C. J. Hawker and G. D. Stucky, 'Facile RAFT precipitation polymerization for the microwave-assisted synthesis of well-defined, double hydrophilic block copolymers and nanostructured hydrogels', *J. Am. Chem. Soc.*, 2007, **129**, 14493–14499.

28 C. A. Figg, A. Simula, K. A. Gebre, B. S. Tucker, D. M. Haddleton and B. S. Sumerlin, 'Polymerization-induced thermal self-assembly (PITSA)', *Chem. Sci.*, 2015, **6**, 1230–1236.

29 V. J. Cunningham, M. J. Derry, L. A. Fielding, O. M. Musa and S. P. Armes, 'RAFT aqueous dispersion polymerization of N-(2-(methacryloyloxy)ethyl)pyrrolidone: A convenient low viscosity route to high molecular weight water-soluble copolymers', *Macromolecules*, 2016, **49**, 4520–4533.

30 M. B. Einarson and J. C. Berg, 'Electrosteric stabilization of colloidal latex dispersions', *J. Colloid Interface Sci.*, 1993, **155**, 165–172.

31 M. S. Romero-Cano, A. Martín-Rodríguez and F. J. De las Nieves, 'Electrosteric stabilization of polymer colloids with different functionality', *Langmuir*, 2001, **17**, 3505–3511.

32 K. E. Bremmell, G. J. Jameson and S. Biggs, 'Polyelectrolyte adsorption at the solid/liquid interface interaction forces and stability', *Colloids Surfaces A Physicochem. Eng. Asp.*, 1998, **139**, 199–211.

33 S. J. Byard, A. Blanazs, J. F. Miller and S. P. Armes, 'Cationic Sterically Stabilized Diblock Copolymer Nanoparticles Exhibit Exceptional Tolerance toward Added Salt', *Langmuir*, 2019, **35**, 14348–14357.

34 B. Huang, J. Jiang, M. Kang, P. Liu, H. Sun, B. G. Li and W. J. Wang, 'Synthesis of block cationic polyacrylamide precursors using an aqueous RAFT dispersion polymerization', *RSC Adv.*, 2019, **9**, 12370–12383.

35 M. Kikuchi, Y. Terayama, T. Ishikawa, T. Hoshino, M. Kobayashi, H. Ogawa, H. Masunaga, J. I. Koike, M. Horigome, K. Ishihara and A. Takahara, 'Chain dimension of polyampholytes in solution and immobilized brush states', *Polym. J.*, 2012, **44**, 121–130.

36 Y. Y. Jhan and R. Y. Tsay, 'Salt effects on the hydration behavior of zwitterionic poly(sulfobetaine methacrylate) aqueous solutions', *J. Taiwan Inst. Chem. Eng.*, 2014, **45**, 3139–3145.

37 K. E. B. Doncom, N. J. Warren and S. P. Armes, 'Polysulfobetaine-based diblock copolymer nano-objects via polymerization-induced self-assembly', *Polym. Chem.*, 2015, **6**, 7264–7273.

38 E. R. Jones, M. Semsarilar, A. Blanazs and S. P. Armes, 'Efficient synthesis of amine-functional diblock copolymer nanoparticles via RAFT dispersion polymerization of benzyl methacrylate in alcoholic media', *Macromolecules*, 2012, **45**, 5091–5098.

39 C. Bray, R. Peltier, H. Kim, A. Mastrangelo and S. Perrier, 'Anionic multiblock core cross-linked star copolymers: via RAFT polymerization', *Polym. Chem.*, 2017, **8**, 5513–5524.

40 J. T. Lai, D. Filla and R. Shea, 'Functional Polymers from Novel Carboxyl-Terminated Trithiocarbonates as Highly Efficient RAFT Agents', *Macromolecules*, 2002, **35**, 6754–6756.

41 J. F. Miller, K. Schätzel and B. Vincent, 'The determination of very small electrophoretic mobilities in polar and nonpolar colloidal dispersions using phase analysis light scattering', *J. Colloid Interface Sci.*, 1991, **143**, 532–554.

42 E. E. Uzgiris, 'Laser Doppler methods in electrophoresis', *Prog. Surf. Sci.*, 1981, **10**, 53–164.

43 A. M. Feltham and M. Spiro, 'Platinized platinum electrodes', *Chem. Rev.*, 1971, **71**, 177–193.

44 Argonne National Laboratory, Irena package for analysis of small-angle scattering data, https://usaxs.xray.aps.anl.gov/software/irena, (accessed 15 June 2023).

45 R. Weast, *CRC Handbook of Chemistry and Physics*, CRC Press, Boca Raton, Florida, 66th edn., 1985.

46 A. Peyman, C. Gabriel and E. H. Grant, 'Complex permittivity of sodium chloride solutions at microwave frequencies', *Bioelectromagnetics*, 2007, **28**, 264–274.

47 J. S. Sin, 'Ion partitioning effect on the electrostatic interaction between two charged soft surfaces', *Colloids Surfaces A Physicochem. Eng. Asp.*, 2021, **628**, 1–16.

48 S. J. Byard, Synthesis and Characterisation of Stimulus-responsive Diblock Copolymer Nano-objects Prepared by RAFT Aqueous Dispersion Polymerisation, PhD Thesis, University of Sheffield, 2019.

49 N. J. Warren, C. Muise, A. Stephens, S. P. Armes and A. L. Lewis, 'Near-Monodisperse Poly(2-(methacryloyloxy)ethyl phosphorylcholine)-Based macromonomers prepared by atom transfer radical polymerization and thiol-ene click chemistry: Novel reactive steric stabilizers for aqueous emulsion

polymerization', *Langmuir*, 2012, **28**, 2928–2936.

50 M. Williams, N. J. W. Penfold and S. P. Armes, 'Cationic and reactive primary amine-stabilised nanoparticles via RAFT aqueous dispersion polymerisation', *Polym. Chem.*, 2016, **7**, 384–393.

51 A. A. Cockram, R. D. Bradley, S. A. Lynch, P. C. D. Fleming, N. S. J. Williams, M. W. Murray, S. N. Emmett and S. P. Armes, 'Optimization of the high-throughput synthesis of multiblock copolymer nanoparticles in aqueous media: Via polymerization-induced self-assembly', *React. Chem. Eng.*, 2018, **3**, 645–657.

52 M. J. Derry, L. A. Fielding, N. J. Warren, C. J. Mable, A. J. Smith, O. O. Mykhaylyk and S. P. Armes, 'In situ small-angle X-ray scattering studies of sterically-stabilized diblock copolymer nanoparticles formed during polymerization-induced self-assembly in non-polar media', *Chem. Sci.*, 2016, **7**, 5078–5090.

53 S. J. Byard, M. Williams, B. E. McKenzie, A. Blanazs and S. P. Armes, 'Preparation and Cross-Linking of All-Acrylamide Diblock Copolymer Nano-Objects via Polymerization-Induced Self-Assembly in Aqueous Solution', *Macromolecules*, 2017, **50**, 1482–1493.

54 B. R. Parker, M. J. Derry, Y. Ning and S. P. Armes, 'Exploring the Upper Size Limit for Sterically Stabilized Diblock Copolymer Nanoparticles Prepared by Polymerization-Induced Self-Assembly in Non-Polar Media', *Langmuir*, 2020, **36**, 3730–3736.

55 V. J. Cunningham, S. P. Armes and O. M. Musa, 'Synthesis, characterisation and Pickering emulsifier performance of poly(stearyl methacrylate)-poly(N-2-(methacryloyloxy)ethyl pyrrolidone) diblock copolymer nano-objects via RAFT dispersion polymerisation in n-dodecane', *Polym. Chem.*, 2016, **7**, 1882–1891.

56 J. Ilavsky and P. R. Jemian, 'Irena: Tool suite for modeling and analysis of small-angle scattering', *J. Appl. Crystallogr.*, 2009, **42**, 347–353.

57 J. S. Pedersen, 'Form factors of block copolymer micelles with spherical, ellipsoidal and cylindrical cores', *J. Appl. Crystallogr.*, 2000, **33**, 637–640.

58 A. Muratov, A. Moussäd, T. Narayanan and E. I. Kats, 'A Percus-yevick description of the microstructure of short-range interacting metastable colloidal suspensions', *J. Chem. Phys.*, 2009, **131**, 54902.

59 B. Chu and T. Liu, 'Characterization of nanoparticles by scattering techniques', *J. Nanoparticle Res.*, 2000, **2**, 29–41.

60 V. J. Cunningham, S. P. Armes and O. M. Musa, 'Synthesis, characterisation and Pickering emulsifier performance of poly(stearyl methacrylate)-poly(N-2-(methacryloyloxy)ethyl pyrrolidone) diblock copolymer nano-objects via RAFT dispersion polymerisation in n-dodecane', *Polym. Chem.*, 2016, **7**, 1882–1891.

61 B. H. Tan, K. C. Tam, D. Dupin and S. P. Armes, 'Rheological behavior of acid-swellable cationic copolymer latexes', *Langmuir*, 2010, **26**, 2736–2744.

62 C. P. Jesson, C. M. Pearce, H. Simon, A. Werner, V. J. Cunningham, J. R. Lovett, M. J. Smallridge, N. J. Warren and S. P. Armes, 'H2O2 enables convenient removal of RAFT end-groups from block copolymer nano-objects prepared via polymerization-induced self- assembly in water', *Macromolecules*, 2017, **50**, 182–191.

63 X. Liu, D. Chen, Y. Yue, W. Zhang and P. Wang, 'Dispersion copolymerization of acrylamide with acrylic

acid in an aqueous solution of ammonium sulfate: Synthesis and characterization', *J. Appl. Polym. Sci.*, 2006, **102**, 3685–3690.

64 J. Lu, B. Peng, M. Li, M. Lin and Z. Dong, 'Dispersion polymerization of anionic polyacrylamide in an aqueous salt medium', *Pet. Sci.*, 2010, **7**, 410–415.

65 S. Bai, Y. Wang, B. Liu, Y. Zhu and R. Guo, 'Dispersion copolymerization of acrylamide and sodium 2-acrylamido-2-methylpropanesulfonate in aqueous salt solution stabilized with a macro-RAFT agent', *Colloids Surfaces A Physicochem. Eng. Asp.*, 2018, **553**, 446–455.

66 J. F. Miller, 'Determination of Protein Charge in Aqueous Solution Using Electrophoretic Light Scattering: A Critical Investigation of the Theoretical Fundamentals and Experimental Methodologies', *Langmuir*, 2020, **36**, 8641–8654.

67 R. J. Hunter, *Zeta Potential in Colloid Science*, Academic Press, New York, 1981.

68 T. Konno, K. Kurita, Y. Iwasaki, N. Nakabayashi and K. Ishihara, 'Preparation of nanoparticles composed with bioinspired 2-methacryloyloxyethyl phosphorylcholine polymer', *Biomaterials*, 2001, **22**, 1883–1889.

69 M. Ahmed, K. Ishihara and R. Narain, 'Calcium mediated formation of phosphorylcholine-based polyplexes for efficient knockdown of epidermal growth factor receptors (EGFR) in HeLa cells', *Chem. Commun.*, 2014, **50**, 2943–2946.

70 D. H. Napper, *Polymeric Stabilization of Colloidal Dispersions*, Academic Press, London, 1983.

71 J. J. Hermans and H. Fujita, 'Electrophoresis of charged polymer molecules with partial free drainage', *Proc. K. Ned. Akad. Wet., Ser. B Phys. Sci.*, 1955, **58**, 182.

72 J. J. Hermans, 'Sedimentation and electrophoresis of porous spheres', *J. Polym. Sci.*, 1955, **18**, 527–534.

73 H. Ohshima, 'Electrophoresis of soft particles: Analytic approximations', *Electrophoresis*, 2006, **27**, 526–533.

Chapter 4: Synthesis of Industrially Relevant High Molecular Weight Water-Soluble Polyacrylamide-Based Polymers as Low-Viscosity Latex Particles

4.1 Introduction

RAFT polymerisation is known to be amenable to a wide range of vinyl monomers. So far in this Thesis, *N*,*N*-dimethylacrylamide (DMAC) has been evaluated for its use as a suitable core-forming block for PISA formulations in highly salty aqueous media. However, if acrylamide (AM) could be used for the core block this would be significantly more cost-effective. As of December 2023, the cost of DMAC per 100 g on the Sigma Aldrich website is £12.14, whereas AM per 100g costs only £3.20 from the same vendor.[1] Furthermore, using an industrially relevant steric stabiliser such as poly(sodium acrylate) would further reduce the cost compared to the use of a speciality salt-tolerant polyelectrolyte stabiliser such as PMPC. **Scheme 4.1** summarises the industrial chemistry developed in the late 19th and early 20th century for the synthesis of several relevant vinyl monomers (ACN, AM, AA, and NaAc). The advent of free radical chain polymerisation led to the production of many other acrylate and acrylamide monomers.[2–4]

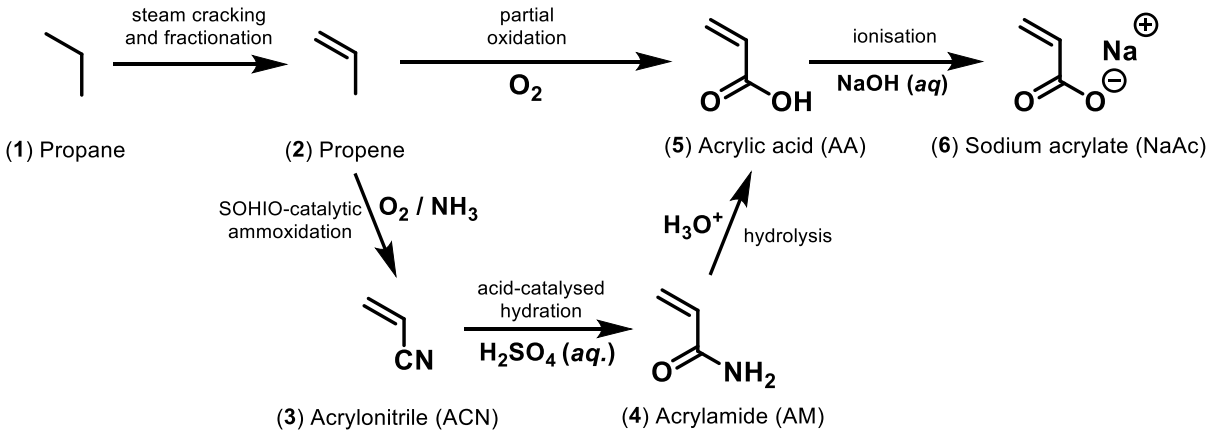

Scheme 4.1 Summary of the industrial manufacture of various commodity vinyl monomers starting from propane, which is derived from the petroleum industry.[3]

Acrylonitrile, acrylamide and acrylic acid are manufactured on a scale of millions of tonnes per annum.[3,5,6] This Chapter reports the use of diblock copolymer particles comprising poly(sodium acrylate) as the steric stabiliser and polyacrylamide-based core-forming blocks. The statistical copolymerisation of DMAC into the core-forming block is also evaluated for its effect on such aqueous dispersion polymerisation formulations.

As discussed in **Chapter 2**, Rimmer and co-workers[7] used potentiometric titration to determine a pK_a of 4.52 - 4.55 for PAA with molecular weights ranging between 6,800 and 73,300 (see **Figure 4.1**). Thus a relatively high pH is required to produce poly(sodium acrylate) as the electrosteric stabiliser. However, strongly alkaline conditions should be avoided to prevent hydrolysis of the organosulfur RAFT end-groups during the polymerisation.[8–10] Thus pH 6 was selected as an appropriate condition for the chain extension of PNaAc in this chapter, which was achieved by the addition of the weak base sodium bicarbonate.

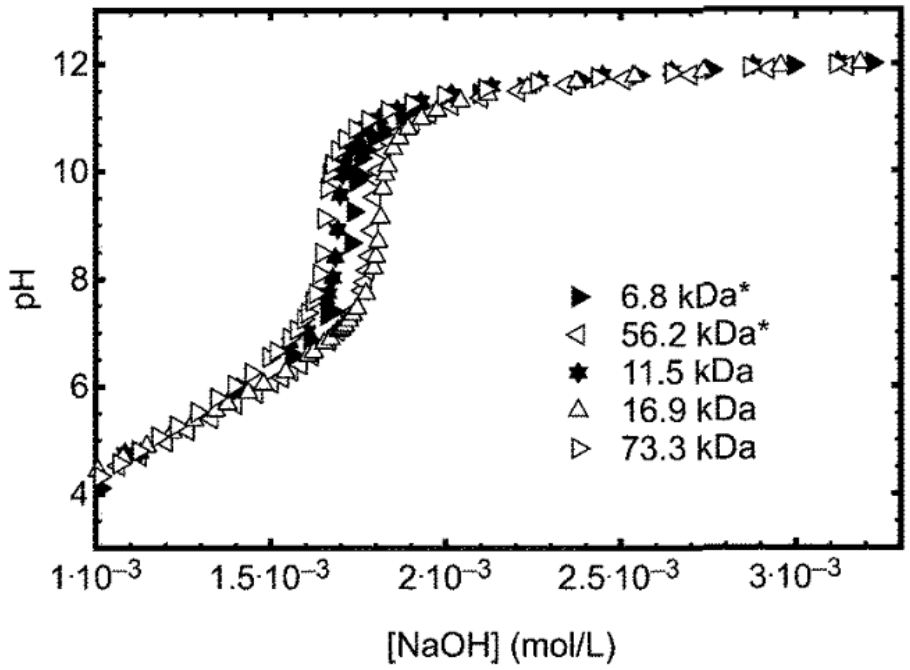

Figure 4.1 Potentiometric titration curve obtained for a series of poly(acrylic acid) homopolymers with molecular weights ranging between 6,800 and 73,300 g mol^{-1}.[7]

4.2 Experimental

4.2.1 Materials

Acrylic acid (AA; 99%; purified with acidic alumina), acidic alumina, basic alumina, acrylamide (AM; 50% w/w aqueous solution), acrylonitrile (ACN; ≥ 99%), *N*,*N*-dimethylacrylamide (DMAC; ≥ 99%), sodium bicarbonate (≥ 99%) and deuterium oxide (D_2O; ≥ 99.9% D) were purchased from Sigma Aldrich (Merck; UK). 2,2′-Azobis(2-imidazolinylpropane) dihydrochloride (VA-044, ≥ 98%) was obtained from Fluorochem Ltd (UK). Sodium hydroxide (≥ 98%) and ammonium sulfate (> 98%) were sourced from Thermo Fisher Scientific (UK). PEO standards were sourced from Agilent/PSS (Church Stretton, UK). Basodrill was supplied by BASF (Germany) and Ultrahib was supplied by SLB (Germany) and potassium chloride (> 99%) by Merck (Germany), with in-house testing conducted by BASF. 2-(((Butylthio)-carbonothioyl)-thio)-2-methylpropanoic acid (BDMAT) was prepared and purified as reported in **Chapter 2**.[11,12] Unless otherwise stated, all solvents and concentrated acids were purchased from Fisher Scientific (UK) and were used as received. Deionised water was used for all experiments.

4.2.2 Characterisation Techniques

Experimental protocols for ^{1}H NMR spectroscopy, UV absorption spectroscopy, DLS, optical microscopy and rotational rheology are described in **Chapter 2**.

Aqueous Gel Permeation Chromatography (GPC)

Experimental details are reported in **Chapter 3**. $PNaAc_{258}$ and its derivatives were analysed at 1.0 mL min^{-1} using Eluent 3, which comprised 0.1 M $NaNO_3$, 0.02 M TEA and 0.05 M $NaHCO_3$ at pH 8.0.

Oilfield Testing (BASF)

An in-house test protocol was conducted at BASF to assess the shale encapsulation potential of selected copolymers for use as drilling fluid additives. A 0.55% w/w copolymer solution was mixed with 1.0% w/w surfactant (Basodrill), 1.0% shale hydration inhibitor (Ultrahib), and 5.0% w/w potassium chloride. A rheometer was used to measure the shear stress of each copolymer as a function of the shear rate. The percentage shale recovery was determined and compared to that of a positive control (Alcomer-115) provided by BASF.

4.2.3 Synthesis of PAA Precursor via RAFT Aqueous Solution Polymerisation of AA at 44°C

AA (34.4 g, 476 mmol), *S*-butyl-*S*′-(α,α′-dimethyl-α′′-acetic acid)trithiocarbonate (BDMAT; 0.404 g, 1.59 mmol), 2,2′-azobis(2-imidazolinylpropane) dihydrochloride (VA-044, 51.3 mg, 159 μmol) and deionised water (52.17 g) were weighed into a 250 mL round-bottom flask equipped with a magnetic flea and the resulting aqueous solution (pH 1.6) was degassed using a stream of nitrogen gas for 30 min at 20°C. The sealed flask was placed in an oil bath set at 44°C and the ensuing polymerisation was allowed to proceed for 90 min, which led 95% AA conversion as judged by ^{1}H NMR spectroscopy. The aqueous polymer solution was purified by dialysis against deionised water adjusted to pH 2 for three days to remove unreacted monomer and then freeze-dried overnight. The mean degree of polymerisation was determined to be 258 ± 1, as judged by end-group analysis using UV spectroscopy at an absorption maximum of 310 nm for the trithiocarbonate end-group. Aqueous GPC analysis indicated an M_n of 19.2 kg mol^{-1} and an M_w/M_n of 1.36 (expressed relative to a series of PEG calibration standards).

4.2.4 Synthesis of $PNaAc_{258}$-PAM_x Diblock Copolymer Particles via RAFT Aqueous Dispersion Polymerisation of Acrylamide (AM) in 3.0 M Ammonium Sulfate at 44°C

A typical protocol for the synthesis of $PNaAc_{258}$-PAM_{3000} particles and 12% w/w solids was conducted as follows. The PAA_{258} precursor (25 mg, 1.33 μmol), $NaHCO_3$ (35 mg, 0.43 mmol), AM (50% w/w in water) (2.264 g, 15.9 mmol) and an aqueous solution of 3.5 M ammonium sulfate (7.19 g) were weighed into a 25 mL carousel tube charged with a magnetic stirrer. The sodium bicarbonate ($NaHCO_3$) was added to deprotonate the PAA_{258} precursor to form $PNaAc_{258}$ and adjust the reaction to pH 6. This tube was loaded into a Radleys 12-reaction carousel station with up to ten further carousel tubes and each solution was degassed using nitrogen gas for 30 min at 20°C. A reference carousel tube containing 10 mL 3.0 M ammonium sulfate and a thermal probe was also loaded onto the carousel. The temperature was then set to 44°C and a separately degassed solution of VA-044 initiator in 3.0 M ammonium sulfate (1.33 μmol; 0.10% w/w, 0.36 mL) was added. The carousel tube was not sealed, but a positive nitrogen over-pressure was always maintained with a cold-water condenser at the top of the apparatus to minimise water loss owing to evaporation. After 18 h, the polymerisation was quenched by exposing the reaction mixture to air while cooling to 20°C. The final AM conversion was 97%, as judged by ^{1}H NMR spectroscopy (the integrated vinyl signals assigned to AM monomer at 5.6–6.2 ppm were compared to the integrated polymer backbone signals at 1.1–2.3 ppm). Aqueous GPC analysis indicated an M_n of 192.8 kg mol^{-1} and an M_w/M_n of 3.01 (expressed relative to a series of PEG calibration standards).

4.2.5 Synthesis of $PNaAc_{258}$-P(AM-*stat*-DMAC)$_x$ Diblock Copolymer Particles via RAFT Aqueous Dispersion Polymerisation of AM and *N,N*-Dimethylacrylamide (DMAC) in 3.0 M Ammonium Sulfate at 44°C

A typical protocol for the synthesis of $PNaAc_{258}$-P(AM-*stat*-DMAC)$_{12000}$ particles (AM/DMAC = 3/1) at pH 6 and 12% w/w solids was conducted as follows. The PAA_{258}

precursor (25 mg, 1.33 μmol), $NaHCO_3$ (35 mg, 0.43 mmol), AM (50% w/w in water) (1.698 g, 11.9 mmol), DMAC (394 mg, 3.98 mmol) and an aqueous solution of 3.5 M ammonium sulfate (8.29 g) were weighed into a 25 mL carousel tube charged with a magnetic stirrer. The sodium bicarbonate ($NaHCO_3$) was added to deprotonate the PAA_{258} precursor to form $PNaAc_{258}$ and adjust the reaction to pH 6. This tube was loaded into a Radleys 12-reaction carousel station with up to ten further carousel tubes and each solution was degassed using nitrogen gas for 30 min at 20°C. A reference carousel tube containing 10 mL 3.0 M ammonium sulfate and a thermal probe was also loaded onto the carousel. The temperature was then set to 44°C and a separately degassed solution of VA-044 initiator in 3.0 M ammonium sulfate (1.33 μmol; 0.10% w/w, 0.36 mL) was added. The carousel tube was not sealed, but a positive nitrogen over-pressure was always maintained with a cold-water condenser at the top of the apparatus to minimise water loss owing to evaporation. After 18 h, the polymerisation was quenched by exposing the reaction mixture to air while cooling to 20°C. The final monomer conversion was 98%, as judged by ^{1}H NMR spectroscopy (the integrated vinyl signals assigned to monomers at 5.6–6.2 ppm were compared to the integrated polymer backbone signals at 1.1–2.3 ppm).

4.3 Results and Discussion

The synthesis of the PAA precursor required filtration of the acrylic acid monomer through an acidic alumina column to remove MEHQ inhibitor. Analysis of a ^{1}H NMR spectrum for the purified monomer indicated the presence of less than 1 mol % acrylic acid dimer (i.e. 2-carboxyethyl acrylate; CEA). The concentration of acrylic dimer in a bottle of acrylic acid monomer increases over time owing to Michael addition; if desired, this impurity can be removed by fractional distillation.[13,14] Further consideration of this dimer is made in **Chapter 6.** The RAFT solution polymerisation of AA was conducted in acidic aqueous solution (pH 1.6) at 44°C using a trithiocarbonate-based RAFT agent (BDMAT). The mean degree of

polymerisation (DP) of the resulting PAA homopolymer was determined to be 258 ± 1 via end-group analysis using the UV absorption maximum at 310 nm and the Beer-Lambert law (see **Figure 4.2**). GPC data shown in **Figure 4.4**.

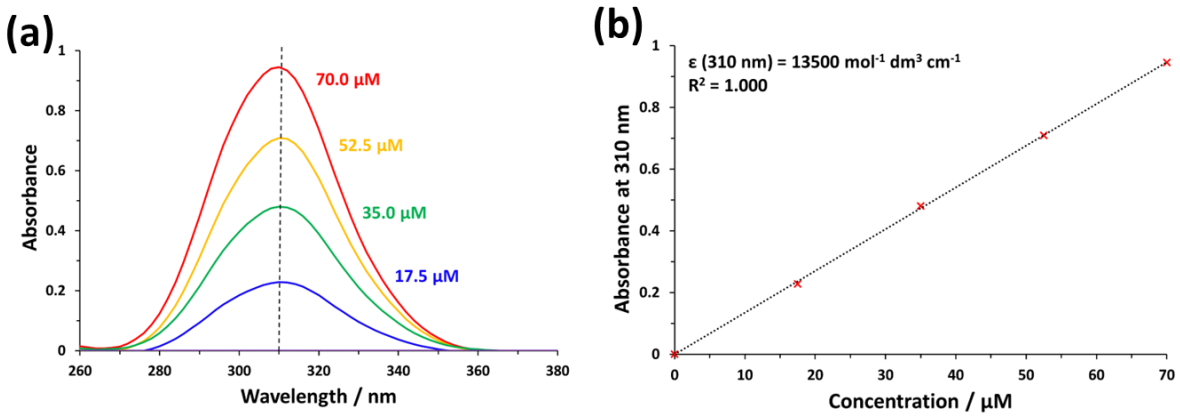

Figure 4.2 (a) UV absorption spectra recorded for S-butyl-S′-(α,α′-dimethyl-α′′-acetic acid)trithiocarbonate (BDMAT) in methanol for a series of concentrations ranging from 0 µM to 70.0 µM. (b) Beer-Lambert calibration plot constructed for BDMAT in methanol to calculate its molar extinction coefficient (ε) at the absorption maximum of 310 nm.

Deprotonation of the PAA_{258} precursor at pH 6 forms $PNaAc_{258}$; this is necessary to maintain the precursor solubility in 3.0 M ammonium sulfate for use as a suitable steric stabiliser. Subsequently, the RAFT aqueous dispersion polymerisation of AM was conducted in the presence of 3.0 M ammonium sulfate at 44°C using the $PNaAc_{258}$ precursor as a salt-tolerant electrosteric stabiliser block at pH 6, as outlined in **Scheme 4.2a**. The highest solids content shown to reproducibly result in free-flowing turbid particle dispersions without macroscopic precipitation occurring for this $PNaAc_{258}$-PAM_x formulation was 12% w/w. This is much lower than for other water-in-water aqueous polymer systems, for example the $PATAC_{242}$-$PDMAC_x$ system in **Chapter 2** was able to successfully target 20 – 40% w/w solids. As more commercially relevant monomers, it is disappointing that a lower solids content is required for polyacrylamide. A two-fold dilution of the resulting turbid aqueous dispersions using deionised water produced a viscous transparent solution, which for the PAM_{12000} formulation corresponds to a sample with a gel-like consistency, as shown in **Scheme 4.2b**.

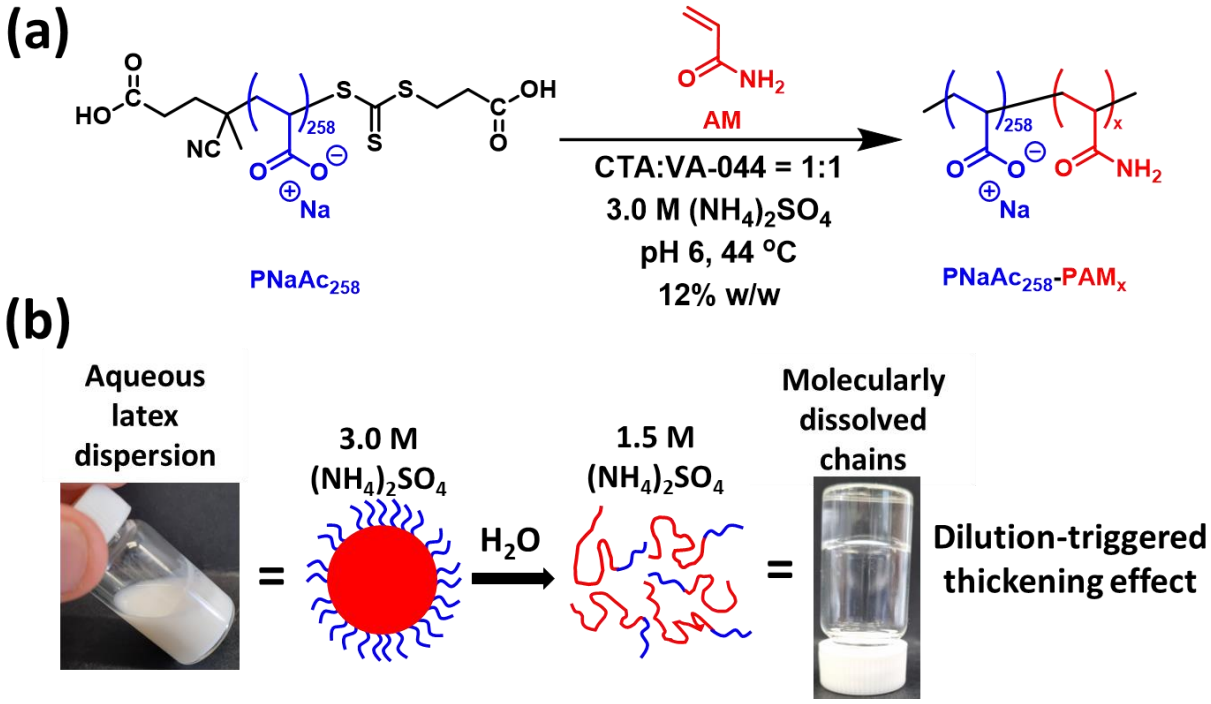

Scheme 4.2 (a) Synthesis of $PNaAc_{258}$-PAM_x (x = 1,000 to 13,000) diblock copolymer particles at 12% w/w solids via RAFT aqueous dispersion polymerisation of AM at 44°C in the presence of 3.0 M ammonium sulfate. (b) Schematic cartoon and corresponding digital images to illustrate the sterically-stabilised $PNaAc_{258}$-PAM_{12000} diblock copolymer particles in the presence of 3.0 M ammonium sulfate. A two-fold dilution of this aqueous dispersion with deionised water halves the salt concentration and results in spontaneous dissociation of the particles, with the concomitant formation of a highly viscous transparent aqueous solution comprising molecularly-dissolved diblock copolymer chains.

PNaAc was selected as an anionic stabiliser block owing to its low cost and its aqueous solubility even in the presence of 4.0 M ammonium sulfate. In contrast, 3.0 M ammonium sulfate is sufficient to salt out the non-ionic core-forming PAM block, see **Table 4.1**.[15] There are two cations present in such formulations, Na^+ from the $NaHCO_3$ used to adjust the solution pH and NH_4^+ derived from the ammonium sulfate. The NH_4^+/Na^+ molar ratio increases from 8/1 – 105/1 for the syntheses of a target PAM DP increasing from 1,000 to 13,000. At pH 6 and temperatures less than 70°C, the salt will dissociate to form ammonium ions with no aqueous ammonia present.[16] In summary, there are two cations associated with acrylate/polyacrylate, with the major species being NH_4^+.

Additive	Aqueous $(NH_4)_2SO_4$ solution / mol dm^{-3}				
	0	1.0	2.0	3.0	4.0
NaAc monomer	Soluble	Soluble	Soluble	Soluble	Soluble
$PNaAc_{258}$	Soluble	Soluble	Soluble	Soluble	Soluble
AM monomer	Soluble	Soluble	Soluble	Soluble	Insoluble
PAM_{500}	Soluble	Soluble	Soluble	Insoluble	Insoluble

Table 4.1 Aqueous solubility of NaAc monomer, $PNaAc_{258}$ homopolymer, AM monomer and PAM_{500} homopolymer at 2.0% w/w solids in the presence of zero to 4.0 M ammonium sulfate as judged by visual inspection at pH 6.0 and 20°C.

^{1}H NMR spectra recorded for each monomer and homopolymer are shown in **Figure 4.3**. Unfortunately, the PNaAc and PAM backbone signals *c*, *d*, *g*, *h* overlap at 1.3 – 2.5 ppm, which means that these two blocks cannot be readily differentiated from each other. For most of the copolymer formulations discussed in this Chapter, the PAM DP is substantially higher than the PNaAc stabiliser DP. In principle, an internal or external NMR reference could be used to calculate the monomer conversion and in retrospect this approach should be less susceptible to experimental uncertainty. However, in practice acrylamide conversions were calculated by comparing the integrated monomer vinyl signals at 5.6 – 6.4 ppm with the polymer backbone signals. This method does not take into account the contribution from the $PNaAc_{258}$ stabiliser (e.g. signals *c* and *d*), but full conversions are obtained for PAM DPs up to 7,000 (see **Table 4.2**).

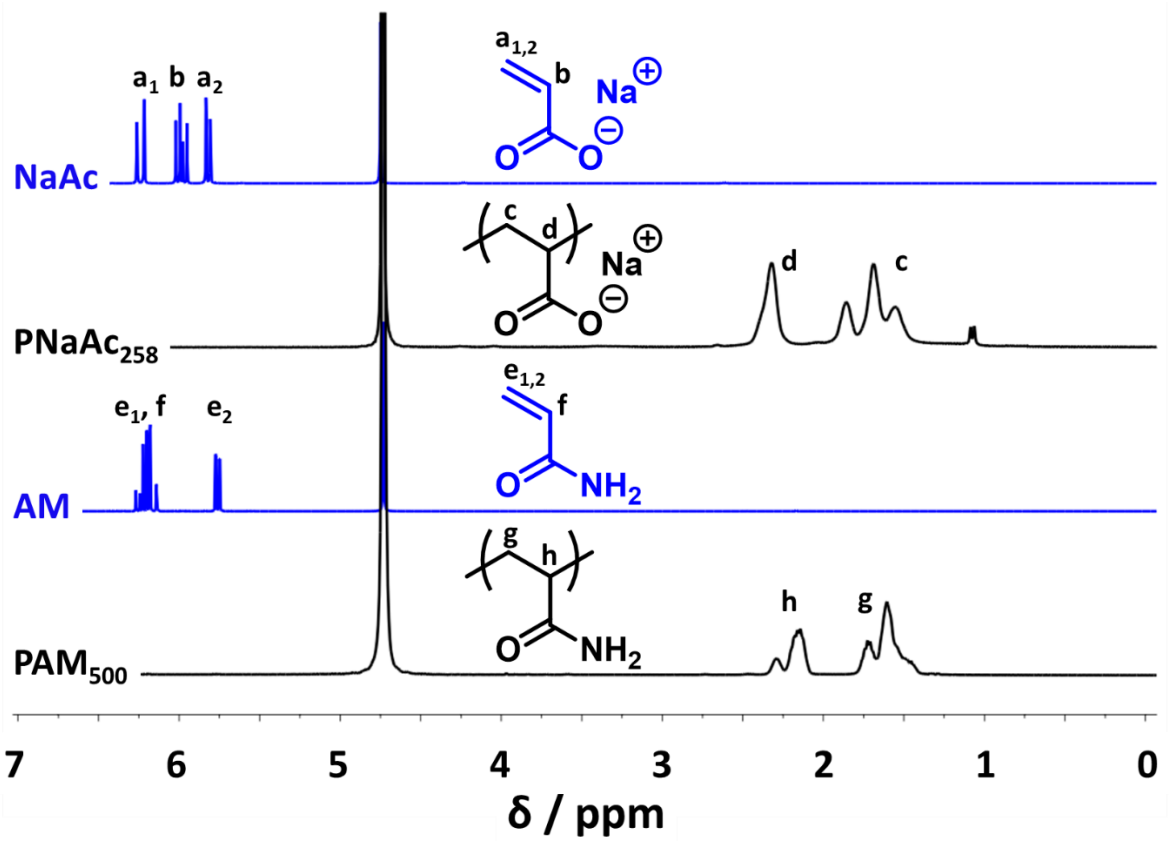

Figure 4.3 Assigned ^{1}H NMR spectra recorded for NaAc, $PNaAc_{258}$, AM and PAM_{500} in deuterium oxide.

The series of aqueous PISA syntheses summarised in **Table 4.2** were conducted at 44°C using VA-044 initiator while targeting 12% w/w solids at pH 6. The $PNaAc_{258}$ precursor afforded colloidally stable dispersions of increasing turbidity when targeting PAM DPs ranging from 1,000 to 12,000. However, macroscopic precipitation was observed either when targeting a PAM DP of 13,000 or when the target copolymer concentration exceeded 12% w/w solids.

PAM DP (x)	Conversion[a] / %	M_n[a] / kg mol^{-1}	GPC M_n[b] / kg mol^{-1}	M_w / M_n [b]	D_z[c] / nm	PDI[c]
1,000	> 99	89.7	68.5	1.85	123	0.27
3,000	> 99	231.8	120.5	2.10	142	0.10
5,000	> 99	374.0	146.3	2.06	195	0.08
7,000	> 99	516.1	156.0	2.64	392	0.23
10,000	99	722.2	173.7	3.07	769	0.25
12,000	97	845.9	192.8	3.01	2,040	0.21
13,000[d]	99	933.4	214.4	3.27	Macroscopic precipitation	

Table 4.2 Summary of ^{1}H NMR conversion, GPC and DLS data obtained for the RAFT aqueous dispersion polymerisation of AM at 44°C using a $PNaAc_{258}$ precursor when targeting 12% w/w solids. (a) Determined by ^{1}H NMR spectroscopy (integrated vinyl signals assigned to AM monomer at 5.6 – 6.4 ppm were compared with the integrated polymer backbone signals at 1.3 – 2.5 ppm). M_n values are calculated from the respective monomer conversions. (b) Determined by aqueous GPC (Eluent 3) using a refractive index detector and expressed relative to a series of near-monodisperse PEO calibration standards. (c) DLS measurements of hydrodynamic z-average diameter (D_z) and particle polydispersity (PDI). (d) macroscopic precipitation is observed for this sample.

Comparing these ^{1}H NMR-derived M_n values to those determined by aqueous GPC suggests a significant systematic error for the latter technique. This is understandable because the PEO calibration standards are unlikely to be accurate for the analysis of PAM-rich diblock copolymers. Very high AM conversions (> 97%) were obtained for each of these syntheses as judged by ^{1}H NMR spectroscopy studies. Targeting a PAM DP of 1,000 (or lower) produced a translucent gel, but lowering the solids concentration led to free-flowing dispersions. These gels are most likely caused by such relatively short PAM chains remaining partially solvated in the presence of 3.0 M ammonium sulfate. There is a monotonic increase in particle diameter when targeting higher PAM DPs, with a particularly large increase from sub-micron to > 2 μm particles observed when increasing the DP from 10,000 to 12,000. Similar observations have been reported for various other PISA formulations that produce kinetically-trapped spheres.[17–20] However, macroscopic precipitation was observed when targeting a PAM DP of 13,000. The

dynamic viscosities and refractive indices of various salt concentrations are shown in **Table 2.6**; these parameters were required for DLS analysis. For example, the solution viscosity of 3.0 M ammonium sulfate solution (2.030 Pa s) is twice that of deionised water at 20°C (1.000 Pa s).

Aqueous GPC analysis of the $PNaAc_{258}$ precursor indicated an apparent M_n of 19.2 kg mol^{-1} which is comparable to the theoretical value of 24.4 kg mol^{-1}. The full series of GPC curves are shown in **Figure 4.4**. These data indicate relatively high chain extension efficiency for this precursor. However, the $PNaAc_{258}$-PAM_{1000} formulation exhibits a low molecular weight shoulder, suggesting a significant fraction of unreacted $PNaAc_{258}$ precursor in this case. This particular formulation was not further optimised, not least because the *in situ* self-assembly of the amphiphilic diblock copolymer chains was relatively inefficient in this case.

RAFT agent/initiator molar ratios of 5-10 are typically required for well-controlled RAFT polymerisations,[17,21,22] although lower molar ratios of 0.5-3.3 are also utilised for PISA syntheses.[23–27] A low molar ratio of 1.0 was selected as it proved essential to ensure high final monomer conversions were achieved when targeting high polymer DPs. Unfortunately, this pragmatic choice inevitably leads to inferior RAFT control, as evidenced by the relatively broad molecular weight distributions observed in **Figure 4.4**.

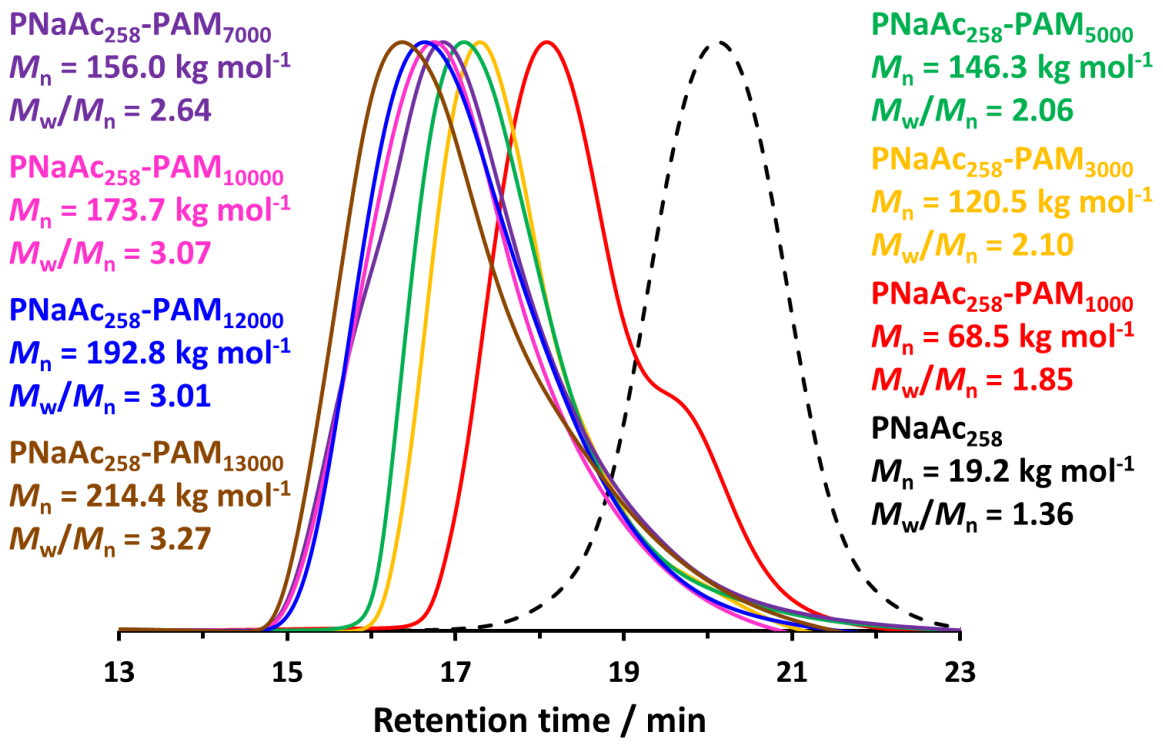

Figure 4.4 Aqueous GPC curves recorded for the $PNaAc_{258}$ precursor and a series of $PNaAc_{258}$-PAM_x diblock copolymers prepared by chain extension via RAFT aqueous dispersion polymerisation of AM at 44°C in the presence of 3.0 M ammonium sulfate. M_n values are calculated relative to a series of near-monodisperse PEO calibration standards. Eluent 3 was used which consisted of 0.1 M $NaNO_3$, 0.02 M TEA and 0.05 M $NaHCO_3$ at pH 8.0.

The synthesis of $PNaAc_{258}$-PAM_{10000} nanoparticles via RAFT aqueous dispersion polymerisation of AM was conducted by the method outlined in **Scheme 4.2a**. This reaction mixture was periodically sampled to enable the kinetics of polymerisation and evolution of the MWD to be monitored via ^{1}H NMR spectroscopy (**Figure 4.5a**) and GPC (**Figure 4.5b**), respectively. The resulting conversion vs. time curve (blue data points) indicated that 95% conversion was achieved within 2.5 h at 30°C and essentially full AM conversion is obtained within 4 – 5 h when targeting 12% w/w solids. The corresponding semi-logarithmic plot (red data points) suggests that this polymerisation exhibits first-order kinetics with respect to monomer. However, there is some (admittedly weak) evidence for a slower rate of polymerisation in the first 30 min, presumably because nucleation is yet to occur on this time scale. Selected aliquots taken during this kinetic experiment were also subjected to aqueous

GPC analysis to examine the evolution in M_n (green data points). Generally, a linear evolution in M_n is observed with increasing AM conversion, which is characteristic of a pseudo-living polymerisation. However, most of the MWDs recorded by aqueous GPC were immediately bimodal between the growing polymer chains and residual $PNaAc_{258}$ precursor. The M_w/M_n values (purple data points) determined for the diblock copolymers range between 4.0 and 5.5 which is higher than the values determined from the final product GPCs in **Figure 4.4**.

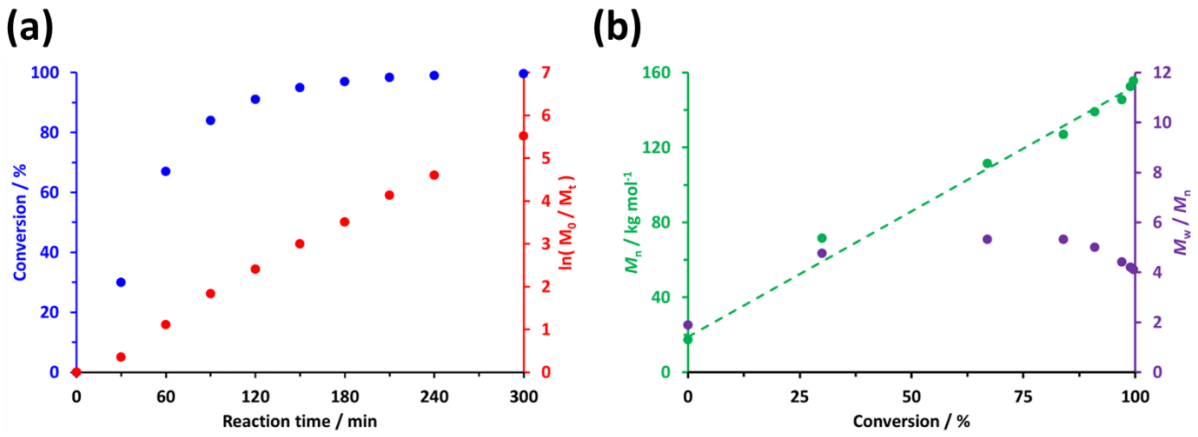

Figure 4.5 (a) Conversion vs. time curve and corresponding semi-logarithmic plot determined by ^{1}H NMR spectroscopy for the RAFT aqueous dispersion polymerisation of AM at 30°C in 3.0 M ammonium sulfate when targeting a PAM DP of 10,000 at 12% w/w solids. (b) Evolution of M_n and M_w/M_n with conversion for the same formulation.

Like the PDMAC formulations discussed in **Chapters 2 & 3**, dilution of the PAM-core samples for particle size analysis required the use of an aqueous solution of 3.0 M ammonium sulfate to prevent *in situ* particle dissolution. This relatively high level of background electrolyte makes electron microscopy studies problematic owing to the formation of salt crystals during sample preparation. Instead, optical microscopy was used to image an aqueous dispersion of $PNaAc_{258}$-PAM_{10000} particles, see **Figure 4.6**. This technique indicates a polydisperse population of micron-sized particles, while DLS studies indicate a z-average particle diameter of 769 nm. The former observations are close to the lower resolution limit for optical microscopy, which is therefore likely to 'oversize' the particles.

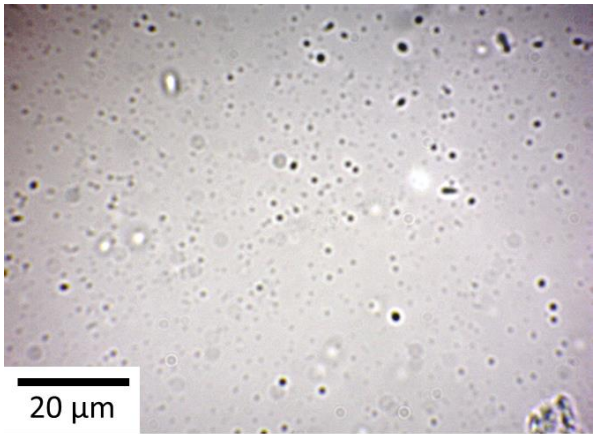

Figure 4.6 Optical microscopy image recorded for 0.2% w/w dilution of $PNaAc_{258}$-PAM_{10000} particles prepared at 12% w/w solids by RAFT aqueous dispersion polymerisation of AM at 44°C in the presence of 3.0 M ammonium sulfate.

^{1}H NMR spectroscopy was used to examine the extent of solvation of the core-forming PAM block before and after dilution of a 12% w/w aqueous dispersion. Accordingly, $PNaAc_{258}$-PAM_{7000} particles were prepared in D_2O in the presence of 3.0 M ammonium sulfate using the same reaction conditions summarised in **Scheme 4.2a**. ^{1}H NMR spectra were recorded for the initial aqueous dispersion and the resulting aqueous solutions obtained after serial dilution using D_2O (see **Figure 4.7**). The weakly solvated polymer backbone protons are visible at 1.3 – 2.5 ppm in 3.0 M ammonium sulfate, but they are fully resolved after a two-fold dilution. At this point, the initially turbid aqueous dispersion has become a highly viscous transparent solution, indicating complete molecular dissolution of the original particles. The intermediate 9.0% w/w $PNaAc_{258}$-PAM_{7000} in 2.25 M ammonium sulfate is partially solvated, in this case the sample is slightly turbid and slightly more viscous than the 12% dispersion. The NMR backbone proton signal is not fully resolved but is more intense than the as-synthesised dispersion.

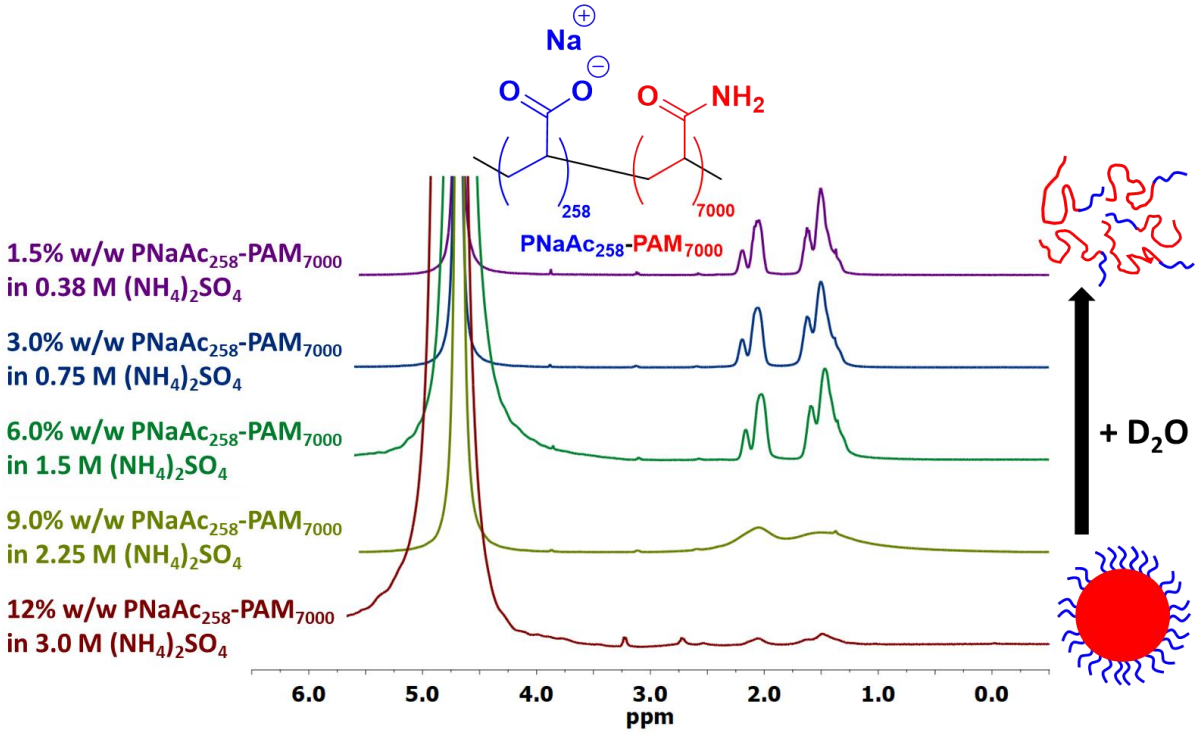

Figure 4.7 ^{1}H NMR spectra recorded for a PNaAc$_{258}$-PAM$_{7000}$ diblock copolymer prepared via RAFT aqueous dispersion polymerisation of AM targeting 12% w/w solids in the presence of 3.0 M ammonium sulfate in D_2O, see red spectrum. On serial dilution of this dispersion with D_2O, both the background salt concentration and the copolymer concentration are systematically reduced. A two-fold dilution of the initial turbid dispersion is sufficient to cause molecular dissolution of the particles as the PAM block becomes solvated in 1.5 M ammonium sulfate. Further dilution results in indistinguishable ^{1}H NMR spectra.

DMAC and ACN are less hydrophilic than AM.[28,29] Hence incorporation of such comonomers into the core-forming block should aid particle formation by *in situ* self-assembly. **Table 4.3** summarises the relative aqueous solubilities of the three corresponding homopolymers in water, 1.5 M ammonium sulfate or 3.0 M ammonium sulfate. PACN is insoluble in aqueous solution even in the absence of any salt, while PDMAC becomes water-insoluble in the presence of 1.5 M ammonium sulfate. In contrast, PAM only becomes water-insoluble in the presence of 3.0 M ammonium sulfate. These observations are consistent with the following order of hydrophobic character: PACN > PDMAC > PAM. Unusually, ACN is not a solvent for its corresponding homopolymer, so a pure PACN core block would not be solvated by unreacted monomer, which would prevent PISA from occurring after particle

nucleation.[30,31] However, successful PISA syntheses should be feasible for the statistical copolymerisation of a relatively low amount of ACN with AM.

	PNaAc	PAM	PDMAC	PACN
Water	Soluble	Soluble	Soluble	Insoluble
1.5 M $(NH_4)_2SO_4$	Soluble	Soluble	Insoluble	Insoluble
3.0 M $(NH_4)_2SO_4$	Soluble	Insoluble	Insoluble	Insoluble

Table 4.3 Summary of aqueous solubilities of $PNaAc_{258}$, PAM_{500}, $PDMAC_{500}$ and $PACN_x$ at 2.0% w/w solids in the presence of zero salt, 1.5 M ammonium sulfate or 3.0 M ammonium sulfate as judged by visual inspection at pH 6 and 20°C.

The synthesis of $PNaAc_{258}$-P(AM_x-*stat*-$DMAC_y$) diblock copolymers is illustrated in **Scheme 4.3**. The reaction conditions are analogous to those in **Scheme 4.2a**, but DMAC is statistically copolymerised with AM.

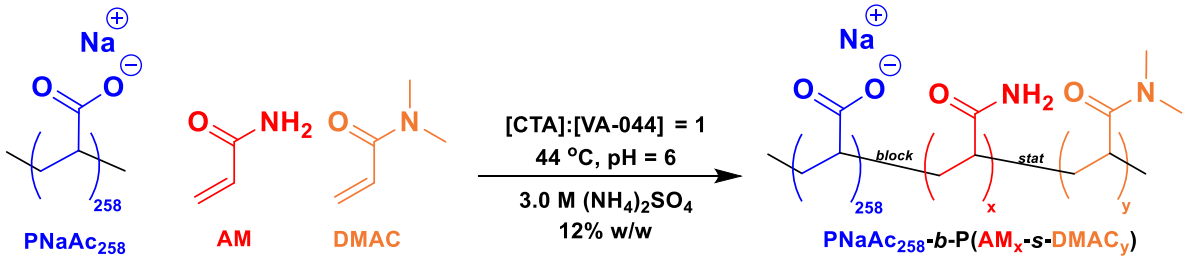

Scheme 4.3 Synthesis of $PNaAc_{258}$-P(AM_x-*stat*-$DMAC_y$) diblock copolymer particles via RAFT aqueous dispersion copolymerisation of AM with DMAC at 44°C in the presence of 3.0 M ammonium sulfate targeting 12% w/w solids and using a $PNaAc_{258}$/VA-044 molar ratio of 1.0.

The overall core-forming block DP was fixed at 12,000 and the DMAC comonomer content was varied from 0 to 25 mol%. Furthermore, two $PNaAc_{258}$-P(AM_{11000}-*stat*-$DMAC_{2500}$) copolymers were synthesised at 12% w/w and 14% w/w solids in order to identify the highest possible DP and copolymer concentration while still maintaining a free-flowing homogeneous dispersion. High comonomer conversions (> 97%) were achieved for all syntheses, as shown in **Table 4.4**. Perhaps surprisingly, there was no discernible trend in the DLS particle diameter for this series of formulations, with consistently high PDIs obtained for all formulations.

P(AM$_x$-stat-DMAC$_y$)		Conversion[a] / %	M_n[a] / kg mol^{-1}	D_z[b] / nm	PDI[b]
x	y				
12,000	0	97	846	2,040	0.21
11,500	500	> 99	886	1,860	0.27
11,000	1,000	> 99	829	990	0.23
10,500	1,500	> 99	914	1,365	0.04
10,000	2,000	98	909	1,248	0.43
9,500	2,500	98	923	2,410	0.49
9,000	3,000	98	937	367	0.80
11,000	2,500	> 99	1,048	1,583	0.44
11,000[c]	2,500[c]	> 99	1,048	1,342	0.14

Table 4.4 Summary of ^{1}H NMR conversion and DLS data obtained for the RAFT aqueous dispersion copolymerisation of AM and DMAC using a PNaAc$_{258}$ precursor targeting 12% w/w solids. (a) Determined by ^{1}H NMR spectroscopy (the integrated vinyl signals assigned to the AM and DMAC comonomers at 5.6 – 6.4 ppm were compared to the integrated backbone signals at 1.3 – 2.5 ppm). M_n values were calculated from comonomer conversions. (b) D_z denotes the z-average diameter and PDI denotes the DLS polydispersity index. (c) experiment was conducted at 14% w/w solids.

The synthesis of PNaAc$_{258}$-P(AM$_x$-*stat*-ACN$_y$) diblock copolymers is illustrated in **Scheme 4.4**. The reaction conditions are analogous to **Scheme 4.2a**, but with the addition of ACN comonomer. Unfortunately, because the Radley carousel apparatus is not a sealed system, most (if not all) of the relatively volatile ACN evaporated from the heated reaction vessel rather than undergoing copolymerisation with the AM, so no results are reported for this formulation.

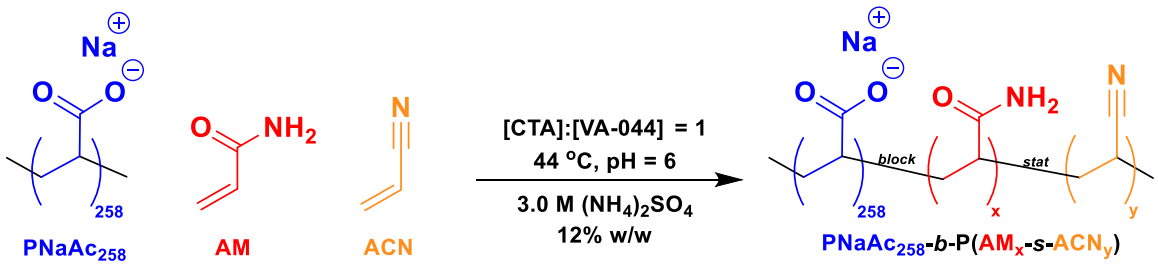

Scheme 4.4 Synthesis of PNaAc$_{258}$-P(AM$_x$-*stat*-ACN$_y$) diblock copolymer particles via RAFT aqueous dispersion copolymerisation of AM with ACN at 44°C in the presence of 3.0 M ammonium sulfate targeting 12% w/w solids and using a PNaAc$_{258}$/VA-044 molar ratio of 1.0.

The rheology of the PNaAc$_{258}$-P(AM$_{11000}$-*stat*-DMAC$_{2500}$) sample shown in **Figure 4.8a** indicates that this diblock copolymer is shear-thinning. It does not exhibit a linear viscoelastic region in its most viscous form (obtained via two-fold dilution with water). However, a plateau region can be identified at all other dilutions examined. The copolymer forms a transparent free-standing gel after a two-fold dilution and plotting the storage modulus against the salt concentration in **Figure 4.8b** suggests that this may correspond to the maximum value. However, verification of this hypothesis would require further analysis of copolymer dilutions in the presence of 0.75 M and 2.25 M ammonium sulfate.

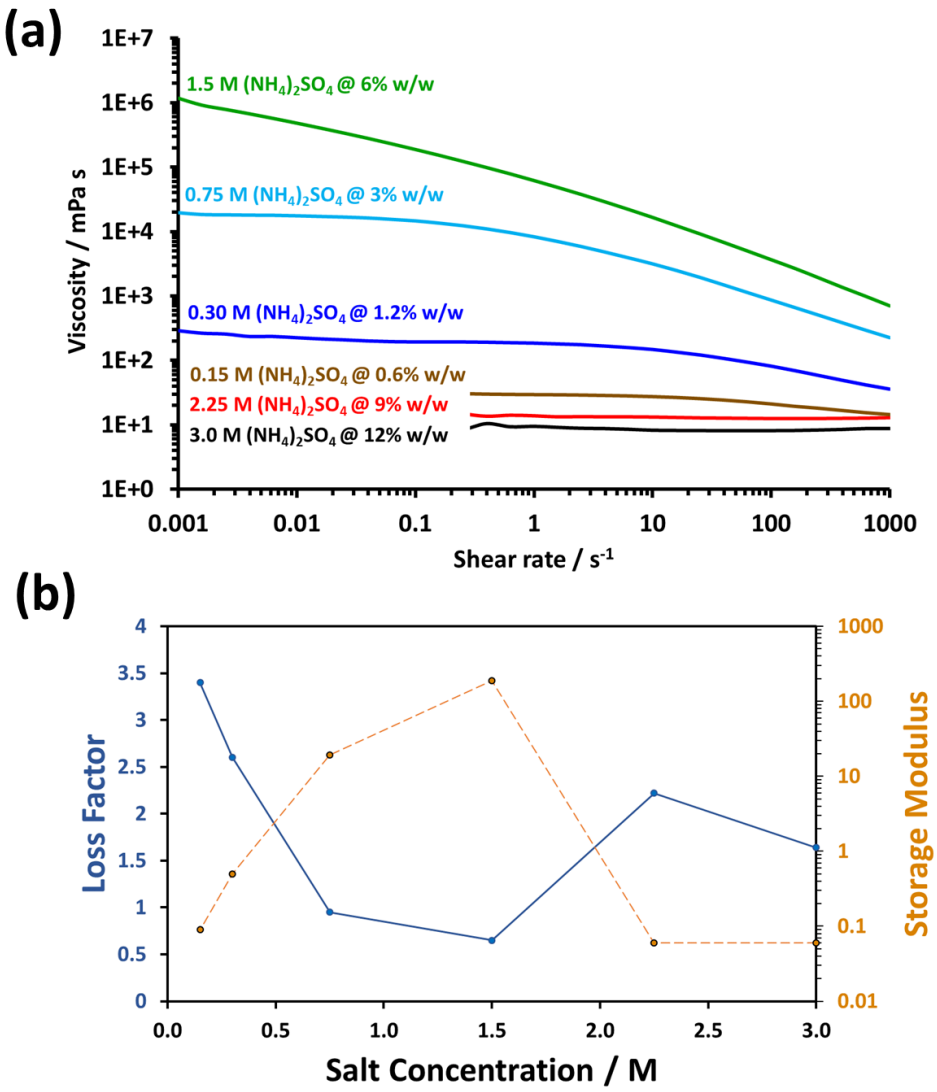

Figure 4.8 (a) Rheology profiles for PNaAc$_{258}$-P(AM$_{11000}$-*stat*-DMAC$_{2500}$) recorded at copolymer concentrations ranging from 0.6% to 12% w/w and salt concentrations of 3.0 M to 0.15 M ammonium sulfate. (b) Salt concentration dependence of the storage modulus and loss factor observed for the same copolymer.

The two highest molecular weight formulations are the PNaAc$_{258}$-P(AM$_{11000}$-*stat*-DMAC$_{2500}$) copolymers synthesised at 12 and 14% w/w solids, respectively. These formulations were selected for an in-house evaluation by BASF for a shale encapsulation test to evaluate their suitability for enhanced oil recovery applications. This industrial testing was only made available for these two PAM-containing formulations.

The extent of shale recovery was determined for a blank sample, an industry standard Alcomer-115 (solid PAM) flocculant (positive control) and the two PNaAc$_{258}$-P(AM$_{11000}$-*stat*-DMAC$_{2500}$) copolymers. The aim of this sieve test for the separation of drill solids is to prevent water from entering the bentonite clay to avoid swelling, which makes filtration more difficult and reduces shale recovery. Shale hydration inhibitor and surfactant (Ultrahib and Basodrill) were added to enhance the performance of each of the three polymers. All experiments were conducted in the presence of 5% w/w potassium chloride. The results indicated that the two PNaAc$_{258}$-P(AM$_{11000}$-*stat*-DMAC$_{2500}$) copolymers exhibited a relatively flat viscosity profile (**Figure 4.9a**) with shale recoveries of 48 – 55% being achieved. This is less than the 73% shale recovery obtained for Alcomer-115 but substantially more than the blank sample (26% shale recovery) (**Figure 4.9b**). The flat viscosity profile is not observed for all formulations, and it could be interesting to explore whether this has any benefits in terms of its commercial application. Although the two new copolymers do not currently meet the threshold for industrial use, they do show some promise after this initial screen. Further optimisation is likely to lead to better shale recovery performance, particularly if M_w can be maximised.

(a)

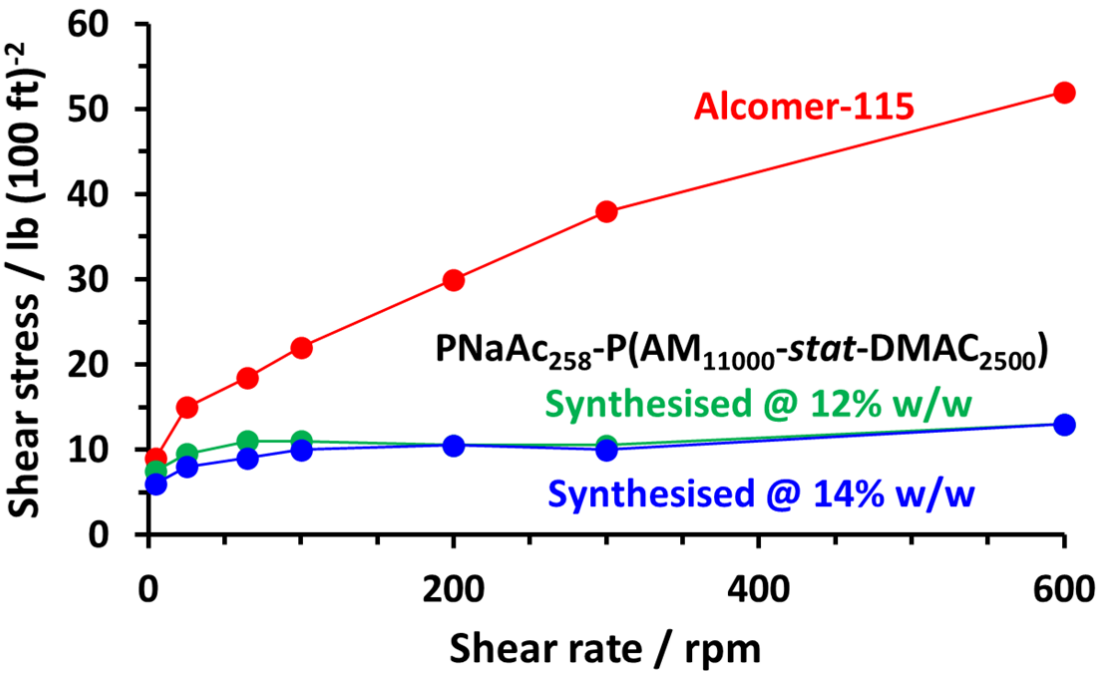

(b)

Polymer Sample	Shale Recovery / %
Blank	26
Alcomer-115 (solid PAM)	73
$PNaAc_{258}$-P(AM_{11000}-*stat*-$DMAC_{2500}$), 12% w/w	49
$PNaAc_{258}$-P(AM_{11000}-*stat*-$DMAC_{2500}$), 14% w/w	55

Figure 4.9 Oilfield test in-house evaluation conducted by BASF. (a) Rheology profile of copolymer samples vs. shear rate. (b) Shale recovery values obtained via shale encapsulation test.

4.4 Conclusions

We report the synthesis of sterically-stabilised diblock copolymer particles via RAFT aqueous dispersion (co)polymerisation in highly salty media using commodity monomers. Prior to chain extension of the poly(acrylic acid) precursor, a small quantity of sodium bicarbonate was added to produce anionic poly(sodium acrylate) ($PNaAc_{258}$) chains, which are soluble in 3.0 M ammonium sulfate. This precursor acts as an effective steric stabiliser for subsequent chain extension via either homopolymerisation of AM or statistical copolymerisation of AM with DMAC, but only at relatively low solids contents (< 15% w/w).

Relatively high DPs are targeted for the salt-insoluble block so this component dominates the formulation. This approach enables high molecular weight commodity water-soluble polymers to be prepared in a highly convenient low-viscosity form. Subsequent two-fold dilution of such copolymer dispersions using deionised water lowers the background salt concentration and hence causes *in situ* molecular dissolution of the particles, which leads to a substantial thickening effect and the formation of highly viscous transparent aqueous solutions. Interestingly, a P(AM-*stat*-DMAC) core-forming block formed a free-standing hydrogel rather than a pure PAM core-forming block which formed a highly viscous solution. The organosulfur content of a 14% w/w aqueous copolymer dispersion of $PNaAc_{258}$-P(AM_{11000}-*stat*-$DMAC_{2500}$) particles is only approximately 11 ppm. Thus the well-known negative aspects of using RAFT agents (i.e. their cost, colour and malodour) are minimised for such formulations.

A preliminary comparison of such copolymers with current BASF commercial products suggests that these new formulations may offer some potential for oilfield applications. More specifically, the $PNaAc_{258}$-P(AM_{11000}-*stat*-$DMAC_{2500}$) copolymer exhibits a relatively flat shear stress profile, although its shale recovery percentage is not as high as that achieved when using Alcomer-115. Nevertheless, further development of such a formulation could lead to its use for such industrial applications.

4.5 References

1 Sigma Aldrich Chemical Company (Merck), https://www.sigmaaldrich.com/GB/en, (accessed 10 December 2023).

2 A. G. Evans, M. Polanyi, H. S. Lilley, L. B. Morgan, H. A. Skinner, P. H. Plesch, M. G. Evans, H. W. Melville, G. B. B. M. Sutherland, W. Cooper, J. H. Baxendale, G. Gee, H. W. Thompson, J. L. Stoves, F. Brown, C. W. Bunn, D. J. Crisp and I. MacArthur, 'Discussion on "some aspects of the chemistry of macromolecules"', *J. Chem. Soc.*, 1947, 252–306.

3 C. E. Habermann, in *Kirk-Othmer Encyclopedia of Chemical Technology*, Wiley, 2002.

4 P. Molyneux, *Water-Soluble Synthetic Polymers*, CRC Press, Boca Raton, 1983.

5 T. Ohara, T. Sato, N. Shimizu, G. Prescher, H. Schwind, O. Weiberg, K. Marten, H. Greim, T. D. Shaffer and P. Nandi, in *Ullmann's Encyclopedia of Industrial Chemistry*, Wiley, 2020, pp. 1–21.

6 E. M. Karp, T. R. Eaton, V. Sànchez i Nogué, V. Vorotnikov, M. J. Biddy, E. C. D. Tan, D. G. Brandner, R. M. Cywar, R. Liu, L. P. Manker, W. E. Michener, M. Gilhespy, Z. Skoufa, M. J. Watson, O. S. Fruchey, D. R. Vardon, R. T. Gill, A. D. Bratis and G. T. Beckham, 'Renewable acrylonitrile production', *Science*, 2017, **358**, 1307–1310.

7 T. Swift, L. Swanson, M. Geoghegan and S. Rimmer, 'The pH-responsive behaviour of poly(acrylic acid) in aqueous solution is dependent on molar mass', *Soft Matter*, 2016, **12**, 2542–2549.

8 C. L. McCormick and A. B. Lowe, 'Aqueous RAFT polymerization: Recent developments in synthesis of functional water-soluble (Co)polymers with controlled structures', *Acc. Chem. Res.*, 2004, **37**, 312–325.

9 D. B. Thomas, A. J. Convertine, R. D. Hester, A. B. Lowe and C. L. McCormick, 'Hydrolytic Susceptibility of Dithioester Chain Transfer Agents and Implications in Aqueous RAFT Polymerizations', *Macromolecules*, 2004, **37**, 1735–1741.

10 M. Mertoglu, A. Laschewsky, K. Skrabania and C. Wieland, 'New water soluble agents for reversible addition-fragmentation chain transfer polymerization and their application in aqueous solutions', *Macromolecules*, 2005, **38**, 3601–3614.

11 C. Bray, R. Peltier, H. Kim, A. Mastrangelo and S. Perrier, 'Anionic multiblock core cross-linked star copolymers: via RAFT polymerization', *Polym. Chem.*, 2017, **8**, 5513–5524.

12 J. T. Lai, D. Filla and R. Shea, 'Functional Polymers from Novel Carboxyl-Terminated Trithiocarbonates as Highly Efficient RAFT Agents', *Macromolecules*, 2002, **35**, 6754–6756.

13 S. S. Cutié, G. J. Kallos and P. B. Smith, 'Separation and characterization of acrylic acid oligomers by nuclear magnetic resonance spectroscopy and thermospray ion-exchange liquid chromatography-mass spectrometry', *J. Chromatogr. A*, 1987, **408**, 349–355.

14 T. L. Staples and P. K. Chatterjee, 2002, pp. 283–322.

15 S. J. Byard, Synthesis and Characterisation of Stimulus-responsive Diblock Copolymer Nano-objects Prepared by RAFT Aqueous Dispersion Polymerisation, PhD Thesis, University of Sheffield, 2019.

16 Z. Jamaludin, S. Rollings-Scattergood, K. Lutes and C. Vaneeckhaute, 'Evaluation of sustainable scrubbing agents for ammonia recovery from anaerobic digestate', *Bioresour. Technol.*, 2018, **270**, 596–602.

17 S. J. Byard, A. Blanazs, J. F. Miller and S. P. Armes, 'Cationic Sterically Stabilized Diblock Copolymer Nanoparticles Exhibit Exceptional Tolerance toward Added Salt', *Langmuir*, 2019, **35**, 14348–14357.

18 M. Williams, N. J. W. Penfold and S. P. Armes, 'Cationic and reactive primary amine-stabilised nanoparticles via RAFT aqueous dispersion polymerisation', *Polym. Chem.*, 2016, **7**, 384–393.

19 A. A. Cockram, R. D. Bradley, S. A. Lynch, P. C. D. Fleming, N. S. J. Williams, M. W. Murray, S. N. Emmett and S. P. Armes, 'Optimization of the high-throughput synthesis of multiblock copolymer nanoparticles in aqueous media: Via polymerization-induced self-assembly', *React. Chem. Eng.*, 2018, **3**, 645–657.

20 R. J. McBride, J. F. Miller, A. Blanazs, H. J. Hähnle and S. P. Armes, 'Synthesis of High Molecular Weight Water-Soluble Polymers as Low-Viscosity Latex Particles by RAFT Aqueous Dispersion Polymerization in Highly Salty Media', *Macromolecules*, 2022, **55**, 7380–7391.

21 P. Biais, P. Beaunier, F. Stoffelbach and J. Rieger, 'Loop-stabilized BAB triblock copolymer

morphologies by PISA in water', *Polym. Chem.*, 2018, **9**, 4483–4491.

22 C. Dommanget, F. D'Agosto and V. Monteil, 'Polymerization of Ethylene through Reversible Addition–Fragmentation Chain Transfer (RAFT)', *Angew. Chemie Int. Ed.*, 2014, **53**, 6683–6686.

23 O. J. Deane, O. M. Musa, A. Fernyhough and S. P. Armes, 'Synthesis and Characterization of Waterborne Pyrrolidone-Functional Diblock Copolymer Nanoparticles Prepared via Surfactant-free RAFT Emulsion Polymerization', *Macromolecules*, 2020, **53**, 1422–1434.

24 E. Read, A. Guinaudeau, D. J. Wilson, A. Cadix, F. Violleau and M. Destarac, 'Low temperature RAFT/MADIX gel polymerisation: Access to controlled ultra-high molar mass polyacrylamides', *Polym. Chem.*, 2014, **5**, 2202–2207.

25 A. Favier, F. D'Agosto, M.-T. Charreyre and C. Pichot, 'Synthesis of N-acryloxysuccinimide copolymers by RAFT polymerization, as reactive building blocks with full control of composition and molecular weights', *Polymer*, 2004, **45**, 7821–7830.

26 B. Huang, J. Jiang, M. Kang, P. Liu, H. Sun, B. G. Li and W. J. Wang, 'Synthesis of block cationic polyacrylamide precursors using an aqueous RAFT dispersion polymerization', *RSC Adv.*, 2019, **9**, 12370–12383.

27 S. Bai, Y. Wang, B. Liu, Y. Zhu and R. Guo, 'Dispersion copolymerization of acrylamide and sodium 2-acrylamido-2-methylpropanesulfonate in aqueous salt solution stabilized with a macro-RAFT agent', *Colloids Surfaces A Physicochem. Eng. Asp.*, 2018, **553**, 446–455.

28 H. Zhang, X. Tong and Y. Zhao, 'Diverse Thermoresponsive Behaviors of Uncharged UCST Block Copolymer Micelles in Physiological Medium', *Langmuir*, 2014, **30**, 11433–11441.

29 C. Baggiani, P. Baravalle, C. Giovannoli and C. Tozzi, 'Binding behaviour of pyrimethanil-imprinted polymers prepared in the presence of polar co-monomers', *J. Chromatogr. A*, 2006, **1117**, 74–80.

30 S. L. Canning, G. N. Smith and S. P. Armes, 'A Critical Appraisal of RAFT-Mediated Polymerization-Induced Self-Assembly', *Macromolecules*, 2016, **49**, 1985–2001.

31 M. Kopeć, P. Krys, R. Yuan and K. Matyjaszewski, 'Aqueous RAFT Polymerization of Acrylonitrile', *Macromolecules*, 2016, **49**, 5877–5883.

Chapter 5: Synthesis of Non-Ionic High Molecular Weight Water-Soluble Polymers as Low-Viscosity Latex Particles in Low Salt Media by RAFT Aqueous Dispersion Polymerisation

Reproduced with permission from [R. J. McBride, E. Geneste, A. Xie, A. J. Ryan, A. Blanazs, C. Rösch, J. F. Miller and S. P. Armes, *Macromolecules,* 2024, **57**, 2432−2445]

5.1 Introduction

It is well-known that water-soluble polymers can differ markedly in terms of their sensitivity towards added salt. For example, zwitterionic polymers such as poly(2-(methacryloyloxy)ethyl phosphorylcholine) are remarkably salt-tolerant and can remain water-soluble even in the presence of 5 M NaCl.[1] On the other hand, the salt sensitivity of poly(2-(*N*-morpholino)ethyl methacrylate) (PMEMA) has been exploited to design several examples of so-called 'schizophrenic' AB diblock copolymers that can form either A-core or B-core micelles in aqueous media depending on the precise solution pH, temperature or salt concentration.[2–4] In each case, PMEMA-core micelles were obtained on addition of 0.7 to 1.0 M sodium sulfate.

Another well-known morpholine-functionalised water-soluble polymer is poly(*N*-acryloylmorpholine) (PNAM). The reversible addition-fragmentation chain transfer (RAFT) solution homopolymerisation of NAM was first reported twenty years ago.[5–7] More recently, PNAM has been used as the water-soluble steric stabiliser block for various polymerisation-induced self-assembly (PISA) syntheses conducted in aqueous media.[8–11] The non-ionic, highly biocompatible nature of PNAM has been exploited for various biomedical applications, including the sustained delivery of nitric oxide,[12] as an alternative to PEGylation for protein conjugation,[13] and the efficient harvesting of cell sheets from a micropatterned brush grown from a planar substrate.[14] Given this prior literature, we were rather surprised to find that there are apparently no studies of the salt sensitivity of PNAM in aqueous solution, which is comparable to that of PMEMA.

The synthesis of various high molecular weight water-soluble polymers via RAFT solution polymerisation has been explored by Destarac et al.[15], An and co-workers[16–18] and Sumerlin et al.[19,20] Unfortunately, this approach inevitably leads to highly viscous solutions or gels, which makes further processing somewhat problematic. To address this problem, an inverse miniemulsion polymerisation strategy has been developed by Olson et al.[21] However, such

formulations require use of an organic solvent (cyclohexane) and a relatively large amount of surfactant (Span 60) to stabilise the aqueous droplets.

Recently, we and others have developed RAFT aqueous dispersion polymerisation formulations to prepare highly asymmetric double-hydrophilic diblock copolymers in the form of low-viscosity sterically-stabilised particles.[22–24] This is achieved by preparing a suitable salt-tolerant water-soluble polymer and then growing a salt-sensitive polymer from this precursor in the presence of sufficient added salt. For example, in **Chapter 3** a zwitterionic, cationic or an anionic precursor for the RAFT aqueous dispersion polymerisation of *N,N'*-dimethylacrylamide (DMAC) in the presence of 2.0 M ammonium sulfate.[24] Interestingly, DMAC conversions of more than 99% could be obtained at up to 20% w/w solids even when targeting PDMAC DPs as high as 5000. Similarly, Huang et al.[22] statistically copolymerised acrylamide with 2-(methacryloyloxy)ethyl trimethylammonium chloride (METAC) and examined the resulting series of cationic water-soluble precursors for the RAFT aqueous dispersion polymerisation of acrylamide in the presence of ammonium sulfate at 45-55°C. METAC-rich copolymer precursors with higher DPs favored the formation of colloidally stable polyacrylamide-core particles. Narrow molecular weight distributions were achieved (typically M_w/M_n = 1.10 to 1.20) but the target core-forming block DP was only varied from 600 to 1200, which is insufficient for optimal performance as an industrial flocculant.[25] Moreover, the target solids content was relatively low at 3-6 % w/w, which meant that the final acrylamide conversion was typically around 90-95%.[22]

In a related study, Bai et al.[26] chain-extended a trithiocarbonate-capped poly(sodium 2-acrylamido-2-methylpropanesulfonate) (PAMPS) precursor via statistical copolymerisation of sodium 2-acrylamido-2-methylpropanesulfonate (AMPS) with acrylamide in the presence of approximately 2.0 M ammonium sulfate. These RAFT aqueous dispersion polymerisation syntheses were conducted under zero shear using a bifunctional precursor to produce ABA-

type triblock copolymer particles of around 1-3 μm diameter at up to 20% w/w solids. Final comonomer conversions of up to 99% were achieved and GPC curves were obtained but no molecular weight data were reported.

Herein we report the RAFT aqueous dispersion polymerisation of NAM using a salt-tolerant water-soluble poly(2-hydroxyethyl acrylamide) (PHEAC) precursor in the presence of added salt (see **Scheme 5.1**). Unlike the prior studies described above, this formulation involves the synthesis of a *wholly non-ionic* diblock copolymer using a *relatively low level of added salt* (just 0.60 M ammonium sulfate). ^{1}H NMR spectroscopy is used to study the kinetics of polymerisation, molecular weight distributions are evaluated using DMF GPC, absolute weight-average molecular weights are determined by static light scattering in aqueous media, and the mean particle diameter is assessed using dynamic light scattering, laser diffraction and transmission electron microscopy. Finally, aqueous electrophoresis and rotational rheology are used to examine the particle surface charge and dispersion/solution viscosity, respectively.

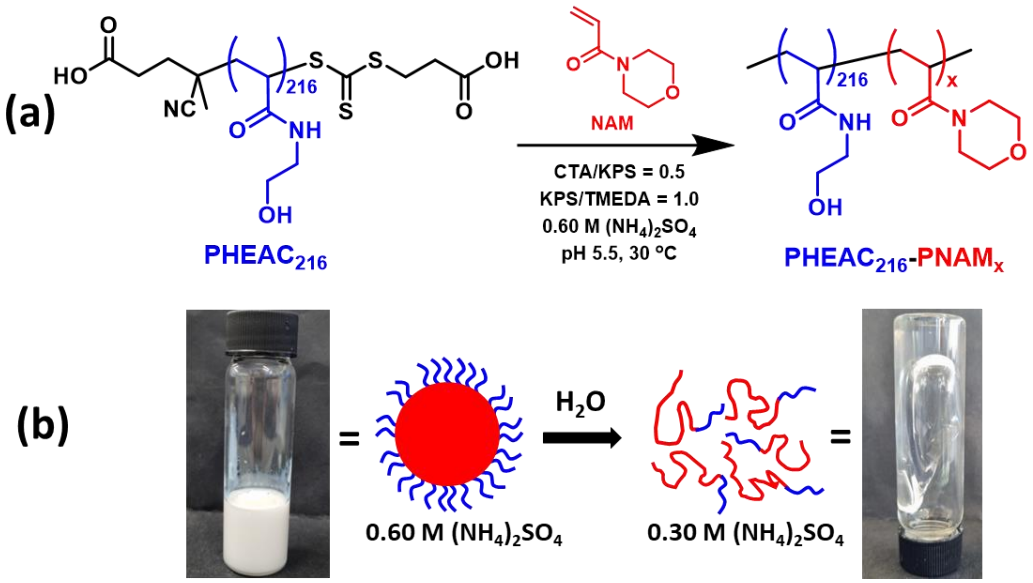

Scheme 5.1 (a) Reaction scheme for the synthesis of **PHEAC$_{216}$-PNAM$_x$** (x = 1,000 to 6,000) diblock copolymer particles at 20% w/w solids via RAFT aqueous dispersion polymerisation of NAM at 30°C in the presence of 0.60 M ammonium sulfate. Conditions: PHEAC$_{216}$/KPS molar ratio = 0.50; KPS/TMEDA molar ratio = 1.0 and time ≥ 18 h. (b) Schematic cartoon and corresponding digital images to illustrate the sterically-stabilised **PHEAC$_{216}$-PNAM$_x$** diblock copolymer particles in the presence of 0.60 M ammonium sulfate obtained after RAFT aqueous dispersion polymerisation of NAM. A two-fold dilution of this aqueous dispersion with deionised water halves the salt concentration and results in spontaneous dissociation of the

particles, with the concomitant formation of a highly viscous transparent aqueous solution comprising molecularly-dissolved diblock copolymer chains.

5.2 Experimental

5.2.1 Materials

2-Hydroxyethyl acrylamide (HEAC, ≥ 96%), *N*-acryloylmorpholine (NAM, ≥ 97%), *N,N,N',N*'-tetramethylethylenediamine (TMEDA, >99%) and D_2O (D_2O; ≥ 99.9% D) were purchased from Sigma-Aldrich Ltd (UK). Potassium persulfate (KPS, 99%) and 2,2′-azobis(2-imidazolinylpropane) dihydrochloride (VA-044, ≥98%) were obtained from Fluorochem Ltd (UK). Ammonium sulfate (>98% purity) was purchased from Alfa Aesar (UK). The 4-(((2-(carboxyethyl)thio)carbonothioyl)thio)-4-cyanopentanoic acid RAFT agent (BM1433, >95%) used in this study was kindly donated by Boron Molecular (Victoria, Australia). *S*-Butyl-*S*′-(α,α′-dimethyl-α″-acetic acid)trithio-carbonate, methyl ester (MeBDMAT) was synthesised in-house. Each of the above chemicals was used as received. All solvents were purchased from Fisher Scientific (UK) and were used as received. Deionised water was used for all experiments.

5.2.2 Characterisation Techniques

Experimental protocols for ^{1}H NMR spectroscopy, UV absorption spectroscopy and rotational rheology are described in **Chapter 2**.

Gel Permeation Chromatography (GPC)

Molecular weights and dispersities were determined for the various homopolymers and diblock copolymers using an Agilent 1260 Infinity GPC instrument. This set-up comprised a pump, a degasser, two PL-gel 5 μm Mixed-C columns in series and a refractive index detector. The column and detector temperature was set to 60°C and the flow rate was 1.0 mL min^{-1}. HPLC-grade DMF containing 10 mM LiBr was used as the eluent and the flow rate was 1.0

mL min^{-1}. Calibration was achieved using ten near-monodisperse poly(methyl methacrylate) standards (370 to 2,520,000 g mol^{-1}) and data were analysed using Agilent Technologies GPC/SEC software.

Static Light Scattering (SLS)

A Dawn Helios II light scattering instrument (Wyatt Technology Corp. USA; equipped with a 130 mW linearly polarised gallium arsenide laser source operating at 658 mm and 18 detectors placed at angles ranging from 22.5° to 147°) was used to determine the absolute weight-average molecular weight (M_w) of each diblock copolymer. This instrument was connected in series to an Agilent 1260 Infinity GPC instrument comprising a pump, a degasser, three GPC columns (PL-Aquagel Mixed-H, OH-30 and OH-40) and a Optilab T-rEX differential refractometer, which was used as a concentration detector in online mode. The eluent was an aqueous solution comprising 0.10 M $NaNO_3$, 0.02 M TEA and 0.05 M $NaHCO_3$ at pH 8. The column and detector temperature was set to 30°C and the flow rate was 0.5 mL min^{-1}. Copolymers were dissolved in the above GPC eluent at a relatively high concentration (> 1 mg/ml) and injected using an autosampler. Data were analysed using Astra 7 software according to Zimm formalisms. For Zimm plots, copolymer concentrations were varied by adjusting the injection volume. Thus 10 µl, 25 µl, or 50 µl of each copolymer solution was injected and a linear correlation was assumed between the injection volume and the light scattering detector signal.

Differential refractive index (dn/dc) measurements. An Optilab T-rEX differential refractometer (Wyatt Technology Corp. USA) was used in batch mode to determine the dn/dc value for copolymers dissolved in the GPC eluent at pH 8. Copolymer solutions of varying concentration (0.5, 1.5, 2.5, 3.5, or 4.5 g dm^{-3}) were injected consecutively (lowest concentration first) into the instrument at the same flow rate used for the online mode experiments using a syringe pump. A linear calibration plot of refractive index versus

copolymer concentration enables a dn/dc value to be calculated directly from the gradient. Hence the copolymer concentrations used for the online mode measurements can be calculated.

Dynamic Light Scattering (DLS)

Analysis was performed using a Malvern Zetasizer Nano ZS instrument equipped with a 4 mW He–Ne 633 nm laser and an avalanche photodiode detector. The instrument was configured to automatically determine the experimental duration and optical attenuation. Each polymer was diluted in 0.60 M $(NH_4)_2SO_4$ to a copolymer concentration of 0.05% w/w and subsequently filtered through a 1.0 μm glass fibre filter. Back-scattered light was detected at an angle of 173° and measurements were conducted at 20 °C in a 10 mm path length quartz cuvette cell. Malvern Zetasizer software v7.11 was used to calculate z-average hydrodynamic diameters (D_z) via the Stokes-Einstein equation, which assumes perfectly monodisperse, non-interacting spherical particles. Data were averaged over at least three consecutive runs with at least ten measurements being recorded for each run. The viscosity of 0.60 M ammonium sulfate is 1.113 Pa s and the refractive index is 1.345.[27] Each dilute aqueous dispersion was passed through a 1 μm ultrafilter to remove dust prior to analysis. Standard deviations were calculated from the DLS polydispersity index (PDI) using the following relationship: standard deviation $= \sqrt{\text{PDI}} \times \text{DLS diameter}$.

Laser Diffraction

Laser diffraction studies were performed using a Malvern Mastersizer 3000 instrument equipped with a Hydro EV dispersion unit (stirring rate = 2,000 rpm). A HeNe laser operating at 633 nm and a solid-state blue laser operating at 466 nm were used to analyse polymer dispersions to determine the volume-average particle diameter. After each measurement, the cell was rinsed three times with water and the laser was aligned central to the detector prior to data acquisition.

Transmission Electron Microscopy (TEM)

Cu/Pd TEM grids (Agar Scientific, UK) were coated in-house with a thin film of amorphous carbon and then treated with a plasma glow discharge for 30 seconds to generate a hydrophilic surface. A 10 μL droplet of a freshly diluted 0.5% w/w aqueous copolymer dispersion was pipetted onto a hydrophilic grid for 1 min, then carefully blotted with filter paper to remove excess sample. Then, a single 10 μL droplet of a 0.75% w/w aqueous solution of uranyl formate was pipetted onto the grid for 20 sec to stain the deposited particles. Excess stain was carefully blotted and dried using a vacuum hose. Imaging was performed using an FEI Tecnai Spirit 2 microscope equipped with an Orius SC1000B camera operating with an accelerating voltage of 80 kV.

Potentiometric titration

Potentiometric titration was performed manually. 25.0 mL of acidified copolymer dispersion was placed in a 250 mL glass beaker and stirred with a magnetic flea. Titrant aqueous solution (0.6 M ammonium sulfate plus 0.2 M potassium hydroxide) was placed in a volumetric 50 mL burette, and a standard glass pH electrode was immersed in the dispersion sample. A total of 5.0 mL of titrant was added in aliquots of typically 0.5 mL, with smaller aliquots being used to determine the equivalence point of the titration. The apparent pH of the copolymer dispersion was recorded after addition of each aliquot and the solution pH restabilised within 30 seconds in each case. All pH measurements were performed at 22 ± 1°C. Approximately 0.75 mL of the aqueous copolymer dispersion was removed at suitable intervals for subsequent electrophoretic light scattering (ELS) analysis. No attempt was made to remove dissolved CO_2 or to prevent its dissolution. Thus it was assumed that these aqueous copolymer dispersions were saturated with dissolved CO_2.

Electrophoretic light scattering (ELS)

Electrophoretic mobilities were determined using NG-ELS (Next Generation Electrophoretic Light Scattering, Enlighten Scientific LLC, Hillsborough, NC). The functional design and operation of this instrument is based on the original phase analysis light scattering (PALS) apparatus,[28] which employed a crossed-beam optical configuration (in contrast to the more common reference beam configuration used in commercial ELS instruments). The electrode assembly used for the NG-ELS equipment was based on that described by Uzgiris[29]. Disposable polystyrene semi-micro cuvettes (4 mm path length) were used as the sample holders. Two identical parallel plate platinised platinum[30] electrodes, 4 mm apart, were used to provide the driving voltage across the sample. The sample volume required for measurement was approximately 0.75 mL and aliquots of aqueous copolymer dispersions were analysed without further dilution. A miniature NTC-type thermistor was placed in direct contact with each aqueous copolymer dispersion. This temperature probe was positioned at the mid-point between the electrodes and approximately 1 mm above the intersection point of the two laser beams. Temperature control was achieved by placing the sample cuvette in an aluminum block that ensured efficient heat transfer to a circulating water supply. The water temperature depended on the degree of Joule heating of the aqueous copolymer dispersion, which in turn depended on both its ionic conductivity and the applied voltage. Complex impedance analysis of the electrode waveform was used to quantify electrode polarisation and Joule heating. Mobility measurements were made using sinusoidal electrode signal waveforms with an amplitude of 3.0 V at frequencies of either 32 or 64 Hz. The sample temperature was maintained at 24.5 ± 1.0°C during measurement. The scattered light was analysed for 60 seconds using both the PALS and the laser Doppler electrophoresis (LDE) methods simultaneously. i.e., the same data were used to calculate the electrophoretic mobility for each method. For each sample, ten independent measurements were made at each electrode signal

frequency. This provided twenty measurements per sample from which a mean value and standard deviation were calculated.

5.2.3 Synthesis of PHEAC Precursor via RAFT Aqueous Solution Polymerisation of HEAC at 46°C

HEAC (30.33 g, 0.26 mol), 4-((((2-carboxyethyl)thio)carbonothioyl)thio)-4-cyanopentanoic acid (BM1433; 0.270 g, 879 μmol), 2,2′-azobis(2-imidazolinylpropane) dihydrochloride (VA-044, 028.4 mg, 87.9 μmol) and deionised water (46.2 g) were weighed into a 250 mL round-bottom flask with a magnetic flea and the resulting reaction solution was degassed using a stream of nitrogen gas for 30 min at 20°C. The sealed flask was immersed into an oil bath set at 46°C and the ensuing polymerisation was allowed to proceed for 3 h achieving 89% HEAC conversion. The aqueous polymer solution was purified by dialysis for three days to remove unreacted monomer and initiator and then freeze-dried overnight. The mean degree of polymerisation was determined to be 216, as judged by end-group analysis using UV spectroscopy at the absorption maximum of 306 nm. DMF GPC analysis indicated an M_n of 23.93 kg mol^{-1} and an M_w/M_n of 1.27.

5.2.4 Preparation of Aqueous Stock Solutions of Ammonium Sulfate, KPS Initiator and TMEDA

Ammonium sulfate (39.65 g) was added to a 500 mL round-bottom flask, which was subsequently charged with deionised water to obtain a 0.60 M aqueous solution. Stock solutions of potassium persulfate (KPS; 5%, 1% or 0.1% w/w) and *N,N,N',N*'-tetramethylethylene diamine (TMEDA; 5%, 1% or 0.1% w/w) were prepared using this 0.60 M $(NH_4)_2SO_4$ aqueous solution. Each stock solution was degassed separately using a stream of nitrogen gas for 30 min at 20°C.

5.2.5 Synthesis of $PHEAC_{216}$-$PNAM_x$ Diblock Copolymer Particles via RAFT Aqueous Dispersion Polymerisation of *N*-Acryloylmorpholine (NAM) in 0.60 M Ammonium Sulfate at 30°C

A typical protocol for the synthesis of $PHEAC_{216}$-$PNAM_{3000}$ diblock copolymer particles at 20% w/w solids was conducted as follows. The $PHEAC_{216}$ precursor (40 mg, 1.59 μmol), NAM (675 mg, 4.78 mmol) and the aqueous solution of 0.60 M ammonium sulfate (1.628 g) were weighed into a 10 mL round-bottom flask charged with a magnetic flea and degassed with N_2 for 30 min at 20°C. This flask was then immersed in an oil bath set at 30°C and KPS (3.19 μmol; 8.61 mg of a 0.1% w/w aqueous stock solution) and TMEDA (3.19 μmol; 370 mg of a 0.1% w/w aqueous stock solution) were added simultaneously to initiate the NAM polymerisation. After 18 h, the final NAM conversion was judged to be more than 99% using ^{1}H NMR spectroscopy (the integrated vinyl monomer signals at 5.7-6.6 ppm were compared to the integrated acrylamide backbone signals at 2.5-2.8 ppm). DMF GPC analysis indicated an M_n of 117.18 kg mol^{-1} and an M_w/M_n of 1.92. Higher PNAM DPs were targeted by reducing the concentration of the $PHEAC_{216}$ precursor while maintaining a constant NAM concentration.

5.2.6 Synthesis of MeBDMAT RAFT Chain Transfer Agent

The initial synthesis of *S*-butyl-*S*′-(α,α′-dimethyl-α′′-acetic acid)trithio-carbonate (BDMAT) is based on protocols reported by Lai *et al.* and Bray *et al.*[31,32]

1-Butanethiol (24 mL), acetone (12 mL) and an aqueous solution of 5 M NaOH (44 mL) were added to a 500 mL round-bottomed flask equipped with a magnetic flea and stirred for 25 min at 20°C to produce a light pink solution. On addition of carbon disulfide (15 mL), the reaction solution turned orange and stirring was continued for a further 30 min. Then the flask was immersed in an ice bath. 2-Methyl-2-bromopropanoic acid was heated to 50°C (i.e. above its melting point range of 44 – 47°C) and 38.4 g was slowly dripped into the ice-cold flask, which caused the reaction solution to turn yellow. The flask was removed from the ice bath,

the reaction mixture was poured into an aqueous solution of 5 M NaOH (44 mL), and the resulting solution was stirred for 20 h at 20°C. This solution was then diluted with deionised water (200 mL) and washed four times with *n*-hexane (4 x 200 mL). The orange aqueous phase was placed in a flask, which was immersed in an ice bath prior to addition of an aqueous solution of 1.0 M HCl (230 mL) to produce a final solution pH of 3. The resulting yellow precipitate was isolated and washed with water prior to dissolution in chloroform (200 mL). After drying with anhydrous $MgSO_4$ and removing the solvent under vacuum, the BDMAT product was isolated as a viscous orange-yellow liquid, which crystallised to form a yellow solid when poured into a glass vial. Subsequently, BDMAT (2.50 g, 9.92 mmol) and anhydrous dichloromethane (25.0 g) were added to an oven-dried 250 mL round-bottomed flask equipped with a magnetic flea. This flask was immersed in an ice bath to 0°C for 5 min. Then DMAP (279.0 mg, 2.28 mmol) and excess methanol (1.59 g, 49.6 mmol) were added and *N*,*N*′-dicyclohexylcarbodiimide (2.15 g, 10.4 mmol) was gradually added over 5 min. The reaction mixture was stirred overnight at 20°C. The insoluble *N*,*N*′-dicyclohexylurea by-product was removed *via* filtration and the crude product was purified by silica column chromatography using dichloromethane as the mobile phase prior to drying in a vacuum oven overnight to isolate a viscous yellow oil; *S*-butyl-*S*′-(α,α′-dimethyl-α′′-acetic acid)trithio-carbonate, methyl ester (MeBDMAT, 1.95 g, 74%), m/z 267 (M^+), δ_H (400 MHz; CD_2Cl_2; $(CH_3)_4Si$) 0.97 (3 H, t, −C**H**$_3$), 1.45 (2 H, q, −C**H**$_2$−), 1.69 (8 H, s, −(C**H**$_3$)$_2$, q, −C**H**$_2$−), 3.33 (2 H, t, −C**H**$_2$−) 3.70 (3 H, s, −OC**H**$_3$).

5.2.7 One-Pot Synthesis of $PHEAC_{220}$-$PNAM_{6000}$ Particles via RAFT Aqueous Dispersion Polymerisation of NAM in the presence of 0.60 M Ammonium Sulfate

The one-pot protocol for the synthesis of $PHEAC_{220}$-$PNAM_{6000}$ diblock copolymer particles at 20% w/w solids was conducted as follows. HEAC (952 mg, 8.27 mmol), MeBDMAT (10.0 mg, 37.6 μmol) and deionised water (315 mg; targeting 70% w/w solids) were weighed into a

250 mL round-bottomed flask equipped with a magnetic flea and the resulting reaction solution was degassed using a stream of nitrogen gas for 45 min at 20°C. The flask was sealed using a rubber septum and immersed in an oil bath set at 30°C. Then KPS (3.76 μmol; 101.6 mg of a 1.0% w/w aqueous stock solution) and TMEDA (3.76 μmol; 43.7 mg of a 1.0% w/w aqueous stock solution) were added to the reaction mixture via syringe. The ensuing HEAC polymerisation was allowed to proceed for 3.5 h at 30°C. Then a degassed mixture of NAM (15.2 g, 113 mmol) in an aqueous solution of 0.60 M ammonium sulfate (134.0 g) was added to target a final copolymer concentration of 20% w/w solids. Simultaneously, KPS initiator (75.2 μmol; 0.40 mL of a 5.0% w/w degassed aqueous stock solution) and TMEDA (75.2 μmol; 0.17 mL of a 5.0% w/w degassed aqueous stock solution) were also added to the reaction mixture. After stirring at 30°C for 20 h, the final comonomer conversion was judged to be more than 99% using ^{1}H NMR spectroscopy.

5.3 Results and Discussion

The RAFT solution polymerisation of HEAC was conducted in 0.6 M ammonium sulfate solution at 46°C using a trithiocarbonate-based RAFT agent (either BM1433 or MeBDMAT). The mean degree of polymerisation (DP) of the resulting PHEAC homopolymer was determined to be 216 ± 1 via end-group analysis using UV absorption spectroscopy (calibration plots shown in **Figure 5.1**).

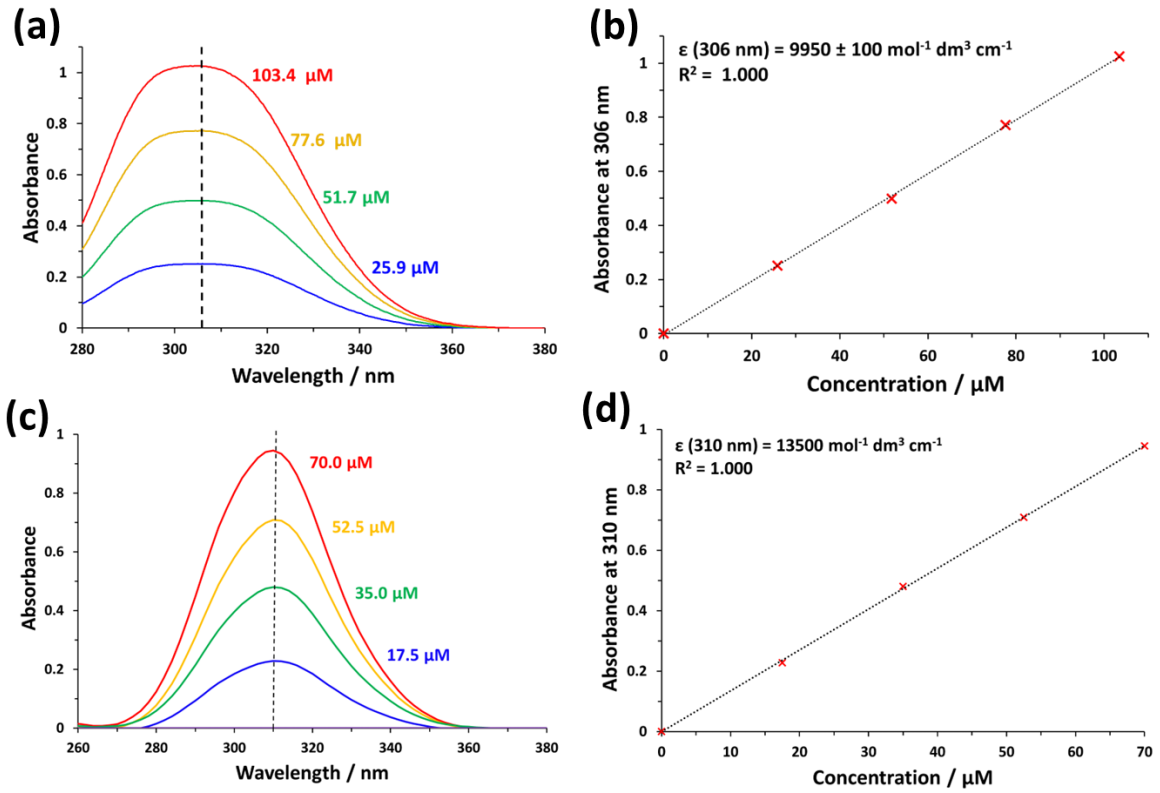

Figure 5.1 (a) UV absorption spectra recorded for 4-(((2-(carboxyethyl)thio)carbonothioyl) thio)-4-cyanopentanoic acid (BM1433) in water for a series of concentrations ranging from 0 µM to 103.4 µM. (b) Beer-Lambert calibration plot constructed for BM1433 in water to calculate its molar extinction coefficient (ε) at the absorption maximum of 306 nm. (c) UV absorption spectra recorded for S-butyl-S′-(α,α′-dimethyl-α′′-acetic acid)trithiocarbonate, methyl ester (MeBDMAT) in methanol for a series of concentrations ranging from 0 µM to 70.0 µM. (d) Beer-Lambert calibration plot constructed for MeBDMAT in methanol to calculate its molar extinction coefficient (ε) at the absorption maximum of 310 nm.

Over the past 25 years, various studies have demonstrated that PMEMA is a salt-intolerant water-soluble polymer.[2,3,33,34] Herein we show that a second morpholine-functional water-soluble polymer, PNAM, exhibits similar behaviour (see **Table 5.1**). More specifically, visual inspection studies (see digital photographs shown in **Figure 5.2**) confirm that $PNAM_{500}$ homopolymer is soluble in the presence of 0.40 M ammonium sulfate at 30°C but becomes insoluble when this salt concentration is increased to 0.60 M. Furthermore, NAM monomer remains water-miscible in the presence of 0.60 M, 1.0 M or 2.0 M ammonium sulfate and only becomes water-immiscible at 3.0 M ammonium sulfate. In view of these observations, an ammonium sulfate concentration of 0.60 M was selected for the aqueous dispersion

polymerisation formulation explored in the present study. This salt concentration is significantly lower than that reported in the literature for a wide range of aqueous dispersion polymerisation formulations conducted in the presence of ammonium sulfate.[22–24,26,35–43]

Additive	Aqueous $(NH_4)_2SO_4$ solution / mol dm^{-3}					
	0	0.40	0.60	1.0	2.0	3.0
HEAC monomer	Soluble	Soluble	Soluble	Soluble	Soluble	Soluble
$PHEAC_{216}$	Soluble	Soluble	Soluble	Soluble	Insoluble	Insoluble
NAM monomer	Soluble	Soluble	Soluble	Soluble	Soluble	Insoluble
$PNAM_{500}$	Soluble	Soluble	Insoluble	Insoluble	Insoluble	Insoluble

Table 5.1 Summary of the aqueous solubilities of HEAC monomer, NAM monomer, $PHEAC_{216}$ homopolymer and $PNAM_{500}$ homopolymer at 2.0% w/w solids in the presence of up to 3.0 M $(NH_4)_2SO_4$ as judged by visual inspection at pH 5.5 and 30°C. Representative digital photographs were recorded above and below the critical salt concentration for each aqueous solution (see **Figure 5.2**).

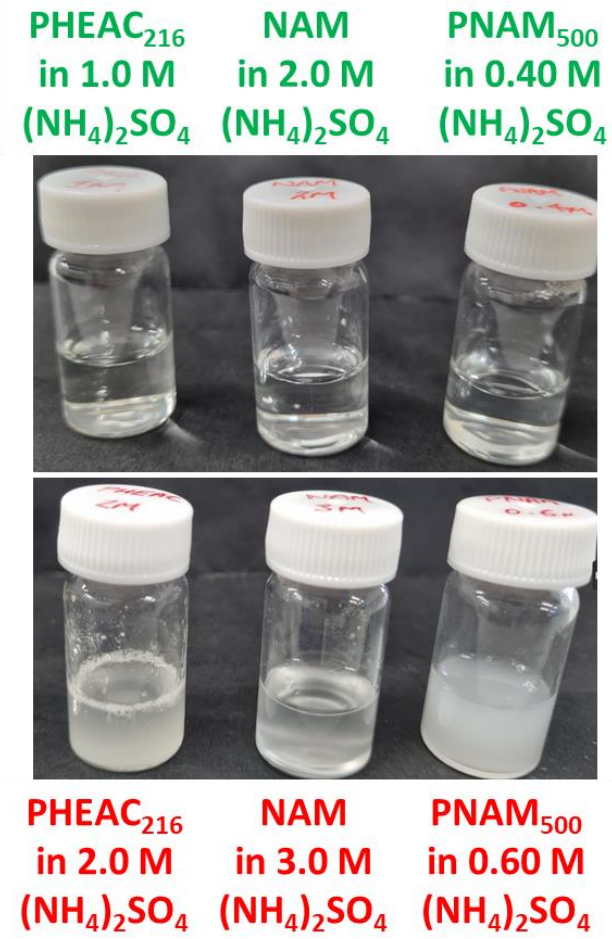

Figure 5.2 Aqueous salt solubility tests. Digital photographs recorded at 30°C illustrating the visual appearance of 2.0% w/w aqueous solutions of NAM monomer, $PHEAC_{216}$ homopolymer and $PNAM_{500}$ homopolymer containing up to 3.0 M ammonium sulfate at pH 5.5.

Furthermore, we explore the first example of an aqueous dispersion polymerisation formulation performed in the presence of salt in which solely *non-ionic* vinyl monomers are used to prepare both the relatively short steric stabiliser block and the much higher molecular weight core-forming block. More specifically, poly(2-hydroxyethyl acrylamide) (PHEAC) is employed as the salt-tolerant steric stabiliser precursor and PNAM is selected as the salt-intolerant core-forming block (see **Scheme 5.1a**). In striking contrast, all prior literature reports of similar aqueous dispersion polymerisation syntheses conducted in the presence of salt involve using cationic, anionic or zwitterionic comonomers.[22–24,26,38–43] This is no doubt because these ionic components confer electrosteric stabilisation. This mechanism ensures colloidal stability even in the presence of 2.0 – 3.0 M ammonium sulfate, i.e. an ionic strength 3 – 5 times higher than that employed in the current study.

In an initial experiment, the RAFT aqueous dispersion polymerisation of NAM was conducted at 30°C in the presence of 0.60 M ammonium sulfate when targeting $PHEAC_{216}$-$PNAM_{3000}$ particles at 20% w/w solids. This reaction mixture was periodically sampled to enable the kinetics of the NAM polymerisation to be monitored via ^{1}H NMR spectroscopy. The resulting conversion vs. time curve (blue data points) indicated that 95% conversion was achieved within 2 h and essentially full conversion was obtained within 3-4 h (see **Figure 5.3a**). The corresponding semi-logarithmic plot (red data points) reveals a change in gradient at around 38 min, which signifies the onset of particle nucleation.[44–47] This occurs at approximately 42% NAM conversion, which corresponds to a mean PNAM DP of 1260. At this point, the unreacted NAM monomer diffuses into the nascent growing particles, which leads to a significantly faster rate of polymerisation. The change in gradient indicates an approximate 2.6-fold increase in the rate of polymerisation after nucleation. This is a more modest rate enhancement compared to that reported for other RAFT aqueous dispersion

polymerisation formulations.[44,48] The final reaction mixture is a free-flowing, low-viscosity, turbid dispersion of $PHEAC_{216}$-$PNAM_{3000}$ particles (see inset photograph in **Figure 5.3a**).

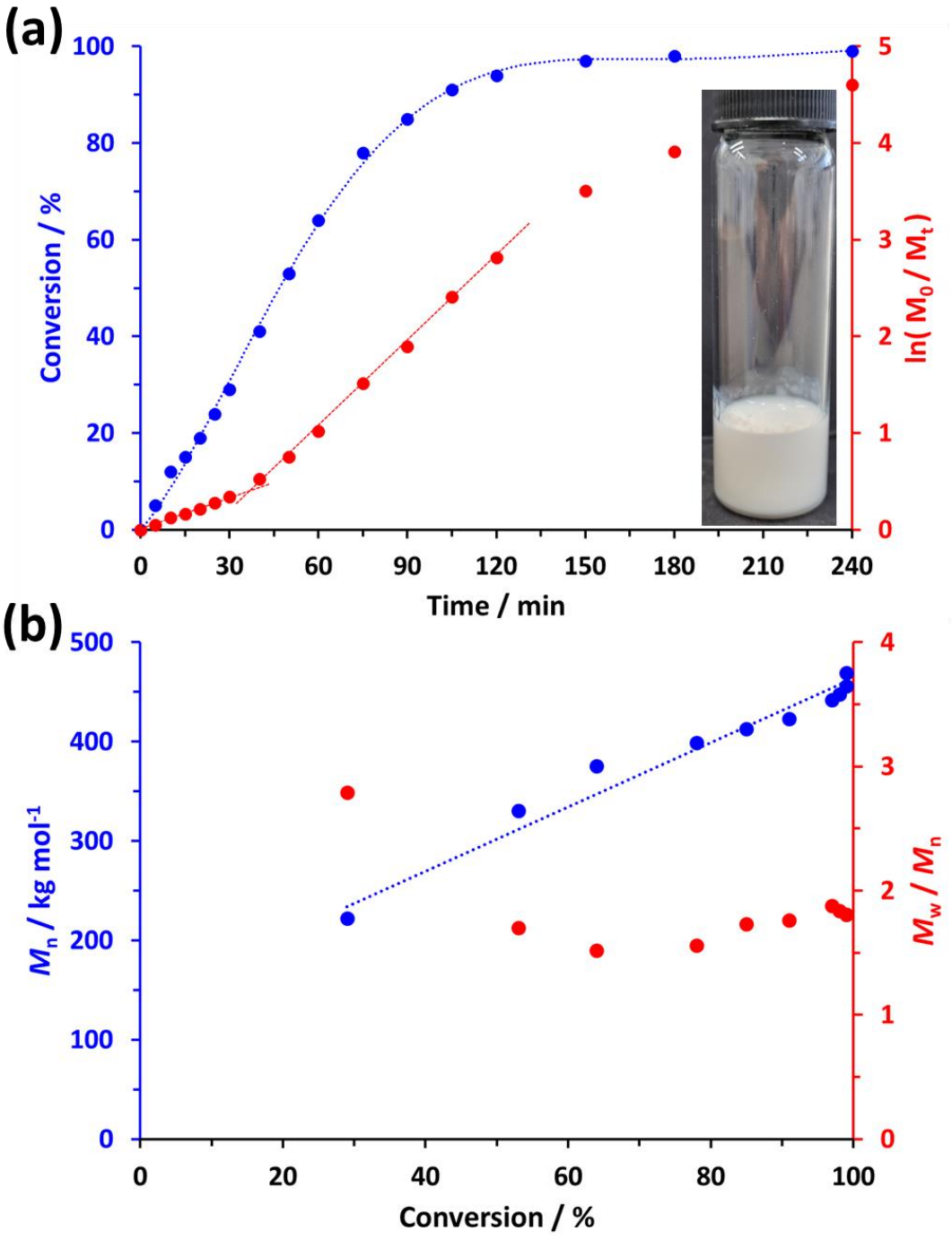

Figure 5.3 (a) Conversion vs. time curve and corresponding semi-logarithmic plot determined by ^{1}H NMR spectroscopy for the RAFT aqueous dispersion polymerisation of NAM at 30°C in the presence of 0.60 M ammonium sulfate when targeting $PHEAC_{216}$-$PNAM_{3000}$ particles at 20% w/w solids. (b) Evolution of M_n and M_w/M_n vs. conversion plot as determined by DMF GPC analysis.

Selected aliquots taken during the above kinetic experiments were subjected to DMF GPC analysis (see **Figure 5.3b**). A linear evolution in M_n was observed with increasing conversion, which is typically characteristic of a RAFT polymerisation. However, the M_w/M_n values are relatively high at around 1.8. This is not unexpected given the relatively low $PHEAC_{216}$/initiator molar ratio of 0.50 employed for these syntheses: this is sub-optimal for a well-controlled RAFT polymerisation but essential to ensure a high final monomer conversion when targeting PNAM DPs of up to 7000.[22,26,49–51] In contrast, a BM1433/initiator molar ratio of 10 was employed for the synthesis of the $PHEAC_{216}$ precursor, which had a relatively low dispersity (M_w/M_n = 1.27).[52–54] Subsequently, this precursor was employed to examine the effect of systematically varying the target DP from 1000 to 7000 for the salt-intolerant PNAM block (see **Table 5.2**).

NAM conversions ranged from 96% to more than 99% for all seven aqueous PISA syntheses, indicating an efficient polymerisation in each case. When targeting a PNAM DP of 1,000, a low-turbidity dispersion of relatively high-viscosity was obtained. In contrast, lower viscosity dispersions were obtained when targeting higher PNAM DPs. These observations are consistent with the kinetic data presented in **Figure 5.3a**, which suggests that a minimum PNAM DP of 1,260 is required for particle nucleation when targeting a PNAM DP of 3,000. On the other hand, DLS studies of the $PHEAC_{216}$-$PNAM_{1000}$ formulation indicate a z-average diameter of approximately 154 nm (see later), which indicates that nucleation has already occurred when targeting this somewhat shorter PNAM block.

PNAM DP (x)	Conversion / %	M_n [a] / kg mol^{-1}	GPC M_n [b] / kg mol^{-1}	M_w / M_n [b]	M_w [c] / kg mol^{-1}	R_g [c] / nm	c* [c] / mg mL^{-1}	D_z [d] / nm	PDI [d]
1000	> 99	166	117	1.92	357	–	–	154	0.01
2000	98	302	166	2.35	548	20.2	110	228	0.03
3000	99	444	226	2.26	837	33.3	38	276	0.06
4000	99	584	401	2.24	1235	49.2	17	377	0.09
5000	96	702	538	2.29	1452	55.4	14	460	0.11
6000	97	846	766	2.11	2091	66.1	12	485	0.07
7000 [e]	99	1002	855	2.21	Macroscopic precipitation			570	0.09

Table 5.2 Summary of monomer conversions, GPC and multi-angle laser light scattering (MALLS) molecular weight data and radius of gyration for a series of $PHEAC_{216}$-$PNAM_x$ diblock copolymer particles (x = 1,000 to 7,000) prepared by RAFT aqueous dispersion polymerisation of NAM in the presence of 0.60 M ammonium sulfate (pH 5.5) using a redox initiator at 30°C for at least 18 h (see **Scheme 5.1a** for further reaction conditions). (a) Calculated M_n corrected for the final NAM conversion, as determined by ^{1}H NMR spectroscopy (assuming 100% chain extension efficiency). (b) M_n and M_w/M_n values, as determined by DMF GPC. (c) The M_w, radius of gyration (R_g) and coil overlap concentration (c*) data are determined by MALLS. (d) D_z denotes z-average diameter and PDI denotes polydispersity index as determined by DLS. (e) A macroscopic precipitate was obtained for this formulation, rather than a colloidally stable aqueous dispersion. For this reason, SLS analysis was not performed.

However, in view of its relatively high viscosity, this $PHEAC_{216}$-$PNAM_{1000}$ dispersion most likely contains a fraction of soluble copolymer chains in addition to sterically stabilised particles. This is understandable given that NAM monomer is a good solvent for PNAM. Clearly, the critical PNAM DP required for nucleation depends on the target PNAM DP, no doubt because the latter parameter dictates how much unreacted NAM monomer is present at the onset of nucleation. Inspecting the penultimate column in **Table 5.2**, SLS studies (see **Figure 5.4** for the corresponding MALLS plots) indicate a monotonic increase in the weight-average molecular weight (M_w) for the $PHEAC_{216}$-$PNAM_{1000\text{-}6000}$ series.

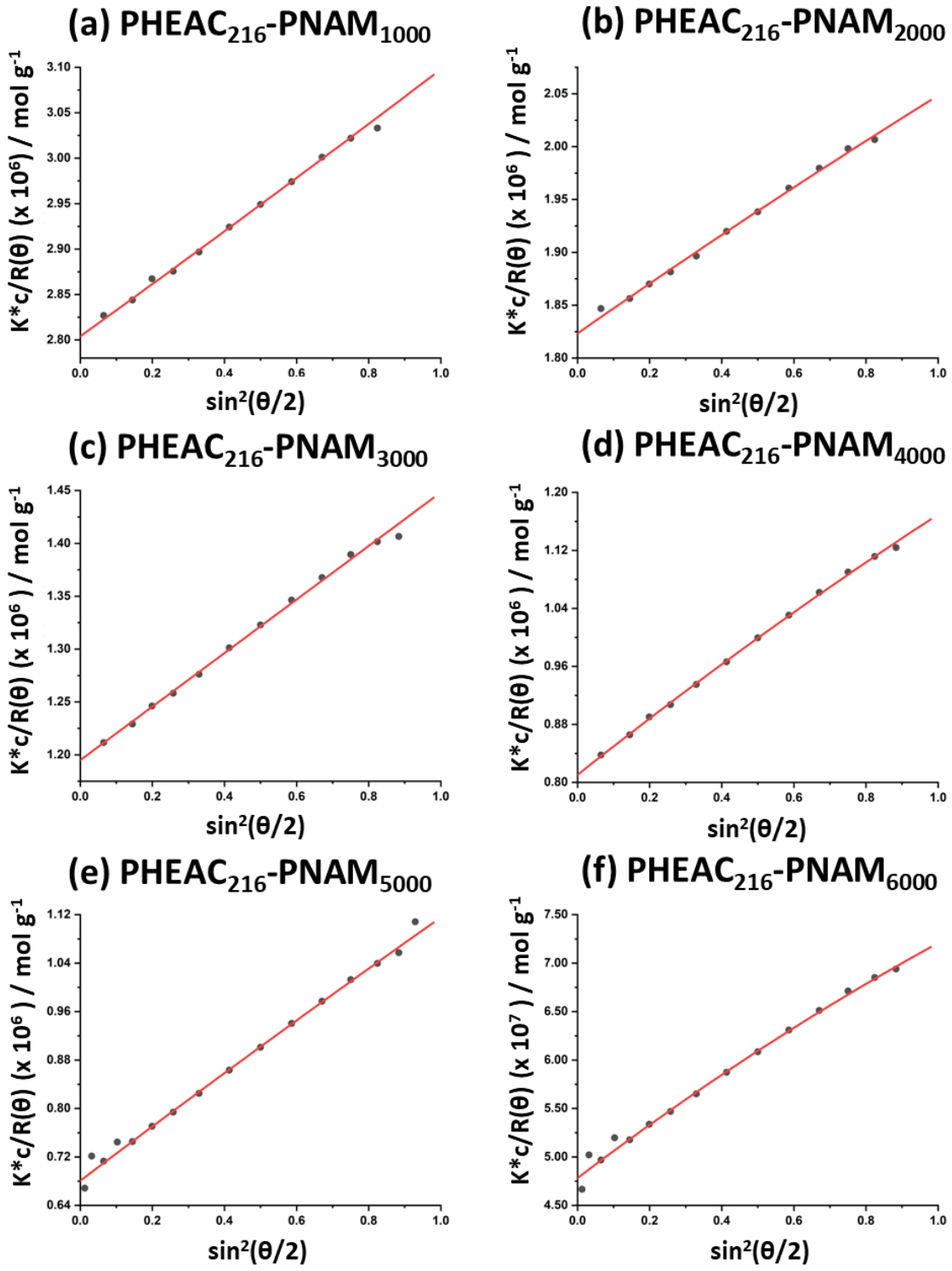

Figure 5.4 Static light scattering plots obtained using a MALLS-GPC detector to determine M_w values for six $PHEAC_{216}$-$PNAM_{1000\text{-}6000}$ diblock copolymers. Measurements were performed on dilute aqueous solutions in the presence of approximately 0.01 M ammonium sulfate.

The same technique also enables the mean radius of gyration (R_g) to be calculated for five of these six samples (the exception being for the lowest molecular weight copolymer, $PHEAC_{216}$-$PNAM_{1000}$). Finally, macroscopic precipitation is observed when targeting a PNAM DP of 7000, although a very high final monomer conversion is obtained even for this unsuccessful formulation. Thus a PNAM DP of 6000 appears to represent the effective upper limit for this new 'low salt' RAFT aqueous dispersion polymerisation, at least under the stated reaction conditions.

One advantage of targeting *non-ionic* diblock copolymers is that such compositions are amenable to GPC analysis in common organic solvents. Indeed, the PHEAC-PNAM diblock copolymers investigated herein are soluble in DMF, which is a widely used GPC eluent. Accordingly, DMF GPC curves for a series of $PHEAC_{216}$-$PNAM_x$ diblock copolymers are shown in **Figure 5.5**. Increasing the target DP for the salt-intolerant PNAM block from 1000 to 6000 produces a monotonic increase in M_n while the dispersity (M_w/M_n) remains essentially constant. The discrepancy between the theoretical M_n values and the GPC M_n data simply reflects the use of poly(methyl methacrylate) calibration standards for GPC studies. Such standards inevitably incur a systematic error when used for the analysis of $PHEAC_{216}$-$PNAM_{1000\text{-}6000}$ diblock copolymers. Importantly, all six MWD curves are unimodal and efficient chain extension of the $PHEAC_{216}$ precursor (see black curve) is achieved for each synthesis. This means that a well-defined diblock copolymer architecture is obtained in each case, although the dispersity of the PNAM block is undoubtedly high. This is not uncommon when targeting very high core-forming block DPs in PISA syntheses.[49,55,56] For the present formulation, this is exacerbated by the relatively low [BM1433]/[KPS] molar ratio of 0.50 used for these aqueous PISA syntheses. As mentioned above, RAFT agent/initiator molar ratios of 5-10 are typically required for well-controlled RAFT polymerisations,[52–54] although lower molar ratios of 0.5-3.3 are often utilised for PISA syntheses.[22,26,49–51] For the present system, a

significantly lower molar ratio (i.e. a higher initiator concentration) was essential to ensure high final monomer conversions when targeting such high PNAM DPs. This pragmatic choice inevitably leads to inferior RAFT control, as evidenced by the relatively broad molecular weight distributions observed in **Figure 5.5**. However, such high dispersities can be beneficial if such salt-sensitive diblock copolymers are to be employed as viscosity modifiers (see later). One reviewer of this work has suggested that our RAFT aqueous dispersion polymerisation formulations are likely to generate PNAM homopolymer, as well as the target diblock copolymer chains. We cannot discount this possibility but we note that such contamination would have no bearing on the intended application).

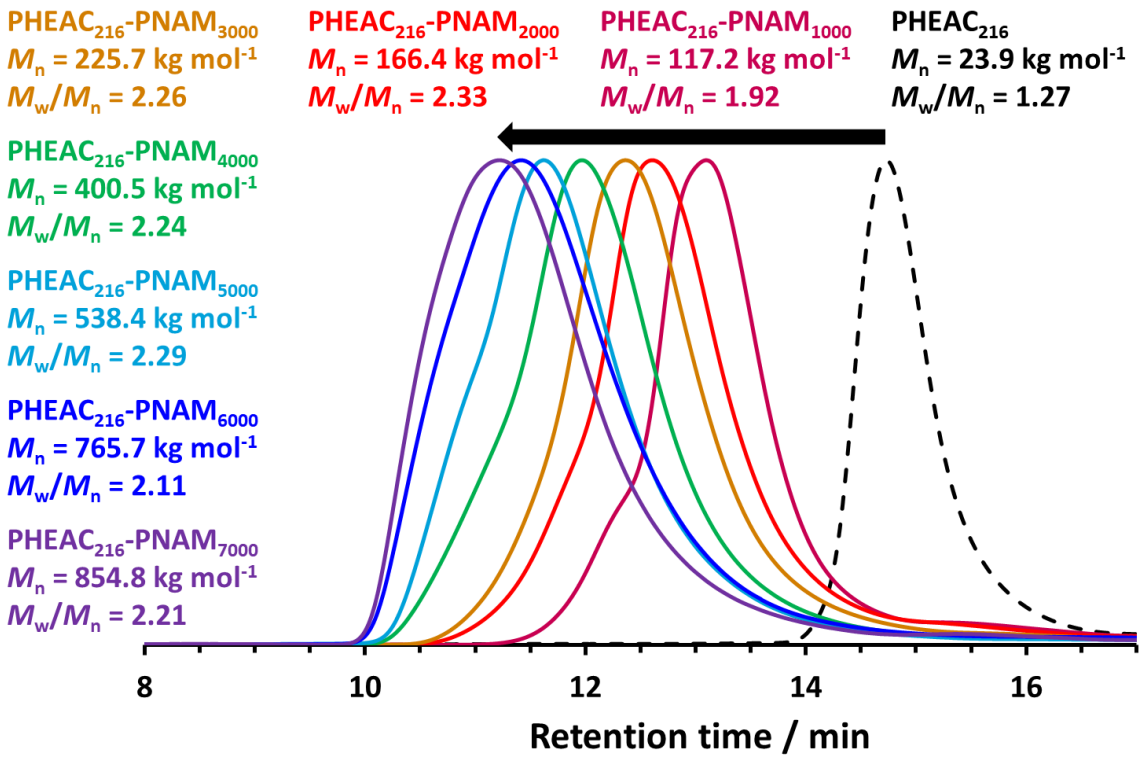

Figure 5.5 Normalised DMF GPC curves recorded for the $PHEAC_{216}$ precursor and a series of $PHEAC_{216}$-$PNAM_x$ diblock copolymers prepared by chain extension via RAFT aqueous dispersion polymerisation of NAM at 30°C in the presence of 0.60 M ammonium sulfate. M_n values are calculated relative to a series of near-monodisperse poly(methyl methacrylate) calibration standards.

A ^1H NMR spectrum recorded for $PHEAC_{216}$-$PNAM_{3000}$ particles (see lowest black spectrum) prepared in D_2O at 20% w/w solids in the presence of 0.60 M ammonium sulfate is

shown in **Figure 5.6**. This sample is then serially diluted to 15%, 10% and 5% w/w solids with D_2O and an NMR spectrum is recorded in each case. Visual inspection confirms that the initially turbid aqueous dispersion became completely transparent at either 10% or 5% w/w, indicating particle dissolution to afford molecularly dissolved copolymer chains. Notably, such transparent copolymer solutions are not coloured, which is consistent with the relatively low levels of RAFT agents required for such syntheses. To aid spectral assignments, NMR reference spectra are also recorded for a $PNAM_{500}$ homopolymer (red spectrum) and a $PHEAC_{216}$ homopolymer (blue spectrum) in the absence of salt. For the as-synthesised 20% w/w aqueous dispersion of $PHEAC_{216}$-$PNAM_{3000}$ particles, only a single broad signal at around 3.6 ppm is visible in the presence of 0.60 M ammonium sulfate, which is assigned to the relatively mobile pendent morpholine protons *e* and *f*. Under such conditions, the acrylamide backbone signals *g* and *h* are not detected. Nevertheless, this spectrum suggests partial (albeit low) hydration of the PNAM chains in the presence of 0.60 M ammonium sulfate. Dilution to 15% w/w using D_2O lowers this salt concentration to 0.45 M. Under such conditions, the *e* and *f* signals are slightly better resolved. Moreover, the backbone proton signals *g* and *h* are now just about discernible at around 1.6 and 2.6 ppm. However, further dilution to 10% w/w is sufficient to cause particle dissociation because the salt-intolerant PNAM block becomes water-soluble in the presence of 0.30 M ammonium sulfate. Now the PNAM proton signals are essentially indistinguishable from those of the $PNAM_{500}$ homopolymer dissolved in pure D_2O (compare the uppermost black spectrum with the red spectrum). These observations are consistent with the schematic cartoon shown in **Scheme 5.1b**. It is also worth mentioning that there is no evidence for the $PHEAC_{216}$ steric stabiliser in any of the four black spectra. However, this is understandable because this constitutes only a minor component of the overall diblock copolymer chains.

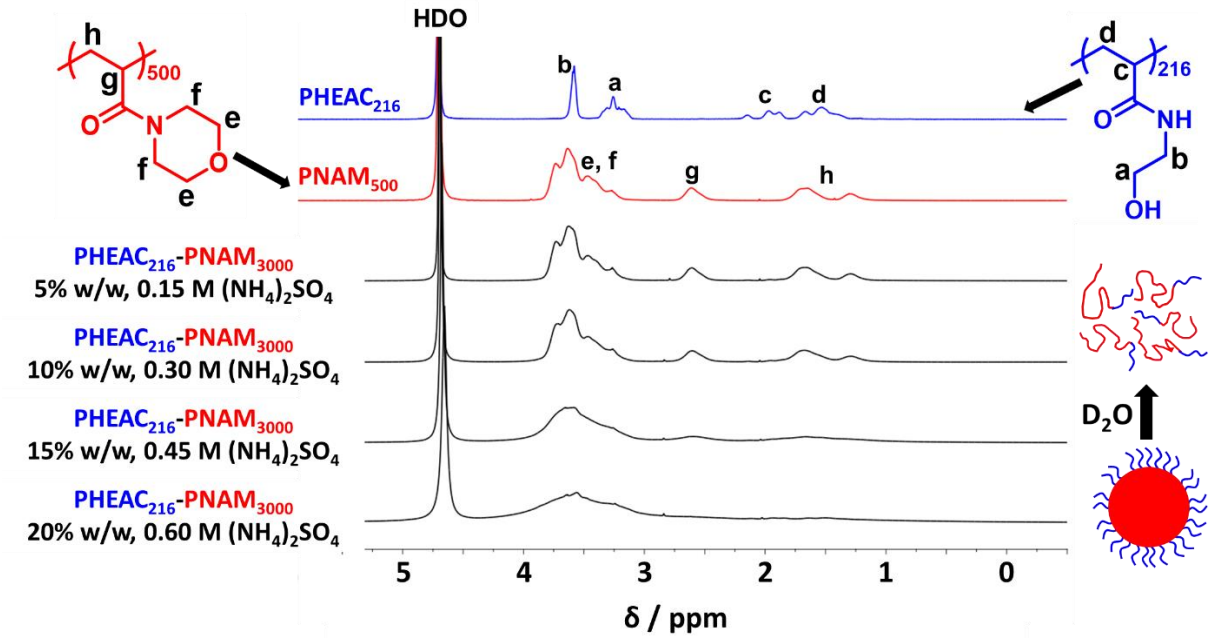

Figure 5.6 Partial ^{1}H NMR spectra (D_2O) recorded for a $PNAM_{500}$ (red spectrum) homopolymer and a $PHEAC_{216}$ (blue spectrum) homopolymer in the absence of salt, as well as $PHEAC_{216}$-$PNAM_{3000}$ diblock copolymer particles prepared in D_2O at 20% w/w solids in the presence of 0.60 M ammonium sulfate, see lowest black spectrum. When this 20% w/w $PHEAC_{216}$-$PNAM_{3000}$ dispersion is diluted with D_2O, both the background salt concentration and the corresponding copolymer concentration are systematically reduced (see other three black spectra).

TEM studies of the $PHEAC_{216}$-$PNAM_{6000}$ particles confirm the presence of spheres with a mean number-average diameter of 420 nm, see **Figure 5.7**. Given the highly asymmetric diblock composition, this suggests a kinetically-trapped copolymer morphology. This is no doubt because the relatively long PHEAC DP confers effective steric stabilisation, which is sufficient to prevent sphere-sphere fusion during the aqueous PISA synthesis.[57]

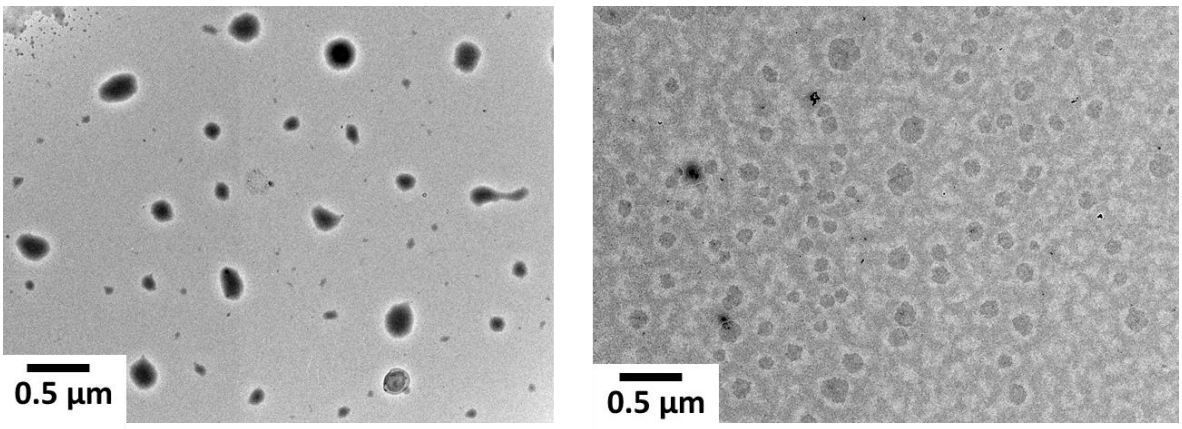

Figure 5.7 Representative TEM images recorded for $PHEAC_{216}$-$PNAM_{6000}$ particles.

DLS analysis of the six aqueous dispersions of $PHEAC_{216}$-$PNAM_{1000-6000}$ particles reveals relatively narrow particle size distributions with z-average diameters that increase monotonically with the PNAM DP. A log-log plot of this data set is shown in **Figure 5.8**.

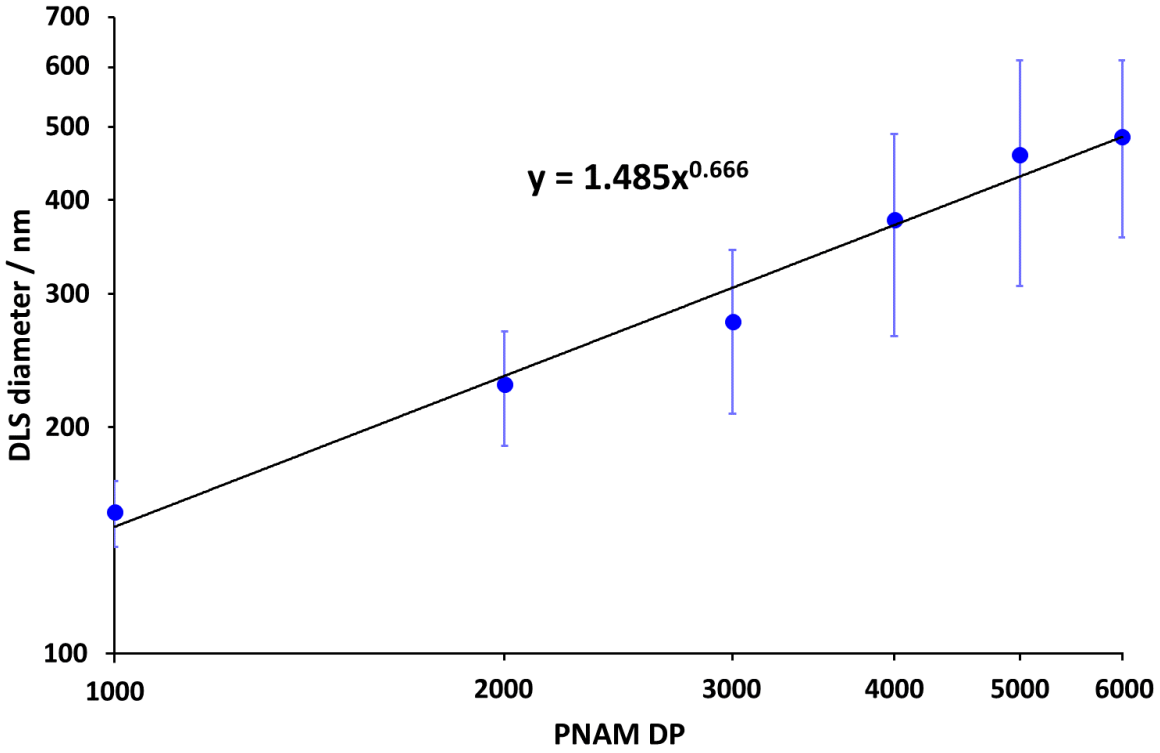

Figure 5.8 Relationship between the z-average diameter (reported by dynamic light scattering) and the mean degree of polymerisation (DP) of the core-forming PNAM block for a series of six $PHEAC_{216}$-$PNAM_x$ particles (x = 1000 to 6000) prepared via RAFT aqueous dispersion polymerisation of NAM at 30°C in the presence of 0.60 M ammonium sulfate (see **Table 5.1**). [N.B. The standard deviations indicate the width of each particle size distribution rather than the experimental uncertainty].

If targeting a longer core-forming block leads to larger particles, there must be a corresponding increase in the inter-separation distance between neighboring steric stabiliser chains within the coronal layer. Eventually, this must result in ineffective steric stabilisation, which accounts for the failure of the $PHEAC_{216}$-$PNAM_{7000}$ formulation (see **Table 5.2**). If the particles were fully dehydrated, the theoretical gradient for the linear plot shown in **Figure 5.8** should be 0.50.[57] However, this gradient is approximately 0.67, which suggests that the core-forming PNAM chains are partially hydrated in the presence of 0.60 M ammonium sulfate.[58–60] This observation is consistent with the ^{1}H NMR data discussed above. The six aqueous

PHEAC$_{216}$-PNAM$_{1000-6000}$ dispersions were also analysed using laser diffraction. This sizing technique reports comparable particle diameters to those obtained using DLS (see **Figure 5.9**).

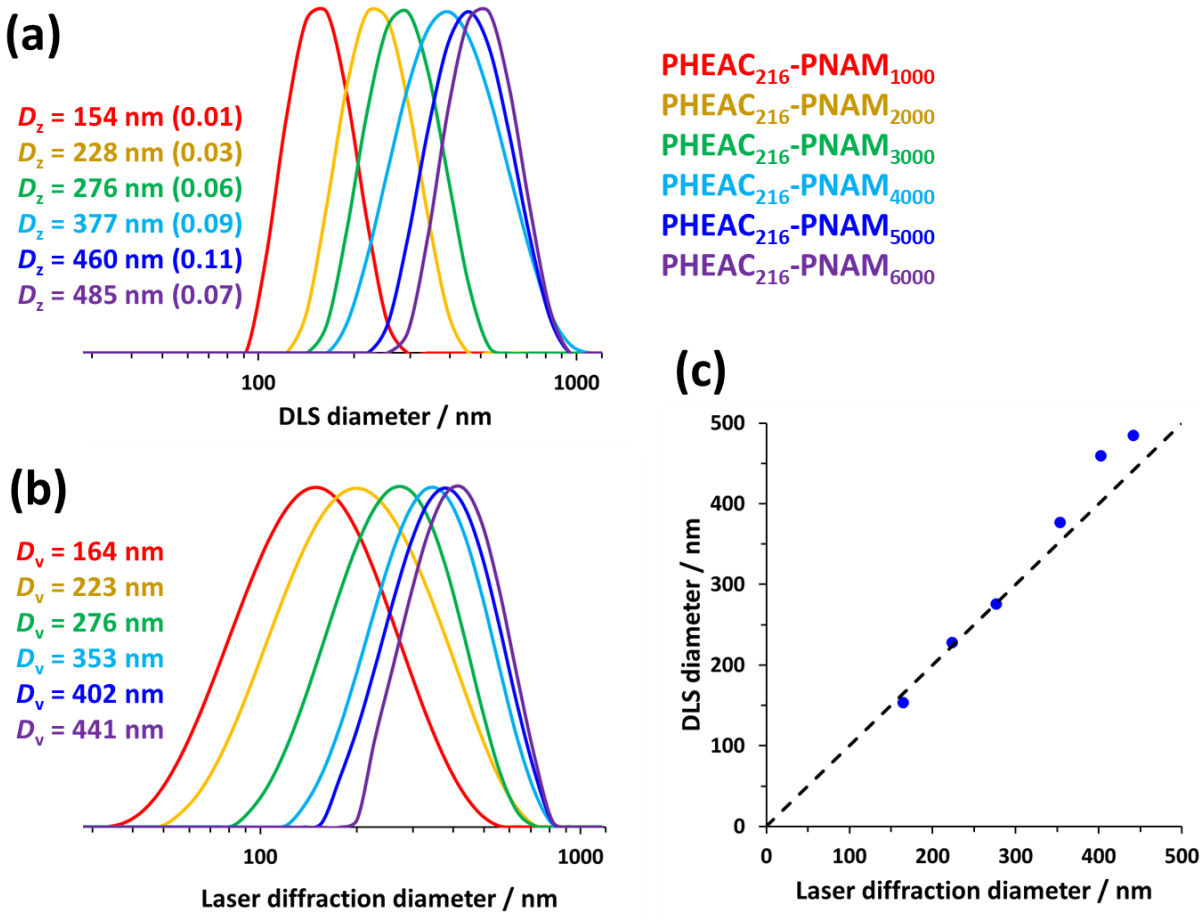

Figure 5.9 (a) DLS particle size distributions recorded for six aqueous dispersions of PHEAC$_{216}$-PNAM$_{1000-6000}$ particles (see **Table 5.2**). Hydrodynamic z-average diameter (D_z) and polydispersity data are indicated for each sample. (b) Laser diffraction particle size distributions recorded for the same six aqueous dispersions of PHEAC$_{216}$-PNAM$_{1000-6000}$ particles. Volume-average diameter (D_v) data are indicated for each sample. (c) Comparison of DLS with laser diffraction diameters. A line of unity is included for reference.

Given that DMF GPC analysis only affords relative molecular weight data, static light scattering (SLS) was used to determine absolute M_w values for the series of six PHEAC$_{216}$-PNAM$_{1000-6000}$ copolymers. First, differential refractometry studies indicate a dn/dc value of 0.17 for such copolymers. For the SLS measurements, an online multi-angle laser light scattering detector was employed in combination with an aqueous GPC instrument. SLS experiments in aqueous solution are usually considered to be rather difficult owing to the

ubiquitous presence of dust and/or air bubbles but fortunately the GPC columns act as an effective filtration system to minimise this problem.

Figure 5.10 shows the strikingly similar relationship between the absolute M_w data obtained from SLS studies and the apparent M_w values indicated by DMF GPC analysis (calculated by multiplying the M_n data shown in **Table 5.2** by the corresponding dispersity). The difference between these two data sets is attributed to the systematic error incurred when using poly(methyl methacrylate) standards as GPC calibrants for the $PHEAC_{216}$-$PNAM_{1000\text{-}6000}$ chains.

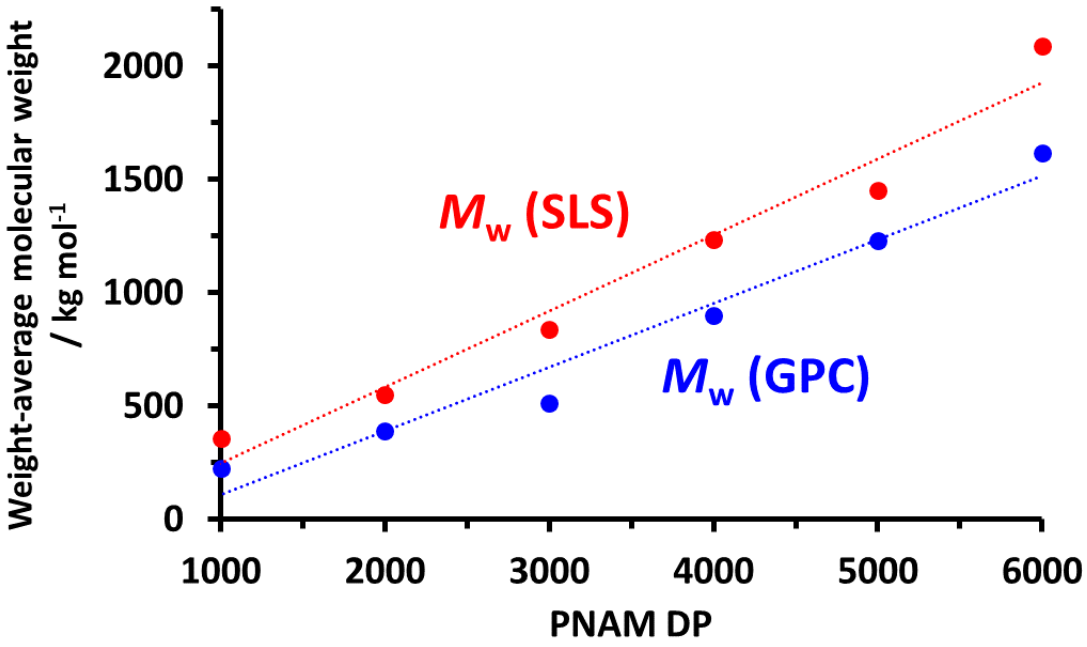

Figure 5.10 Relationship between the weight-average molecular weight (M_w) and the mean degree of polymerisation (DP) of the PNAM block for a series of six $PHEAC_{216}$-$PNAM_x$ diblock copolymers (x = 1,000 to 6,000) prepared via RAFT aqueous dispersion polymerisation of NAM at 30°C. The red data set was obtained by static light scattering studies whereas the blue data set was calculated by multiplying each M_n value obtained by DMF GPC (see **Table 5.2**) by the corresponding dispersity (M_w/M_n).

The relationship between the radius of gyration, R_g, and weight-average molecular weight, M_w, is presented in **Figure 5.11** (data in **Table 5.2**). The global chain behaviour follows a universal scaling law, $R_g \sim M^v$, where the Flory exponent, v, is related to the molecular weight, the solvent quality and the inherent flexibility of the copolymer chain.[61] Unperturbed flexible chains scale

as $R_g \sim M_w^{1/2}$, which is typical of a Gaussian conformation, In contrast, flexible chains in a good solvent follow self-avoiding walk statistics with $R_g \sim M_w^{3/5}$, while relatively stiff chains behave like rigid rods, for which $R_g \sim M_w$.[62]

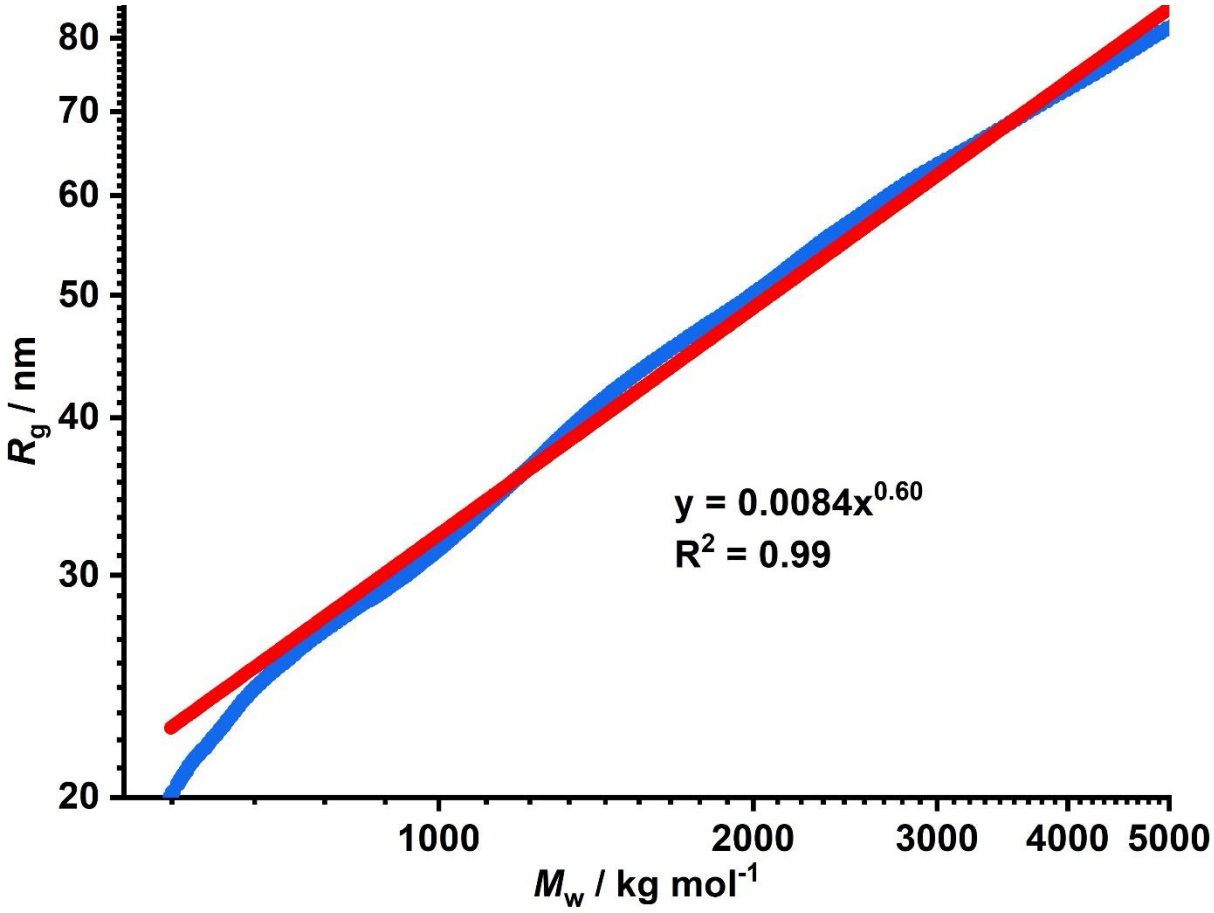

Figure 5.11 Relationship between the radius of gyration (R_g) and the weight-average molecular weight (M_w) obtained by GPC-SLS analysis of $PHEAC_{216}$-$PNAM_{1000}$, $PHEAC_{216}$-$PNAM_{3000}$ and $PHEAC_{216}$-$PNAM_{5000}$ diblock copolymers. These three copolymer MWDs overlap to provide a continuous relationship between M_w and R_g. The solid red line is a power law fit with an exponent of 0.60, indicating dilute copolymer coils in a good solvent. The downturn observed in the low M_w limit simply represents the SLS resolution limit.

The behaviour of semi-flexible chains can be described using the worm-like chain (WLC) model, also known as the Kratky-Porod model.[63] On sufficiently short length scales, semi-flexible chains behave as rigid rods. However, over longer length scales, entropic considerations ensure that the copolymer chains form coils. For the WLC model, R_g can be

expressed as a function of the contour length (molecular weight) and persistence length (intrinsic stiffness), according to the following relationship:[63]

$$R_g^2 = 2l_pL - 2l_p^2(1 - e^{-L/l_p}) \qquad \textbf{(1)}$$

where L is the contour length and l_p is the persistence length. A fit to the WLC model using the data set shown in **Figure 5.11** gives $L > R_g >> l_p \approx 0.7$ nm.

For each copolymer, we have calculated the coil overlap concentration (c*; shown in, where N_A is Avogadro's number:[64]

$$c^* \geq \frac{M_w}{N_A * {R_g}^3} \qquad \textbf{(2)}$$

The copolymer with the highest M_w ($PHEAC_{216}$-$PNAM_{6000}$) has c* = 12 g dm^{-3} (see **Table 5.2**). In a GPC measurement, the copolymer chains are fractionated according to their hydrodynamic volume, so the most concentrated solutions for SLS analysis were 0.60 g dm^{-3} (PNAM DP = 2,000) and 0.12 g dm^{-3} (PNAM DP = 6,000). Hence all SLS measurements were performed in the dilute solution regime. For a flexible copolymer chain in a good solvent, $R_g \sim M_w^{3/5}$. According to **Figure 5.11**, the Flory exponent, ν, is approximately 0.60, which confirms that the GPC eluent provides a good solvent environment for the $PHEAC_{216}$-$PNAM_x$ series.

A representative Zimm plot[65] constructed for the highest molecular weight diblock copolymer ($PHEAC_{216}$-$PNAM_{6000}$) is shown in **Figure 5.12**. The double extrapolation to zero copolymer concentration and zero scattering angle yields a common intercept at 3.920 x 10^{-7}, which corresponds to an M_w of 2.5 x 10^6 g mol^{-1}. This value is considered more accurate than the M_w of 2.09 x 10^6 g mol^{-1} indicated in **Table 5.2**, which is calculated from the static light scattering plot (see **Figure 5.4**). From the gradient for the zero-angle extrapolation, a second virial coefficient, A_2, of –4.8 x 10^{-5} cm^3 mol g^{-1} is calculated. This suggests that the aqueous pH 8 eluent must be fairly close to a good solvent for the PNAM chains at 25°C. This is

consistent with our observation of inverse temperature solubility behaviour for $PNAM_{500}$ homopolymer, which precipitates at only 32 – 36°C in the presence of 0.30 M ammonium sulfate but at more than 95°C in deionised water, as judged by turbidimetry studies (data not shown). Finally, the radius of gyration, R_g, for five of the six diblock copolymers listed in **Table 5.2** ($PHEAC_{216}$-$PNAM_{2000\text{-}6000}$) ranges from approximately 20 to 66 nm.

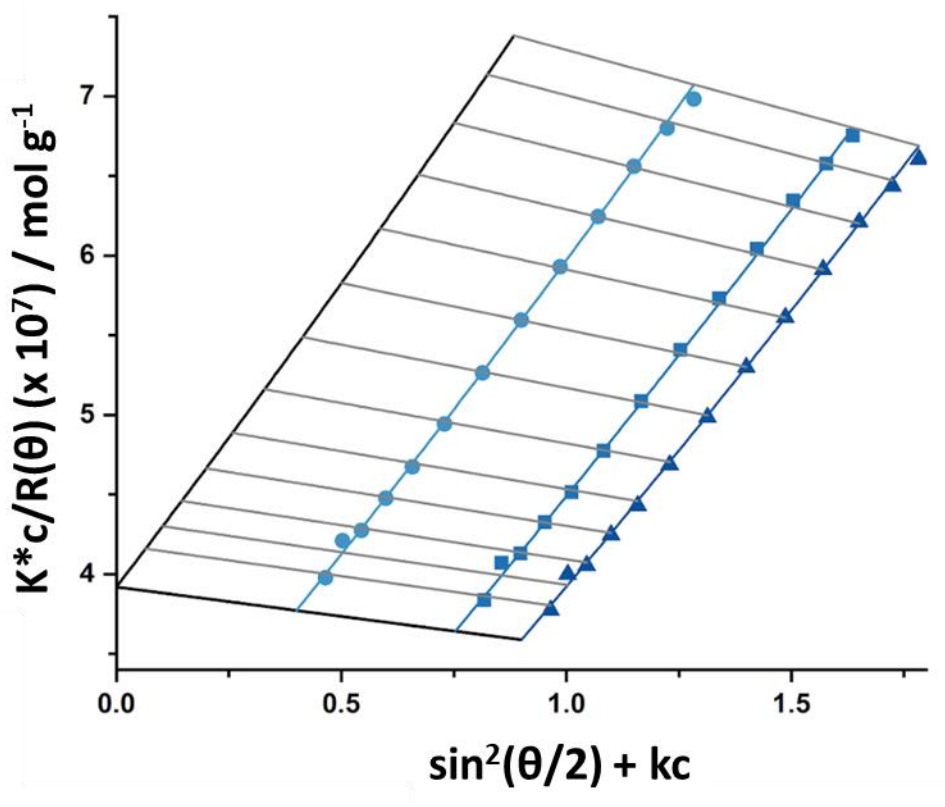

Figure 5.12 Zimm plot obtained by static light scattering analysis of $PHEAC_{216}$-$PNAM_{6000}$ diblock copolymer chains in aqueous solution (0.10 M $NaNO_3$, 0.02 M TEA and 0.05 M $NaHCO_3$ at pH 8). The common intercept at 3.920 x 10^{-7} indicates an M_w of 2.5 x 10^6 g mol^{-1}.

Two-fold dilution of each of the six turbid aqueous dispersions obtained from the successful PISA formulations summarised in **Table 5.2** using deionised water produces a transparent viscous solution comprising molecularly dissolved copolymer chains in each case.

A viscosity vs. shear rate plot recorded for the as-synthesised 20% w/w turbid aqueous dispersion comprising $PHEAC_{216}$-$PNAM_{6000}$ particles in the presence of 0.60 M ammonium sulfate confirms their shear-thinning nature, see **Figure 5.13**. Further rotational rheology

studies of the latter aqueous solutions affords the viscosity vs. shear rate data shown in **Figure 5.14**. Notably, each solution viscosity plateau observed at low shear (i.e. at shear rates of 0.05 to 5.0 s^{-1}) correlates closely with the PNAM chain length.

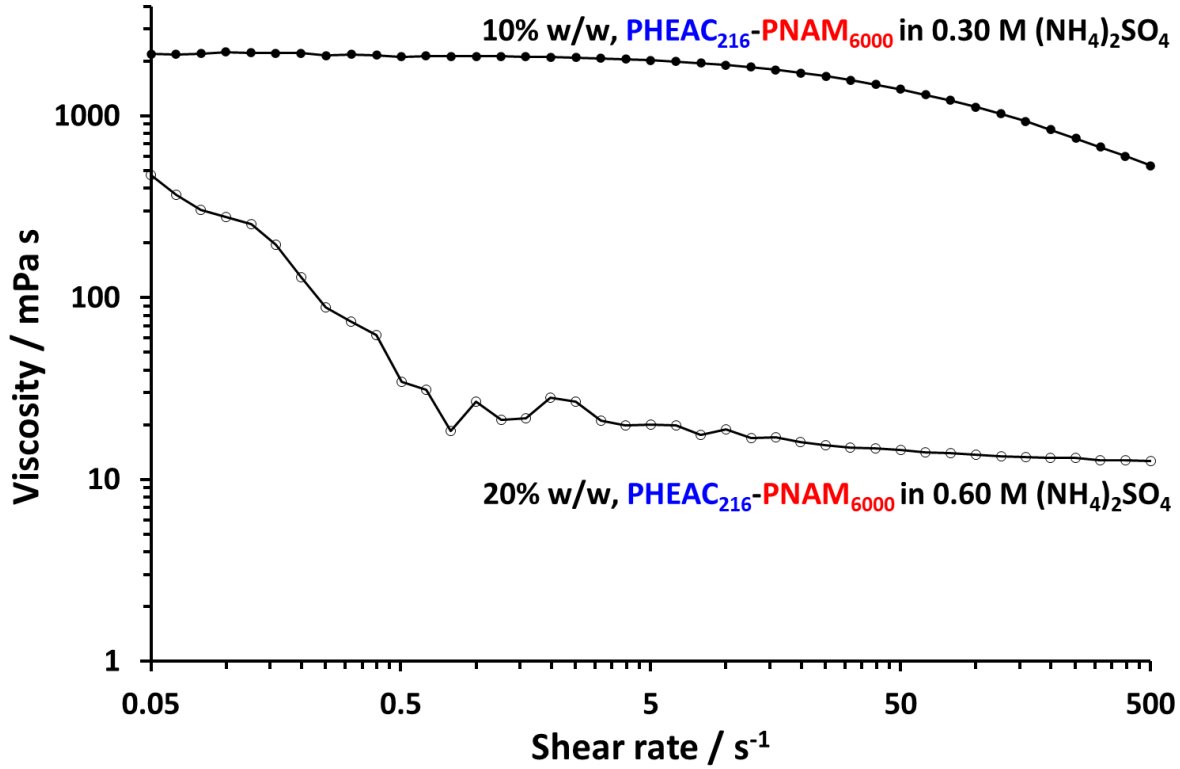

Figure 5.13 Viscosity vs. shear rate plot obtained by rotational rheology studies of a 20% w/w aqueous *dispersion* of $PHEAC_{216}$-$PNAM_{6000}$ particles in the presence of 0.60 M $(NH_4)_2SO_4$ compared to that for a 10% w/w aqueous *solution* of the same copolymer in the presence of 0.30 M ammonium sulfate (i.e. after a two-fold dilution using deionised water).

A two-fold dilution of each dispersion with deionised water produces a transparent viscous aqueous solution in each case owing to molecular dissolution of the diblock copolymer chains in the presence of 0.30 M ammonium sulfate (see **Scheme 5.1b**). Each copolymer *dispersion* behaves as a Newtonian fluid and exhibits a viscosity that is almost independent of shear rate (see **Figure 5.13** and **Figure 5.14**). In contrast, the corresponding copolymer *solutions* formed after two-fold dilution with water exhibit shear-thinning behaviour at high shear. For the dispersions, the torque sensitivity of the rheometer is poor at low shear rates, which produces rather noisy data. The 10% $PHEAC_{216}$-$PNAM_{6000}$ copolymer solution exhibits a zero-shear

plateau and shear-thinning behaviour under applied shear (see **Figure 5.13**). Under zero-shear conditions, the solution viscosity is approximately two orders of magnitude higher for the final molecularly-dissolved $PHEAC_{216}$-$PNAM_{6000}$ chains (≈ 2120 mPa s) compared to the initial aqueous dispersion of $PHEAC_{216}$-$PNAM_{6000}$ particles (≈ 20-35 mPa s). In principle, such dilution-triggered thickening could be useful for home and personal care product formulations. In this context, it is worth emphasising that the relatively high copolymer dispersities are beneficial because the solution viscosity depends on the viscosity-average molecular weight, M_v. Since this parameter correlates much more closely with M_w than M_n, the approximate two-fold increase in M_w achieved by using a relatively high initiator concentration compared to that of the RAFT agent leads to a corresponding increase in the dilution-triggered thickening effect.

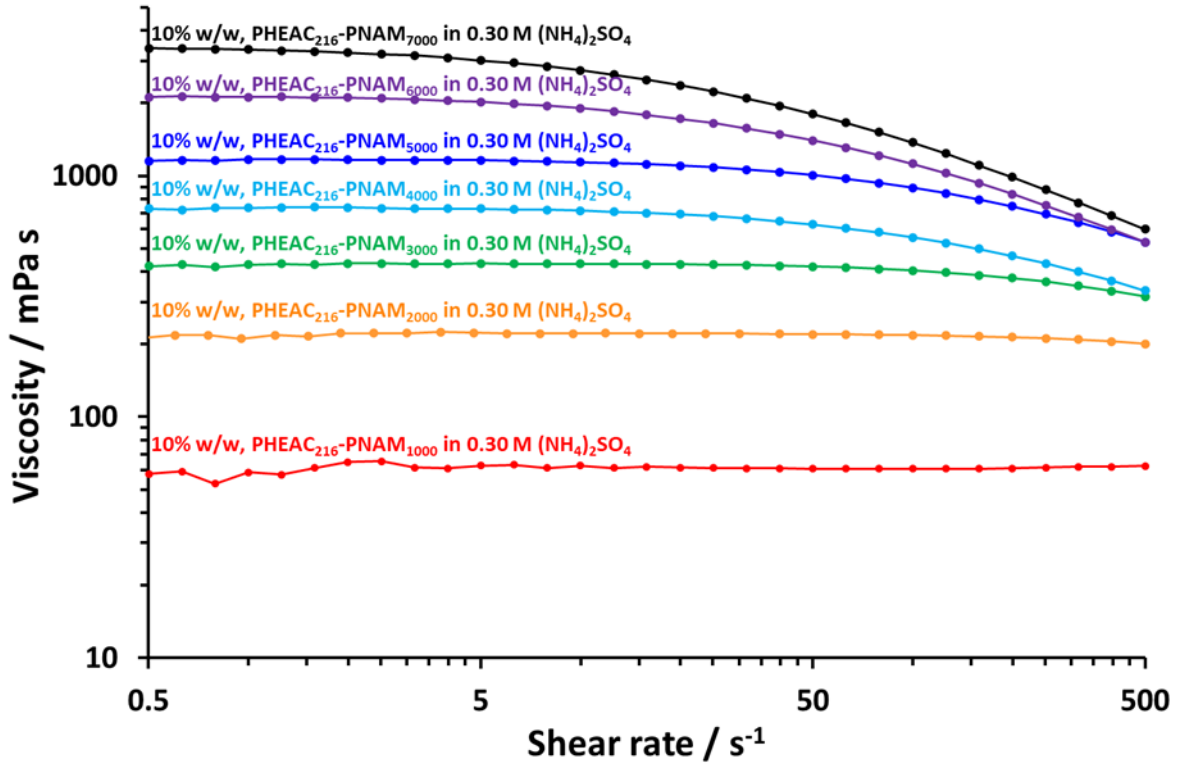

Figure 5.14 Viscosity vs. shear rate plots obtained by rotational rheology studies of 10% w/w aqueous *solutions* of molecularly-dissolved $PHEAC_{216}$-$PNAM_{1000\text{-}6000}$ chains in the presence of 0.30 M ammonium sulfate.

A water-soluble dicarboxylic acid-functionalised trithiocarbonate-based RAFT agent (BM1433) was selected for the aqueous PISA syntheses shown in **Table 5.2**. However, with

the benefit of hindsight, this RAFT agent is most likely present in its anionic carboxylate form under the reaction conditions summarised in **Scheme 5.1a** (i.e. at pH 5.5). According to the aqueous PISA literature, such terminal anionic charge can enhance the colloidal stability of the final diblock copolymer nanoparticles via an electrosteric stabilisation mechanism.[53,66,67] Moreover, literature precedent suggests that a higher chain extension efficiency and a lower final dispersity are usually obtained when employing a one-pot synthesis protocol, rather than when utilising a purified water-soluble precursor (e.g. $PHEAC_{216}$ in the present study).[68–70] Accordingly, we decided to explore the feasibility of conducting the one-pot synthesis of $PHEAC_{220}$-$PNAM_{6000}$ diblock copolymer particles using a *non-ionic* RAFT agent (MeBDMAT) under the reaction conditions shown in **Scheme 5.2**. The initial synthesis of the $PHEAC_{220}$ precursor was conducted at 70% w/w solids to enable the HEAC monomer to act as a co-solvent for the otherwise water-insoluble MeBDMAT reagent.

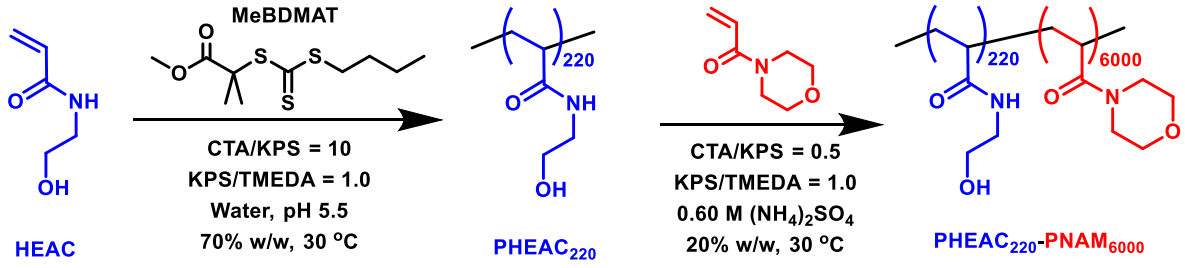

Scheme 5.2 One-pot synthesis of sterically-stabilised $PHEAC_{220}$-$PNAM_{6000}$ diblock copolymer particles via (i) RAFT aqueous solution polymerisation of HEAC at 30°C targeting $PHEAC_{220}$ at 70% w/w solids followed by (ii) RAFT aqueous dispersion polymerisation of NAM at 30°C targeting $PHEAC_{220}$-$PNAM_{6000}$ particles at 20% w/w solids.

Kinetic studies confirm that this first-stage polymerisation proceeds to around 90% conversion within 3.5 h at 30°C (see **Figure 5.15**). On subsequent addition of the NAM monomer, a turbid, free-flowing aqueous copolymer dispersion is obtained after a further 20 h at 30°C, with visual inspection indicating no signs of macroscopic precipitation. ^{1}H NMR spectroscopy studies confirmed a final comonomer conversion of more than 99% and DLS analysis of the as-synthesised particles indicated a z-average diameter of 460 nm (DLS polydispersity = 0.06), which is comparable to the z-average diameter of 485 nm (DLS

polydispersity = 0.07) reported for the $PHEAC_{216}$-$PNAM_{6000}$ particles prepared using the two-step protocol summarised in **Scheme 5.1a**. This suggests that the terminal anionic carboxylate group on the $PHEAC_{216}$ precursor has minimal effect on the colloidal stability, particle size and molecular weight distribution of the final diblock copolymer particles/chains. Moreover, this successful one-pot protocol augurs well for the potential scale-up of such 'low salt' aqueous PISA formulations.

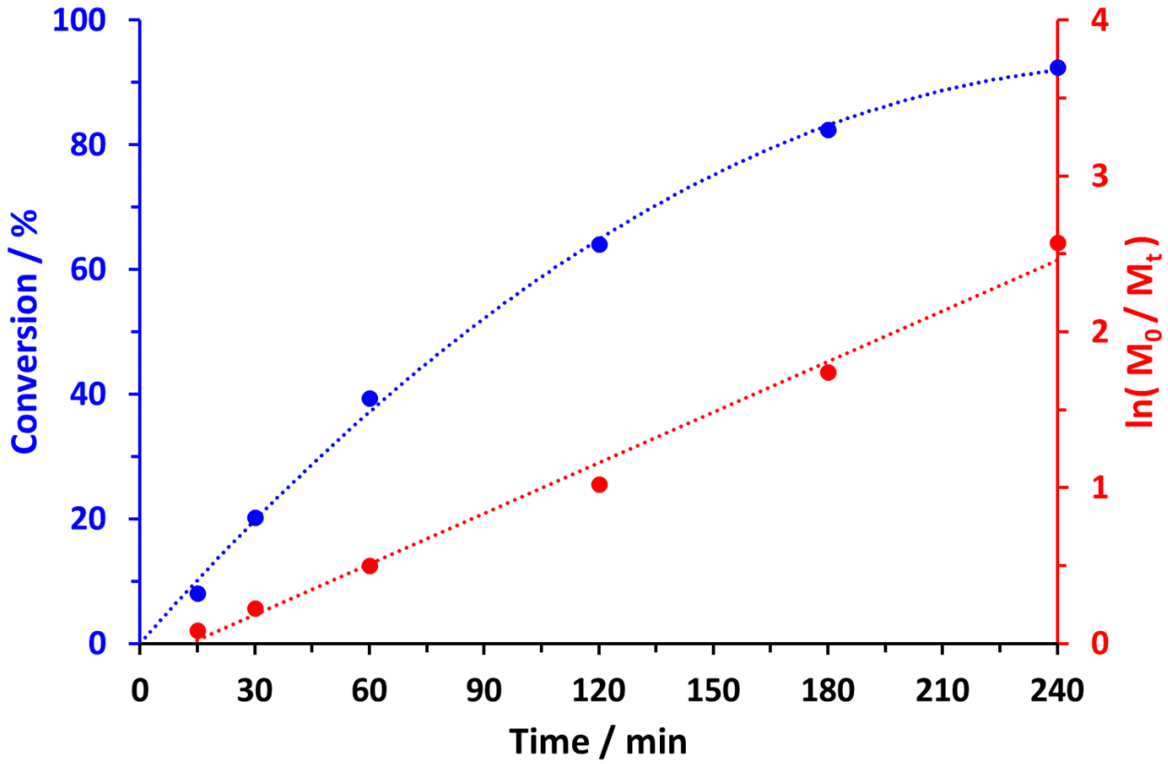

Figure 5.15 Conversion vs time curve obtained when targeting $PHEAC_{220}$ using MeBDMAT RAFT agent.

Three alternative steric stabilisers were also evaluated for the RAFT aqueous dispersion polymerisation of NAM conducted in the presence of 0.60 M ammonium sulfate. To complement the non-ionic salt-tolerant $PHEAC_{216}$ steric stabiliser, we evaluated a cationic polyelectrolyte ($PATAC_{242}$), an anionic polyelectrolyte ($PAMPS_{230}$) and a zwitterionic polyelectrolyte ($PMPC_{139}$), see **Scheme 5.3**. Each of these water-soluble polymers has been reported to exhibit salt-tolerant behaviour.[22,24,26,39,42] The target PNAM DP was 3,000 and ^{1}H

NMR spectroscopy studies of the final reaction mixture confirmed that more than 99% NAM conversion was obtained in each case.

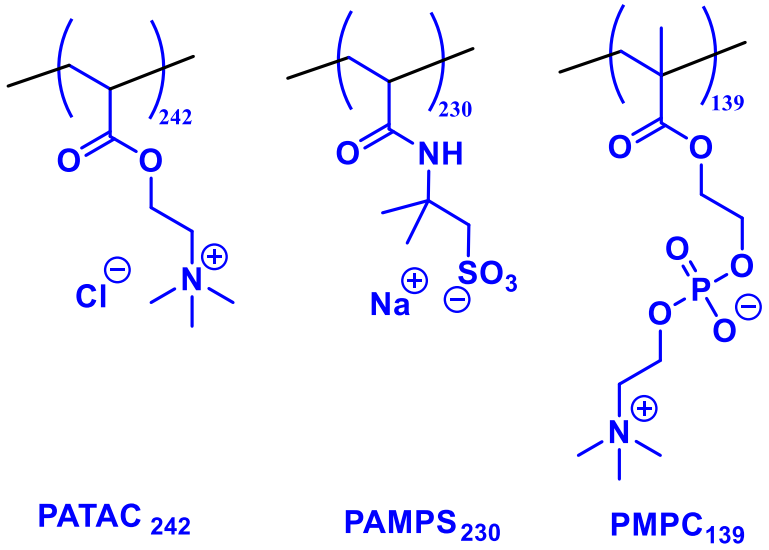

Scheme 5.3 Chemical structures of the cationic $PATAC_{242}$, anionic $PAMPS_{230}$ and zwitterionic $PMPC_{139}$ precursors used to stabilise PNAM-rich diblock copolymer particles prepared via RAFT aqueous dispersion polymerisation of NAM in 0.60 M $(NH_4)_2SO_4$.

As discussed in our previous publications, aqueous electrophoresis experiments cannot be performed in highly salty media using conventional commercial instruments.[24,71] Instead, we used a state-of-the-art instrument to determine the electrophoretic mobility for the $PHEAC_{216}$-$PNAM_{3000}$, $PATAC_{242}$-$PNAM_{3000}$, $PAMPS_{230}$-$PNAM_{3000}$ or $PMPC_{139}$-$PNAM_{3000}$ particles during the addition of known amounts of KOH in the presence of 0.60 M ammonium sulfate. The apparent pH of each aqueous copolymer dispersion was determined using an Ag/AgCl glass reference electrode without any compensation to offset the effect of the high ionic strength on the electrode response (although a temperature sensor within the electrode assembly did enable temperature compensation). Accordingly, zeta potentials calculated using the Smoluchowski model[72] are denoted as 'apparent zeta potentials'.

Apparent zeta potential data determined by electrophoretic light scattering (ELS) for the four aqueous copolymer dispersions as a function of added KOH are shown in **Figure 5.16**.

Data obtained for the $PHEAC_{216}$-$PNAM_{3000}$ particles prepared using the carboxylic acid-based RAFT agent are included, whereas the corresponding data obtained for $PHEAC_{216}$-$PNAM_{3000}$ particles prepared using a non-ionic RAFT agent are shown in **Figure 5.17**. Interestingly, there is no significant difference between these datasets. As expected, the characteristic electrophoretic footprint observed for each type of particle is dictated by the chemical nature of the steric stabiliser chains. Thus, the cationic $PATAC_{242}$-$PNAM_{3000}$ particles possess positive apparent zeta potentials of +19.4 ± 1.6 mV, whereas the anionic $PAMPS_{230}$-$PNAM_{3000}$ particles exhibit negative apparent zeta potentials of –32.2 ± 1.8 mV. Finally, the zwitterionic $PMPC_{139}$-$PNAM_{3000}$ particles and the non-ionic $PHEAC_{216}$-$PNAM_{3000}$ particles exhibit near-zero apparent zeta potentials of +1.6 ± 1.8 mV and –3.0 ± 1.7 mV, respectively. These observations are consistent with previous data reported by us for such steric stabilisers.[24]

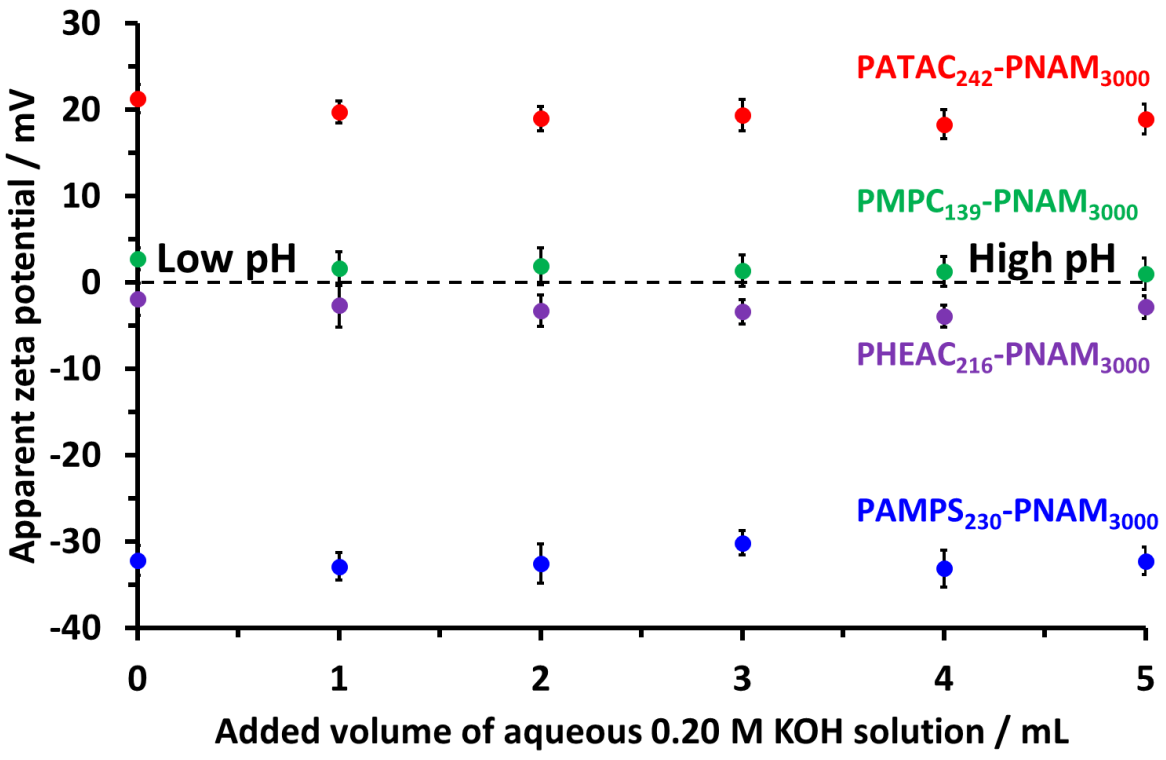

Figure 5.16 Apparent zeta potentials observed on addition of 0.20 M KOH to 0.1% w/w aqueous copolymer dispersions containing 0.6 M ammonium sulfate: $PHEAC_{216}$-$PNAM_{3000}$ (purple circles), $PATAC_{242}$-$PNAM_{3000}$ (red circles), $PAMPS_{230}$-$PNAM_{3000}$ (blue circles) and $PMPC_{139}$-$PNAM_{3000}$ (green circles). Standard deviations are indicated for each data point.

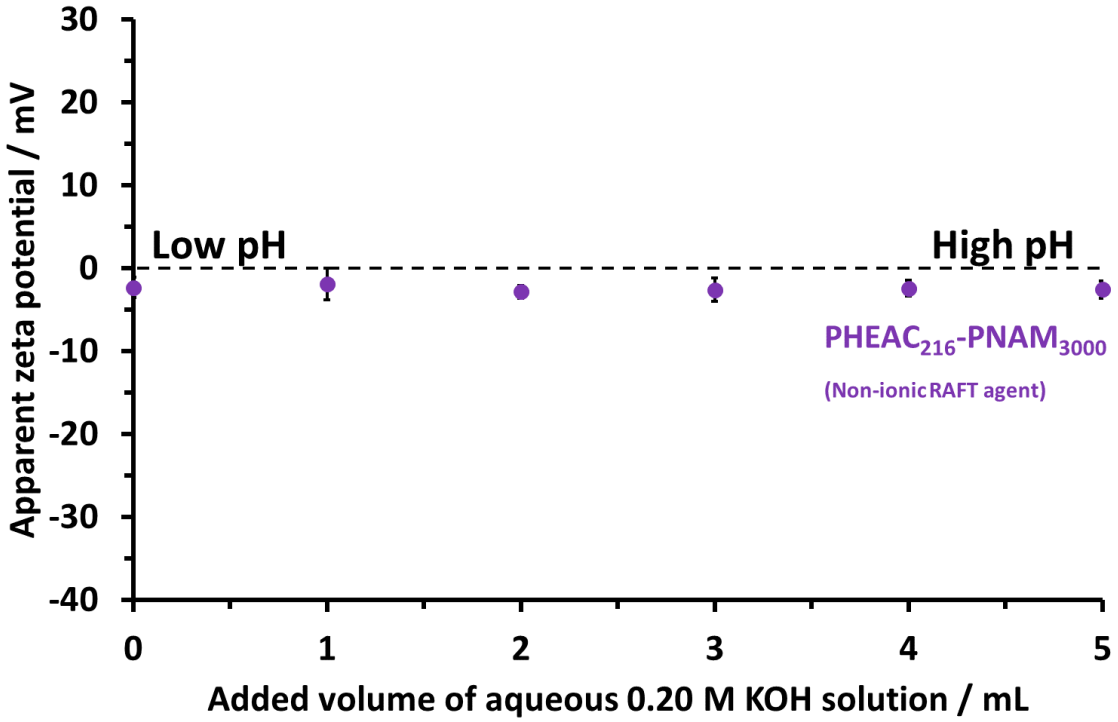

Figure 5.17 Apparent zeta potentials observed on addition of 0.20 M KOH to a 0.1% w/w aqueous dispersion of $PHEAC_{216}$-$PNAM_{3000}$ particles containing 0.6 M ammonium sulfate. Standard deviations are indicated for each data point.

5.4 Conclusions

The RAFT aqueous dispersion polymerisation of NAM is conducted using a water-soluble salt-tolerant PHEAC precursor in the presence of a relatively low level of added salt (0.60 M ammonium sulfate) to produce a colloidal dispersion of sterically-stabilised particles comprising wholly non-ionic diblock copolymer chains at 20% w/w solids.

Kinetic studies confirm that relatively high NAM conversions (94-99%) can be achieved within 2 h at 30°C. DMF GPC studies indicate relatively efficient chain extension of the PHEAC precursor but relatively broad molecular weight distributions (M_w/M_n > 1.92) for the final diblock copolymer chains. Systematic variation of the target DP of the salt-intolerant PNAM block leads to a progressive increase in the mean particle diameter as judged by dynamic light scattering and laser diffraction. Static light scattering (Zimm plot) indicates that M_w values of up to 2.5 x 10^6 g mol^{-1} can be obtained using this aqueous PISA formulation.

^{1}H NMR spectroscopy studies confirm that a two-fold dilution of an aqueous dispersion of such diblock copolymer particles using deionised water leads to their molecular dissolution. Rotational rheology studies indicate that the ensuing dilution-triggered thickening increases the solution viscosity by up to two orders of magnitude, which may be sufficient to offer potential commercial applications. Importantly, such high molecular weight copolymers contain minimal amounts of RAFT chain-ends: an as-synthesised 20% w/w aqueous dispersion of PHEAC$_{216}$-PNAM$_{6000}$ particles contains just 23 ppm sulfur, which is reduced to just 11.5 ppm sulfur for the final dilution-thickened aqueous solution.

5.5 References

1 M. Kikuchi, Y. Terayama, T. Ishikawa, T. Hoshino, M. Kobayashi, H. Ogawa, H. Masunaga, J. I. Koike, M. Horigome, K. Ishihara and A. Takahara, 'Chain dimension of polyampholytes in solution and immobilized brush states', *Polym. J.*, 2012, **44**, 121–130.

2 V. Bütün, N. C. Billingham and S. P. Armes, 'Unusual aggregation behavior of a novel tertiary amine methacrylate- based diblock copolymer: Formation of Micelles and reverse Micelles in aqueous solution [12]', *J. Am. Chem. Soc.*, 1998, **120**, 11818–11819.

3 V. Bütün, A. Atay, C. Tuncer and Y. Baş, 'Novel multiresponsive microgels: Synthesis and characterization studies', *Langmuir*, 2011, **27**, 12657–12665.

4 Y. Samav, B. Akpinar, G. Kocak and V. Bütün, 'Preparation of Responsive Zwitterionic Diblock Copolymers Containing Phosphate and Phosphonate Groups', *Macromol. Res.*, 2020, **28**, 1134–1141.

5 F. D'Agosto, R. Hughes, M.-T. Charreyre, C. Pichot and R. G. Gilbert, 'Molecular Weight and Functional End Group Control by RAFT Polymerization of a Bisubstituted Acrylamide Derivative', *Macromolecules*, 2003, **36**, 621–629.

6 A. Favier, C. Ladavière, M.-T. Charreyre and C. Pichot, 'MALDI-TOF MS Investigation of the RAFT Polymerization of a Water-Soluble Acrylamide Derivative', *Macromolecules*, 2004, **37**, 2026–2034.

7 C. Chamignon, D. Duret, M. Charreyre and A. Favier, '1 H DOSY NMR Determination of the Molecular Weight and the Solution Properties of Poly(N -acryloylmorpholine) in Various Solvents', *Macromol. Chem. Phys.*, 2016, **217**, 2286–2293.

8 J. Lesagedelahaye, X. Zhang, I. Chaduc, F. Brunel, M. Lansalot and F. D'Agosto, 'The Effect of Hydrophile Topology in RAFT-Mediated Polymerization-Induced Self-Assembly', *Angew. Chemie - Int. Ed.*, 2016, **55**, 3739–3743.

9 I. Chaduc, E. Reynaud, L. Dumas, L. Albertin, F. D'Agosto and M. Lansalot, 'From well-defined poly(N -acryloylmorpholine)-stabilized nanospheres to uniform mannuronan- and guluronan-decorated nanoparticles by RAFT polymerization-induced self-assembly', *Polymer*, 2016, **106**, 218–228.

10 R. Takahashi, S. Miwa, F. H. Sobotta, J. H. Lee, S. Fujii, N. Ohta, J. C. Brendel and K. Sakurai,

'Unraveling the kinetics of the structural development during polymerization-induced self-assembly: Decoupling the polymerization and the micelle structure', *Polym. Chem.*, 2020, **11**, 1514–1524.

11 P. Galanopoulo, N. Gil, D. Gigmes, C. Lefay, Y. Guillaneuf, M. Lages, J. Nicolas, F. D'Agosto and M. Lansalot, 'RAFT-Mediated Emulsion Polymerization-Induced Self-Assembly for the Synthesis of Core-Degradable Waterborne Particles', *Angew. Chemie Int. Ed.*, 2023, **62**, e202302093.

12 Y. S. Jo, A. J. van der Vlies, J. Gantz, T. N. Thacher, S. Antonijevic, S. Cavadini, D. Demurtas, N. Stergiopulos and J. A. Hubbell, 'Micelles for Delivery of Nitric Oxide', *J. Am. Chem. Soc.*, 2009, **131**, 14413–14418.

13 J. Morgenstern, G. Gil Alvaradejo, N. Bluthardt, A. Beloqui, G. Delaittre and J. Hubbuch, 'Impact of Polymer Bioconjugation on Protein Stability and Activity Investigated with Discrete Conjugates: Alternatives to PEGylation', *Biomacromolecules*, 2018, **19**, 4250–4262.

14 H. Takahashi, M. Nakayama, K. Itoga, M. Yamato and T. Okano, 'Micropatterned Thermoresponsive Polymer Brush Surfaces for Fabricating Cell Sheets with Well-Controlled Orientational Structures', *Biomacromolecules*, 2011, **12**, 1414–1418.

15 E. Read, A. Guinaudeau, D. J. Wilson, A. Cadix, F. Violleau and M. Destarac, 'Low temperature RAFT/MADIX gel polymerisation: Access to controlled ultra-high molar mass polyacrylamides', *Polym. Chem.*, 2014, **5**, 2202–2207.

16 R. Li and Z. An, 'Achieving Ultrahigh Molecular Weights with Diverse Architectures for Unconjugated Monomers through Oxygen-Tolerant Photoenzymatic RAFT Polymerization', *Angew. Chemie - Int. Ed.*, 2020, **59**, 22258–22264.

17 Z. An, '100th Anniversary of Macromolecular Science Viewpoint: Achieving Ultrahigh Molecular Weights with Reversible Deactivation Radical Polymerization', *ACS Macro Lett.*, 2020, **9**, 350–357.

18 Q. Ma, G. G. Qiao and Z. An, 'Visible Light Photoiniferter Polymerization for Dispersity Control in High Molecular Weight Polymers', *Angew. Chemie - Int. Ed.*, 2023, e202314729.

19 R. N. Carmean, T. E. Becker, M. B. Sims and B. S. Sumerlin, 'Ultra-High Molecular Weights via Aqueous Reversible-Deactivation Radical Polymerization', *Chem*, 2017, **2**, 93–101.

20 R. N. Carmean, M. B. Sims, C. A. Figg, P. J. Hurst, J. P. Patterson and B. S. Sumerlin, 'Ultrahigh Molecular Weight Hydrophobic Acrylic and Styrenic Polymers through Organic-Phase Photoiniferter-Mediated Polymerization', *ACS Macro Lett.*, 2020, **9**, 613–618.

21 R. A. Olson, M. E. Lott, J. B. Garrison, C. L. G. Davidson, L. Trachsel, D. I. Pedro, W. G. Sawyer and B. S. Sumerlin, 'Inverse Miniemulsion Photoiniferter Polymerization for the Synthesis of Ultrahigh Molecular Weight Polymers', *Macromolecules*, 2022, **55**, 8451–8460.

22 B. Huang, J. Jiang, M. Kang, P. Liu, H. Sun, B. G. Li and W. J. Wang, 'Synthesis of block cationic polyacrylamide precursors using an aqueous RAFT dispersion polymerization', *RSC Adv.*, 2019, **9**, 12370–12383.

23 Y. Zhang, X. Li, X. Ma, S. Bai, J. Zhang and R. Guo, 'Critical phase separation concentration of acrylamide and 2-acrylamido-2-methylpropanesulfonate copolymers in ammonium sulfate aqueous solution and its influence factors', *Colloids Surfaces A Physicochem. Eng. Asp.*, 2020, **590**, 124485.

24 R. J. McBride, J. F. Miller, A. Blanazs, H. J. Hähnle and S. P. Armes, 'Synthesis of High Molecular Weight Water-Soluble Polymers as Low-Viscosity Latex Particles by RAFT Aqueous Dispersion

Polymerization in Highly Salty Media', *Macromolecules*, 2022, **55**, 7380–7391.

25 D. F. Bagster, in *Processing of Solid–Liquid Suspensions*, ed. P. Ayazi Shamlou, Butterworth-Heinemann, Online edn, 1993, pp. 26–58.

26 S. Bai, Y. Wang, B. Liu, Y. Zhu and R. Guo, 'Dispersion copolymerization of acrylamide and sodium 2-acrylamido-2-methylpropanesulfonate in aqueous salt solution stabilized with a macro-RAFT agent', *Colloids Surfaces A Physicochem. Eng. Asp.*, 2018, **553**, 446–455.

27 R. Weast, *CRC Handbook of Chemistry and Physics*, CRC Press, Boca Raton, Florida, 66th edn., 1985.

28 J. F. Miller, K. Schätzel and B. Vincent, 'The determination of very small electrophoretic mobilities in polar and nonpolar colloidal dispersions using phase analysis light scattering', *J. Colloid Interface Sci.*, 1991, **143**, 532–554.

29 E. E. Uzgiris, 'Laser Doppler methods in electrophoresis', *Prog. Surf. Sci.*, 1981, **10**, 53–164.

30 A. M. Feltham and M. Spiro, 'Platinized platinum electrodes', *Chem. Rev.*, 1971, **71**, 177–193.

31 J. T. Lai, D. Filla and R. Shea, 'Functional Polymers from Novel Carboxyl-Terminated Trithiocarbonates as Highly Efficient RAFT Agents', *Macromolecules*, 2002, **35**, 6754–6756.

32 C. Bray, R. Peltier, H. Kim, A. Mastrangelo and S. Perrier, 'Anionic multiblock core cross-linked star copolymers: via RAFT polymerization', *Polym. Chem.*, 2017, **8**, 5513–5524.

33 V. Bütün, S. P. Armes, N. C. Billingham, Z. Tuzar, A. Rankin, J. Eastoe and R. K. Heenan, 'The Remarkable "Flip−Flop" Self-Assembly of a Diblock Copolymer in Aqueous Solution', *Macromolecules*, 2001, **34**, 1503–1511.

34 D. Ulker, C. Tuncer, S. B. Sezgin, Y. Toptas, A. Cabuk and V. Bütün, 'An antibacterial composite system based on multi-responsive microgels hosting monodisperse gold nanoparticles', *J. Polym. Res.*, 2017, **24**, 169.

35 T. Lü, X. Liu, D. Qi and H. Zhao, 'Effect of hydrophobic monomer on the aqueous dispersion polymerization of acrylamide with quaternary ammonium cationic monomer', *Iran. Polym. J.*, 2015, **24**, 219–227.

36 C. Zheng and Z. Huang, 'Preparation and Properties of Branched Copolymer P(AM-AA-MACA-EAMA) Using Water in Water Emulsion Polymerization in Aqueous Salt Solution', *J. Dispers. Sci. Technol.*, 2016, **37**, 1132–1139.

37 J. Zhu, G. Zhang and J. Li, 'Preparation of amphoteric polyacrylamide flocculant and its application in the treatment of tannery wastewater', *J. Appl. Polym. Sci.*, 2011, **120**, 518–523.

38 Y. M. Wu, Y. P. Wang, Y. Q. Yu, J. Xu and Q. F. Chen, 'Dispersion polymerization of acrylamide with 2-acrylamido-2-methyl-1- propane sulfonate in aqueous solution', *J. Appl. Polym. Sci.*, 2006, **102**, 2379–2385.

39 X. Liu, D. Chen, Y. Yue, W. Zhang and P. Wang, 'Dispersion copolymerization of acrylamide with acrylic acid in an aqueous solution of ammonium sulfate: Synthesis and characterization', *J. Appl. Polym. Sci.*, 2006, **102**, 3685–3690.

40 D. Chen, X. Liu, Y. Yue, W. Zhang and P. Wang, 'Dispersion copolymerization of acrylamide with quaternary ammonium cationic monomer in aqueous salts solution', *Eur. Polym. J.*, 2006, **42**, 1284–1297.

41 X. Liu, S. Xiang, Y. Yue, X. Su, W. Zhang, C. Song and P. Wang, 'Preparation of poly(acrylamide-co-acrylic acid) aqueous latex dispersions using anionic polyelectrolyte as stabilizer', *Colloids Surfaces A*

Physicochem. Eng. Asp., 2007, **311**, 131–139.

42 J. Lu, B. Peng, M. Li, M. Lin and Z. Dong, 'Dispersion polymerization of anionic polyacrylamide in an aqueous salt medium', *Pet. Sci.*, 2010, **7**, 410–415.

43 H. Park, S. Lim, J. Yang, C. Kwak, J. Kim, J. Kim, S. S. Choi, C. Bin Kim and J. Lee, 'A Systematic Investigation on the Properties of Silica Nanoparticles "Multipoint"-Grafted with Poly(2-acrylamido-2-methylpropanesulfonate- co -acrylic Acid) in Extreme Salinity Brines and Brine–Oil Interfaces', *Langmuir*, 2020, **36**, 3174–3183.

44 A. Blanazs, J. Madsen, G. Battaglia, A. J. Ryan and S. P. Armes, 'Mechanistic insights for block copolymer morphologies: How do worms form vesicles?', *J. Am. Chem. Soc.*, 2011, **133**, 16581–16587.

45 F. L. Hatton, M. J. Derry and S. P. Armes, 'Rational synthesis of epoxy-functional spheres, worms and vesicles by RAFT aqueous emulsion polymerisation of glycidyl methacrylate', *Polym. Chem.*, 2020, **11**, 6343–6355.

46 A. Czajka and S. P. Armes, 'Time-Resolved Small-Angle X-ray Scattering Studies during Aqueous Emulsion Polymerization', *J. Am. Chem. Soc.*, 2021, **143**, 1474–1484.

47 E. J. Cornel, S. Van Meurs, T. Smith, P. S. O'Hora and S. P. Armes, 'In Situ Spectroscopic Studies of Highly Transparent Nanoparticle Dispersions Enable Assessment of Trithiocarbonate Chain-End Fidelity during RAFT Dispersion Polymerization in Nonpolar Media', *J. Am. Chem. Soc.*, 2018, **140**, 12980–12988.

48 S. J. Byard, M. Williams, B. E. McKenzie, A. Blanazs and S. P. Armes, 'Preparation and Cross-Linking of All-Acrylamide Diblock Copolymer Nano-Objects via Polymerization-Induced Self-Assembly in Aqueous Solution', *Macromolecules*, 2017, **50**, 1482–1493.

49 O. J. Deane, O. M. Musa, A. Fernyhough and S. P. Armes, 'Synthesis and Characterization of Waterborne Pyrrolidone-Functional Diblock Copolymer Nanoparticles Prepared via Surfactant-free RAFT Emulsion Polymerization', *Macromolecules*, 2020, **53**, 1422–1434.

50 E. Read, A. Guinaudeau, D. J. Wilson, A. Cadix, F. Violleau and M. Destarac, 'Low temperature RAFT/MADIX gel polymerisation: Access to controlled ultra-high molar mass polyacrylamides', *Polym. Chem.*, 2014, **5**, 2202–2207.

51 A. Favier, F. D'Agosto, M.-T. Charreyre and C. Pichot, 'Synthesis of N-acryloxysuccinimide copolymers by RAFT polymerization, as reactive building blocks with full control of composition and molecular weights', *Polymer*, 2004, **45**, 7821–7830.

52 S. J. Byard, A. Blanazs, J. F. Miller and S. P. Armes, 'Cationic Sterically Stabilized Diblock Copolymer Nanoparticles Exhibit Exceptional Tolerance toward Added Salt', *Langmuir*, 2019, **35**, 14348–14357.

53 P. Biais, P. Beaunier, F. Stoffelbach and J. Rieger, 'Loop-stabilized BAB triblock copolymer morphologies by PISA in water', *Polym. Chem.*, 2018, **9**, 4483–4491.

54 C. Dommanget, F. D'Agosto and V. Monteil, 'Polymerization of Ethylene through Reversible Addition–Fragmentation Chain Transfer (RAFT)', *Angew. Chemie Int. Ed.*, 2014, **53**, 6683–6686.

55 V. J. Cunningham, M. J. Derry, L. A. Fielding, O. M. Musa and S. P. Armes, 'RAFT aqueous dispersion polymerization of N-(2-(methacryloyloxy)ethyl)pyrrolidone: A convenient low viscosity route to high molecular weight water-soluble copolymers', *Macromolecules*, 2016, **49**, 4520–4533.

56 S. J. Byard, Synthesis and Characterisation of Stimulus-responsive Diblock Copolymer Nano-objects

Prepared by RAFT Aqueous Dispersion Polymerisation, PhD Thesis, University of Sheffield, 2019.

57 A. Blanazs, A. J. Ryan and S. P. Armes, 'Predictive phase diagrams for RAFT aqueous dispersion polymerization: Effect of block copolymer composition, molecular weight, and copolymer concentration', *Macromolecules*, 2012, **45**, 5099–5107.

58 M. J. Derry, L. A. Fielding, N. J. Warren, C. J. Mable, A. J. Smith, O. O. Mykhaylyk and S. P. Armes, 'In situ small-angle X-ray scattering studies of sterically-stabilized diblock copolymer nanoparticles formed during polymerization-induced self-assembly in non-polar media', *Chem. Sci.*, 2016, **7**, 5078–5090.

59 F. S. Bates and G. H. Fredrickson, 'Block copolymer thermodynamics: Theory and experiment', *Annu. Rev. Phys. Chem.*, 1990, **41**, 525–557.

60 S. Förster, M. Zisenis, E. Wenz and M. Antonietti, 'Micellization of strongly segregated block copolymers', *J. Chem. Phys.*, 1996, **104**, 9956–9970.

61 P. J. Flory, *Statistical Mechanics of Chain Molecules*, Wiley Interscience, New York, 1969.

62 P.-G. De Gennes, *Scaling Concepts in Polymer Physics*, Cornell University Press, Ithaca, 1979.

63 O. Kratky and G. Porod, 'Röntgenuntersuchung gelöster Fadenmoleküle', *Recl. des Trav. Chim. des Pays-Bas*, 1949, **68**, 1106–1122.

64 P. Lindner and T. H. Zemb, in *Static Properties of Polymers*, Amsterdam, Elsevier., 2002, pp. 288–291.

65 B. H. Zimm, 'Application of the Methods of Molecular Distribution to Solutions of Large Molecules', *J. Chem. Phys.*, 1946, **14**, 164–179.

66 R. R. Gibson, S. P. Armes, O. M. Musa and A. Fernyhough, 'End-group ionisation enables the use of poly(: N -(2-methacryloyloxy)ethyl pyrrolidone) as an electrosteric stabiliser block for polymerisation-induced self-assembly in aqueous media', *Polym. Chem.*, 2019, **10**, 1312–1323.

67 D. L. Beattie, O. J. Deane, O. O. Mykhaylyk and S. P. Armes, 'RAFT aqueous dispersion polymerization of 4-hydroxybutyl acrylate: Effect of end-group ionization on the formation and colloidal stability of sterically-stabilized diblock copolymer nanoparticles', *Polym. Chem.*, 2022, **13**, 655–667.

68 S. J. Byard, C. T. O'Brien, M. J. Derry, M. Williams, O. O. Mykhaylyk, A. Blanazs and S. P. Armes, 'Unique aqueous self-assembly behavior of a thermoresponsive diblock copolymer', *Chem. Sci.*, 2020, **11**, 396–402.

69 C. György, C. Verity, T. J. Neal, M. J. Rymaruk, E. J. Cornel, T. Smith, D. J. Growney and S. P. Armes, 'RAFT Dispersion Polymerization of Methyl Methacrylate in Mineral Oil: High Glass Transition Temperature of the Core-Forming Block Constrains the Evolution of Copolymer Morphology', *Macromolecules*, 2021, **54**, 9496–9509.

70 S. M. North and S. P. Armes, 'One-pot synthesis and aqueous solution properties of pH-responsive schizophrenic diblock copolymer nanoparticles prepared via RAFT aqueous dispersion polymerization', *Polym. Chem.*, 2021, **12**, 5842–5850.

71 J. F. Miller, 'Determination of Protein Charge in Aqueous Solution Using Electrophoretic Light Scattering: A Critical Investigation of the Theoretical Fundamentals and Experimental Methodologies', *Langmuir*, 2020, **36**, 8641–8654.

72 R. J. Hunter, *Zeta Potential in Colloid Science*, Academic Press, New York, 1981.

Chapter 6: Synthesis of High Molecular Weight Polyelectrolytes as Low-Viscosity Latex Particles by RAFT Aqueous Dispersion Polymerisation at Low pH

6.1 Introduction

As discussed in **Section 1.3.6**, Armes and co-workers utilised the ionisation of carboxylic acid groups located at the end of steric stabiliser chains to confer minimal charge for sterically-stabilised diblock copolymer nanoparticles.[1,2] For certain formulations, lowering the solution pH led to nanoparticle flocculation because this caused protonation of the terminal anionic carboxylate groups and hence loss of surface charge. The present Chapter examines the use of a weak anionic polyelectrolyte as the core-forming block for RAFT aqueous dispersion polymerisation formulations. If such syntheses are conducted at sufficiently low pH, the polyelectrolyte chains are uncharged and hence hydrophobic. In principle, raising the solution pH after the aqueous PISA synthesis should lead to extensive ionisation of the core-forming block and hence cause *in situ* nanoparticle dissolution to form a highly viscous gel. Carbopol products are an example of a commercial line of crosslinked PAA microgels manufactured by Lubrizol. Such particles provide effective rheology modification (solution thickening) for a range of applications, including laundry detergents, surface cleaners and batteries. These polymer products generally exists as powders, though emulsion formulations are also available.[3]

Accordingly, an anionic $PAMPS_{230}$ precursor was chain-extended using a suitable carboxylic acid based vinyl monomer at pH 2.0 – 2.5 (i.e. well below the pK_a of the corresponding anionic polyelectrolyte homopolymer). Both acrylic acid (AA) and 2-carboxyethyl acrylate (CEA) were evaluated in this context and their structures when protonated and ionised are shown in **Scheme 6.1**.

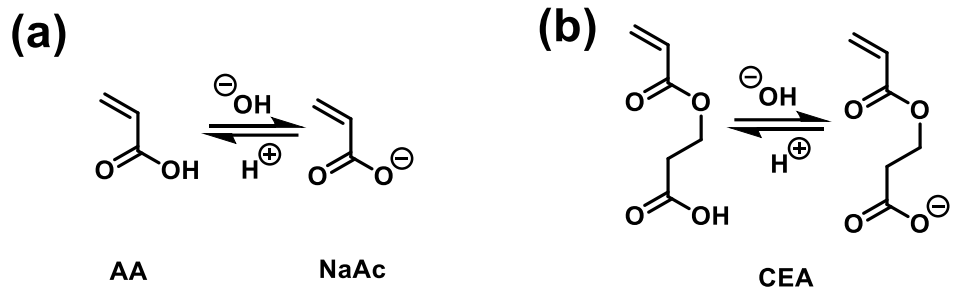

Scheme 6.1 Chemical structures of (a) acrylic acid (AA) and (b) 2-carboxyethyl acrylate (CEA) in protonated and deprotonated forms.

Rimmer and co-workers used potentiometric titration with NaOH (*aq*) to determine a pK_a of 4.52 – 4.55 for PAA as discussed in **Section 2.3.3**.[4] This work has determined the pK_a of PCEA to be approximately 5.1, also via potentiometric titration. This was achieved by identifying the midpoint between the titration equivalence points (i.e., the inflection points observed at low and high pH). A structurally comparable monomer to CEA has been reported in work by Bories-Azeau et al.[5,6]: monosuccinic acid ester of 2-hydroxyethyl methacrylate (SEMA), with a pK_a of 5.5 determined by potentiometric titration. Although PSEMA has a similar pKa to poly(methacrylic acid)[7] and are both water-soluble in their ionised form, protonation of the pendent carboxylic acid groups below pH 4 causes macroscopic precipitation of PSEMA, whereas the neutral PMAA chains remain hydrophilic.[6] This same observation is made in this work for PCEA.

The CEA monomer can be formed by dimerisation of AA. Indeed, it is known that AA can be contaminated with CEA, as indicated in work published by López-Pérez et al..[8] These authors noticed that when they used 'pure' AA in a homopolymerisation with a bifunctional RAFT agent (**Figure 6.1a**), there are additional monomer and polymer signals that are consistent with residual CEA and statistically copolymerised CEA repeat units. As well as the proton signals expected for PAA (and residual AA monomer), see **Figure 6.1b**. Subsequently, they verified that the commercial sample of AA used was contaminated with ca. 10 mol % of this dimer. However, as stated in **Section 4.3**, only 1 mol % dimer contamination of AA was

detected via ^{1}H NMR in the monomer used in this work. If desired, this impurity can be removed by fractional distillation.[9,10]

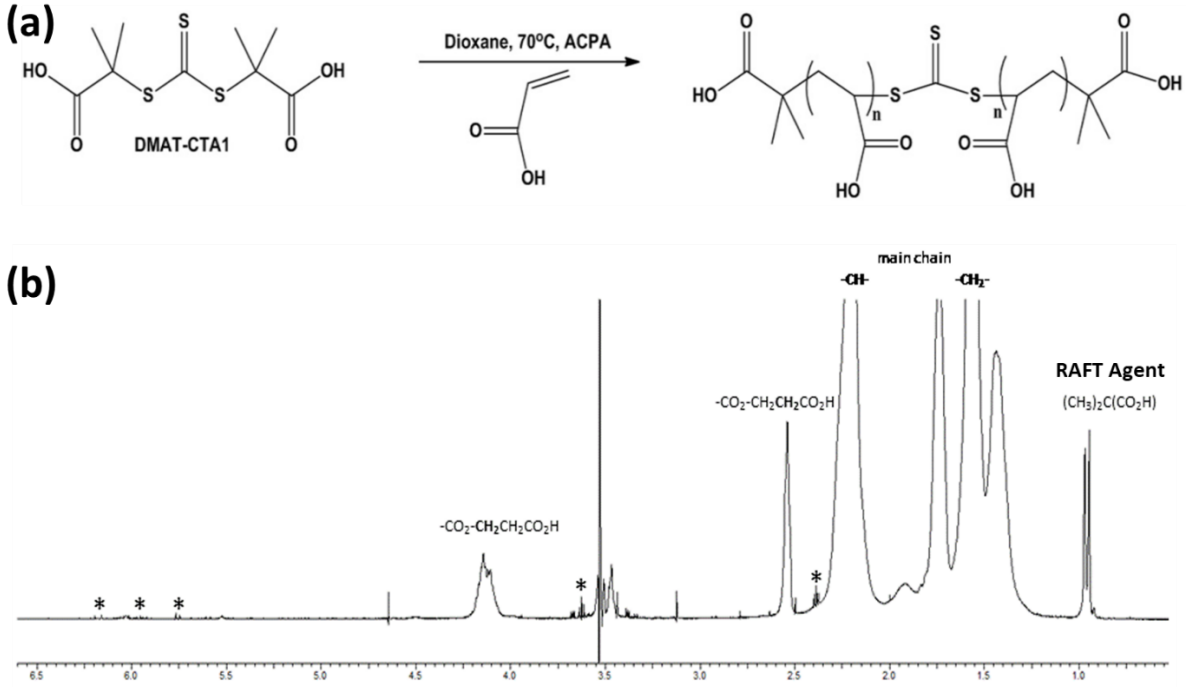

Figure 6.1 (a) Reaction scheme for the synthesis of PAA by **López-Pérez** et al. with 99% monomer conversion and M_n = 11.6 kg mol^{-1}.[8] (b) Associated ^{1}H NMR spectrum of poly(acrylic acid) containing traces of 2-carboxyethyl acrylate (CEA). This AA dimer is a known impurity in AA and is assigned to the proton signals denoted by an asterisk (*). The corresponding proton signals for statistically copolymerised CEA repeat units are indicated at 2.5 and 4.2 ppm.[8] [Adapted from López-Pérez et al., *Polymer*, 2019, 168, 116–125]

Both CEA and PCEA are readily susceptible to hydrolysis, particularly when the carboxylic acid groups are deprotonated in alkaline solution. Moreover, in a study published by North et al.,[11] a significant quantity of the β-lactic acid (β-LA) hydrolysis product was formed during the one-pot synthesis of PDEA$_{67}$-PCEA$_{135}$ diblock copolymer nanoparticles via RAFT aqueous dispersion polymerisation at pH 2 (**Figure 6.2a**), as shown by the signals *g* and *h* in **Figure 6.2b**. This observation was not noticed by North et al., but the work in this Thesis Chapter has identified this issue. Unfortunately, the presence of (unwanted) statistically copolymerised AA residues in the copolymer chains cannot be confirmed by ^{1}H NMR spectroscopy owing to overlapping backbone proton signals. However, the extent of (P)CEA hydrolysis can be

estimated by comparing the intensity of the β-LA side-product signals (*g* and *h*) at either 2.4 or 3.7 ppm with the integrated PCEA side-chain signals (*e* and *f*) at either 2.6 or 4.25 ppm. This process is valid for syntheses with full CEA monomer conversions, for incomplete CEA polymerisation, the residual monomer peaks must also be accounted for.

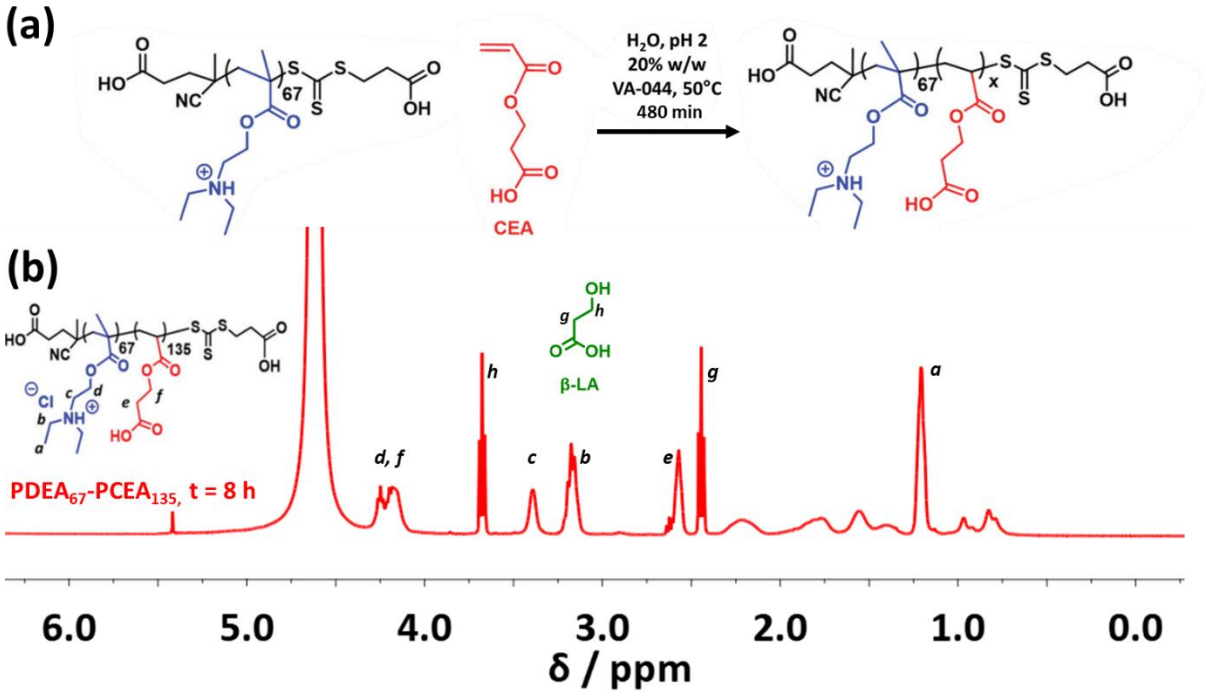

Figure 6.2 (a) Reaction scheme for the synthesis of $PDEA_{67}$-$PCEA_{135}$ by North et al. with > 99% monomer conversion and M_n = 22.0 kg mol^{-1}.[8] (b) ^1H NMR spectrum recorded after conducting the one-pot synthesis of such diblock copolymer nanoparticles via RAFT aqueous dispersion polymerisation of CEA for 8 h at 50°C and pH 2, spectrum adapted from North and co-workers.[11] The hydrolysis by-product β-lactic acid (β-LA) can be identified in this ^1H NMR spectrum. [Adapted from North et al., *Polym. Chem.*, 2021, 12, 5842-5850]

Like PMAA, PAA remains water-soluble at pH 2.0 – 2.5 in the absence of added salt. However, preliminary salting out studies summarised in **Chapter 2** indicate that PAA becomes insoluble in the presence of 2.8 M ammonium sulfate, see **Table 6.1**. This suggests that the RAFT aqueous dispersion polymerisation of AA should be feasible at pH 2.0 – 2.5 in the presence of at least 3.0 M ammonium sulfate. Under such conditions, the PAA acts as the salt-intolerant core block in its deprotonated form. At low pH, PAA chains adopt a compact,

globular conformation.[4] However, ionisation occurs on increasing the pH and the chains expand to their fully solvated open coil conformation.[12]

Additive	Aqueous $(NH_4)_2SO_4$ solution / mol dm^{-3}				
	0	1.0	2.0	3.0	4.0
$PNaAc_{500}$ (pH 8.0)	Soluble	Soluble	Soluble	Soluble	Soluble
PAA_{500} (pH 2.5)	Soluble	Soluble	Soluble	Insoluble	Insoluble

Table 6.1 Aqueous solubility of $PNaAc_{500}$ at pH 8.0 and PAA_{500} at pH 2.5.

The aim of this work is to design a high molecular weight pH-responsive weak polyelectrolyte for viscosity modification in a liquid form. It is worth noting that this Thesis chapter utilises a different approach to earlier chapters as it does not rely on dilution and it results in the formation of a charged thickener.

6.2 Experimental

6.2.1 Materials

Acrylic acid (AA; ≥ 99%; purified with acidic alumina), acidic alumina, basic alumina, 2-carboxyethyl acrylate (CEA; ≥ 99%), 2-acrylamido-2-methylpropanesulfonic acid, sodium salt (AMPS; 50% w/w aqueous solution), phosphate buffered saline (PBS) tablets, sodium nitrate, sodium bicarbonate, sodium deuteroxide solution (NaOD; 40% w/w, 99.5% D) and deuterium oxide (D_2O; ≥ 99.9% D) were sourced from Sigma Aldrich (Merck; UK). 2,2'- Azobis(2-(2-imidazolin-2-yl)propane)dihydrochloride (VA-044; ≥ 98%) was sourced from Fluorochem. CD_2Cl_2 (≥ 99.8% D) was sourced from Cambridge Isotope Laboratories (UK). 2-Ethylhexanoyl tert-butyl peroxide (T-21S; ≥ 97%) was obtained from AkzoNobel (Netherlands). Sodium hydroxide (≥ 98%) and ammonium sulfate (> 98%) were sourced from Thermo Fisher Scientific (UK). PEO standards were sourced from Agilent/PSS (Church Stretton, UK). 2-(((butylthio)-carbonothioyl)-thio)-2-methylpropanoic acid (BDMAT) was prepared as reported in **Chapter 2**.[13,14] Triethylamine (≥ 99%) was sourced from Fisher

Scientific (UK). Unless otherwise stated, all solvents and concentrated acids were purchased from Fisher Scientific (UK) and were used as received. Deionised water was used for all experiments.

6.2.2 Characterisation Techniques

Experimental protocols for ^{1}H NMR spectroscopy (solvent: 0.1 M NaOD), UV absorption spectroscopy, DLS, optical microscopy and rotational rheology are described in **Chapter 2**.

Aqueous Gel Permeation Chromatography (GPC)

Experimental details are reported in **Chapter 3**. PAMPS-PCEA copolymers were analysed at 1.0 mL min^{-1} using Eluent 3, which comprised 0.1 M $NaNO_3$, 0.02 M TEA and 0.05 M $NaHCO_3$ at pH 8.0. PAMPS-PAA copolymers were analysed at 0.8 mL min^{-1} using Eluent 4, which comprised 70% v/v 0.2 M $NaNO_3$ and 0.01 M NaH_2PO_4 at pH 7.0 plus 30% v/v methanol.

Potentiometric Titration

The pK_a value for the PCEA block within a $PAMPS_{230}$-$PCEA_{2000}$ diblock copolymer was determined by titrating an acidified 2.5% w/w copolymer dispersion at pH 2.0 using 0.1 M NaOH solution at 20°C. Solution pH was monitored using a HANNA pH sensor, which was calibrated using pH 4.0, 7.0, and 10.0 buffers. Identification of the midpoint between the titration equivalence points (from the inflection points at low and high pH) enabled determination of the pK_a value.

Transmission Electron Microscopy (TEM)

Cu/Pd TEM grids (Agar Scientific, UK) were coated in-house with a thin film of amorphous carbon and then treated with a plasma glow discharge for 30 seconds to generate a hydrophilic surface. A 10 μL droplet of freshly diluted 0.1% w/w aqueous copolymer dispersion was

pipetted onto a hydrophilic grid for 1 min, then carefully blotted with universal indicator paper to remove excess sample and check an acidic pH was maintained. No stain was added to samples, as this was shown to cause an increase in the sample pH and particle dissolution. The grid was dried with the aid of a vacuum hose. Imaging was performed using an FEI Tecnai Spirit 2 microscope equipped with an Orius SC1000B camera operating with an accelerating voltage of 80 kV.

6.2.3 Synthesis of PAMPS Precursor via RAFT Solution Polymerisation of 2-Acrylamido-2-methylpropanesulfonic acid, sodium salt (AMPS) in Water at 90°C

AMPS (55% w/w in water) (61.9 g, 149 mmol), BDMAT (0.15 g, 594 μmol), T-21S (0.026 g, 119 mmol) and PBS (23.5 g) were weighed into a 250 mL round-bottom flask charged with a magnetic stirrer to form an aqueous solution (pH 7), which was degassed using a stream of nitrogen gas for 45 min at 20°C. The sealed flask was then immersed into an oil bath set at 90°C for 180 min and the polymerisation was subsequently quenched by removing the flask from the oil bath and exposing the reaction mixture to air while cooling to room temperature. The final AMPS conversion was 99%, as judged by ^{1}H NMR spectroscopy (the integrated vinyl signals assigned to AMPS monomer at 5.5 – 6.3 ppm were compared to the integrated methacrylic backbone signals at 1.0 – 2.5 ppm). The aqueous PAMPS solution was purified by dialysis for three days to remove unreacted monomer and initiator and then freeze-dried. The mean degree of polymerisation was determined to be 230 ± 1, as judged by end-group analysis using UV spectroscopy at the absorption maximum of 310 nm. Aqueous GPC analysis indicated an M_n of 28 kg mol^{-1} and an M_w/M_n of 1.82 in 70% v/v 0.2 M $NaNO_3$ and 0.01 M NaH_2PO_4 at pH 7.0 plus 30% v/v methanol (Eluent 4) and an M_n of 32 kg mol^{-1} and an M_w/M_n of 1.33 in 0.1 M $NaNO_3$, 0.02 M TEA and 0.05 M $NaHCO_3$ at pH 8.0 (Eluent 3).

6.2.4 Synthesis of $PAMPS_{230}$-PAA_x Diblock Copolymer Particles via RAFT Aqueous Dispersion Polymerisation of Acrylic acid (AA) in the Presence of 3.0 M Ammonium Sulfate at 46°C

A typical protocol for the synthesis of $PAMPS_{230}$-PAA_{1000} spheres at 10% w/w solids was conducted as follows. The $PAMPS_{230}$ precursor (140 mg, 2.64 μmol), AA monomer (191 mg, 2.64 mmol), an aqueous solution of VA-044 initiator (427 mg, 2.64 μmol) and 3.0 M ammonium sulfate (2.55 g) were weighed into a 14 mL vial charged with a magnetic stirrer. An aqueous solution of 37% w/w HCl (≈ 40 mg) was added to adjust the solution to pH 2.5 before being degassed using a stream of nitrogen gas for 30 min at 20°C. The sealed flask was then immersed into an oil bath set at 46°C. After 18 h, the AA polymerisation was quenched by removing the flask from the oil bath and exposing the reaction mixture to air while cooling to 20°C. The final AA conversion was 96% as judged by ^{1}H NMR spectroscopy (the integrated vinyl signals assigned to AA monomer at 5.8 – 6.3 ppm were compared to the integrated acrylic backbone signals at 1.1 – 2.6 ppm). Aqueous GPC analysis in pH 8.0 eluent indicated an M_n of 49 kg mol^{-1} and an M_w/M_n of 1.88.

6.2.5 Synthesis of $PAMPS_{230}$-$PCEA_x$ Diblock Copolymer Particles via RAFT Aqueous Dispersion Polymerisation of 2-Carboxyethyl acrylate (CEA) in Acidic Solution at 46°C

A typical protocol for the synthesis of $PAMPS_{230}$-$PCEA_{2000}$ spherical nanoparticles at 30% w/w solids was conducted as follows. The $PAMPS_{230}$ precursor (150 mg, 2.83 μmol), CEA (816 mg, 5.66 mmol), an aqueous solution of VA-044 initiator (549 mg, 5.66 μmol) and deionised water (1.71 g) were weighed into a 14 mL vial charged with a magnetic stirrer. An aqueous solution of 37% w/w HCl (≈ 40 mg) was added to adjust the solution pH to pH 2.0 prior to degassing using a stream of nitrogen gas for 30 min at 20°C. The sealed flask was then immersed into an oil bath set at 46°C. After 18 h, the polymerisation was quenched by removing the flask from the oil bath and exposing the reaction mixture to air while cooling to

20°C. The final CEA conversion was more than 99% as judged by ^{1}H NMR spectroscopy (the integrated vinyl signals assigned to CEA monomer at 5.6 – 6.2 ppm were compared to the integrated acrylic backbone signals at 1.1 – 2.5 ppm). Aqueous GPC analysis in pH 8.0 eluent indicated an M_n of 89 kg mol^{-1} and an M_w/M_n of 2.90.

6.3 Results and Discussion

The synthesis of the PAMPS homopolymer was based on the protocol by Bray et al., who used phosphate buffered saline (PBS) to maintain the solution at pH 7.4. Subsequent purification by dialysis removed the salts from the PAMPS precursor prior to freeze-drying which yielded a free-flowing powder. ^{1}H NMR spectroscopy studies indicated that almost complete conversion was achieved within 3 h. PAMPS remained water-soluble even in the presence of 4.0 M ammonium sulfate, so it was considered to be a suitable electrosteric stabiliser. Both AMPS monomer and PAMPS polymer are essentially permanently ionised in aqueous solution because their respective pK_a values are less than 2.[15]

The PAMPS$_x$ homopolymer was determined to have a DP of x = 230 ± 1, via end-group analysis using UV absorption spectroscopy. This was calculated by constructing a linear calibration curve based on the Beer-Lambert law, as shown in **Figure 6.3**.

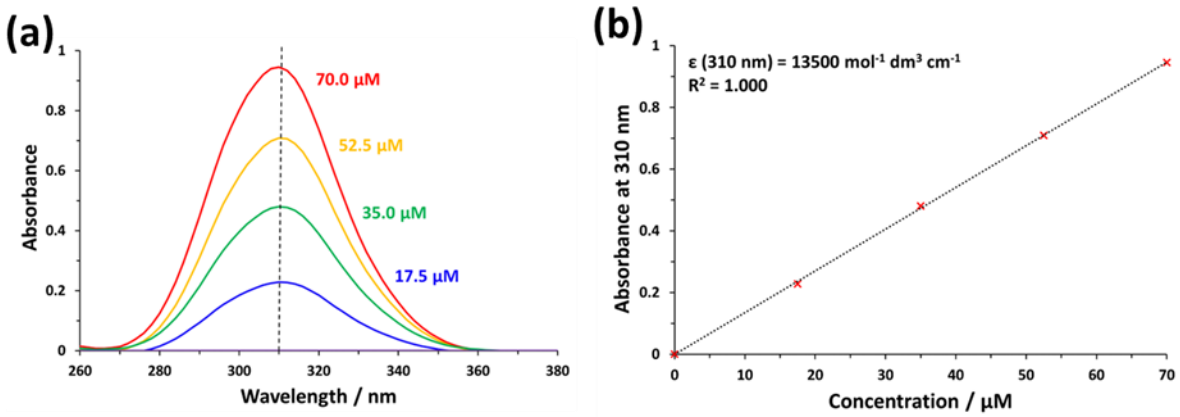

Figure 6.3 (a) UV absorption spectra recorded for S-butyl-S′-(α,α′-dimethyl-α′′-acetic acid)trithio-carbonate (BDMAT) in methanol for a series of concentrations ranging from 0 µM to 70.0 µM. (b) Beer-Lambert linear calibration plot constructed for BDMAT in methanol to calculate its molar extinction coefficient (ε) at the absorption maximum of 310 nm.

Preliminary chain extension experiments using acrylic acid demonstrated that both 3.0 M ammonium sulfate and pH 2.5 were insufficient to form nanoparticle dispersions with the synthesis shown in **Scheme 6.2**.

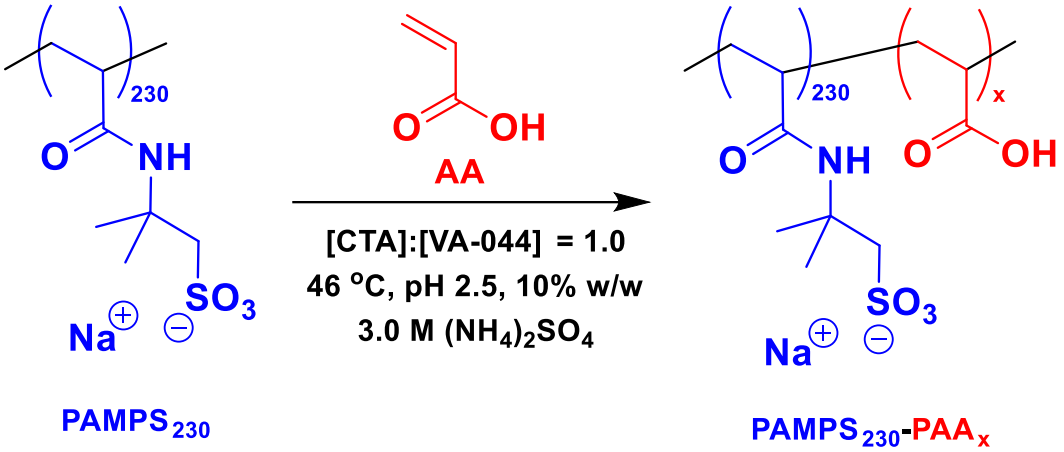

Scheme 6.2 Synthesis of $PAMPS_{230}$-PAA_x diblock copolymers (x = 1,000 to 3,000) via RAFT polymerisation of AA at 46°C in the presence of 3.0 M ammonium sulfate at pH 2.5.

The corresponding GPC curves are shown in **Figure 6.4** with a reasonably high chain extension efficiency being observed as the target PAA DP is increased from 1,000 to 3,000. However, relatively high M_w/M_n values are obtained for the $PAMPS_{230}$ precursor and the diblock copolymers. The tailing observed in the GPC traces is attributed to the high initiator concentration relative to the RAFT agent concentration.

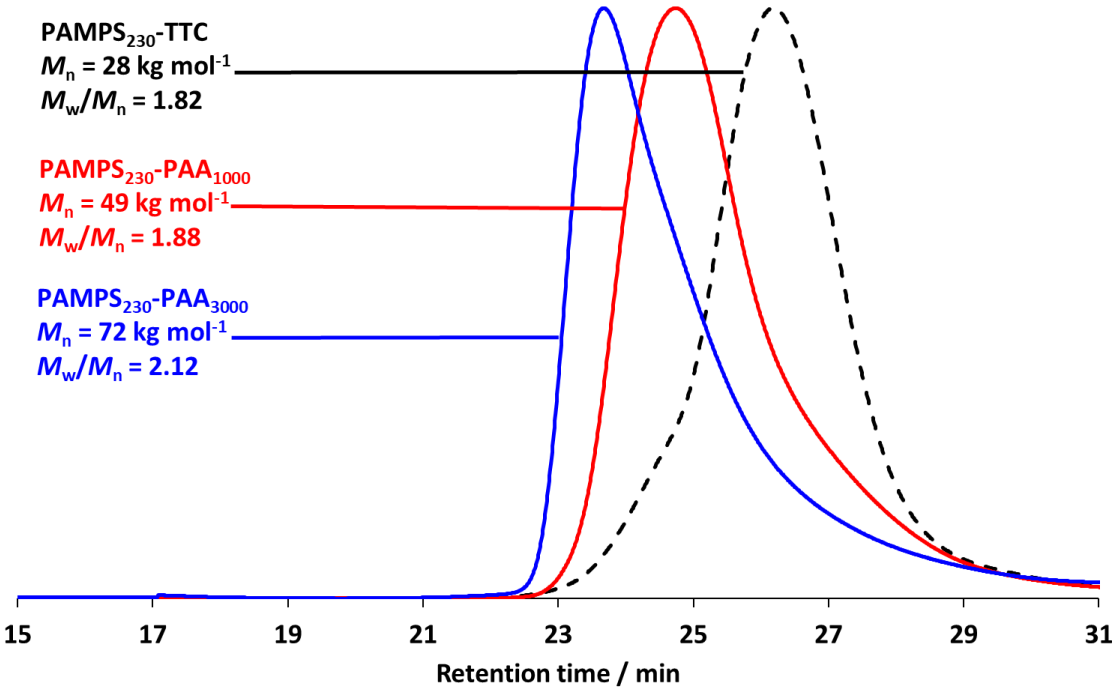

Figure 6.4 Aqueous GPC curves recorded for the $PAMPS_{230}$ precursor and a series of $PAMPS_{230}$-PAA_x diblock copolymers prepared by chain extension via RAFT aqueous dispersion polymerisation of AA at 46°C in the presence of 3.0 M ammonium sulfate at pH 2.5. M_n values are calculated relative to a series of near-monodisperse PEO calibration standards. Eluent 4 was used which consisted of 70% v/v 0.2 M $NaNO_3$ and 0.01 M NaH_2PO_4 at pH 7.0 plus 30% v/v methanol.

This initial low pH synthesis of $PAMPS_{230}$-PAA_x copolymers in the presence of added salt led to the hypothesis that a more hydrophobic carboxylic acid-based monomer could be used for a dispersion polymerisation. Accordingly, a $PAMPS_{230}$-$PCEA_x$ formulation was investigated at pH 2.0 with no salt required. Unfortunately, an even higher initiator concentration was required to ensure that the RAFT aqueous dispersion polymerisation of CEA proceeded to full conversion under the stated reaction conditions, see **Scheme 6.3**.

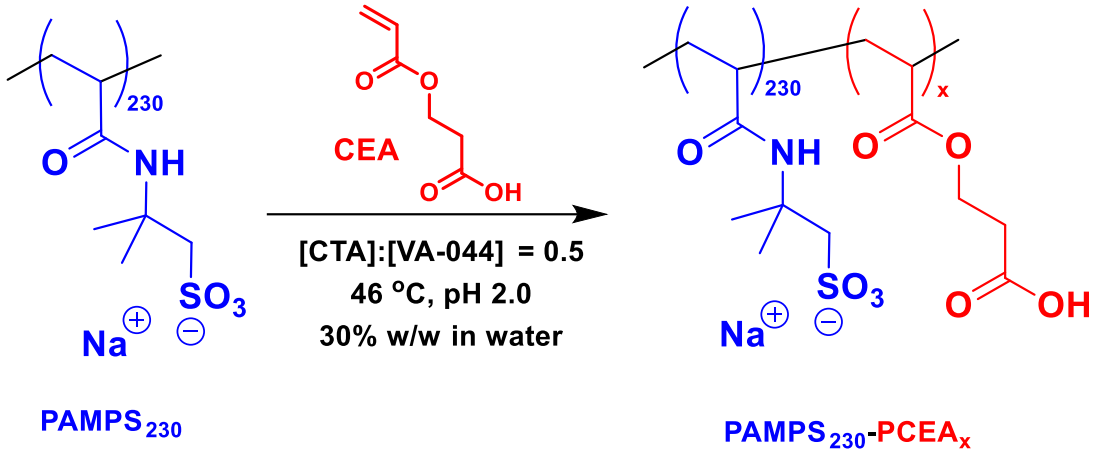

Scheme 6.3 Reaction scheme for the synthesis of $PAMPS_{230}$-$PCEA_x$ diblock copolymer particles via RAFT aqueous dispersion polymerisation of CEA at 46°C in highly acidic media. Conditions: 30% w/w solids; $PAMPS_{230}$/VA-044 molar ratio = 0.50; pH 2.0; x = 2,000 to 12,000.

The subsequent addition of an aqueous solution of NaOH causes ionisation of the carboxylic acid groups within the $PCEA_{8000}$ chains and hence converts the initial low-viscosity turbid dispersion into a highly viscous, free-standing transparent gel, as illustrated by the two digital images shown in **Scheme 6.4**.

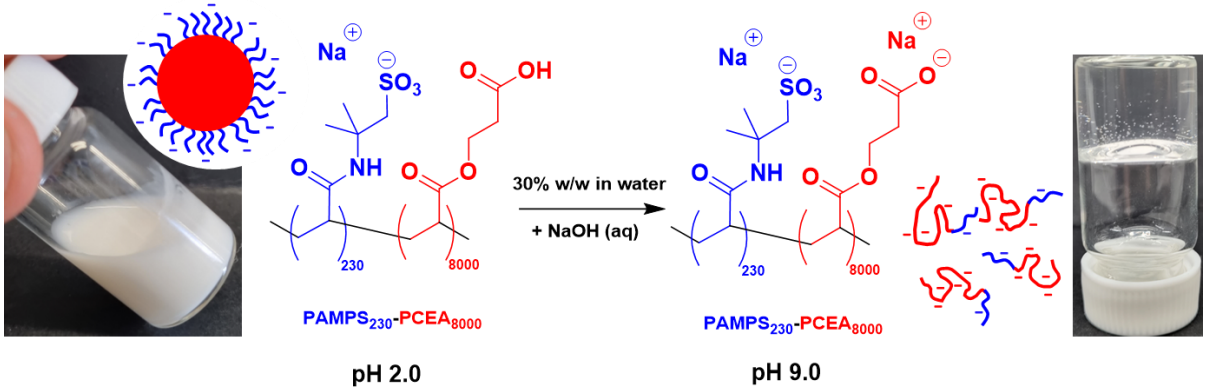

Scheme 6.4 Schematic cartoon and corresponding digital images to illustrate the behaviour of the initial sterically-stabilised $PAMPS_{230}$-$PCEA_{8000}$ diblock copolymer particles in aqueous solution. Raising the solution pH from pH 2.0 to pH 9.0 using NaOH leads to *in situ* dissociation of the original particles and the concomitant formation of a viscous transparent gel comprising molecularly-dissolved diblock copolymer chains.

A potentiometric titration of the $PAMPS_{230}$-$PCEA_{2000}$ diblock copolymer chains was conducted in order to determine the pK_a value for the PCEA block, as shown in **Figure 6.5**. Given the relatively low pK_a of the PAMPS block,[15] these permanently ionised chains are

considered to have no effect on the titration data. The pH value obtained from the midpoint of the titration equivalence points (where the degree of ionisation is 0.50) was used to calculate an effective pK_a of 5.1 for the PCEA block. Importantly, this titration curve confirmed the requirement to use a relatively acidic solution (pH 2.0) for the RAFT aqueous dispersion polymerisation of CEA to ensure full protonation of the resulting PCEA chains. To more accurately quantify the pK_a of the PCEA block, a homopolymer could have been used for the potentiometric titration, although macroscopic precipitation of the PCEA at low pH values makes this less convenient than using the electrosterically stabilised nanoparticles.

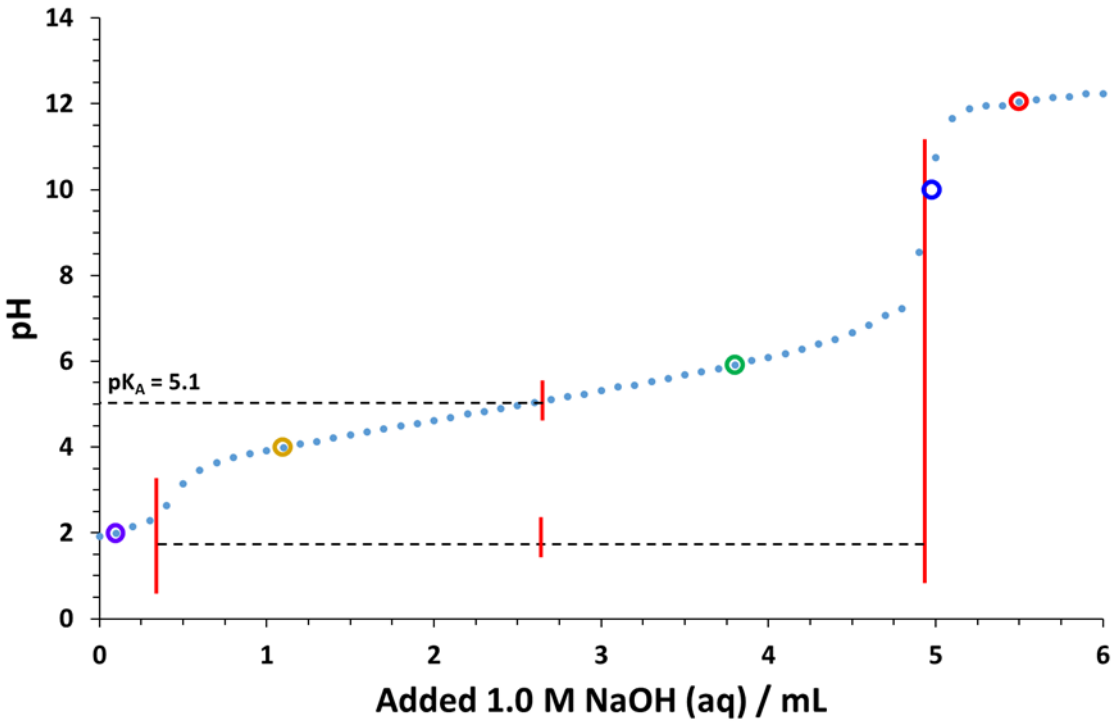

Figure 6.5 Potentiometric titration of a 2.5% w/w solution of $PAMPS_{230}$-$PCEA_{2000}$ diblock copolymer with an aqueous solution of 1.0 M NaOH to determine the two equivalence points and thus the effective pK_a of the PCEA block.

Table 6.2 summarises the results obtained for the $PAMPS_{230}$-$PCEA_{2000\text{-}12000}$ formulation when targeting 30% w/w solids. CEA conversions of 96% to 99% were obtained for six aqueous PISA syntheses, although some macroscopic precipitation was observed when targeting a PCEA DP ≥ 10,000. Low-viscosity turbid dispersions were obtained for all six syntheses and the final solution pH was still pH 2.0 at the end of each CEA polymerisation.

Aqueous GPC analysis indicated a monotonic increase in M_n, albeit with systematic under-estimation of this parameter owing to the choice of PEO calibration standards. The volume-average particle diameter reported by laser diffraction also increased monotonically with respect to the PCEA DP.

PCEA DP (x)	Conversion[a] / %	M_n[b] / kg mol^{-1}	M_w/M_n[b]	D_v [4,3][c] / µm	Span[c]	Uniformity[c]
2,000	> 99	89	2.90	0.31	1.14	0.35
4,000	> 99	134	3.25	1.06	0.88	0.27
6,000	99	182	3.81	1.17	0.72	0.23
8,000	98	197	4.01	1.48	0.56	0.17
10,000[d]	96	262	2.94	1.74	0.52	0.16
12,000[d]	97	244	3.43	2.05	0.57	0.17

Table 6.2 Summary of series of six $PAMPS_{230}$-$PCEA_x$ (x = 2,000 to 12,000) diblock copolymer particles prepared via RAFT aqueous dispersion polymerisation of CEA at pH 2.0. Conditions: 30% w/w solids; 46°C; $PAMPS_{230}$/VA-044 molar ratio = 0.50. (a) CEA conversions obtained via ^{1}H NMR spectroscopy, (b) M_n and M_w/M_n values, as determined by aqueous GPC (Eluent 3), (c) particle size data via laser diffraction (D_v [4,3] = volume-average diameter) and (d) some macroscopic precipitation observed.

The GPC protocol used for analysis of the anionic $PAMPS_{230}$ precursor and each $PAMPS_{230}$-$PCEA_x$ diblock copolymer could also be conducted at this higher solution pH. However, in view of the susceptibility of the PCEA block to undergo base-catalysed hydrolysis, the solution pH should ideally not exceed pH 8.0. Various protocols were examined for GPC analysis of the $PAMPS_{230}$-$PCEA_x$ diblock copolymers, with a pH 8 eluent selected and corresponding data shown in **Figure 6.6**. Relatively high chain extension efficiencies were always observed, regardless of the eluent type. However, the addition of methanol co-solvent, which is commonly used for the analysis of PAMPS homopolymers,[13,16,17] caused extensive tailing and M_w/M_n values increased to between 5 – 15 (data not shown). This is believed to be an artefact owing to column adsorption.

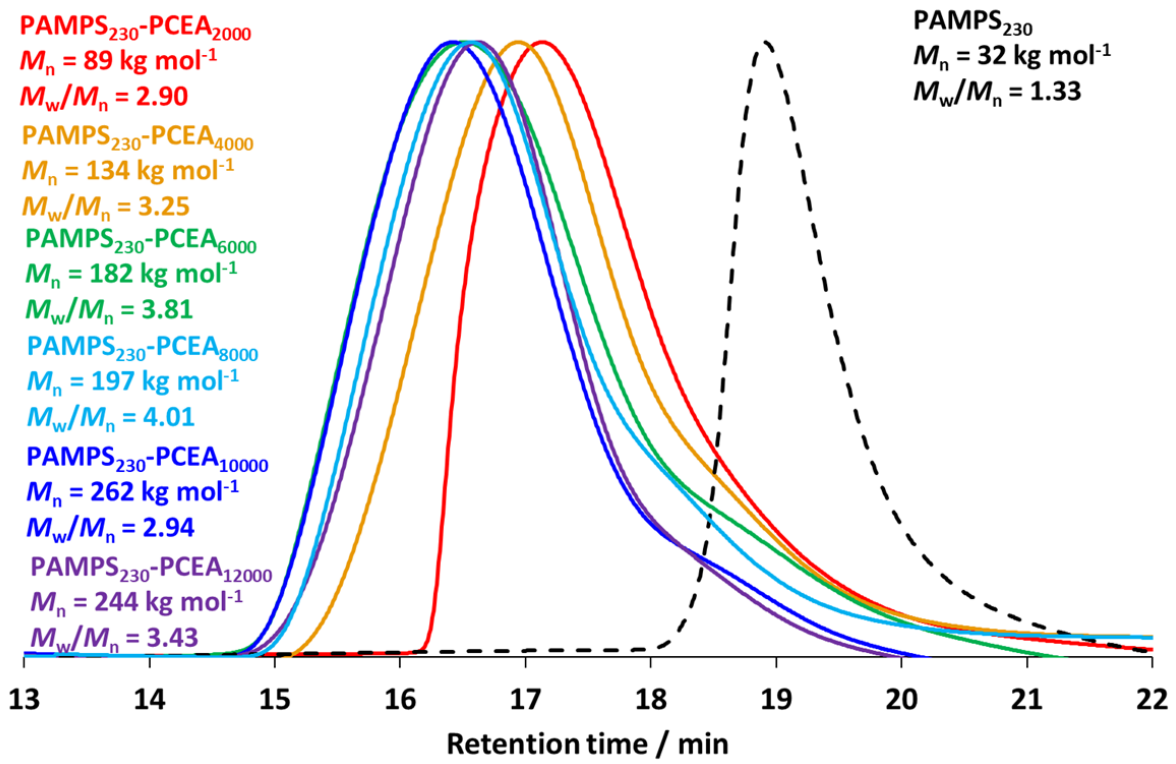

Figure 6.6 Aqueous GPC curves recorded for the $PAMPS_{230}$ precursor and a series of $PAMPS_{230}$-$PCEA_x$ diblock copolymers prepared by chain extension via RAFT aqueous dispersion polymerisation of CEA at 46°C at pH 2.0. M_n values are calculated relative to a series of near-monodisperse PEO calibration standards. Eluent 3 was used which consisted of 0.1 M $NaNO_3$, 0.02 M TEA and 0.05 M $NaHCO_3$ at pH 8.0.

The ^{1}H NMR spectra of AA (blue spectrum), CEA (red spectrum) and β-LA (green spectrum) were prepared directly from the chemical supplier bottles in deuterium oxide and are shown in **Figure 6.7**. The β-LA peaks are shifted upfield relative to the corresponding CEA peaks due to the reduced electron withdrawing effect of the β-LA alcohol group compared to the CEA ester group.

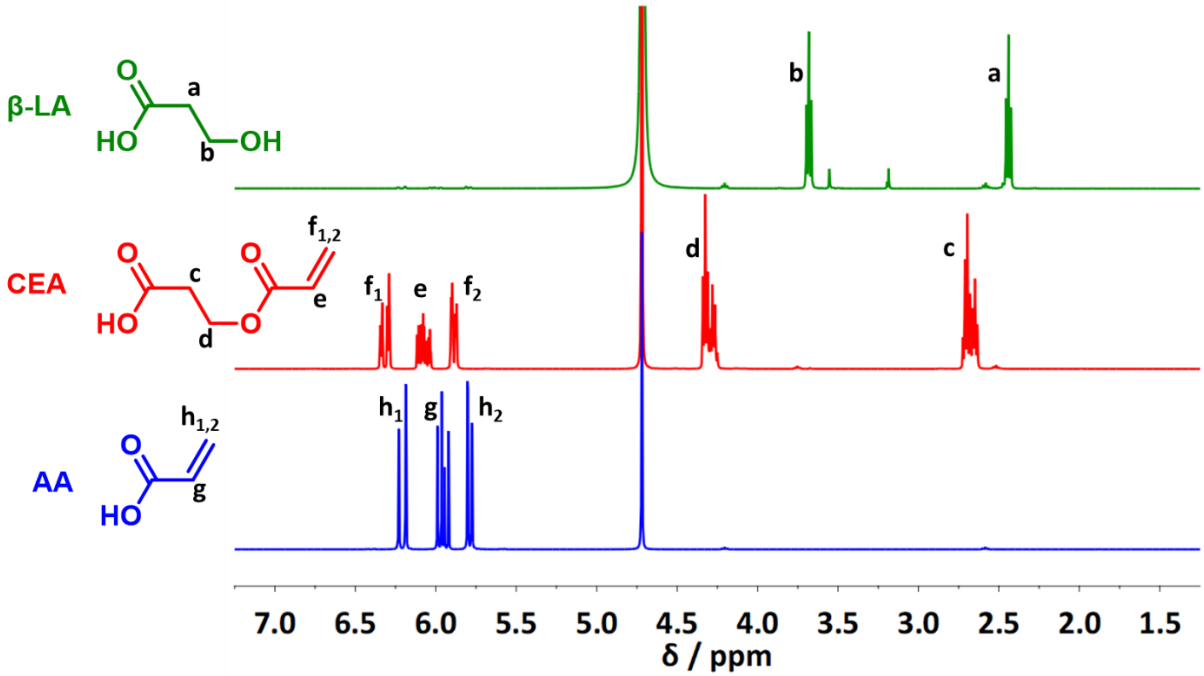

Figure 6.7 Annotated ^{1}H NMR spectra (recorded in D_2O) of acrylic acid (AA), 2-carboxyethyl acrylate (CEA) and β-lactic acid (β-LA).

Subsequently, ^{1}H NMR spectroscopy was used to study the kinetics of the CEA polymerisation at 46°C when targeting $PAMPS_{230}$-$PCEA_{8000}$ particles at 30% w/w solids (see **Figure 6.8a**). Periodic sampling of the reaction mixture confirmed that a CEA conversion of 98% was achieved within 17 h under such conditions. The protons corresponding to the PCEA and PAA (hydrolysis product) polymer repeat units have been annotated on **Figure 6.8b**. The quantity of β-LA formed by hydrolysis of the (P)CEA species has been determined to be about 23 mol % in the final ^{1}H NMR spectrum. Further investigation into the minimisation of this hydrolysis needs to be considered. For example, it is proposed that the addition of 0.1 M NaOD to the polymer in the ^{1}H NMR preparation could cause some hydrolysis before the solution pH has time to equilibrate to pH 5.

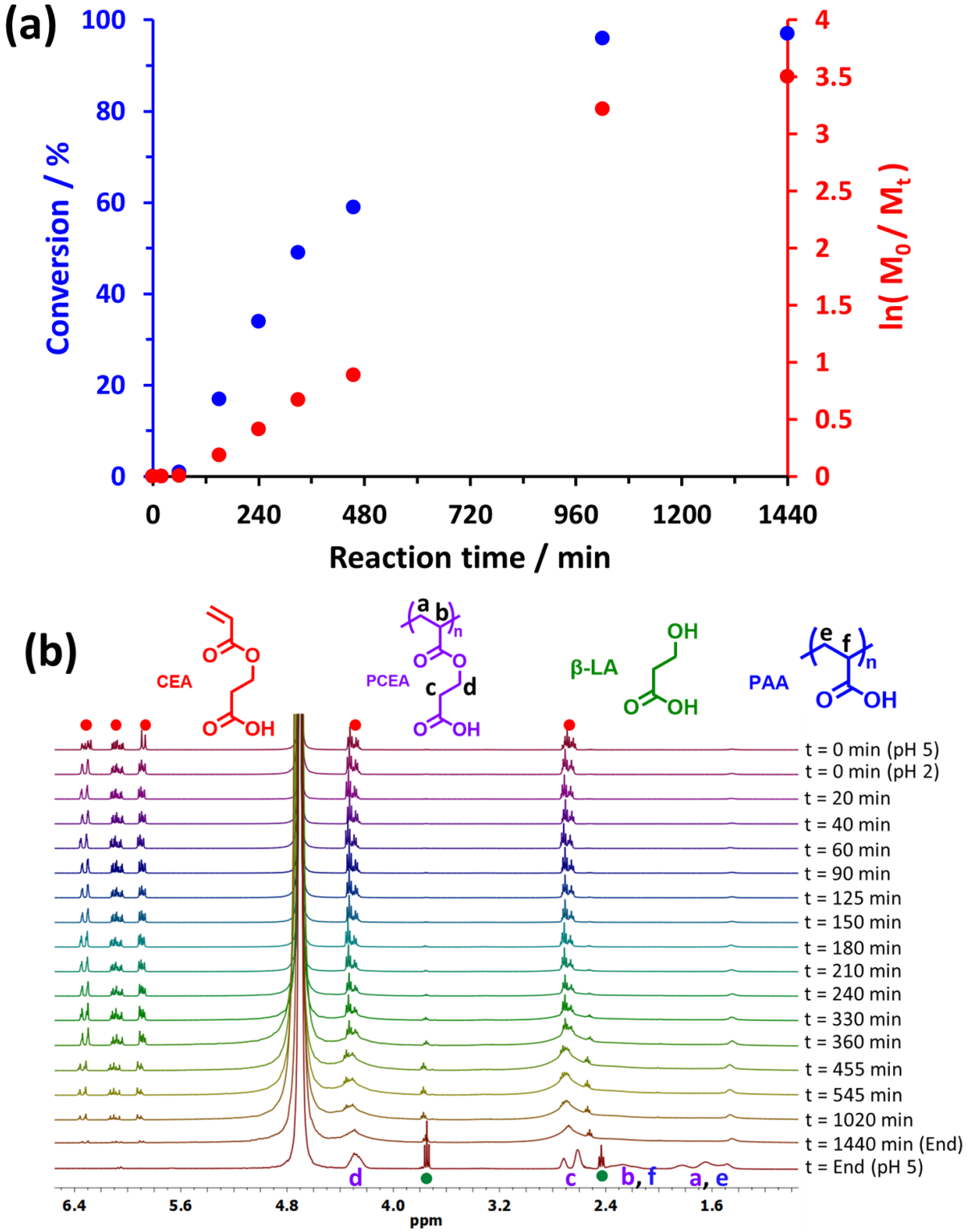

Figure 6.8 (a) Conversion vs. time curve determined by ^{1}H NMR spectroscopy studies of the RAFT aqueous dispersion polymerisation of CEA at 46°C when targeting a PCEA DP of 8,000 at 30% w/w solids and pH 2.0 over a 24 h (1440 min) timescale. (b) ^{1}H NMR kinetic samples obtained for this polymerisation. Samples were run at pH 2.0 unless specified otherwise.

^{1}H NMR spectra were recorded for the $PAMPS_{230}$-$PCEA_{2000}$ as a function of solution pH. The effect of hydrolysis has been discussed previously, so for clarity in the NMR spectra, the polymer was dialysed against deionised water (pH 6.5) and the purified polymer was carefully adjusted to specific pH values which were analysed and are shown in **Figure 6.9**. The acrylic backbone signals are weakly visible at pH 2.0 because the PCEA chains – which form the major component of this diblock copolymer – are not solvated under such conditions. These signals are resolved at pH 4 owing to solvation of the partially ionised PCEA chains. However, they become poorly resolved at pH 6 and 9 owing to the high solution viscosity conferred by the molecularly dissolved copolymer chains. Above pH 9, base-catalysed hydrolysis of the ester groups within the PCEA chains leads to the elimination of β-LA as a small molecule side-product. The degree of hydrolysis for the pH 12 sample which was left for about 3 hours before analysis is approximately 46 mol %. The large singlet peak in **Figure 6.9** shifts from 2.7 ppm when the carboxylic acid group is protonated, to 2.5 ppm when the group is ionised. This peak represents the two methylene protons (*c*) adjacent to the carboxylic acid group and its chemical shift is pH dependent. For the solvated polymer spectrum at pH 9.0 this peak is a singlet at 2.5 ppm, whereas at pH 6.0 a large peak at 2.5 ppm is present alongside a small peak at 2.7 ppm which indicates a small portion of protonated PCEA remains. Furthermore, the final *ca*. pH 5 NMR spectrum shown in **Figure 6.8b** has both peaks which indicates partial ionisation of the carboxylic acid groups. This is consistent with the measured pK_a value of 5.1 being at the 50% degree of ionisation point.

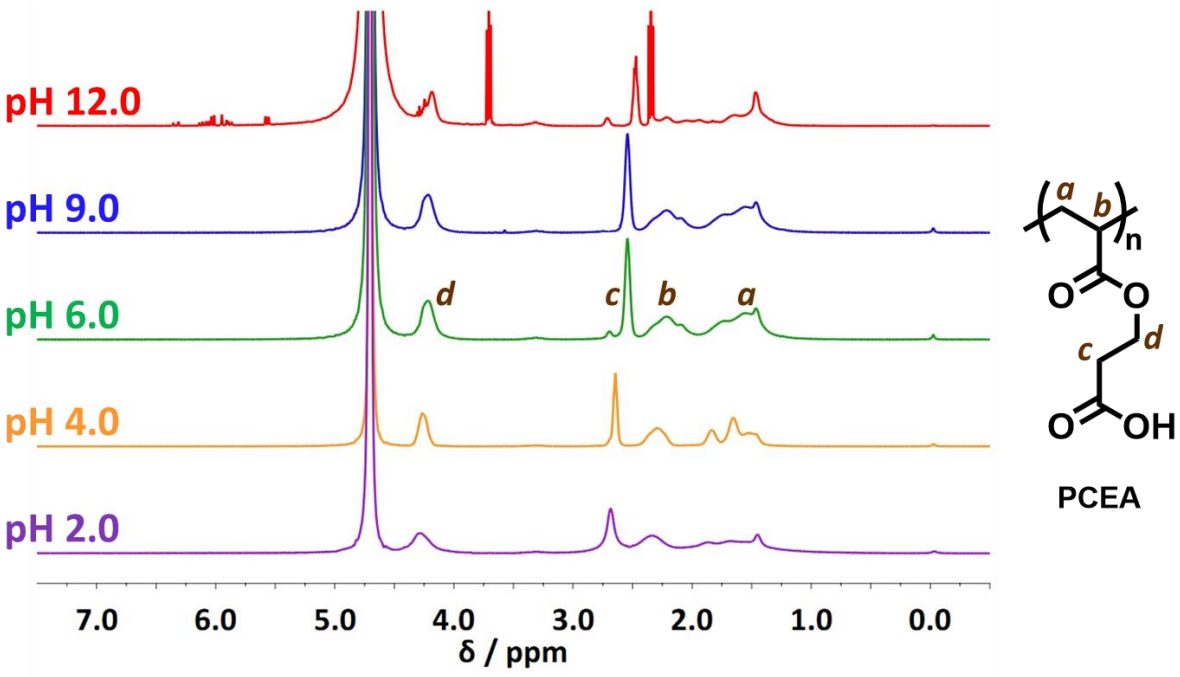

Figure 6.9 ^{1}H NMR spectroscopy studies of a $PAMPS_{230}$-$PCEA_{2000}$ diblock copolymer when varying the solution pH from pH 2.0 to pH 12.0. Careful addition of NaOD/D_2O to the dried purified polymer enabled spectra to be recorded at pH 2.0 (purple spectrum), pH 4.0 (orange spectrum), pH 6.0 (green spectrum), pH 9.0 (blue spectrum) and pH 12.0 (red spectrum).

Laser diffraction has been well-established as a particle sizing technique for micron-sized particles.[18–21] The Malvern Mastersizer 3000 instrument used in this study is equipped with a dispersion unit. Each aqueous dispersion is constantly stirred and pumped through the sample chamber, so particles cannot undergo gravitational sedimentation on the time scale of the measurement. A double log plot reveals that the volume-average particle diameter increases monotonically with the PCEA DP, see **Figure 6.10**. According to the literature, the power law exponent of 1.06 suggests that these particles are likely to have a relatively high degree of hydration.[22–24]

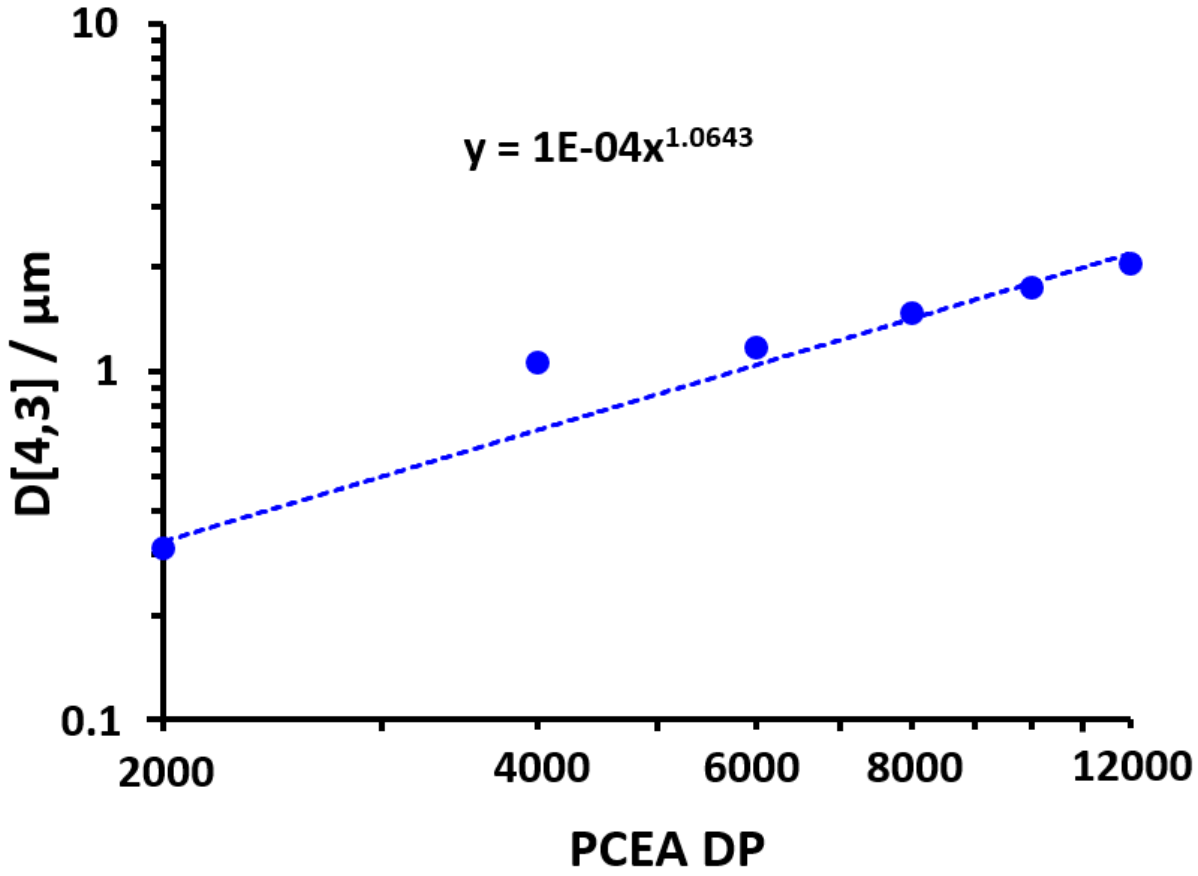

Figure 6.10 Logarithmic relationship between the volume-average diameter (D_v, reported by laser diffraction) and the mean degree of polymerisation (DP) of the core-forming PCEA block for a series of six $PAMPS_{230}$-$PCEA_x$ particles (x = 2,000 to 12,000) prepared via RAFT aqueous dispersion polymerisation of CEA at 46°C in pH 2.0 aqueous solution (see **Table 6.2**).

The optical microscopy image shown in **Figure 6.11a** indicates that the $PAMPS_{230}$-$PCEA_{8000}$ particles have a spherical morphology with a mean diameter of 1.80 ± 0.56 µm (which is the effective resolution limit for this imaging technique). Furthermore, since there is no salt present in these copolymer dispersions, they are amenable to electron microscopy techniques unlike some other formulations in this Thesis. A representative TEM image is shown in **Figure 6.11b** which finds the mean diameter of the spherical particle to be 2.10 ± 0.12 µm. These values are very similar to each other and are both larger than the D_v of 1.48 µm determined by laser diffraction. These particle sizing techniques are more appropriate for assessing particles diameters > 1 µm compared to DLS.[25]

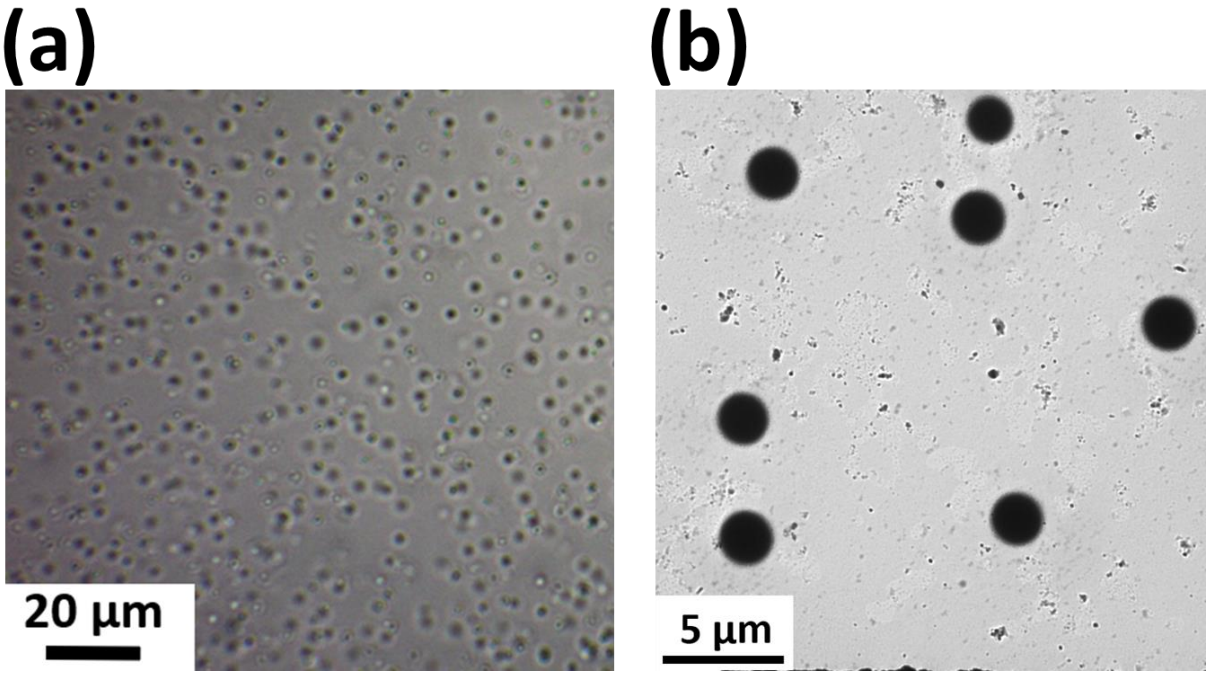

Figure 6.11 (a) Representative optical microscopy image recorded for $PAMPS_{230}$-$PCEA_{8000}$ particles prepared at 30% w/w solids by RAFT aqueous dispersion polymerisation of CEA at 46°C in acidic aqueous solution (pH 2.0). (b) Representative TEM image recorded for the same particles.

Viscosity data obtained via rheometry for a shear sweep from 0.005 to 100 s^{-1} for the $PAMPS_{230}$-$PCEA_{8000}$ formulation is shown in **Figure 6.12**. A low solution viscosity is measured across all shear rates for the as-synthesised particle dispersion at pH 2.0. This sample is a free-flowing turbid dispersion which exhibits shear thinning behaviour. Increasing the solution pH from 2 to 4 led to a significant increase in viscosity at all shear rates as some of the PCEA chains are ionised which causes the polymer to have a higher degree of dissolution in the solvent. Further increasing the pH to 6 continued to increase the solution (or gel) viscosity owing to further ionisation of the PCEA. The titration data in **Figure 6.5** indicates that the corresponding increase in the degree of ionisation is from 20 to 76% for this pH change. The gel viscosity is almost unchanged at pH 9, whereas a significant reduction in gel viscosity occurs at pH 12 owing to *in situ* hydrolysis of the ester bonds in the PCEA chains which reduces the polymer molecular weight. Additionally, although the resulting acrylic acid repeat units are

also ionised under these conditions, the β-LA side-product acts as a salt to screen the repulsive interactions between the anionic P(CEA-*stat*-AA) chains.

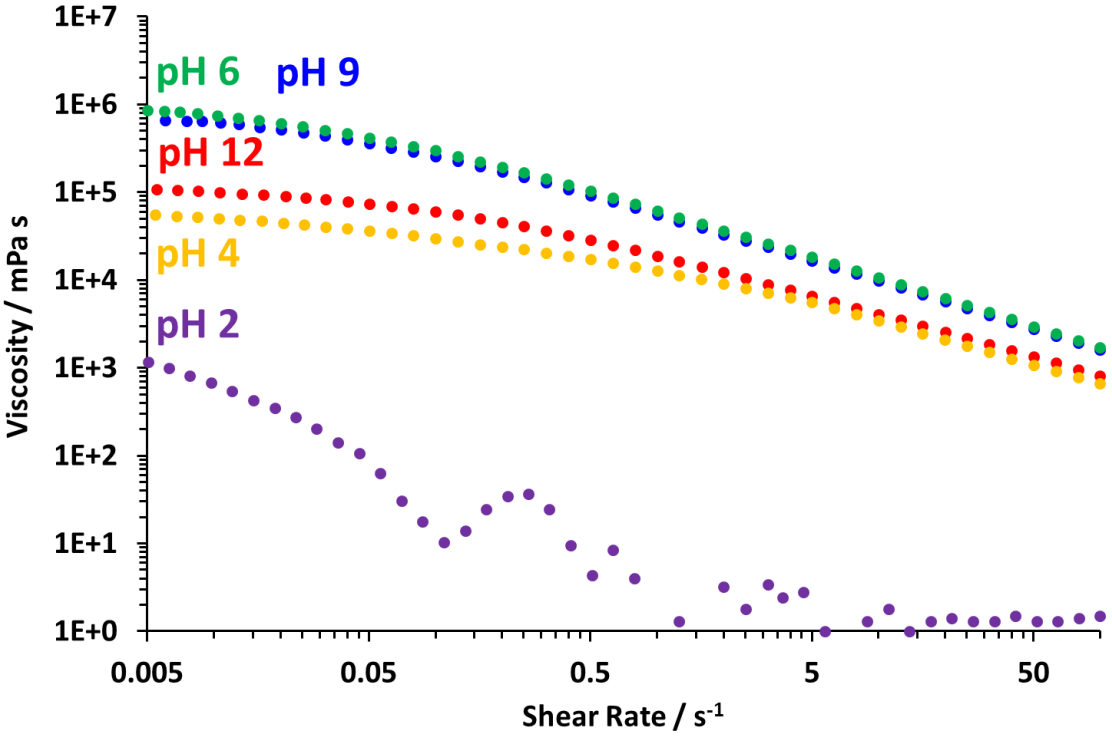

Figure 6.12 Solution viscosity data obtained for $PAMPS_{230}$-$PCEA_{8000}$ via rotational rheometry as a function of shear rate for a 5.0% w/w copolymer concentration at pH 2 (purple), pH 4 (orange), pH 6 (green), pH 9 (blue) and pH 12 (red).

The data in **Figure 6.12** does not show a linear zero-shear viscosity regime with the conditions used, so it is appropriate to compare datasets at a fixed shear rate value. Further study of the $PAMPS_{230}$-$PCEA_{8000}$ formulation at 0.5 s^{-1} with variation of the copolymer concentration between 0.3 and 5% w/w across the range of pH values is shown in **Figure 6.13**. As expected, reducing the copolymer concentration led to lower solution viscosities. It was not convenient to characterise more concentrated gels via rheometry because they were too viscous to load into the instrument. A 5% copolymer dispersion is a turbid, free-flowing fluid, whereas the 5% w/w copolymer solution formed a transparent free-standing gel (e.g. η = 105 Pa s at a shear rate of 0.5 s^{-1}) at pH 6. The intrinsic viscosity [η] is related to the viscosity-average molecular weight (M_v) by the Mark-Houwink relation[26] and it is known that the M_v is usually

comparable to M_w (within 10%).[27] This means that the polymers synthesised, which are reported to have relatively large M_w/M_n values, form solutions with greater viscosities than those with narrower MWDs.

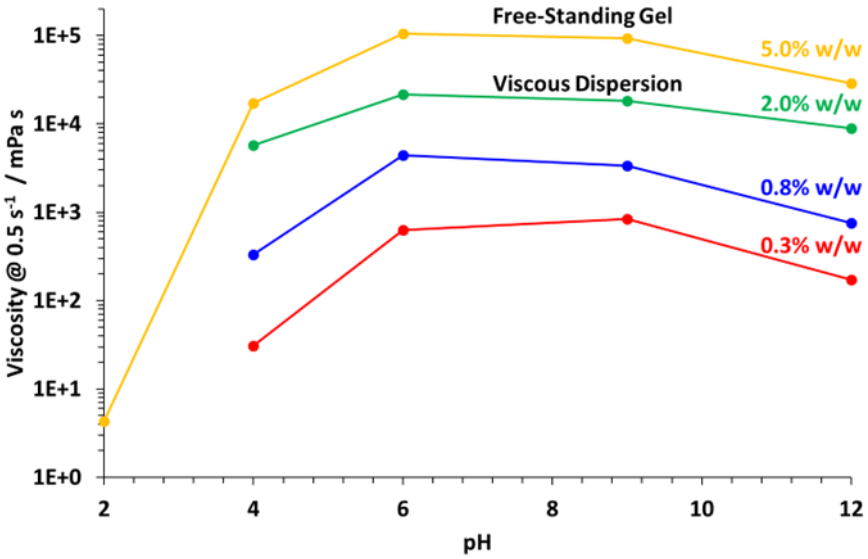

Figure 6.13 Viscosity data obtained for $PAMPS_{230}$-$PCEA_{8000}$ via rotational rheometry measurements at pH 4, 6, 9 or 12 with a shear rate of 0.50 s^{-1} and copolymer concentrations of 5.0% w/w (orange), 2.0% w/w (green), 0.8% w/w (blue) or 0.3% w/w (red).

It is well-known that the addition of salt to polyelectrolytes results in a reduction in the solution viscosity.[28,29] However, no discernible reduction in the gel viscosity for a pH 6 solution of 5.0% w/w $PAMPS_{230}$-$PCEA_{8000}$ was observed, even in the presence of 1.0 M $(NH_4)_2SO_4$. This unexpected observation means that the $PAMPS_x$-$PCEA_y$ formulation may be suitable for a wide range of commercial applications, including in the oilfield and mining sectors which may require thickeners which can cope with a high background electrolyte concentration.

6.4 Conclusions

An anionic PAMPS steric stabiliser was selected for its excellent salt tolerance and its ability to confer electrosteric stabilisation. We report the zero-salt synthesis of a series of sterically-stabilised $PAMPS_{230}$-$PCEA_x$ diblock copolymer particles (x = 2,000 to 12,000) via RAFT aqueous dispersion polymerisation of CEA at 30% w/w solids in acidic aqueous media (pH

2.0). Under such conditions, ionisation of the PCEA block is suppressed and these neutral chains become hydrophobic at a certain critical DP, which drives self-assembly to form sterically-stabilised particles. The ionisation variation with pH was identified via potentiometric titration, which also enabled determination of the pK_a of the PCEA block. The resulting diblock copolymer particles formed turbid low-viscosity dispersions at pH 2.0. Optical microscopy and TEM indicated the presence of micron-sized particles with a polydisperse spherical morphology. Laser diffraction data were consistent with these observations and confirmed a modest increase in particle size when targeting higher PCEA DPs. The realistic upper limit PCEA DP was judged to be 10,000 because partial precipitation was observed when targeting a higher PCEA DP. Aqueous GPC analysis of the anionic diblock copolymer chains indicated reasonably efficient chain extension of the $PAMPS_{230}$ precursor and a systematic increase in molecular weight when targeting higher PCEA DPs. However, rather broad molecular weight distributions (M_w/M_n > 2.0) were obtained owing to the relatively low $PAMPS_{230}$/VA-044 ratio required for such syntheses, which proved to be essential to ensure high CEA conversions.

Raising the solution pH caused ionisation of the PCEA block and hence molecular dissolution of the diblock copolymer particles, which led to a substantial increase in viscosity. The initial gel contained trapped air bubbles, which disappeared overnight to produce a free-standing transparent gel. The theoretical M_n value for $PAMPS_{230}$-$PCEA_{8000}$ is approximately 1.18 x 10^6 g mol^{-1}, respectively. Given that the corresponding M_w/M_n values is 4.01, this suggests a corresponding M_v value of the order of 4.73 x 10^6 g mol^{-1}, which accounts for the relatively high solution viscosity observed for this formulation at pH 6.0.

Base-catalysed hydrolysis of the ester groups within the PCEA block has been observed by ^{1}H NMR spectroscopy. This side-reaction also occurred in a study reported by North et al. but was not recognised at the time.[11] This problem can be minimised by avoiding alkaline

conditions when adding NaOH (*aq.*) to ionise the PCEA block. ^{1}H NMR spectroscopy can be used to monitor the increasing solvation of the PCEA block when raising the solution pH. In addition, this technique can be used to quantify the extent of *in situ* hydrolysis of the PCEA block, which generates β-LA as a side-product. Further investigation into the most appropriate storage conditions for $PAMPS_{230}$-$PCEA_x$ diblock copolymers should be made. The particles are known to be stable around pH 2, though potential acid hydrolysis in this environment should also be considered. The use of buffers could also assist in maintaining an appropriate pH value, although the mixing of salt with the polyelectrolyte may cause a reduction in solution viscosity.

Rheological studies of the $PAMPS_{230}$-$PCEA_{8000}$ formulation as a function of shear rate at various copolymer concentrations and solution pH values has enabled identification of the conditions required to maximise the thickening effect. Remarkably, the highly viscous, free-standing transparent gels formed by the highly anionic $PAMPS_{230}$-$PCEA_{8000}$ diblock copolymer chains seem to be relatively insensitive to the addition of added salt (1.0 M ammonium sulfate).

6.5 References

1 R. R. Gibson, S. P. Armes, O. M. Musa and A. Fernyhough, 'End-group ionisation enables the use of poly(: N -(2-methacryloyloxy)ethyl pyrrolidone) as an electrosteric stabiliser block for polymerisation-induced self-assembly in aqueous media', *Polym. Chem.*, 2019, **10**, 1312–1323.

2 D. L. Beattie, O. J. Deane, O. O. Mykhaylyk and S. P. Armes, 'RAFT aqueous dispersion polymerization of 4-hydroxybutyl acrylate: Effect of end-group ionization on the formation and colloidal stability of sterically-stabilized diblock copolymer nanoparticles', *Polym. Chem.*, 2022, **13**, 655–667.

3 Lubrizol: Carbopol, https://www.lubrizol.com/Home-Care/Products/Carbopol-Polymers.

4 T. Swift, L. Swanson, M. Geoghegan and S. Rimmer, 'The pH-responsive behaviour of poly(acrylic acid) in aqueous solution is dependent on molar mass', *Soft Matter*, 2016, **12**, 2542–2549.

5 X. Bories-Azeau, S. P. Armes and H. J. W. Van Den Haak, 'Facile Synthesis of Zwitterionic Diblock Copolymers without Protecting Group Chemistry', *Macromolecules*, 2004, **37**, 2348–2352.

6 X. Bories-Azeau, T. Mérian, J. V. M. Weaver, S. P. Armes and H. J. W. Van Den Haak, 'Synthesis of near-monodisperse acidic homopolymers and block copolymers from hydroxylated methacrylic

copolymers using succinic anhydride under mild conditions', *Macromolecules*, 2004, **37**, 8903–8910.

7 J. Zhang and N. A. Peppas, 'Synthesis and Characterization of pH- and Temperature-Sensitive Poly(methacrylic acid)/Poly(N -isopropylacrylamide) Interpenetrating Polymeric Networks', *Macromolecules*, 2000, **33**, 102–107.

8 L. López-Pérez, H. Maldonado-Textle, L. E. Elizalde-Herrera, J. G. Telles-Padilla, R. Guerrero-Santos, S. Collins, E. J. Jiménez-Regalado and C. St Thomas, 'Methylation of poly(acrylic acid), prepared using RAFT polymerization, with trimethylsilyldiazomethane: A metamorphosis of the thiocarbonyl group to a thiol-end group', *Polymer*, 2019, **168**, 116–125.

9 S. S. Cutié, G. J. Kallos and P. B. Smith, 'Separation and characterization of acrylic acid oligomers by nuclear magnetic resonance spectroscopy and thermospray ion-exchange liquid chromatography-mass spectrometry', *J. Chromatogr. A*, 1987, **408**, 349–355.

10 T. L. Staples and P. K. Chatterjee, 2002, pp. 283–322.

11 S. M. North and S. P. Armes, 'One-pot synthesis and aqueous solution properties of pH-responsive schizophrenic diblock copolymer nanoparticles prepared via RAFT aqueous dispersion polymerization', *Polym. Chem.*, 2021, **12**, 5842–5850.

12 A. Katchalsky and H. Eisenberg, 'Molecular weight of polyacrylic and polymethacrylic acid', *J. Polym. Sci.*, 1951, **6**, 145–154.

13 C. Bray, R. Peltier, H. Kim, A. Mastrangelo and S. Perrier, 'Anionic multiblock core cross-linked star copolymers: via RAFT polymerization', *Polym. Chem.*, 2017, **8**, 5513–5524.

14 J. T. Lai, D. Filla and R. Shea, 'Functional Polymers from Novel Carboxyl-Terminated Trithiocarbonates as Highly Efficient RAFT Agents', *Macromolecules*, 2002, **35**, 6754–6756.

15 E. V. Piletska, A. R. Guerreiro, M. Romero-Guerra, I. Chianella, A. P. F. Turner and S. A. Piletsky, 'Design of molecular imprinted polymers compatible with aqueous environment', *Anal. Chim. Acta*, 2008, **607**, 54–60.

16 P. Gurnani, C. P. Bray, R. A. E. Richardson, R. Peltier and S. Perrier, 'Heparin-Mimicking Sulfonated Polymer Nanoparticles via RAFT Polymerization-Induced Self-Assembly', *Macromol. Rapid Commun.*, 2019, **40**, 1–7.

17 R. J. McBride, J. F. Miller, A. Blanazs, H. J. Hähnle and S. P. Armes, 'Synthesis of High Molecular Weight Water-Soluble Polymers as Low-Viscosity Latex Particles by RAFT Aqueous Dispersion Polymerization in Highly Salty Media', *Macromolecules*, 2022, **55**, 7380–7391.

18 J. Ormond-Prout, D. Dupin, S. P. Armes, N. J. Foster and M. J. Burchell, 'Synthesis and characterization of polypyrrole-coated poly(methyl methacrylate) latex particles', *J. Mater. Chem.*, 2009, **19**, 1433.

19 D. H. Chan, A. Millet, C. R. Fisher, M. C. Price, M. J. Burchell and S. P. Armes, 'Synthesis and Characterization of Polypyrrole-Coated Anthracene Microparticles: A New Synthetic Mimic for Polyaromatic Hydrocarbon-Based Cosmic Dust', *ACS Appl. Mater. Interfaces*, 2021, **13**, 3175–3185.

20 D. H. H. Chan, E. L. Kynaston, C. Lindsay, P. Taylor and S. P. Armes, 'Block Copolymer Nanoparticles are Effective Dispersants for Micrometer-Sized Organic Crystalline Particles', *ACS Appl. Mater. Interfaces*, 2021, **13**, 30235–30243.

21 D. H. H. Chan, J. L. Wills, J. D. Tandy, M. J. Burchell, P. J. Wozniakiewicz, L. S. Alesbrook and S. P. Armes, 'Synthesis of Autofluorescent Phenanthrene Microparticles via Emulsification: A Useful

Synthetic Mimic for Polycyclic Aromatic Hydrocarbon-Based Cosmic Dust', *ACS Appl. Mater. Interfaces*, 2023, **15**, 54039–54049.

22 M. J. Derry, L. A. Fielding, N. J. Warren, C. J. Mable, A. J. Smith, O. O. Mykhaylyk and S. P. Armes, 'In situ small-angle X-ray scattering studies of sterically-stabilized diblock copolymer nanoparticles formed during polymerization-induced self-assembly in non-polar media', *Chem. Sci.*, 2016, **7**, 5078–5090.

23 F. S. Bates and G. H. Fredrickson, 'Block copolymer thermodynamics: Theory and experiment', *Annu. Rev. Phys. Chem.*, 1990, **41**, 525–557.

24 S. Förster, M. Zisenis, E. Wenz and M. Antonietti, 'Micellization of strongly segregated block copolymers', *J. Chem. Phys.*, 1996, **104**, 9956–9970.

25 'International Organisation for Standardisation: Particle size analysis, Dynamic light scattering (DLS), ISO 22412: 2017', 1–34.

26 J. D. Ferry, *Viscoelastic Properties of Polymers (2nd Ed.)*, John Wiley & Sons, New York, 2nd edn., 1970.

27 J. W. Gooch, in *Encyclopedic Dictionary of Polymers*, Springer, New York, 2011, pp. 799–799.

28 G. Chen, A. Perazzo and H. A. Stone, 'Influence of Salt on the Viscosity of Polyelectrolyte Solutions', *Phys. Rev. Lett.*, 2020, **124**, 177801.

29 J. Barrat and F. Joanny, in *Theory of Polyelectrolyte Solutions*, Wiley, New York, 1996, pp. 1–66.

Chapter 7: Conclusions and Outlook

7.1 Conclusions and Outlook

The ubiquitous use of modern synthetic polymers has been driven by the desire for a diverse range of materials for bespoke applications. This demand remains high, although the focus has shifted towards more efficient, sustainable formulations.[1–3] This Thesis reports the development of a novel class of thickeners, which are initially prepared in the form of free-flowing low-viscosity particles. Subsequently, either lowering the salt concentration or raising the solution pH leads to a substantial increase in viscosity by several orders of magnitude to produce transparent free-standing gels. This PhD project was sponsored by BASF which is a company who manufacture a range of polymeric thickeners for their Nutrition & Care, Oilfield, and Materials businesses. Furthermore, they hold many patents in the manufacture of latex particles at high solids.[4–7] Current commercial thickeners such as anionic polyacrylamide Alcomers produced by BASF are widely used as dewatering additives in the oilfield sector. Such copolymers also exhibit a strong thickening effect when dissolved in water. However, they are dispensed in powdered form and dissolution in aqueous solution is quite slow and requires thorough mixing.[8]

Chapter 2 reports the synthesis of various trithiocarbonate-based RAFT agents that are suitable for the controlled polymerisation of a range of vinyl monomers, including acrylates, methacrylates, acrylamides and methacrylamides. These reagents enabled the synthesis of eighteen homopolymers via RAFT solution polymerisation. Aqueous solubility tests for each hydrophilic monomer and its corresponding water-soluble homopolymer were conducted across a range of ammonium sulfate concentrations. Visual inspection was used to judge whether full solubility had been achieved. Comparison of the critical salt concentration required to precipitate each homopolymer allowed the identification of suitable salt-tolerant stabiliser blocks and salt-intolerant core-forming blocks. Judicious selection of appropriate

aqueous PISA formulations was then made. The same tests also indicated when certain water-miscible vinyl monomers became water-immiscible in the presence of salt.

Chapter 2 also includes further experimental details regarding the PATAC-PDMAC formulation reported by Byard that led to the current PhD project.[9] In her prior study, the PATAC stabiliser DP was 100. In contrast, a PATAC DP of 242 was chosen for the experiments reported in **Chapter 2** to aid the electrosteric stabilisation of polymer particles when targeting relatively long core-forming blocks. This approach was expected to enhance the colloidal stability of the nanoparticles: according to the PISA literature, it would likely result in a kinetically-trapped spherical morphology, which is desirable to minimise the dispersion viscosity.[10,11] RAFT aqueous dispersion polymerisation syntheses conducted at 20% w/w solids enabled high monomer conversions to be achieved up to a PDMAC DP of 12,400, which corresponds to a theoretical molecular weight of 1.2 x 10^6 g mol^{-1}. Relative molecular weight data can be determined experimentally using GPC, where M_n values from the RI detector are calculated relative to a set of calibration standards. In addition, M_w values can be obtained by static light scattering using a MALLS GPC detector. The former detector requires PEO calibration standards, which results in systematic under-estimation of M_n; in contrast, the latter detector determines absolute M_w values. For the highest molecular weight $PATAC_{242}$-$PDMAC_{12400}$ diblock copolymer, an M_w of more than 2.0 x 10^6 g mol^{-1} is reported. Moreover, a unimodal MWD was obtained, whereas Byard reported a bimodal MWD in her preliminary experiments. Rheological studies enabled quantification of the thickening effect achieved over a wide range of shear rates. For example, the solution viscosity of $PATAC_{242}$-$PDMAC_{6200}$ was three orders of magnitude higher than the initial dispersion viscosity at an arbitrary shear rate of 3.0 s^{-1}. Furthermore, a monomer-starved feed protocol was employed to target copolymer particles at higher solids. This approach produced rather polydisperse particles, but the final

DMAC conversion was typically more than 97% and free-standing gels were obtained after a four-fold dilution with deionised water.

Chapter 3 reports the use of a highly salt-tolerant zwitterionic PMPC steric stabiliser for the synthesis of PMPC-PDMAC nanoparticles in 2.0 M ammonium sulfate.[11] A series of colloidally stable copolymer dispersions were obtained at 20% w/w solids: targeting higher PDMAC DPs produced a monotonic increase in both the GPC M_n and the hydrodynamic z-average particle diameter. When targeting a PDMAC DP of either 500 or 1,000, some of the copolymer chains remain in the aqueous continuous phase, producing a translucent gel instead of a free-flowing turbid dispersion. Selected copolymer dispersions were characterised using synchrotron SAXS at Diamond Light Source.[12] Volume-average diameters were calculated by fitting SAXS patterns using a spherical model and were slightly lower than the z-average diameters reported by DLS. The DMAC polymerisation exhibited first-order kinetics as judged by ^{1}H NMR spectroscopy and aqueous GPC analysis confirmed a monotonic increase in M_n with target PDMAC DP. Analysis of the electrophoretic mobility of the $PMPC_{139}$-$PDMAC_{1000}$ particles in the presence of 2.0 M ammonium sulfate was performed by Dr. John F. Miller of Enlighten Scientific LLC using his state-of-the-art instrument. This protocol was repeated for two other PDMAC-based copolymer dispersions prepared using either an anionic or a cationic steric stabiliser block. The resulting apparent zeta potential vs. pH plots indicated the formation of neutral (PMPC stabiliser), anionic (PAMPS stabiliser) or cationic (PATAC stabiliser) copolymer particles, with little variation in the apparent zeta potential being observed over a wide pH range.

Chapter 4 examines industrially relevant aqueous PISA formulations using commodity monomers such as acrylic acid, acrylamide and acrylonitrile.[13] First, a poly(acrylic acid) stabiliser was prepared by RAFT solution polymerisation. Prior to its chain extension, a small quantity of sodium bicarbonate was added to produce poly(sodium acrylate) (PNaAc) chains,

which are soluble in 3.0 M ammonium sulfate. The RAFT synthesis of cationic polyacrylamide-based particles has been reported by Huang et al.,[14] while Bai et al.[15] have described the preparation of anionic polyacrylamide-based particles. However, such studies did not focus on maximising either the upper limit solids content or PAM DP achievable at high monomer conversions. As the salt concentration was reduced from 3.0 M to 1.5 M ammonium sulfate via two-fold dilution using deionised water, ^{1}H NMR spectroscopy studies of a PNaAc-PAM copolymer confirmed full hydration of the PAM chains. Small quantities of DMAC as a comonomer was introduced into the core-forming block via statistical copolymerisation with AM. As expected, the resulting P(AM-*stat*-DMAC) core-forming block formed a free-standing hydrogel at a lower DP than that required for a PAM homopolymer. Use of ACN may also be possible, but due to its high volatility, it was not amenable to the experimental procedures used. A preliminary viscosity evaluation of such samples relative to BASF's Alcomer products suggests that these formulations may offer some potential for oilfield applications.

A new 'low salt' aqueous PISA formulation based on a wholly non-ionic diblock copolymer is developed in **Chapter 5**. More specifically, an efficient one-pot synthesis protocol is devised for the preparation of a series of six $PHEAC_{216}$-$PNAM_{1000\text{-}6000}$ particles, where PNAM is a particularly salt-intolerant water-soluble polymer. Both laser diffraction and dynamic light scattering were used to assess mean particle diameters and good agreement was observed when targeting PNAM DPs from 1,000 to 6,000. The use of a GPC MALLS detector enabled absolute M_w values to be measured once the dn/dc value of such copolymers had been determined. A Zimm plot was constructed for $PHEAC_{216}$-$PNAM_{6000}$, which indicated an M_w of approximately 2.5 x 10^6 g mol^{-1}. Static laser light scattering was also used to estimate the radius of gyration for five of the six copolymers: this parameter increased from 20 to 66 nm as the target PNAM DP was raised from 2,000 to 6,000.

Finally, **Chapter 6** considers the use of a carboxylic acid-based core-forming block to prepare sterically-stabilised particles at pH 2.0 – 2.5. In this case, the objective was to design a high molecular weight pH-responsive polyelectrolyte for viscosity modification. An anionic PAMPS steric stabiliser was selected for its excellent salt tolerance and its ability to confer electrosteric stabilisation. Subsequently, a new 'zero salt' aqueous PISA formulation was developed based on the RAFT aqueous dispersion polymerisation of 2-carboxyethyl acrylate (CEA) at pH 2.0 using the same PAMPS precursor. A potentiometric titration indicated that the resulting core-forming PCEA block had a pK_a of approximately 5.1. A series of $PAMPS_{230}$-$PCEA_{2000\text{-}12000}$ particles were prepared and laser diffraction studies indicated volume-average particle diameters ranging from 0.3 to 2.0 μm. These results were corroborated by optical microscopy studies, which indicated a polydisperse spherical morphology for the larger particles. On adjusting the solution pH from pH 2 to pH 6 for a $PAMPS_{230}$-$PCEA_{8000}$ formulation, ionisation of the PCEA block led to *in situ* molecular dissociation of the initial particles to produce a highly viscous transparent gel. Moreover, these gels remained free-standing on dilution to 5.0% w/w copolymer concentration. Clearly the initial acidity may be problematic for some applications, but such copolymers are undoubtedly effective viscosity modifiers.

A summary of all of the highest MW aqueous PISA syntheses is provided in **Table 7.1**, which enables comparison of the chemical and physical properties of such formulations.

Stabiliser Block	Core-forming Block	Solids / % w/w	Conversion / %	Theoretical M_n / kg mol^{-1}	Sulfur Content / ppm	Viscosity @ 0.1 s^{-1} / Pa s	Viscosity Comment
$PATAC_{242}$	$PDMAC_{12400}$	20	96	1227	16	— (5% w/w)	highly viscous
$PATAC_{242}$	$PDMAC_{10000}$*	40	99	1031	37	— (10% w/w)	free-standing gel
$PMPC_{139}$	$PDMAC_{6000}$	20	99	629	31	3.3 (10% w/w)	highly viscous
$PNaAc_{258}$	PAM_{12000}	12	97	846	14	— (6% w/w)	very highly viscous
$PNaAc_{258}$	$P(AM_{11000}$-*stat*-$DMAC_{2500})$	14	> 99	1048	13	188 (7% w/w)	free-standing gel
$PHEAC_{216}$	$PNAM_{6000}$	20	97	846	23	2.1 (10% w/w)	highly viscous
$PAMPS_{230}$	$PCEA_{8000}$	30	98	1182	24	300 (5% w/w)	free-standing gel

Table 7.1 Summary of the maximum core block DP, solids content, monomer conversion, theoretical M_n, sulfur content and solution viscosity obtained for the various new aqueous PISA formulations developed in this Thesis. * The $PATAC_{242}$-$PDMAC_{10000}$ diblock copolymer was synthesised at 40% w/w solids using a monomer-starved feed protocol.

The organosulfur content of each of the reported formulations is less than 37 ppm for the as-synthesised dispersions, so the undesirable colour and malodour conferred by the RAFT agent is minimised. As the RAFT agent is the most expensive component in such syntheses, the manufacturing cost is also significantly reduced. The solids content of the final diblock copolymer nanoparticles ranges from 12 to 40% w/w. This is comparable to that claimed by Destarac et al., who claimed that up to 50% w/w solids could be obtained via 'water-in-water' RAFT polymerisation.[16]

One of the most promising formulations is $PAMPS_{230}$-$PCEA_{8000}$, which produces a free-standing gel after pH adjustment with NaOH. Even after a six-fold dilution to 5% w/w, the anionic carboxylate groups on the PCEA chains produce a free-standing gel with a viscosity of 300 mPa s at a shear rate of 0.5 s^{-1}. The organosulfur content contained per polymer chain is amongst the lowest of all the formulations, it corresponds to just 24 ppm for the as-synthesised 30% w/w copolymer dispersion. The main disadvantages of this formulation is the relatively low pH and the likelihood of further hydrolysis of the ester groups on the PCEA chains during low-term storage under such conditions, which would cause premature gelation. In principle, optimal pH control during and after the synthesis could mitigate this problem. Alternatively, other carboxylic acid-containing monomers such as 3-methacryloylaminopropionic acid (MAAP) could be evaluated since the corresponding polymer should be much more resistant to hydrolytic degradation. Alternatively, a molecule such as 4-vinylphenol, which is predicted to have a pKa of 9.95 using ACD/Labs software,[17] may form particles at low and intermediate pH values, but will solubilise into chains only in alkaline media. The aromatic group in the structure of this monomer should cause it to be highly resistant to hydrolytic degradation.

The most innovative formulation reported in this Thesis is the $PHEAC_{216}$-$PNAM_{6000}$ copolymer. As a fully non-ionic system, its one-pot aqueous synthesis in the presence of just 0.60 M ammonium sulfate shows how such formulations can be devised even if the steric

stabiliser block is not particularly salt-tolerant. The low salt concentration is more cost-effective and also made such formulations amenable to transmission electron microscopy studies, which are problematic for higher salt concentrations. Nonetheless, highly viscous copolymer solutions were obtained after a two-fold dilution with water. Future work on this system could involve using a higher reaction temperature, which should enable even lower salt concentrations to be used. This is because PNAM exhibits inverse temperature solubility behaviour at 32 – 36°C in the presence of 0.30 M ammonium sulfate, which is only 2 – 6°C higher than the current synthesis temperature. It is well-known that the critical solution temperature (or LCST) of thermoresponsive polymers is typically lower in the presence of salt; for example, Cremer et al. reported such observations for PNIPAM.[18]

Further GPC characterisation of each system using a multi-angle laser light scattering (MALLS) detector would be useful. Most of the aqueous GPC results in this Thesis are reported relative to PEG calibrants using an RI detector, which inevitably introduces a systematic error. Obtaining absolute M_w values via MALLS is more likely to be useful for predicting the copolymer solution viscosity after dissolution of the initial low-viscosity particles.

Preliminary results of the all-cationic formulations; $PATAC_x$-$PBzDA_y$, $PMETAC_x$-$PBzDA_y$ and $PMETAC_x$-$PBzDMA_y$ indicate high conversions and free-flowing turbid dispersions when prepared in the presence of 3.0 M ammonium sulfate. The difficulty with such formulations is the GPC analysis. Initial characterisation using aqueous GPC protocols led to no copolymer elution: this observation is attributed to their irreversible adsorption onto the GPC columns. Thus, if such systems are to be further investigated, a suitable hydrolysis/methylation protocol should be developed (such as that reported by North et al.[19]) to enable GPC analysis in a suitable organic solvent (e.g. THF, DMF or chloroform). On the other hand, MALLS could be used in its offline mode to determine absolute M_w values (although no MWD information is obtained from such measurements).

The use of alternative steric stabilisers for either PNAM or PAM core-forming blocks could also be considered. Suitable electrosteric stabilisers could be PATAC, PAMPS or PMPC while the ammonium sulfate concentration could be maintained at either 0.60 M or 3.0 M respectively. Gel polymerisation methods, as reported by Destarac[20] and Sumerlin[21], for the production of UHMW polymers have been discussed in **Chapter 1**. Low-temperature RAFT solution polymerisations using either redox initiator or UV light respectively apparently lead to efficient syntheses with minimal chain transfer. No free-flowing low-viscosity copolymer particles have been prepared using such techniques, but M_n values greater than 1 MDa have been reported for PAM and PDMAC homopolymers.

7.2 References

1 H. Jung, G. Shin, H. Kwak, L. T. Hao, J. Jegal, H. J. Kim, H. Jeon, J. Park and D. X. Oh, 'Review of polymer technologies for improving the recycling and upcycling efficiency of plastic waste', *Chemosphere*, 2023, **320**, 138089.

2 A. Samir, F. H. Ashour, A. A. A. Hakim and M. Bassyouni, 'Recent advances in biodegradable polymers for sustainable applications', *npj Mater. Degrad.*, 2022, **6**, 68.

3 A. W. Fortenberry, P. E. Jankoski, E. K. Stacy, C. L. McCormick, A. E. Smith and T. D. Clemons, 'A Perspective on the History and Current Opportunities of Aqueous RAFT Polymerization', *Macromol. Rapid Commun.*, 2022, **43**, e2200414.

4 A. Guyot, F. Chu, M. Schneider, C. Graillat and T. F. McKenna, 'High solid content latexes', *Prog. Polym. Sci.*, 2002, **27**, 1573–1615.

5 Aqueous Polymer Dispersion, O. Aydin, Oral, M. Portugall, J.Neutzner, W. Maechtle, BASF, US5340859A, 1994.

6 Aqueous Polymer Dispersion, O. Aydin, Oral, M. Portugall, J.Neutzner, W. Maechtle, BASF, US5624992A, 1997.

7 Process for producing aqueous polyacrylamide solutions, T. J. Zimmermann, F.-A. El-Toufaili, H. Sprakfe, BASF, US11384177B2, 2022.

8 C. Castillo, P. Fawell and A. Costine, 'Optimising the activity of acrylamide-based polymer solutions used to flocculate mineral processing tailings suspensions – A review', *Chem. Eng. Res. Des.*, 2023, **199**, 214–237.

9 S. J. Byard, Synthesis and Characterisation of Stimulus-responsive Diblock Copolymer Nano-objects Prepared by RAFT Aqueous Dispersion Polymerisation, PhD Thesis, University of Sheffield, 2019.

10 A. Blanazs, A. J. Ryan and S. P. Armes, 'Predictive phase diagrams for RAFT aqueous dispersion polymerization: Effect of block copolymer composition, molecular weight, and copolymer concentration',

Macromolecules, 2012, **45**, 5099–5107.

11 R. J. McBride, J. F. Miller, A. Blanazs, H. J. Hähnle and S. P. Armes, 'Synthesis of High Molecular Weight Water-Soluble Polymers as Low-Viscosity Latex Particles by RAFT Aqueous Dispersion Polymerization in Highly Salty Media', *Macromolecules*, 2022, **55**, 7380–7391.

12 A. J. Smith, S. G. Alcock, L. S. Davidson, J. H. Emmins, J. C. Hiller Bardsley, P. Holloway, M. Malfois, A. R. Marshall, C. L. Pizzey, S. E. Rogers, O. Shebanova, T. Snow, J. P. Sutter, E. P. Williams and N. J. Terrill, 'I22: SAXS/WAXS beamline at Diamond Light Source – an overview of 10 years operation', *J. Synchrotron Radiat.*, 2021, **28**, 939–947.

13 C. E. Habermann, in *Kirk-Othmer Encyclopedia of Chemical Technology*, Wiley, 2002.

14 B. Huang, J. Jiang, M. Kang, P. Liu, H. Sun, B. G. Li and W. J. Wang, 'Synthesis of block cationic polyacrylamide precursors using an aqueous RAFT dispersion polymerization', *RSC Adv.*, 2019, **9**, 12370–12383.

15 S. Bai, Y. Wang, B. Liu, Y. Zhu and R. Guo, 'Dispersion copolymerization of acrylamide and sodium 2-acrylamido-2-methylpropanesulfonate in aqueous salt solution stabilized with a macro-RAFT agent', *Colloids Surfaces A Physicochem. Eng. Asp.*, 2018, **553**, 446–455.

16 Controlled Radical Polymerization in Water-in-Water Dispersion, M. Destarac, J. D. Wilson, S. Silvia, Rhodia, WO2013132108A1, 2013.

17 Calculated using Advanced Chemistry Development (ACD/Labs) Software V11.02 (© 1994-2023 ACD/Labs), .

18 Y. Zhang, S. Furyk, L. B. Sagle, Y. Cho, D. E. Bergbreiter and P. S. Cremer, 'Effects of Hofmeister Anions on the LCST of PNIPAM as a Function of Molecular Weight', *J. Phys. Chem. C*, 2007, **111**, 8916–8924.

19 S. M. North and S. P. Armes, 'Synthesis of polyampholytic diblock copolymers: Via RAFT aqueous solution polymerization', *Polym. Chem.*, 2021, **12**, 4846–4855.

20 E. Read, A. Guinaudeau, D. J. Wilson, A. Cadix, F. Violleau and M. Destarac, 'Low temperature RAFT/MADIX gel polymerisation: Access to controlled ultra-high molar mass polyacrylamides', *Polym. Chem.*, 2014, **5**, 2202–2207.

21 R. N. Carmean, T. E. Becker, M. B. Sims and B. S. Sumerlin, 'Ultra-High Molecular Weights via Aqueous Reversible-Deactivation Radical Polymerization', *Chem*, 2017, **2**, 93–101.